C9ORF72 ALS
from pathology to therapy

Gomez Deza, Jorge

Awarding institution:
King's College London

C9ORF72 ALS: From pathology to therapy

Jorge Gómez-Deza

Maurice Wohl Clinical Neurosciences Institute

Institute of Psychiatry Psychology and Neuroscience

King's College London

Thesis submitted for degree of Doctor in Philosophy

Declaration

I hereby declare that this work is original and all my own. Contributions from other people have been clearly stated. I have performed all experiments and subsequent analysis of results unless otherwise stated. Previous work has been reported and referenced accordingly. This work has not been submitted to any degree. Some of the work presented in Chapter 3 has been published in (Gomez-Deza et al., 2015).

Acknowledgements

Although I may use the word “I” extensively in this thesis, all of my work could’ve not been achieved with the help of many people. Firstly I would like to thank my founders; the King's Bioscience Institute, the Guy’s and St. Thomas’ Charity and the Motor Neurone Disease Association that have made it possible for me to experiment, explore, become a scientist and live in such an amazing place as London.

My two amazing supervisors, Prof. Christopher Shaw and Dr. Jean-Marc Gallo have been essential for this work, they have put up with my crazy ideas and guided me so that I could pursue them without getting lost in them. A big special thank you to my two scientific mentors. Dr. Youn-Bok Lee taught me how to love science with his endless enthusiasm, crazy Korean stories and existential conversations whilst miniprepping, extracting RNA or god knows what. Dr. Agnes Nishimura has taught me pretty much everything I know about iPSCs and has helped me out when everything was failing and assured me everything would be ok.

Secondly I would like to thank you for reading this thesis. Please note that from now on, I’m going to take the liberty of acknowledging people in a very personal way. I have worked on this for over 4 years and none of it would be possible with the help and support of all of my friends. I have decided to acknowledge them by the WhatsApp group name they have used to support me. I would like to thank all of the “lad” components of “Gü” (Adam, Swamit, Numa, Kane, Danny, KP, Niko, Bob and De Souza) and that have given me a science-less refuge, weekends (and weeks) away, football, economic and political discussion and have been pretty much become my second family. An essential part of that second family that I have developed is the components of “this is fucking awesome” (Sarah, Patrick, Laura and Josh (and Ruth and Beth). Nothing would’ve been the same without them. Thanks for dinners, pub lunches, secret Hitler and cards against humanity and everything that comes

with them. “Hastinianos Londinenses” (Rosanna, Maria, Nata, Irene and David) have provided me with much needed “Spanglish” relief when I needed it, including corqueta nights, brugal and silly Spanish laughter. The “Astor Class of ‘09” (Ela, Marina, Ines, Yasir, Danny and Andrew) with whom I met in my first year and they are still as awesome as ever. Also thanks to all of those friends in Spain including “Soom” and “Fiesta biatch” and all those people that have shared my time in London (you know who you are).

I must thank all of the components of the Shaw lab; Caroline, Jackie, Simon, Brad, Alinda, Claire, Graham, Sarah and Bex. They have made my day to day so special and have had to put up with me. Their advice and help is invaluable and much of my success is thanks to them. Special mention to Han-Jou Chen for being ruthlessly honest and to Holly barker for being my NSC partner. Thanks to the “>0-------88-----<” members (Athina, Erin, Martina, Nada, Ricky, Sharky, Valentina, Wong, Wejdan, Carole and James) with whom I have shared pretty much every lunchtime laughing, moaning and having a lovely time. Also many thanks to Bea, Patricia, Maria and Aurelio for providing me with some good old fashion Spanish support in the lab. Coming to the lab was an absolute delight thanks all to them.

By name I have specially thank a couple of people too. Laura Stone has been just too good. We met after that famous “I hate Lauras” and she still became my best friend. Laura Kolserman has listened to me when I needed it the most and although we don’t see each other much, I know she is just there when I need her. My undergraduate and my PhD wouldn’t have been the same without Anaïs Cassaignau. Luis Alejandro Gonzalez for being silly, making rhymes and being a great support. Pia Mendaro for her architecture lessons. Martina De Majo for being her, being that Mediterranean support inside and outside the lab. I lived with Ed and Merrick for pretty much the entirety of my PhD. Four years of Catan, Junip, squash, Game of thrones and so much more. You guys have been the absolute best and I could not have asked for better flatmates.

I have to thank my family (My tio Pablo and Miguel, tia Lola, Susana, la Aba y el Bubu) that had the courage of asking me what I was studying every time I went back to visit. Last but not least I have to thank my mum, dad and my brother. Absolutely nothing would've happened without their endless support. Thank you for trusting (and funding) me when I decided to come to London. Thank you for taking so much care of me and being my role models. I owe them so much for making me who I am, passing on their values and always being there for me.

Abstract

A hexanucleotide GGGGCC (G4C2) repeat expansion in the chromosome 9 open reading frame 72 (*C9ORF72*) gene is the most common cause of familial amyotrophic lateral sclerosis (ALS) and frontotemporal dementia (FTD). The expansion is transcribed from the sense and the antisense strands and accumulates in the nucleus of cells as RNA foci. Moreover, it is translated into five dipeptide repeat (DPR) proteins that accumulate in the brain and spinal cord and causes a decrease in *C9ORF72* transcripts and protein levels. In the present study, we reported that there are very few DPR inclusions in the spinal cord of ALS-C9ORF72 cases and we have assessed the presence of sense and antisense RNA foci in the spinal cords of ten *C9ORF72*-ALS cases. We have shown that sense RNA foci are more common that antisense foci in the spinal cord, and significantly more common in spinal motor neurons of *C9ORF72*-ALS cases. This suggests that the presence of intranuclear sense RNA foci may be the main contributor to toxicity. We have designed non-degrading antisense phosphorodiamidate morpholino oligomers (PMOs) that bind, but not degrade G4C2 target transcripts as a potential therapeutic strategy. We tested the PMOs in HEK-293T cells expressing EGFP-72(G4C2) constructs showing that PMOs bind and reduce the number of pathological RNA foci. We have also shown that the use of PMOs reverse *C9ORF72*-specific phenotypes in neuronal progenitor cells (NPCs) and neurons from C9ORF72-ALS patient-derived induced pluripotent stem cells (iPSC). All together our results suggest that sense RNA foci may be the main contributor to *C9ORF72*-associated toxicity and that its effect can be mitigated using non-degrading PMOs targeting the G4C2 repeats. Finally, our results highlight an alternative therapeutic approach which consists in blocking the G4C2 expanded RNA transcripts but not degrading them, which may be important given that haploinsufficiency of *C9ORF72* may also be a strong component of C9ORF72 ALS pathogenic mechanism.

Abbreviations

AChE	Acetylcholinesterase enzyme
AD	Alzheimer's disease
AFP	α-fetoprotein
ALS	Amyotrophic lateral sclerosis
ALS-*C9ORF72*	Amyotrophic lateral sclerosis case carrying the *C9ORF72* expansion
ALS2	Autosomal recessive juvenile-onset form of ALS
ANOVA	Analysis of variants
ASO	Antisense oligonucleotide
ATG	Adenine-thymine-guanine
ATXN2	Ataxin 2
Aβ	Amyloid beta
βIII-tubulin	Beta III tubulin
BAC	Bacterial artificial construct
BDNF	Brain-derived neurotrophic factor
bFGF	Basic fibroblast growth factor
bp	Base pair
BSA	Bovine serum albumin
C4G2	CCCCGG
C-terminal	Carboxy terminal
CDM	Chemically defined medium
cDNA	Complementary DNA
CHAPS	Dimethyl[3-(propyl]. azaniumyl}propane-1-sulfonate
CHMPB2	Charged multivesicular body protein 2B
CMT	Charcot-Marie-Tooth

CNS	Central nervous system
CRISPR	Clustered regularly interspaced short palindromic repeats
CSF	Cerebral spinal fluid
CO_2	Carbon dioxide
C9ORF72	Chromosome 9 open reading frame 72
DAPI	4',6-diamidino-2-phenylindole
DMPK	DM protein kinase
DMSO	Dimethyl sulphoxide
DNA	Deoxyribonucleic acid
DPR	Dipeptide repeat
EB	Embryoid body
EDTA	Ethylenediaminetetraacetic acid
EGFP	Enhanced green fluorescent protein
ELP3	Elongator protein 3
ER	Endoplasmic reticulum
ESCRTIII	Endosomal sorting complex required for transport III
EWSR-1	Ewing's sarcoma RNA binding protein 1
fALS	Familial Amyotrophic lateral sclerosis
FACS	Fluorescent activated cell sorting
FDA	Federal drugs agency
Fig	Figure
FIG4	Phosphoinsoited phosphatase
FISH	Fluorescent *in situ* hybridisation
FTD	Frontotemporal dementia
FUS	Fused in sarcoma
g	Grams

G4C2	GGGGCC
GDNF	Glial cell-derived neurotrophic factor
GTP	Guanosine triphosphate
HA	Hemagglutinin
hESC	Human embryonic stem cell
hnRNP	Heterogeneous nuclear ribonucleoprotein
IBMPFD	Paget disease of the bone and frontotemporal dementia
iPSC	Induced pluripotent stem cell
iPSC-MNs	Motor neurons differentiated from induced pluripotent stem cells
iPSN	neurons differentiated from induced pluripotent stem cells
HEK-293T	Human embryonic kidney cells
HRP	Horse radish peroxidase
ICC	Immunocytochemistry
ICV	Intracerebroventricular
IHC	Immunohistochemistry
IT	Intrathecal
kDa	Kilo Daltons
KO	Knock out
L	Litre
LB	Luria Bertani
LNA	Locked nucleic acid
L-C9ORF72	Long isoform of C9ORF72 protein
m	Meter
M	Molar (moles/litre)
MAP2	Microtubule-associated protein 2
MATR3	Matrin 3

MBNL1	Mucleblind like 1
$MgCl_2$	Magnesium chloride
MOPS	4-Morpholinepropanesulfonic acid
miRNA	Micro RNA
mRNA	Messenger RNA
NEK1	NIMA-related kinase 1
min	Minutes
N-terminal	Amino terminal
NCI	Nuclear cytoplasmic inclusions
NLS	Nuclear localisation signal
NMJ	Neuromuscular junction
MN	Motor neuron
NPC	Neural progenitor cell
n.s.	Not significant
OCT4	Octamer-binding transcription factor 4
OPTN	Optineurin
P-body	Processing body
PBS	Phosphate saline buffer
PBST	Phosphate saline buffer with Tween 20
PCR	Polymerase chain reaction
PFN1	Profilin 1
PMD	Post-mortem delay
PMO	Phosphorodiamitate morpholino oligomer
Poly-GA	poly-Gly-Ala
Poly-GP	poly-Gly-Pro
Poly-GR	poly-Gly-Arg

Poly-HEMA	Poly (2-hydrixyethylmethacrylate)
Poly-PA	poly-Pro-Ala
Poly-PR	poly-Pro-Arg
Poly-Q	poly-Glutamine
PPMO	Peptide-coupled Phosphorodiamitate morpholino oligomer
PTPIP51	Protein tyrosine phosphatase-interacting protein-51
qPCR	Quantitative polymerase chain reaction
RAN	Repeat-associated non-ATG
RA	Retinoic acid
RIPA	Ratio immunoprecipitation assay
ROCK	Rho-associated kinase
ROS	Reactive oxygen species
RNA	Ribonucleic acid
RNAi	RNA interference
RISC	RNA-induced silencing complex
RNAP II	RNA polymerase II
RNS	Reactive nitrogen species
RRM	RNA recognition motif
RT-PCR	reverse transcriptase polymerase chain reaction
s	Second
sALS	Familial Amyotrophic lateral sclerosis
SCA2	Spinocerebellar ataxia type 2
S-C9ORF72	Short isoform of C9ORF72 protein
SDS	Sodium Dodecyl sulphate
SEM	Standard error of the mean
shRNA	Small hairpin RNA

siRNA	Small interfering RNA
SMA	spinal muscular atrophy
SOD1	Superoxide dismutase 1
SQSTM1	Sequestosome 1
TAF-15	Tata-binding protein associated factor 2N
Taq	*Thermophilus aquaticus*
TALEN	Transcription activator-like endonuclease
TBK1	TANK-binding kinase
TARDBP/TDP- 43	Transactive response DNA-binding protein 43
TBS	Tris-buffered saline
TBST	Tris-buffered saline with Tween 20
tRNA	Transfer RNA
UPS	Ubiquitin proteasome system
UV	Ultraviolet
V	Volts
VAPB	VAMP Associated Protein B and C (VAPB)
VCP	Valosin-containing protein
w/v	Weight/volume
WT	Wild Type

CONTENTS

Table of Figures

Table of Tables

1 INTRODUCTION

1.1 AMYOTROPHIC LATERAL SCLEROSIS

Amyotrophic lateral sclerosis (ALS) is a progressive neurodegenerative disease characterised by the loss of motor neurons in the brain and spinal cord, causing progressive paralysis of limb and bulbar muscles and death due to respiratory failure within an average of three years from symptom onset. Cytoplasmic inclusions containing the transactive response DNA-binding protein (TDP-43) are the neuropathological hallmark in ~95 % of ALS cases (Neumann et al., 2006).

The clinical signs of lower motor neuron degeneration include fasciculations, muscle wasting and weakness, while signs of upper motor neuron degeneration include spasticity, hyper-reflexia and an extensor plantar response (Babinski sign). There is currently no cure, and the sole disease-modifying treatment, riluzole, has only a modest effect on survival; increasing life expectancy by only three months during an 18 month clinical trial (Cheah et al., 2010). The management of ALS is largely palliative and focussed on reducing the impact of symptoms arising from muscle weakness in the throat causing difficulty swallowing or limbs decreasing mobility and independence in the tasks of daily living. When respiratory weakness develops non-invasive or even invasive mechanical ventilation is instituted (Mitsumoto et al., 2014). The relentless progression of disabilities and loss of autonomy are reasons given as to why so many ALS patients seek euthanasia and in the Netherlands. Around 20% of ALS patients chose to die by “Physician assisted suicide” (Veldink et al., 2002).

ALS is regarded as a rare condition with a prevalence of 3 to 6 per 100.000 people and an incidence of 3 per 100.000 people (Chio et al., 2013) however it appears as the cause of death in 1 in 300 UK death certificates (Johnston et al., 2006). Due to improvements in healthcare and increase in life expectancy this number is expected to rise significantly as the incidence

of ALS increases with age. ALS is mainly a late onset disease although juvenile onset (<25 years) and early onset (<45 years) account for ~1 and ~20% of all ALS cases respectively (Turner et al., 2012).

ALS and frontotemporal dementia (FTD) are strongly pathologically and genetically linked and are increasingly regarded as two ends of a phenotypic spectrum. TDP-43 aggregates, common in ALS, are present in the frontal cortex of ~50% of FTD cases. Moreover the hexanucleotide repeat GGGGCC (G4C2) expansion in the chromosome 9 open reading frame 72 (*C9ORF72*) gene occurs in in 20-50% of familial (Snowden et al., 2012) and 10% of sporadic ALS and FTD cases (DeJesus-Hernandez et al., 2011). FTD is the second most common cause of dementia with an onset <65 years after Alzheimer's disease. It is characterised by the loss of neurons in the frontal and temporal lobes leading to personality and behavioural changes and the loss of language skills. Frank dementia is rare in ALS but round 30-50% of ALS cases present with subtle cognitive and language deficits that are typical of FTD and it is estimated that 15% of FTD cases develop subtle signs of upper and lower motor neuron degeneration and the diagnostic criteria for ALS (Ling et al., 2013).

1.2 DIAGNOSIS

There are currently no disease specific biomarkers to diagnose ALS. Diagnosis according to El Escorial criteria is based on the history of progressive muscle dysfunction and signs of motor neuron degeneration in the absence of radiological evidence of a structural lesion and excluding other conditions that may mimic ALS (Brooks, 1999). These, although generally reliable to diagnose ALS, lack the ability to predict whether the disease will be slow or fast progressing in each case. Moreover, the lack of a reliable biomarker makes it hard to assess the efficacy of drugs tested in clinical trials in an objective manner. The diagnostic tests include magnetic resonance imaging, nerve conduction studies and blood tests for anti-

ganglioside antibodies or a gene test for Kennedy's disease. Diagnostic accuracy exceeds 95% in most experienced centres but post-mortem pathological examination may still be required to confirm a clinical ALS diagnosis in complex cases.

1.3 GENETICS

The majority of ALS cases (~90%) appear to be sporadic, with no known family history (sporadic ALS or sALS) (Chio et al., 2013). The remaining 10% of cases have a familial history of ALS or a dementia consistent with FTD (familial ALS or fALS) as shown in figure 1. In 1993 mutations in the superoxide dismutase 1 (*SOD1*) gene were shown to cause ~20% of fALS cases (Rosen et al., 1993). It was not until recently, when with next generation gene sequencing techniques that the number of genes liked to ALS has increased dramatically. To date, mutations in over 30 different genes have been causally associated with ALS with variable degree of certainty (summarised in table 1.1) (White and Sreedharan, 2016).

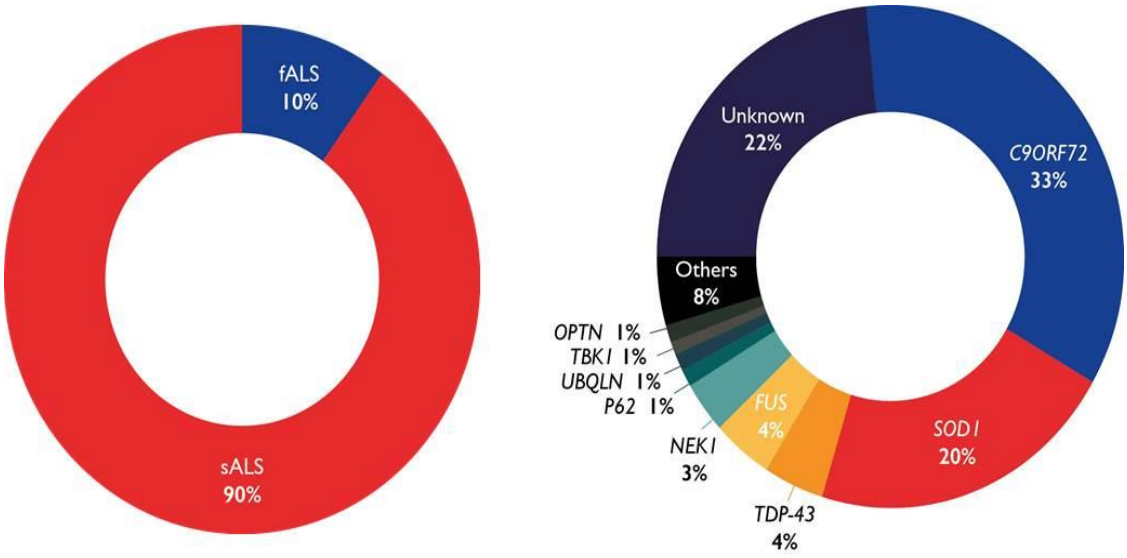

Figure 1.1: Diagram showing the prevalence of genetic mutations in sporadic and familiar ALS cases.

(Special thanks to Micol Montessanti for generating the figure)

Gene ID	Description	Location	Reference
ALS2	Alsin Rho guanine nucleotide factor	2q33.2	(Yang et al., 2001)
ALS3	Amyotrophic lateral sclerosis 3	18q21	(Hentati et al., 1994)
ALS7	Amyotrophic lateral sclerosis 7	20p13	(Hoyer and Hecht, 2000)
ANG	Angiogenin	14q11.1	(Greenway et al., 2004)
ATXN2	Ataxin 2	12q24.1	(Elden et al., 2010)
C9ORF72	Chromosome 9 open reading frame 72	9p21.2	(DeJesus-Hernandez et al., 2011; Renton et al., 2011)
CCNF	Cyclin F1	16p13.3	(Williams et al., 2016)
CHCHD10	Coiled-coil-helix-coiled-coil-helix containing 10	22q11.23	(Bannwarth et al., 2014)
CHMPB2	Charged multivesicular body protein 2B	3p11.2	(Parkinson et al., 2006)
DAO	d-amino-acid oxidase	12q24	(Mitchell et al., 2010)
DCTN1	Dynactin subunit 1	2p13	(Munch et al., 2005; Munch et al., 2004)
ELP3	Elongator acetytransferase complex subunit 3	8p21.1	(Simpson et al., 2009)
ERBB4	Erb-b2 receptor tyrosine kinase	2q33.3-q34	(Takahashi et al., 2013)

Gene ID	Description	Location	Reference
FIG4	FIG4 phosphoinositide 5-phosphatase	6q21	(Chow et al., 2009)
FUS	Fused in Sarcoma	16p11.2	(Kwiatkowski et al., 2009; Vance et al., 2009)
GLE1	GLE1 RNA export mediator	9q34.11	(Kaneb et al., 2015)
HNRNPA1	Heteronuclear ribonucleoprotein A1	12q13.1	(Kim et al., 2013)
LMNB1	Laminin B1	5q23.2	(Johnson et al., 2014)
MATR3	Matrin 3	5q31.2	(Johnson et al., 2014)
NEFH	Neurofilament heavy polypeptide	22q12.2	(Al-Chalabi et al., 1999; Meyer and Potter, 1995)
NEK1	NIMA related kinase 1	4q33	(Brenner et al., 2016; Cirulli et al., 2015; Kenna et al., 2016)
OPTN	Optieneurin	10p13	(Maruyama et al., 2010)
PFN1	Profilin 1	17p13.3	(Daoud et al., 2013)
PRPH	Peripherin	12q13.12	(Gros-Louis et al., 2004; Leung et al., 2004)
SETX	Senataxin	9q34.13	(Chen et al., 2004)
SIGMR1	Sigma nonopioid intracellular receptor 1	9p13.3	(Al-Saif et al., 2011)

Gene ID	Description	Location	Reference
SOD1	Superoxide dismutase 1	21q22.11	(Rosen et al., 1993)
SPAST	Spastin	2p24-p21	(Meyer et al., 2005)
SPG11	Spastic paraplegia 11	15q14	(Daoud et al., 2012)
SQSTM1	Sequestosome 1	5q35	(Fecto et al., 2011)
TAF15	TATA-box binding protein associated factor 15	17q12	(Ticozzi et al., 2011)
TARDBP	Tar DNA protein binding	1p36.22	(Sreedharan et al., 2008)
TBK1	TANK binding kinase 1	12q14.1	(Cirulli et al., 2015; Freischmidt et al., 2015)
TUBA4A	Tubulin alpha 4a	2q35	(Smith et al., 2014)
UBQLN	Ubiquilin 2	Xp11.21	(Deng et al., 2011)
UNC13A	Unc-13 homologue A	19p13.11	(van Es et al., 2009)
VAPB	VAMP associated protein B	20q13.33	(Nishimura et al., 2004)
VCP	Valosin containing protein	9p13.3	(Johnson et al., 2010)

Table 1.1: List of genes causally associated with ALS (adapted and expanded from (White and Sreedharan, 2016)). It must be noted that the exact link between the reported mutations in many of these genes and ALS still remains to be confirmed with the use of cellular and animal models.

1.4 MAIN ALS GENES

1.4.1.1 SOD1

SOD1 gene codes for superoxidase dismutase 1 protein which catalyses the dismutation of peroxide ions to free radicals with oxygen and hydrogen peroxide as substrates (Rosen et al., 1993). Mutations present in the *SOD1* gene were the first to be identified in fALS cases. Initially, 11 missense mutations were discovered by linkage studies; since then over 180 disease-causing mutations have subsequently been reported (Rosen et al., 1993; Scarrott et al., 2015). Cases with *SOD1* mutations do not show the typical TDP-43 pathology identified in 90% of ALS cases. Instead, SOD1 cytoplasmic inclusions are present in the spinal cord of *SOD1* mutation carriers (van Zundert and Brown, 2016).

Pathogenic *SOD1* mutations are predominantly single amino acid changes and account for 20% of fALS and 1% of sALS cases (White and Sreedharan, 2016). The mechanism of toxicity of *SOD1*-linked ALS is caused by misfolding and aggregation of SOD1 protein rather than by impairment of SOD1 activity (Williamson et al., 2000). Mice over-expressing G93A mutant SOD1 human protein develop progressive motor neuron loss and hind limb paralysis and are commonly used for preclinical studies. These mice however do not develop TDP-43 pathology, which is observed in 90% of ALS cases (Picher-Martel et al., 2016).

1.4.1.2 TARDBP (TDP-43)

The *TARDBP* gene encodes for the RNA-binding protein TDP-43. Hyper-phosphorylated, poly-ubiquitinated insoluble cytoplasmic TDP-43 inclusions are present in the spinal cord and frontal cortex of >90% of ALS cases. TDP-43 intracellular inclusions are present in the nucleus and cytoplasm of neurons and glia (Neumann et al., 2009; Neumann et al., 2006). TDP-43 pathology can be found in the majority of ALS patients with the exception of those with SOD1 and FUS mutations. TDP-43 pathology is indistinguishable between patients with and without mutations in the *TARDBP* gene. In 2008, the first

pathogenic mutations in the *TARDBP* were identified (Sreedharan et al., 2008), and since then, over 50 mutations have been reported accounting for 4% of all fALS and 1% of sALS cases. Most mutations are clustered in the low-complexity "prion like" glycine rich carboxyl (C)-terminus of the protein (Ling et al., 2013; Sreedharan et al., 2008).

TDP-43 is a 414 amino acid protein containing two RNA recognition motifs (RRM) (Ling et al., 2013) that shuttles between the nucleus and the cytoplasm and it has been shown to bind ~5,500 different RNA transcripts, including TDP-43 mRNA, self-regulating its expression (Polymenidou et al., 2011; Tollervey et al., 2011). The presence of cytoplasmic aggregates and clearance of nuclear TDP-43 suggests that toxicity may arise though gain or loss-of-function mechanisms and it remains unclear which of the two is the main driver of toxicity (Diaper et al., 2013; Ratti and Buratti, 2016).

Animal models have yielded conflicting results on whether TDP-43 toxicity is due to a loss-of-function or a gain-of-function mechanism. TDP-43 knockout (KO) mice are embryonically lethal, however heterozygous KO mice are viable and fertile with autoregulation maintaining nearly normal TDP-43 levels (Kraemer et al., 2010). Selective removal of TDP-43 from the motor neurons in mice causes weight loss, degeneration of the motor axons and loss of the neuromuscular junction (NMJ), however these mice did not have reduced survival rates and normal life spans (Iguchi et al., 2013b). Furthermore, homozygous KO of TDP-43 in zebrafish causes muscle degeneration and reduced motor neuron axon outgrowth (Schmid et al., 2013). Together this data suggests that loss of TDP-43 may play an important role in adult motor neuron degeneration, but it may not be sufficient to cause fatal motor neurone disease.

Overexpression of TDP-43 in *C. elegans* causes cell death (Ash et al., 2010). This study showed that there was a correlation between endogenous TDP-43 levels and motor deficits. Moreover, the overexpression of wild type (WT) TDP-43 and M337V TDP-43 mutant causes

severe neurodegeneration and short life span in transgenic mice (Mitchell et al., 2015). These mice develop most of the observed pathology in post mortem tissue, including hyperphosphorylated, poly-ubiquitinated TDP-43 aggregates and loss of upper and lower motor neurons. These studies suggest that overexpression of TDP-43 is also capable of causing neurodegeneration and reducing life span. Finally KO and overexpression of the endogenous *tardbp* gene in zebrafish are both sufficient to cause motor phenotypes in zebrafish (Kabashi et al., 2010). These results indicate that motor neuron degeneration may be driven by both the loss of nuclear TDP-43 and the presence of cytoplasmic TDP-43 aggregates.

1.4.1.3 C9ORF72

In 2011 a large intronic hexanucleotide expansion GGGGCC (G4C2) in the chromosome 9 open reading frame 72 (*C9ORF72*) gene was identified and accounts for 20-50% of all fALS cases (DeJesus-Hernandez et al., 2011; Renton et al., 2011). In ALS cases the G4C2 repeat can be expanded up to 2000 times, this contrasts with the presence of 2-20 repeats in healthy individuals (DeJesus-Hernandez et al., 2011; Renton et al., 2011).

The TDP-43 pathology observed in *C9ORF72* cases is indistinguishable from other ALS cases (Mackenzie et al., 2013a), however *C9ORF72* cases also show abundant p62-positive and TDP-43-negative inclusions in non-motor regions such as the cerebellum (Al-Sarraj et al., 2011). Additionally, expanded G4C2 RNA accumulates in the nucleus of neurons and glia as RNA foci in most regions of the brain and the spinal cord (Cooper-Knock et al., 2012; DeJesus-Hernandez et al., 2017; DeJesus-Hernandez et al., 2011; Lee et al., 2013; Mizielinska et al., 2013). Moreover, the repeats can be translated through unconventional repeat-associated non-ATG (RAN) translation of the sense and the antisense strands. Five dipeptide-repeat (DPR) proteins have been identified in post mortem tissues from C9ORF72 ALS and FTD cases; poly-Gly-Pro (GP), Gly-Ala (GA) and Gly-Arg (GR) from the sense strand (Ash et al., 2013; Mori

et al., 2013c) and poly-Gly-Pro (GP), Pro-Ala (PA) and Pro-Arg (PR) from the antisense strand (Gendron et al., 2013; Mori et al., 2013a). Aggregates of these five DPR proteins have been identified to varying degree in many different regions of the brain and spinal cord of *C9ORF72* expansion carriers (Ash et al., 2013; Mori et al., 2013a).

The mechanisms by which the hexanucleotide repeats might exert toxicity are highly controversial. It was initially reported that the presence of the G4C2 repeats lead to a decrease in *C9ORF72* transcripts and protein, therefore suggesting toxicity could be due to haploinsufficiency (DeJesus-Hernandez et al., 2011; Renton et al., 2011). This theory was subsequently not supported as *C9orf72*-KO mice do not develop any neurological defects or any ALS associated pathology and instead have immune deficiency and dysfunctional macrophages and microglia (O'Rourke et al., 2016) (Koppers et al., 2015). Furthermore, homozygous expansion carriers do not develop disease at an earlier age or a more rapidly progressive disease course compared to heterozygous carriers (Fratta et al., 2013), which would be expected if haploinsufficiency was the mechanism.

Sense and antisense transcripts have been identified in the major sites of neurodegeneration in *C9ORF72* expansion carriers as nuclear RNA foci and sequester RNA binding proteins (Lee et al., 2013; Mizielinska et al., 2013). We and others have shown that G4C2 RNA foci can sequester RNA binding proteins such as hnRNP-H, ADARB2 and nucleolin and increase nucleolar stress (Donnelly et al., 2013; Haeusler et al., 2014; Lee et al., 2013). Additionally, expanded transcripts can form secondary structures such as G-quadruplexes and R-loops (DNA-RNA hybrids) that bind proteins and possibly disrupt nucleocytoplasmic transport in the cell (Conlon et al., 2016b; Fratta et al., 2012; Haeusler et al., 2014; Jovicic et al., 2015; Zhang et al., 2015). Finally, the presence of antisense RNA foci has been reported to be correlated with the nuclear depletion of TDP-43 in the spinal motor neurons of a reduced number of C9ORF72 ALS cases. This study failed to observe any correlation between

the nuclear depletion of TDP-43 in motor neurons and the presence of sense RNA foci (Cooper-Knock et al., 2015).

The expression of DPR proteins has also been strongly implicated in causing neurotoxicity. Although it is unclear which specific DPR is toxic; poly-GR and PR have been shown to be toxic in drosophila causing eye degeneration when overexpressed in the retina and reducing life span when expressed under an ELAV neuronal promoter (Mizielinska et al., 2014). The arginine-rich DPRs Poly-GR and PR, may also exert toxicity though impairment of biogenesis of ribosomal RNA (Kwon et al., 2014). Additionally, poly-GA has been shown to be toxic in an aggregation-dependent manner when overexpressed in mice. Poly-GA may exert its toxicity though endoplasmic reticulum stress and caspase-3 activation (Schludi et al., 2017; Zhang et al., 2016a). However, the extremely low presence of DPR inclusions in some areas of maximal neurodegeneration, such as the spinal cord, challenges the idea that DPRs are the main source of toxicity (Gomez-Deza et al., 2015; Mackenzie et al., 2015). It is also unclear whether any of the three mechanisms are sufficient to exert toxicity on their own. Based on the current evidence it is clear that a combination of all three processes may differentially contribute to neurodegeneration in different sites. The recent emergence of *C9ORF72* bacterial artificial construct (BAC) mouse models and neurons derived from induced pluripotent stem cells (iPSCs) carrying the expansion opens the possibility of studying disease mechanisms in a more physiological setting (Jiang et al., 2016; Liu et al., 2016; O'Rourke et al., 2015; Peters et al., 2015)

The main mechanisms though which the *C9ORF72* expansion may be exerting toxicity will be reviewed in greater detail in a later section.

1.4.1.4 FUS

Mutations in the gene fused in sarcoma (*FUS*) gene were reported by two independent groups in 2009 having been previously linked to chromosome 16q (Abalkhail et

al., 2003; Kwiatkowski et al., 2009; Ruddy et al., 2003; Sapp et al., 2003; Vance et al., 2009). FUS is another DNA and RNA binding protein, like TDP-43. Most mutations reside in the extreme C-terminus of the protein and reduce its nuclear import leading to increased cytoplasmic accumulation and aggregation. Pathological studies revealed the presence of large FUS-immunoreactive inclusions in the spinal cord and motor neurons of a subset of ALS cases (Vance et al., 2006). FUS is a 526 amino acid nuclear protein that shuttles between the nucleus and the cytoplasm and can bind single- and double-stranded DNA as well as RNA. It has been shown to participate in multiple cellular processes such as DNA repair, axonal transport of mRNA, RNA splicing and transcriptional regulation (Lagier-Tourenne et al., 2010).

Structurally, FUS belong to a family of FET RNA binding proteins which include FUS, Ewing's sarcoma RNA binding protein 1 (EWSR-1) and Tata-binding protein associated factor 2N (TAF-15). The FET protein family interact with the C-terminal domain of RNA polymerase II (RNAP II) and general transcription factor TFIID (Shang and Huang, 2016).

Interestingly, FUS cases are pathologically distinct as they lack TDP-43 pathology. Instead FUS immunoreactive inclusions of varying morphologies are present in the spinal cord of ALS cases with *FUS* mutations (King et al., 2015; Vance et al., 2009). Moreover, 35% of ALS cases with symptom onset <40 years old carry mutations in the *FUS* gene and more than 60% of cases with *FUS* mutations disease onset before 45 years of age, with many juvenile onset in late teens and early 20's (Baumer et al., 2010; Shang and Huang, 2016).

Several groups have used a wide range of animal models to study the effect on expressing FUS mutant proteins. *In vitro* studies have shown that mutations known to cause ALS increase the levels of cytoplasmic FUS by impairing nuclear import and cause it to aggregate and sequester WT-FUS into cytoplasmic stress granules (Dormann et al., 2010; Vance et al., 2013). FUS knockdown using antisense morpholinos in zebrafish cause motor

and behavioural defects and reductions in the branching and length of motor axons. Morpholino knockdown of zebrafish FUS followed by overexpression of mutant human FUS proteins also cause defects in the neuromuscular junction (NMJ) (Armstrong and Drapeau, 2013). Finally, murine models of FUS show that WT-FUS as well as mutant FUS overexpression causes degeneration in mice. FUS-R521C and FUS-R525L cause more severe dendritic outgrowth deficits than WT-FUS (Mitchell et al., 2013). Interestingly, transgenic mice expressing higher levels of WT-FUS also displayed early onset motor neuron degeneration in a dose-dependent manner (Mitchell et al., 2013).

1.4.2 Genes involved in protein homeostasis

1.4.2.1 UBQLN2 (Ubiquilin 2)

Ubiquilins are known to associate with ubiquitin ligases and proteasomes to mediate protein degradation. Ubiquilin 2 is a 66 kDa protein (Zhang et al., 2014a) is highly homologous to Ubiquilin 1, which has been shown to play a role in mediating the ubiquitin proteasome system (UPS) and as a regulator of autophagy (Zhang et al., 2014a). Additionally, UBQLN2 has been linked to cell cycle regulation, to modulate G-protein coupled receptors in endocytosis and it associates with cytoskeletal elements (Zhang et al., 2014a). Five mutations were initially described in the *UBQLN2* gene to cause ALS (Deng et al., 2011). All mutations were shown to be present in the PXX motif of the protein. ALS patients carrying mutations in the *UBQLN2* gene are associated with an early age of onset and survival of 6 months to 5 years from symptom onset (Deng et al., 2011; Gellera et al., 2013).

The pathology of fALS patients with *UBQLN2* mutations and sALS patients is characterised by the presence of ubiquilin 2 and ubiquitin-positive inclusions which also contain TDP-43, Optineurin and FUS. Ubiquilin 2 inclusions have also been found to be present in the molecular layer of the hippocampus of ALS-*C9ORF72* cases regardless of the presence of *UBQLN2* mutations (Brettschneider et al., 2012; Scotter et al., 2016). In some

cases these inclusions colocalised with other important ALS proteins such as TDP-43 and FUS, however, inclusions in the molecular layer of the hippocampus have been shown to be uniquely present in ALS-*C9ORF72* cases (Brettschneider et al., 2012).

Mutations in *UBQLN2* decrease the interaction with another ALS-linked protein, hnRNPA1 (Gilpin et al., 2015) and have been linked to optineurin defects (Osaka et al., 2015). Furthermore, overexpression of ubiquilin-2 causes neuronal death in transgenic rats (Huang et al., 2016). Finally, transgenic mice overexpressing ALS-linked mutant ubiquilin-2 have TDP-43 pathology, loss of motor neurons and impaired memory. Interestingly, only mice expressing the mutant forms of ubiquilin-2 and not WT showed these symptoms (Le et al., 2016).

1.4.2.2 Sequestosome 1/ p62

The *SQSTM1* gene codes for the 440 amino acid protein commonly known as p62, which amongst other functions, plays a critical role in autophagy. P62 binds poly-ubiquitinated proteins though it's ubiquitin-associated (UBA) domain and directs them into lysosomes. Mutations known to cause ALS and FTD were first reported in 2011 (Fecto et al., 2011), since then, over 40 mutations have been identified accounting for 1.5-3% of familial and sporadic ALS/FTD cases (White and Sreedharan, 2016). Most mutations thought to be causative of ALS are missense mutations but the pathogenic mechanism is unclear. *SQSTM1* patients have classical p62- and TDP-43-positive inclusions and increased p62 and TDP-43 levels in the spinal cord (Teyssou et al., 2013). Knockdown of *SQSTM1* in zebrafish causes motor deficits which can be rescued by human WT p62 overexpression, but not by overexpressing human p62 constructs carrying ALS/FTLD-related mutations (Lattante et al., 2015).

1.4.2.3 Valosin-containing protein/P97 (VCP)

The VCP protein is an AAA ATPase involved in an extensive range of ubiquitin-dependent cellular processes that rely on protein degradation via the UPS or autophagy (Majcher et al., 2015). Mutations in the *VCP* gene account for 1-2% of fALS cases (Johnson et al., 2010; Miller et al., 2012) and are found throughout the protein, making predictions about effect on protein-protein interactions challenging (Majcher et al., 2015). Patients carrying *VCP* mutations showed rapid disease progression and cognitive impairment (Johnson et al., 2010).

Mutations in *VCP* have also been found in Paget disease of the bone and frontotemporal dementia (IBMPFD). A mouse model of the disease-associated VCP R155H mutation was found to be show with muscle weakness and brain pathology with increased TDP-43 and ubiquitin-positive cytoplasmic inclusions (Nalbandian et al., 2013). VCP also plays a role in stress granule formation and processing body (P-body) clearance, delivering them to autophagy for degradation. Disease-associated mutations delay this process, highlighting the interconnection between RNA processing and autophagy defects in ALS (Buchan, 2014). Moreover, cortical neurons derived from ALS patients carrying pathogenic mutations in the *VCP* gene show slower rate of ADP/ATP translocation across the mitochondrial and as a result have impaired cellular energy homeostasis (Ludtmann et al., 2017).

1.4.2.4 **Charged multivesicular body protein 2B / *CHMPB2***

Mutations in the *CHMPB2* gene were the first identified in familial form of FTD linked to Chromosome 3 (Skibinski et al., 2015). *CHMP2B* codes for CHMP2B, which belongs to the charged multivesicular body protein family. As a component of the endosomal sorting complex required for transport III (ESCRTIII) multi-protein complex, CHMP2B is involved in vesicular trafficking, autophagy, and dendritic spine formation and functionality (Urwin et al., 2010; Vernay et al., 2016). Subsequently *CHMP2B* mutations have been reported ALS and

may account for up to 1% of fALS cases (Parkinson et al., 2006) (Cox et al., 2010; White and Sreedharan, 2016) but their role in pathogenesis has not been fully determined. ALS patients carrying mutations in the *CHMP2B* gene have a variable age of onset and show the typical ALS neuropathology with p62-positive TDP-43 neuronal inclusions (Cox et al., 2010; Parkinson et al., 2006) but FTD cases contain p62-positive, TDP-43 negative inclusions (Holm et al., 2007). Mice expressing the disease-causing *CHMP2B*^{intron5} show neuronal loss and lysosomal storage pathology in the form of autofluorescent aggregates in a progressive manner (Clayton et al., 2015). A later study showed that mutant mice expressing *CHMP2B*^{intron5} in a neuronal specific manner show a dose dependent disease phenotype, and paralysis (Vernay et al., 2016).

1.4.2.5 Phosphoinositide phosphatase (FIG4)

Mutations in *FIG4* were reported in about 2% of ALS and primary lateral sclerosis patients in a cohort with European ancestry (Chow et al., 2009). Mutations in *FIG4* have also been previously identified in Charcot-Marie-Tooth (CMT) disease (Chow et al., 2007). Patients with mutations had predominantly dysfunction in their upper extremities and show a typical age of onset and disease duration (Chow et al., 2009). FIG4 is a phosphatase that regulates intracellular vesicle trafficking along the endosomal-lysosomal pathway (Kon et al., 2014). Kon *et al.* (2014) reported that FIG4 does not colocalise with TDP-43 immunoreactive inclusions in ALS cases, however, FIG4-positive inclusions were reported in other neurodegenerative diseases such as Parkinson's disease and dementia with Lewy bodies (Kon et al., 2014).

1.4.2.6 VAPB

In 2004, Nishimura and colleagues reported a novel missense mutation in the *VAPB* gene in a large white Brazilian family and caused severe ALS with rapid disease progression (Nishimura et al., 2004). Mutations in the VAPB protein disrupt the cellular distribution and

increase VAPB aggregation (Landers et al., 2008; Nishimura et al., 2004). VAPB interacts with the mitochondrial protein tyrosine phosphatase-interacting protein-51 (PTPIP51) to regulate Endoplasmic Reticulum-mitochondria association and autophagy (De Vos et al., 2012). Interestingly is has been shown that mutations in TDP-43 known to cause ALS, disrupt this contact and decrease the calcium transmission into the mitochondria, mediated by GSK3β activation (Stoica et al., 2014).

1.4.2.7 TBK1

TANK-binding kinase (TBK1) is a kinase involved in the regulation of many cellular pathways, including immune response, inflammation, autophagy, cell proliferation and insulin signalling (Helgason et al., 2013). Nonsense truncation mutations in the *TBK1* gene were first identified in a large ALS kindred and in a large Exome sequencing study (Cirulli et al., 2015). To date, 77 non-synonymous *TBK1* variants have been identified in patients diagnosed with ALS and/or FTD (Freischmidt et al., 2016; Freischmidt et al., 2015). It is thought that pathogenic mutations in *TBK1* may lead to haploinsufficiency and might impair the regulation of autophagy and/or inflammation signalling pathways regulated by TBK1. Furthermore, mutations in genes encoding two other components of the autophagic pathway interact with and are activated by TBK1; OPTN and SQTM1/p62 are also associated with ALS. Interestingly, a single patient with FTD carrying TBK1 and OPTN mutations resulting in a haploinsufficiency of both proteins has been identified (Pottier et al., 2015). This patient showed late age of onset (68 years) but fast disease progression, suggesting that a more severe disease pattern may arise if this pathway is severely disrupted.

1.4.2.8 Optineurin (OPTN)

Optineurin is a ubiquitin-binding protein that interacts with LC3, regulates autophagy and also plays a role in the turnover of damaged mitochondria (Majcher et al., 2015). Mutations in the *OPTN* gene that codes for Optineurin were first identified to cause

ALS in a small Japanese population (Maruyama et al., 2010) and are known to account for 1-4% of fALS cases (Iguchi et al., 2013a) but are absent from FTD cases (Maruyama et al., 2010). Optineurin-positive immunoreactive inclusions have been reported in sALS and *SOD1*-ALS cases (Maruyama et al., 2010). Interestingly, TBK1 is known to regulate Optineurin activity by phosphorylating it. The crystal structure of the TBK1-Optneurin complex has been resolved predicting that the ALS linked E696K TBK1 mutation disrupts the TBK1-Optneurin complex but has little effect on the NAP1/TBK1 complex (Li et al., 2016a).

1.4.3 Other Genes involved in RNA metabolism

In this section we review some of the most important genes involved in RNA binding and processing that have been identified in ALS cases in addition to TDP-43 and FUS.

1.4.3.1 ELP3

The elongator protein 3 (ELP3) protein is involved in the RNA polymerase II complex and RNA processing (Winkler et al., 2001). Mutations in the *ELP3* gene were identified in ALS by carrying out an association study in UK, USA and Belgian populations (Simpson et al., 2009). This group carried out a mutagenesis screen, where they found out that drosophila carrying two loss-of-function mutations in the ELP3 protein displayed axonal targeting and synaptic transmission deficits. Furthermore they showed that zebrafish showed axonal motor abnormalities when ELP3 levels where decreased using a morpholino in a dose-dependent manner (Simpson et al., 2009). Simpson *et al.* (2009) showed that the expression of ELP3 was decreased in ALS patients carrying risk-associated alleles. The mechanism through which ELP3 leads to motor neuron disease remains unknown but it appears that mutations in the *ELP3* gene may modulate the susceptibility to ALS.

1.4.3.2 SETX

SETX encodes a DNA/RNA helicase involved In DNA repair and RNA production. Mutations in the *SETX* gene were found to cause juvenile onset, slowly progressive ALS, with

a disease onset at <25 years, distal muscle weakness and atrophy, preserved sensation and a normal life span (Chen et al., 2004). Homozygous and compound heterozygous mutations in the *SETX* gene were subsequently identified in people with ataxia with oculomotor apraxia type 2 (Moreira et al., 2004).

1.4.3.3 ATXN2 (Ataxin-2)

Ataxin-2 is an RNA-binding protein containing 15-32 CAG repeats in exon 1 that are translated into poly glutamine (poly-Q) repeats in healthy individuals. However it has been shown that the presence of 33-64 CAG repeats can cause spinocerebellar ataxia type 2 (SCA2). Elden *et al.* (2010) found that intermediate-length expansions of 27-33 CAG repeats in Ataxin-2 confer a significant risk for ALS and are present in 4.7% of all ALS cases (Elden et al., 2010). This finding has been replicated by several other groups (Baumer et al., 2014; Borghero et al., 2015).

ALS patients carrying intermediate Ataxin-2 expansions show immunoreactive Ataxin-2 cytoplasmic aggregates in the spinal cord and have a distinct TDP-43 pathology. The motor neurons of ALS cases with Ataxin-2 poly-Q expansions contained primarily skein-like or filamentous TDP-43 pathology and only rarely, if ever, contained large round inclusions, whereas the ALS cases without Ataxin-2 poly-Q expansions contained abundant round and skein-like TDP-43 pathology (Elden et al., 2010; Hart et al., 2012).

Moreover, recent work has shown that the RNA-dependent interaction of Ataxin-2 and TDP-43 is involved in disease pathogenicity (Hart et al., 2012). Furthermore, Ataxin-2 interacts with FUS and enhances FUS-related pathology (Farg et al., 2013). Finally, it has been recently reported that the Ataxin-2 locus can be bi-directionally transcribed. Ataxin-2 antisense transcripts (*ATXN2-AS*) with CUG repeats are neurotoxic and may also contribute to the disease pathogenicity (Li et al., 2016b). Interestingly, knockout of Ataxin-2 with

antisense oligonucleotides significantly improves survival in TDP-43 transgenic mice (Becker et al., 2017).

1.4.3.4 hnRNP A2/B1 and hnRNP A1

Mutations in *hnRNP A2/B1* and *hnRNP A1* were identified by Kim *et al.* (2013) in patients with inclusion body myopathy with Paget's disease of the bone (IBMPFD) and ALS. Patients carrying mutations in these genes showed hnRNP A2/B1 /hnRNP A1-positive cytoplasmic inclusions and normal TDP-43 pathology. Mutations present in these two genes were centred within the prion-like domains of the proteins. Mutated proteins were shown to have enhanced fibrillisation and were recruited into stress granules, cytoplasmic aggregates and colocalised with TDP-43 inclusions (Kim et al., 2013).

Patient motor neurons differentiated from induced pluripotent stem cells (iPSC-MNs) carrying the ALS-associated hnRNP A2/B1 D290V mutation had abnormal splicing changes, likely due to increased nuclear-insoluble hnRNP A2/B1. Mutant iPSC-MNs also displayed decreased survival in long-term culture and exhibiting hnRNP A2/B1 localization to cytoplasmic granules (Martinez et al., 2016).

1.4.3.5 MATR3

MATR3 encodes a nuclear DNA/RNA-binding protein that interacts with TDP-43 and regulates the alternative splicing of a large amount of genes (Coelho et al., 2015). Mutations in *MATR3* were identified by exon sequencing of a family of European ancestry with dominantly inherited ALS and dementia. *MATR3* cases show heterogeneous phenotypes; one mutation is associated with slow progressing ALS while another presented with classical, rapidly progressing ALS (Johnson et al., 2014). Johnson *et al.* (2014) showed that MATR3 is localised in the nucleus of motor neurons in control individuals but it is occasionally found in the cytoplasm of ALS cases. They hypothesized that ALS-causing mutations in *MATR3*

increased its affinity with TDP-43 and aggregates were identified in a skeletal muscle biopsy from an ALS patient carrying a MATR3 S85C mutation (Johnson et al., 2014).

1.4.3.6 GLE1

Recent candidate screening of *GLE1* in 173 fALS and 760 sALS cases identified novel nonsense and missense mutations in two sALS cases and a splice site mutation in a fALS case (Kaneb et al., 2015). These mutations failed to rescue motor neuron pathology in zebrafish lacking GLE1, indicating pathogenicity though a loss of function/ haploinsufficiency mechanism (Kaneb et al., 2015). GLE1 has important roles in translation initiation, termination and some isoforms have been shown to associate with stress granules. Interestingly, GLE1 localises to the nuclear pore complex and can shuttle between the nucleus and the cytoplasm (Kaneb et al., 2015; White and Sreedharan, 2016), an area of great interest currently in the field of ALS.

1.4.4 Other genes involved in ALS

1.4.4.1 ALS2

Mutations in the *ALS2* gene cause the autosomal recessive juvenile-onset form of ALS (ALS2). ALS2 is a rare form of ALS, characterised by symptom onset in the 20's and slowly progressing disease (Hadano et al., 2001). *ALS2* codes for a guanine nucleotide exchange factor, which activates GTPases to regulate endosomal trafficking. Deletion mutations identified result in a frame shift that generates premature stop codons (Hadano et al., 2001). These mutations are predicted to cause a loss of protein function. Interestingly, simultaneous deletion of SQSTM1 and ALS2 in *SOD1* H46R mice resulted in accelerated disease onset (Hadano et al., 2016).

1.4.4.2 PFN1

Exome sequencing of two large families suffering from ALS showed the presence of mutations within the profiling 1 (*PFN1*) gene. PFN1 is crucial for the conversion of monomeric (G)-actin to filamentous (F)-actin. Exome sequencing of two large ALS families showed different mutations within the PFN1 gene. Further sequence analysis identified 4 mutations in 7 out of 274 fALS cases. Cells expressing PFN1 mutants contain ubiquitinated, insoluble aggregates that in many cases contain the ALS-associated protein TDP-43 (Wu et al., 2012). Transgenic mice expressing ALS-linked C71G mutant PFN1 display progressive motor neuron loss, unlike those expressing WT PFN1. The authors of this study suggested the mutation in the PFN1 caused motor neuron degeneration through gain-of-function toxicity. Mutant, but not wild-type, PFN1 forms insoluble aggregates, disrupts cytoskeletal structure, and elevates ubiquitin and p62 levels in motor neurons in these mice (Yang et al., 2016a).

1.4.4.3 TUBA4A

Only recently, Smith and colleagues (2016) have identified the presence of five non-synonymous pathogenic mutations in the gene encoding the Tubulin, Alpha 4A protein (TUBA4A). Mutations were identified by carrying exon-wide rare burden analysis in 363 fALS index cases. All patients carrying *TUBA4A* mutations presented with spinal onset ALS with upper and lower motor neuron signs and two cases showed cognitive decline consistent with a diagnosis of FTD (Smith et al., 2014). This study also demonstrates the power of collecting exon capture data from fALS index cases and collecting them together in order to discover new pathogenic mutations (Smith et al., 2014). Mutations identified in *TUBA4A*, together with those in *PFN1*, highlight the role of axonal transport and the cytoskeletal in ALS.

1.4.4.4 NEK1

NIMA-related kinase 1 (NEK1) is a ubiquitously expressed, multifunctional kinase involved in many cellular activities including DNA damage response, microtubule stability,

neuronal morphology and axon polarity (Kenna et al., 2016). Interestingly, NEK1 is also known to interact with two known ALS-related proteins; Alsin and VAPB (White and Sreedharan, 2016). Loss of function mutations in the *NEK1* gene were first identified as a minor hit by Cirulli and colleagues (Cirulli et al., 2015) but have since been confirmed by two individual studies by exon sequencing that analysed 265 and 1022 index fALS cases (Brenner et al., 2016; Kenna et al., 2016). In total, Kenna and colleagues (2016) identified *NEK1* variants in almost 3% of ALS cases (Kenna et al., 2016).

1.5 MECHANISMS OF PATHOGENESIS

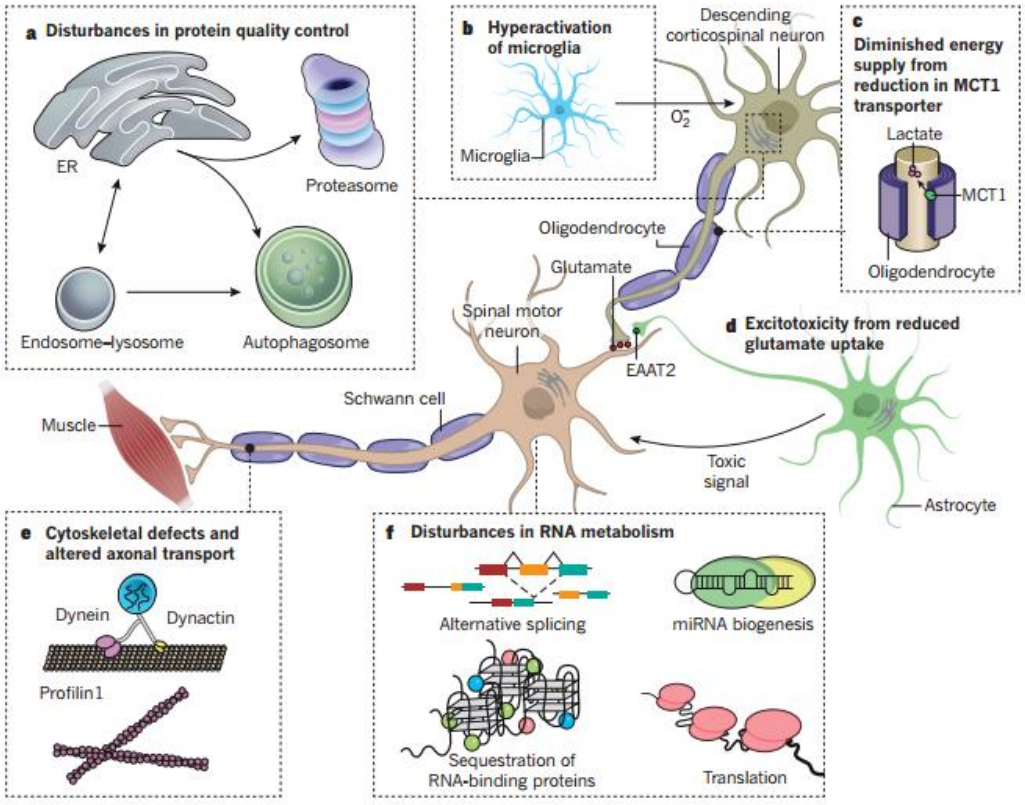

Figure 1.2: Summary of the main cellular mechanisms affected in ALS (adapted from (Taylor et al., 2016))

1.5.1 Failure of the proteasome degradation pathways

As with most neurodegenerative conditions, a hallmark feature of ALS is the presence of pathological protein aggregates in affected tissues. In addition a large number

of ALS mutant genes play a vital role in protein quality control, trafficking and degradation maintaining protein homeostasis, (*VCP*, *UBQLN2*, *OPTN* and *TBK1*). This indicates that defective proteostasis is a key pathogenic mechanism (Blokhuis et al., 2013).

The aggregation of mutant proteins in ALS is well-documented. Mutant SOD1 has been shown to misfold and adopt a conformation to prevent ubiquitin-mediated degradation (Niwa et al., 2007). Mutant SOD1 forms toxic oligomers (Urushitani et al., 2002), which further accumulates as aggregates to induce a stress response in cells (Atkin et al., 2006). The oxidation of WT SOD1 also leads to misfolding and aggregation of the protein in a similar fashion to mutant SOD1. Aggregation of SOD1 has toxic effects on two major protein degradation pathways, the UPS and autophagy.

Similarly, TDP-43 and FUS form insoluble protein aggregates in ALS and FTD but are also present in other neurodegenerative disorders such as Alzheimer's, Parkinson's and Huntington's disease (Neumann et al., 2006; Vance et al., 2009). Mutant TDP-43 and FUS are recruited into cytoplasmic stress granules upon stress. Stress granules are normally resolved by disaggregases and chaperones; however, it is thought that mutant TDP-43 and mutant FUS aggregate with stress granule components in an irreversible manner to give rise to pathological inclusions (Chen et al., 2016; Vance et al., 2013). This may be mediated by mislocalisation from the nucleus to the cytoplasm of the mutant protein and the prion-like domain within the protein structure of TDP-43 and FUS (Hock and Polymenidou, 2016).

1.5.2 RNA metabolism

The first link between alterations in RNA processing and motor neuron degeneration was described over a decade ago. The expression of a neurofilament transgene was found to affect binding of a ribonucleoprotein to the neurofilament mRNA and lead to the degeneration of enteric and motor neurons in transgenic mice (Canete-Soler et al., 1999). The discovery of disease-linked mutations in multiple RNA binding proteins has highlighted

dysfunctional RNA processing as a major pathogenic pathway in ALS (Kwiatkowski et al., 2009; Sreedharan et al., 2008; Vance et al., 2009). Pathological, as well as *in vitro* and *in vivo* studies, have provided evidence of abnormalities in multiple steps of RNA processing, including transcription, splicing, translation and decay (Baloh, 2012). Mutations present in *TARDBP*, the gene encoding for TDP-43, and *FUS*, both coding for RNA binding proteins with hundreds of target transcripts highlight the importance of dysregulated RNA metabolism. Knock-down of TDP-43 and FUS affects the level of thousands of transcripts (Lagier-Tourenne et al., 2012).

1.5.3 Axonal dysfunction

Motor neurons are characterised by a unique morphology. These cells are highly polarised, typified by axonal projections that can reach a meter in length in adult humans. This morphology requires active axonal transport of organelles, cytoskeletal, synaptic components, and trophic factors to maintain normal cellular function. Axonal transport defects have been shown to occur in pre-symptomatic stages of disease in animal models of motor neuron disease, and the selective loss of neuromuscular synapse subtypes are believed to precede motor neuron degeneration (Frey et al., 2000). The accumulation of neurofilaments in the soma and axons of motor neurons in the spinal cord constitutes one of the pathological hallmarks in ALS (Hirano et al., 1984). Additionally, the loss of the neuromuscular junction is common in patients and mouse models of the disease (Mitchell et al., 2015) and ALS-causing mutations in TDP-43 also affect axonal transport in iPSC-derived neurons (iPSN) (Alami et al., 2014).

1.5.4 Mitochondrial dysfunction

Evidence for mitochondrial involvement in ALS was first identified when ultrastructural studies revealed an increase in the number of mitochondria in myelinated axons (Atsumi, 1981). Dysfunctional mitochondria have also been observed in transgenic

mice overexpressing the G93A SOD1 mutant. The presence of mutant SOD1 aggregates correlates with mitochondrial vacuolar degeneration in G93A SOD1 mice (Dal Canto and Gurney, 1995; Wong et al., 1995). Transgenic mice expressing TDP-43 also display mitochondrial abnormalities, such as mitochondrial aggregation, and develop impaired motor function (Xu et al., 2010). Mitochondrial dysfunction may lead to apoptosis through the release of cytochrome-C into the cytoplasm.

1.5.5 Excitotoxicity

Levels of glutamate, one of the main neurotransmitters in the central nervous system (CNS), have been shown to be elevated in the cerebrospinal fluid (CSF) of ALS patients (Shaw et al., 1995a). Moreover, knock down of metabolic glutamate receptor 1 in G93A SOD1 mice extends survival and increase the number of motor neurons (Milanese et al., 2014). SOD1 fALS mutations inhibit the function of excitatory amino acid transporter-2 responsible for glutamate uptake (Trotti et al., 1999). Additionally, iPSN derived from *C9ORF72* expansion carriers show an increased susceptibility to glutamate toxicity (Donnelly et al., 2013). Finally, Riluzole, the only licensed drug for ALS, reduces excitotoxicity through the inhibition of pre-synaptic glutamate release (Cheah et al., 2010).

1.5.6 Oxidative stress

Oxidative stress arises from the imbalance in the production of reactive oxygen (ROS) and reactive nitrogen (RNS) species and their clearance by the cell. ROS are important signalling molecules necessary for a range of physiological processes. However, excessive production of ROS causes damage of biomolecules interfering with their normal functions and leading ultimately to cellular dysfunction or even death.

There is strong evidence showing that oxidative stress may be a contributing factor in the pathogenesis of ALS. Spinal cord samples from ALS patients contain higher levels of oxidative damage markers and free radicals (Ihara et al., 2005; Shaw et al., 1995b).

Most of *in vivo* studies assessing the effect of oxidative stress in ALS have been carried out in the G93A SOD1 mice. The same oxidative stress makers seen to be upregulated in ALS patients have been reported in the spinal cord and cortex of G93A SOD1 transgenic mice (Ferrante et al., 1997). Finally, a recent study has proposed that some DPRs translated from the G4C2 expansion may also induce oxidative stress in iPSC-MNs derived from *C9ORF72* expansion carriers (Lopez-Gonzalez et al., 2016).

1.5.7 Nucleocytoplasmic transport

The efficacy of nucleocytoplasmic transport has been shown to deteriorate significantly during aging (D'Angelo et al., 2009) and studies using iNeurons show that it is particularly affected in neurons derived from old people compared to younger ones (Mertens et al., 2015a). The presence of cytoplasmic aggregates of FUS and TDP-43 are the main pathological hallmark of 98% of ALS cases. Although TDP-43 and FUS are known to shuttle between the nucleus and the cytoplasm, they are mainly nuclear proteins. The existence of cytoplasmic aggregates therefore highlights the possibility of the nucleocytoplasmic transport of proteins may be dysregulated in ALS (Boeynaems et al., 2016b; Dormann and Haass, 2011).

Most pathogenic *FUS* mutations affect its nuclear localisation signal (NLS) and interfere with proper nuclear targeting (Dormann et al., 2010; Vance et al., 2013). Interestingly, the nuclear/cytoplasmic ratio of different FUS mutants inversely correlate with the age of onset in FUS-ALS patients (Dormann et al., 2010). Independently of the amino acid sequence, the methylation of the FUS NLS also perturbs its nuclear targeting and increases its affinity to transportin (Dormann et al., 2012; Suarez-Calvet et al., 2016).

Moreover, a large group of proteins implicated in nucleocytoplasmic transport, the karyopherins, have been shown to be misregulated in ALS and FTD (Nishimura et al., 2010) and a recent study has shown that the presence of cytoplasmic protein aggregates may

interfere with the nucleocytoplasmic transport process (Woerner et al., 2016). Interestingly, DPRs translated from the G4C2 expansion, together with expanded RNA, have also been shown to affect the nucleocytoplasmic transport in several ways which will be reviewed in greater detail later (Boeynaems et al., 2016a; Jovicic et al., 2015; Zhang et al., 2015; Zhang et al., 2016b).

Despite the importance of nucleocytoplasmic transport in aging and ALS pathology, genes regulating nucleocytoplasmic transport have not been strongly implicated in the genetics of the disease. The only exception is *GLE1*, where mutations have been linked to ALS cases and GLE1 knockdown in zebrafish causes motor neuron deficits that can be rescued by wildtype but not mutant Gle1 (Kaneb et al., 2015).

1.5.8 Neuro-inflammation

Another of the main pathological hallmarks of ALS is the presence of activated microglia and infiltrated lymphocytes in the main sites of neurodegeneration (Engelhardt and Appel, 1990). Research using positron emission tomography has provided direct evidence of microglial activation in the brains of living patients with ALS. The intensity of microglial activation was correlated with the severity of disease, suggesting an active involvement of microglial activation in ALS throughout the disease process (Turner et al., 2004). Microgliosis and inflammation have been demonstrated in mutant G93A SOD1 mice and ALS cases. ALS patients contain elevated levels of proinflammatory molecules such as cytokines, reactive oxygen species, chemokines, and glutamate (Komine and Yamanaka, 2015). However it still remains unclear whether the presence of M2, protective microglia and M1, neurotoxic microglia are a response to the loss of neurons of actively contribute to neurodegeneration (Henkel et al., 2009).

Finally, it has been shown that *C9ORF72* KO mice show increased microglia activation, possibly indicating that the G4C2 expansion may be causing a decrease in the levels of C9ORF72 protein and increasing neuroinflamation (O'Rourke et al., 2016).

1.6 MODELLING ALS AND FTD WITH IPSCS

In 2006 a study published by the Yamanaka group showed that mouse fibroblasts could be reprogrammed to become induced embryonic stem cells (ESC) following the expression of only four transcription factors, *OCT3/4*, *KLF4*, *c-MYC* and *SOX2,* now known as the "Yamanaka factors" (Takahashi and Yamanaka, 2006). These cells were capable of differentiation into a wide range of tissues and contribute to chimeric mice. Soon after the same group reprogrammed human fibroblasts into induced pluripotent stem cells (iPSCs) (Takahashi et al., 2007). Pluripotent cells have the ability to be differentiated into any type of cell, including neurons and glia. This technology has facilitated the generation of iPSCs from ALS patients carrying mutations in the *SOD1*, *TARDBP*, *C9ORF72*, *FUS* and *VCP* genes. Studies in these lines have yielded valuable information about the disease patho-mechanism and raised the prospect of utilising these lines for drug discovery purposes. Interestingly, a study in iPSCs derived from Alzheimer's disease (AD) patients are resistant to therapeutically relevant concentrations of NSAID-based GSMs that failed in clinical trials but had an effect on mouse models of the disease (Mertens et al., 2013). Moreover, iPSC-derived neurons from patients with bipolar disorder are responsive to therapeutically relevant lithium levels in the culture medium (Mertens et al., 2015b). These results highlight the potential use of iPSC-derived neurons in order to test potential therapeutic strategies.

iPSCs derived from fibroblasts carrying mutations in the *SOD1* gene were the first to be generated carrying an ALS-causing mutation showing that iPSCs from ALS patients could be differentiated into motor neurons (SOD1-iPSMN) (Dimos et al., 2008). Several studies

have followed showing that spinal motor neurons derived from ALS-*SOD1* patients display neurofilament aggregation and neurite degeneration. These changes were reversed in one of the cell lines by genetic modification using transcription activator-like effector nuclease (TALEN) technology (Chen et al., 2014). A recent study has shown that *SOD1*-iPSMNs show loss of excitability and increased ER stress. These deficits were reversed upon treatment of the FDA approved drug 4-aminopyridine (Naujock et al., 2016). Finally it has been shown that genetic correction of *SOD1* mutant iPSCs using clustered regularly interspaced short palindromic repeats (CRSIPR)-Cas9 mediated gene editing revealed that ERK and JNK activated AP1 played an important role in ALS (Bhinge et al., 2017). This is one of the first studies that utilises CRISPR technology to remove a pathogenic mutation in ALS iPSCs.

Several groups have derived iPSCs by reprograming fibroblasts from ALS patients carrying mutations in the *TARDBP* gene which encodes for TDP-43. iPSC-derived motor neurons (iPSC-MNs) generated from these lines show increased levels of detergent insoluble TDP-43 and decreased motor neuron survival, two key pathological features of ALS (Bilican et al., 2012). The increased levels of detergent insoluble TDP-43 were partially reversed by allele specific knockdown of the mutant allele in neuronal progenitor cells carrying the mutation (Nishimura et al., 2014). A separate study reported decreased levels of total TDP-43, increased levels of cytoplasmic TDP-43 levels as well us downregulation of miRNA9 in iPSC-MNs carrying TDP-43 mutations (Zhang et al., 2013). Finally, iPSC-MNs carrying TDP-43 mutations have also been reported to show cytoplasmic TDP-43 aggregates and increased levels of detergent insoluble TDP-43. The authors of this study showed that the phenotypes could be reversed with the histone acetyl transferase inhibitor anacardic acid (Egawa et al., 2012). This is another example of the potential of iPSC-derived neurons for drug discovery.

The hexanucleotide repeat G4C2 repeat present in the *C9ORF72* gene is the most common cause of fALS and a number of iPSC lines have been generated and have made

important contributions to our understanding of disease mechanisms. All groups have reported the presence of intranuclear RNA foci which sequester a number of RNA binding proteins such as hnRNP-H or ADARB2 in iPSC-derived neurons from *C9ORF72* expansion carriers, but the presence of DPR has not been consistent. These studies have reported several different additional phenotypes which include: elevated p62 levels and dysfunctional proteasome system (Almeida et al., 2013), increased toxicity to glutamate-induced stress (Donnelly et al., 2013), diminished capacity to fire continuous spikes upon depolarization (Sareen et al., 2013), hypermethylation of the *C9ORF72* promoter (Esanov et al., 2016), decreased neurite (Burguete et al., 2015) and axonal outgrowth (Sivadasan et al., 2016), altered ER calcium homeostasis and increased cell death (Dafinca et al., 2016), mitochondrial stress and DNA damage (Lopez-Gonzalez et al., 2016), decreased levels of *C9ORF72* transcript and protein levels (Aoki et al., 2017) and nucleocytoplasmic transport deficits (Zhang et al., 2015). Interestingly one study has shown how iPSN carrying TDP-43 mutations or *C9ORF72* expansion show hyperexcitability followed by loss of action potential output and activity at the synapse (Devlin et al., 2015). Some of these deficits have been reversed with antisense oligonucleotides (Aoki et al., 2017; Donnelly et al., 2013; Sareen et al., 2013; Zhang et al., 2015) and will be reviewed in greater detail in the following section. Once again, it highlights the potential of iPSC-derived neurons to be used as a drug screening tool.

Finally iPSCs have also been derived from ALS patients carrying *FUS* and *VCP* mutations as well as from sALS patients. Several independent groups have shown that iPSN harbouring mutations in the *FUS* gene show increased levels of mislocalised cytoplasmic FUS that is localised into stress granules (Higelin et al., 2016; Ichiyanagi et al., 2016; Lenzi et al., 2015). These deficits were reversed by removal of the pathogenic mutations using TALEN (Lenzi et al., 2015) and CRISPR-Cas9 (Ichiyanagi et al., 2016) genome editing techniques. Moreover, cortical neurons carrying pathogenic mutations in the *VCP* gene show slower rate of ADP/ATP translocation across the mitochondrial membrane and as a result have impaired cellular

energy homeostasis (Ludtmann et al., 2017). Interestingly, astrocytes derived from sALS-iPSCs transplanted into the spinal cord of mice induced motor neuron loss (Qian et al., 2017). Motor neurons differentiated from multiple sALS-iPSCs showed cytoplasmic TDP-43 aggregates. These cell lines apparently carried no mutations known to be implicated in ALS. TDP-43 aggregation was subsequently identified in post-mortem tissue of one of the patients from which the iPSCs were derived (Burkhardt et al., 2013), highlighting that iPSC-derived neurons are an exciting tool by which to model disease.

The use of iPSC-derived neurons to study FTD has also been explored by deriving iPSCs from sporadic FTD and FTD patients carrying pathogenic mutations in the *PGRN* gene encoding progranulin. Comparison between sporadic FTD and *PRGN* neurons showed varying levels of progranulin and contrasting sensitivity to cellular stressors such as kinase inhibitors. Consequently iPSN were used for the validation of small molecules with potential to reverse these deficits (Lee et al., 2014b). A separate study has shown that behavioural variant FTD patient derived neuronal cultures display altered levels of AMPA receptors and miRNA-124 (Gascon et al., 2014).

1.7 CHROMOSOME 9 OPEN READING FRAME 72 (*C9ORF72*)

In this section I will review the main cellular and pathogenic finding of how the expansion in the *C9ORF72* gene may contribute to the pathophysiology of ALS.

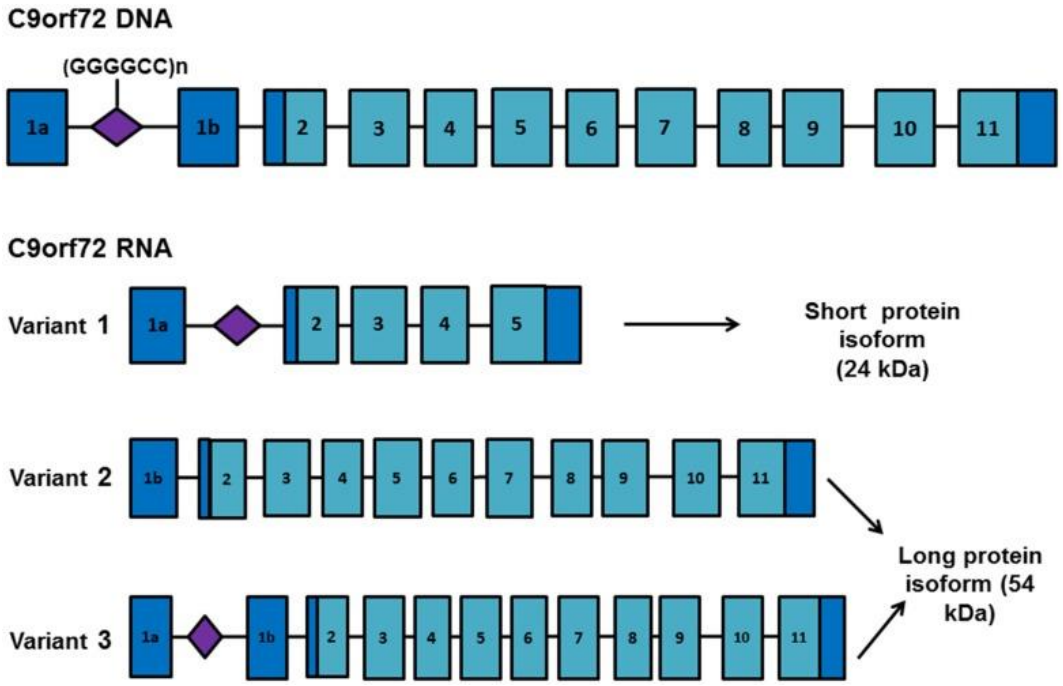

Figure 1.3: Schematic representation of the *C9ORF72* gene and transcript variants (adapted from Barker et al., 2017)

1.7.1 Genetics of the expansion, methylation and genomic instability

In 2011 two groups independently reported the discovery of an intronic hexanucleotide expanded repeat of GGGGCC repeat between the first alternative exons of the *C9ORF72* gene (DeJesus-Hernandez et al., 2011; Renton et al., 2011). Only 2-20 repeats are found in healthy individuals, in contrast between 50 and 3,000 repeats have been identified in ALS and FTD cases. The expansion which is known to cause 20-40% of all fALS cases of European ancestry was thought to have multiple origins that arose about 300-13,000 years ago (Fratta et al., 2015; Smith et al., 2013) and has strikingly low presence is Asian populations (Majounie et al., 2012).

The genomic region around the expanded repeat is unstable as the size of the expansion has been shown to vary widely in different tissues and even different brain regions on Southern blots. Expansion sizes are shorter in white blood samples and the cerebellum compared to the frontal cortex of ALS and FTD patients (van Blitterswijk et al., 2013). In some

cases, expansion size in white blood cells was up to 40 times shorter than in neuronal tissue in the same patient (Nordin et al., 2015). Some studies report that the number of repeats detected in the frontal cortex of ALS and FTD patients correlates with age of onset (van Blitterswijk et al., 2013) and that there is an inverse correlation between the number of G4C2 repeats and disease duration (Suh et al., 2015).

G4C2 repeats can form secondary structures like G-quadruplexes, R-Loops from the sense strand (Fratta et al., 2012; Haeusler et al., 2014) and i-motifs and protonated hairpins from the antisense strand *in vitro* (Kovanda et al., 2015). The presence of G-quadruplexes has been also confirmed in G4C2 repeat-expressing cells and ALS post-mortem tissue (Conlon et al., 2016a). Moreover, *in vitro* studies have shown that the processing of R-loops formed by the expansion increases cellular stress (Reddy et al., 2014). The formation of secondary structures is essential for the initiation of repeat associated non-ATG (RAN) translation and for the formation of RNA foci and sequestration of RNA-binding proteins (Zamiri et al., 2014; Zhang et al., 2015). G-quadruplexes can be disrupted with TMPYP4, reducing the ability of repeats to form intranuclear RNA foci and bind RNA-binding proteins (Zamiri et al., 2014; Zhang et al., 2015). Interestingly, TDP-43 has also been shown to have the ability to bind G-quadruplexes (Ishiguro et al., 2016).

Hypermethylation of the CpG islands 5' of the expansion repeat has been extensively reported and is thought to play a neuroprotective counter mechanism in both ALS (Xi et al., 2013) and FTD (Liu et al., 2014a; Xi et al., 2014) and the expansion itself is hypermethylated (Xi et al., 2015a). The G4C2-expansion was found to be generally methylated in unrelated carriers of alleles >50 repeats (97 %), while small (<22) and intermediate (22-90) repeats are unmethylated in ALS and FTD cases (Xi et al., 2015b). Methylation of the G4C2 repeats alters the secondary structure and influences the affinity of binding to RNA-binding proteins (Zamiri et al., 2015). Neuropathological studies have shown that *C9ORF72* cases with higher

methylation of the *C9ORF72* promoter have less RNA foci and DPR levels. Furthermore, demethylation of mutant *C9ORF72* promoter with 5-aza-deoxycytidine resulted in increased vulnerability of mutant cells to oxidative and autophagic stress (Liu et al., 2014b).

1.7.2 Role of the C9ORF72 protein

At the time of discovery, little was known about the expression pattern and role of the C9ORF72 protein. Bioinformatics analysis revealed that there are two isoforms of the C9ORF72 protein; a short (S-C9ORF72) form including exons 2-5 and a long (L-C9ORF72) form including exons 2-11 (Figure 1.3). C9ORF72 has been linked to the regulation of autophagy by several independent studies. One of them showed that C9ORF72 interacts with Rab1 and the ULK1 complex to regulate autophagy. Furthermore, they showed that iNeurons derived from expansion carriers had low levels of autophagy (Webster et al., 2016). Moreover, two independent studies showed that the C9ORF72 protein interacts with a poorly characterised protein called SMCR8 and regulates autophagy through that pathway too (Amick et al., 2016; Yang et al., 2016b). In motor neurons the C9ORF72 protein has been shown to interact with cofilin and regulate actin dynamics (Sivadasan et al., 2016) and to regulate stress granule formation and its depletion results in increased sensitivity to cellular stress (Maharjan et al., 2016).

In mice, the C9orf72 protein can be observed in synaptic puncta in neurons (Atkinson et al., 2015), however depletion of the C9orf72 protein in KO mouse models does not cause neurodegeneration and instead splenomegaly and disturbed microglia and macrophage function is observed (Atanasio et al., 2016; O'Rourke et al., 2016). Interestingly, many of the pathways dysregulated in *C9orf72* KO mice are also dysregulated in *C9ORF72* patients (O'Rourke et al., 2016). Neuropathological studies have shown that the L-C9ORF72 shows diffuse cytoplasmic staining while S-C9ORF72 shows specific labelling around the nuclear envelope. Co-immunoprecipitation experiments revealed an interaction of the C9ORF72

isoforms with both Importin β1 and Ran-GTPase, components of the nuclear pore complex (Xiao et al., 2016). Thus, a reduction in levels of the C9orf72 protein due to the expanded allele may affect nucleocytoplasmic transport.

1.7.3 Neuropathological features of ALS and FTD C9orf72 expansion carriers

The TDP-43 pathology observed in *C9ORF72* ALS, FTD and ALS/FTD is indistinguishable from sporadic cases (Murray et al., 2011). ALS and FTD cases carrying the *C9ORF72* expansion have a highly distinct P62 (Al-Sarraj et al., 2012) and Ubiquilin-2 pathology in the cerebellar granular layer and the hippocampal molecular layer. This pathological signature is enough to predict the presence of the expansion from port mortem tissue (Brettschneider et al., 2012). Additionally, neuroimaging studies of *C9ORF72*-FTD patients have revealed that these patients have altered connectivity networks (Lee et al., 2014a). C9ORF72 protein levels are decreased in post mortem samples of the motor, frontal and temporal cortex but not in the cerebellum or the spinal cord of *C9ORF72* expansion carriers compared to controls. The generation of isoform specific antibodies revealed that S-C9ORF72 is enriched in the temporal and frontal cortex of *C9ORF72* expansion carriers (Waite et al., 2014; Xiao et al., 2016).

Furthermore, sense and antisense RNA foci are common in the brain and spinal cord of ALS and FTD cases (DeJesus-Hernandez et al., 2017; Mizielinska et al., 2013). Sense RNA foci colocalise with many RNA-binding proteins such as hnRNPA3, ALEYREF or hnRNP-H (Cooper-Knock et al., 2014a; Lee et al., 2013; Mori et al., 2013b). RNA foci are mostly present in the nucleus and cytoplasm of neuronal cells, although they have also been detected in oligodendrocytes, microglia and astrocytes (Mizielinska et al., 2013; Gendron et al., 2013). In the frontal cortex, hippocampus and cerebellum of FTD patients there are a greater number of cells containing sense than antisense RNA foci (Mizielinska et al., 2013). Moreover, sense RNA foci are also present in the spinal cord of ALS and FTD cases and there are a significantly

larger number of sense foci in the spinal motor neurons than hippocampal granular neurons (Cooper-Knock et al., 2014a).

Antisense foci are also present in the frontal cortex, hippocampus, cerebellum and spinal cord of ALS and FTD cases and the number of antisense foci in the motor neurons of ALS patients has been reported to correlate with TDP-43 proteinopathy and bind similar RNA binding proteins than sense foci such as hnRNP-H or ALEYREF (Cooper-Knock et al., 2015). This report suggests that the number of antisense RNA foci in spinal motor neurons correlates with the nuclear depletion of TDP-43 (Cooper-Knock et al., 2015).

The sense and the antisense strand of the G4C2 expansion can be can be translated though non-ATG repeat-associated (RAN) translation yielding five different DPR proteins (poly-GP, GA, GR, PA and PR) which accumulate in the brain and spinal cord of ALS and FTD patients and are largely absent from peripheral tissues (Ash et al., 2013; Gendron et al., 2013; Mori et al., 2013a; Mori et al., 2013c; Zu et al., 2013). It was initially reported that *C9ORF72* ALS and FTD cases contained large numbers of p62 positive/ TDP-43 negative inclusions in the hippocampus and the cerebellum (Al-Sarraj et al., 2011), these inclusions where later identified as containing DPR protein aggregates as well as hnRNP A3 (Mori et al., 2013b; Mori et al., 2013c).

The pattern of DPR pathology is highly consistent amongst cases regardless of their ALS or FTD clinical phenotype with a high DPR load in the cerebellum, the neocortical regions and the hippocampus while moderate in the subcortical regions (Mackenzie et al., 2013a). Interestingly soluble and inclusions from all DPRs are almost absent from the spinal cord of ALS cases (Gomez-Deza et al., 2015; Mackenzie et al., 2015) and the presence of DPR protein inclusions does not correlate with neurodegeneration (Davidson et al., 2016). DPR protein aggregates frequently colocalise with p62 (Mann et al., 2013) but rarely colocalise with TDP-43 (Gomez-Deza et al., 2015) and never with pTDP-43 (Mori et al., 2013c). Different DPRs

occasionally colocalise together (Zu et al., 2013) and occasionally contain hnRNP A3 (Mori et al., 2013b) and drosha (Porta et al., 2015).

1.8 C9ORF72 TOXIC MECHANISMS

The toxic mechanisms of the *C9ORF72* expansion are unknown but three hypotheses have been proposed: i) loss of C9ORF72 protein due to reduced expression and degradation of its mRNA (DeJesus-Hernandez et al., 2011), ii) neuronal toxicity caused by RNA accumulation from the sense and antisense strands into nuclear RNA foci (Lee et al., 2013) and iii) cellular toxicity by repeat-associated non-ATG (RAN) translation of dipeptide repeat (DPR) proteins (Mori et al., 2013c). In the following section I will review the evidence for and against each of the main hypotheses.

1.8.1 Haploinsufficiency

It was initially reported that the presence of the G4C2 hexanucleotide repeat expansion lead to a reduction of *C9ORF72* transcript levels. The presence of the expansion leads to the hypermethylation of its promoter, the use of an alternative start codon and to nuclear transcript retention (Niblock et al., 2016). As a result, C9ORF72 protein levels are reduced in the frontal, temporal and motor cortex but not in the cerebellum of ALS and FTD patients (Waite et al., 2014; Xiao et al., 2016). Moreover it has been proposed that higher levels of C9ORF72 transcripts may be beneficial in ALS and FTD patient (Gijselinck et al., 2016).

In vitro studies have shown that the knockdown of C9ORF72 protein in neurons leads to increased levels of cytoplasmic TDP-43 and cleavage (Sellier et al., 2016) as well as an increased cellular sensitivity to stress (Maharjan et al., 2016). Knock down of the *C. elegans C9ORF72* homologue shows that lack of C9ORF72 protein leads to motor neuron degeneration and increased sensitivity to cellular stress (Therrien et al., 2013). Zebrafish

lacking C9orf72 develop motor deficits (Ciura et al., 2013), however, although the C9orf72 mouse orthologue is enriched in neurons (Suzuki et al., 2013), *C9orf72* KO mice do not develop neurodegeneration, but immune dysregulation (Jiang et al., 2016; Koppers et al., 2015). Interestingly, many of the dysregulated pathways in the brains of *C9orf72* KO mice are also dysregulated in *C9ORF72* expansion carriers who also have impaired microglia and macrophage function (O'Rourke et al., 2016).

Arguing against the possibility that the loss of C9ORF72 protein is the main driver of toxicity is the absence of loss of function mutations in *C9ORF72* (Harms et al., 2013) and that individuals homozygous for the expansion do not develop disease at an earlier onset or progress more rapidly (Cooper-Knock et al., 2013; Fratta et al., 2013). Furthermore, *C9orf72* KO mice do not develop neurodegeneration or motor deficits (Jiang et al., 2016; Koppers et al., 2015), whereas mice overexpressing 66x(G4C2) show TDP-43 and DPR pathology and motor deficits indicating that the G4C2 repeats are sufficient to cause neurodegeneration (Chew et al., 2015b). Although a possibility remains that haploinsufficiency may increase cellular sensitivity to stress, it is not a major contributor to neurodegeneration.

1.8.2 RNA gain-of-function

Toxicity driven by expanded G4C2 RNA transcripts in the nucleus and cytoplasm has attracted a lot of interest in the field. Several studies have demonstrated a length and dosage dependent toxicity of G4C2 repeats *in vitro* (Lee et al., 2013; Rossi et al., 2015; Stopford et al., 2017) and *in vivo* (Freibaum et al., 2015). G4C2 transcripts form secondary structures such as G-quadruplexes and R-loops *in vitro* (Fratta et al., 2012) and *in vivo* (Conlon et al., 2016a). This conformational change promotes their accumulation in the nucleus as RNA foci that can sequester RNA binding proteins. Many RNA binding proteins have been shown to colocalise with intranuclear RNA foci in the brain and spinal cord of ALS and FTD cases, which include hnRNP-H (Cooper-Knock et al., 2014a; Lee et al., 2013), ADARB2 (Donnelly et al.,

2013), hnRNPA3 (Mori et al., 2013b), RanGAP1 (Zhang et al., 2015) and nucleolin (Haeusler et al., 2014). Interestingly, many of the splicing changes observed in human *C9ORF72* brains also correlate with the splicing targets of hnRNP-H (Prudencio et al., 2015).

Studies using iPSCs derived from ALS patients carrying the *C9ORF72* expansion have revealed that the binding of G4C2 RNA causes severe splicing dysregulation (Donnelly et al., 2013), diminished capacity to fire continuous spikes upon depolarization (Sareen et al., 2013), increased levels of abortive transcripts and nucleolar stress (Haeusler et al., 2014; Thys and Wang, 2015). The presence of expanded transcripts in the cytoplasm has also been shown to be toxic, induce neuronal branching deficits and impair vesicular transport (Burguete et al., 2015).

In vivo models of the disease have shown that G4C2 repeats are neurotoxic in *C. elegans* (Kramer et al., 2016), drosophila (Freibaum et al., 2015; Xu et al., 2013) and zebrafish (Lee et al., 2013). Neuropathological studies have also revealed that sense RNA foci are primarily neuronal (Mizielinska et al., 2013) and that there are a significantly greater number of RNA foci in the motor neurons of ALS patients that in the granule layer of the cerebellum (Cooper-Knock et al., 2014b).

Two independent studies expressing G4C2 repeats in drosophila argue against the possibility that the expanded G4C2 RNA is the main driver of toxicity. Mizielinska *et al.* (2014) showed that drosophila expressing ~108 and ~288 G4C2 repeats in the drosophila eye that are not translated into DPR proteins (so called RNA-only repeats) are not neurotoxic. However, a similar number of repeats that are able to be translated into arginine rich DPR proteins (poly-GR and PR) are profoundly neurotoxic in the fly eye and shorten their life span when expressed under a pan-neuronal ELAV promoter (Mizielinska et al., 2014). Additionally, Tran *et al.* (2015) expressed 160 G4C2 repeats in an intronic construct. Flies expressing the repeats have RNA foci but no developmental deficits or toxicity was observed. When the

expression of these constructs was increased by elevating the temperature at which drosophila were grown, DPR proteins were expressed and toxicity was observed (Tran et al., 2015).

1.8.3 Toxicity driven by DPR proteins

The *C9ORF72* G4C2 expansion can be translated through unconventional repeat associated non-ATG (RAN) translation into five different dipeptide repeat proteins. Poly-GP, poly-GA and poly-GR are translated from the sense strand (Ash et al., 2013; Mori et al., 2013c) and poly-PA, poly-PR and poly-GP (Gendron et al., 2013; Mori et al., 2013a; Zu et al., 2013) from the antisense strand. All five DPRs are found to be aggregated in the central nervous system of *C9ORF72* ALS and FTD post-mortem tissue and absent from peripheral tissue such as the heart, the kidney or the spleen (Ash et al., 2013) and DPR pathology precedes overt ALS/FTD symptoms by many years (Baborie et al., 2014; Proudfoot et al., 2014) although none of these studies attempted to quantify the abundance and distribution of RNA foci. Much effort has been spent studying the effect of DPRs generated by ATG sequence of non-repetitive codons which do not form nuclear RNA foci. In this section I will review the main findings for each DPR protein.

Poly-GP can be translated from the sense and the antisense strands. However, poly-GP inclusions are not the most common DPR aggregate in the brain and spinal cord of *C9ORF72* ALS and FTD cases (Gomez-Deza et al., 2015; Mackenzie et al., 2015). Two recent studies have demonstrated that the presence of poly-GP in the cerebrospinal fluid (CSF) and peripheral blood mononuclear cells from *C9ORF72* ALS and FTD patients by immunoassay. The presence of poly-GP in human samples was highly stable and could also be detected in asymptomatic *C9ORF72* carriers (Gendron et al., 2017; Lehmer et al., 2017). This highlights the possible use of this technique as a disease progression and treatment efficacy tool for clinical trials.

Poly-GA is translated from the sense strand and it is the most commonly aggregated DPR in the frontal cortex and spinal cord of ALS and FTD cases (Gomez-Deza et al., 2015; Mackenzie et al., 2015). Poly-GA aggregates colocalise with P62 (Mann et al., 2013) and other DPRs as wells as other proteins, such as drosha (Porta et al., 2015), UNC119 (May et al., 2014; Schludi et al., 2015), hnRNPA3 (Mori et al., 2016) or HR23 (Zhang et al., 2016b) in *C9ORF72* expansion carriers. Transient expression of poly-GA forms nuclear and cytoplasmic aggregates, modelling what is observed in the central nervous system (CNS) of ALS and FTD patients (Schludi et al., 2015). Several studies have revealed that *in vitro* expression of poly GA induces neuronal branching deficits (May et al., 2014), ER stress and UPS impairment (Zhang et al., 2014b) and impairment of nuclear import causing TDP-43 to mislocalise in the cytoplasm (Khosravi et al., 2016).

Moreover, poly GA forms 13 nm filaments and induces cell death (Zhang et al., 2014b). Poly-GA can also form cross β structures that can be transmitted from cell to cells (Chang et al., 2016; Zhou et al., 2017). The aggregation, seeding capacity and transmission of poly-GA can be mitigated with the use of poly-GA-specific antibodies, opening the possibility that these antibodies can be used as a possible immunotherapy in the future (Zhou et al., 2017). *In vivo* models of poly-GA have revealed that the expression of poly-(GA)x80 causes motor neuron loss in zebrafish. Additionally, there have been two published mouse models of poly-GA toxicity to date. Zhang and colleagues (2014) use an AAV serotype 1 vectors to express GFP-(GA)x50 in the mouse CNS. This study shows that aggregated and not soluble poly-GA induces motor deficits and neuronal loss (Zhang et al., 2016b). Shuldi *et al.* (2017) demonstrated that transgenic mice expressing poly-(GA)x149 under a Thy1 promoter have motor deficits but no neuronal loss (Schludi et al., 2017).

Poly-GR and poly-PR are both arginine rich peptides and are translated from the sense and the antisense strand respectively. Addition of arginine rich peptides to the cell

culture media has revealed that these peptides are internalised by cells and migrate into the nucleolus impairing RNA biogenesis and inducing nucleolar stress and cell death (Kwon et al., 2014). Additionally poly-GR and poly-PR impair assembly dynamics and function of membrane less organelles such as the nucleolus or stress granules (Boeynaems et al., 2017; Lee et al., 2016) and bind proteins with low complexity sequences such as TDP-43 (Lin et al., 2016). Similarly to poly-GA, poly-GR and poly-PR can be transmitted from cell to cell in an exosome-dependent manner (Westergard et al., 2016) and poly-PR induced toxicity is thought to be aggregation-dependent (Wen et al., 2014).

Transient expression of poly-GR and poly-PR in cells induces nucleolar stress by colocalising with nucleolin (Tao et al., 2015; Wen et al., 2014), impaired stress granule formation (Tao et al., 2015), DNA damage (Lopez-Gonzalez et al., 2016) and nucleocytoplasmic transport deficits (Jovicic et al., 2016). *In vivo,* poly-GR and poly-PR are toxic when expressed in the drosophila eye and lead to decreased lifespan (Mizielinska et al., 2014). Moreover, *in vivo* genetics screens have shown that poly-GR and poly-PR are toxic by impairing nucleocytoplasmic transport in yeast (Jovicic et al., 2016) and in drosophila (Boeynaems et al., 2016a).

Although numerous studies have shown that the transient expression of poly-GA, poly-GR and poly-PR are toxic *in vivo* and *in vitro* the main argument against the fact that the main source of toxicity is driven by DPRs is that soluble DPRs and DPR inclusions are very rare in the spinal cord of ALS patients and almost absent from motor neurons (Gomez-Deza et al., 2015; Mackenzie et al., 2015). Additionally neurodegeneration in ALS and FTD patients correlates with the presence of TDP-43 inclusions and not with DPR inclusions (Davidson et al., 2016). The fact that some studies have demonstrated the necessity for DPRs to aggregate to induce cell death (Wen et al., 2014; Zhang et al., 2016b) increases the significance of these pathological studies. Moreover, *in vitro* and *in vivo* studies studying DPR toxicity present

contradictory results in which different studies suggest that different DPRs are toxic and only what is observed in cells expressing poly-GA is representative of the human pathology (Schludi et al., 2015).

1.9 APPROVED THERAPEUTIC TREATMENTS

To date, riluzole is the only FDA approved therapeutic treatment for ALS. Although its mechanism of action is unknown, it is thought to reduce glutamate toxicity by inhibiting the levels presynaptic glutamate (Cheah et al., 2010). Riluzole received marketing authorization in 1995 in the USA and in 1996 in Europe. In the years that followed, over 60 molecules have been investigated as a possible treatment for ALS. Despite significant research efforts, the overwhelming majority of human clinical trials have failed to demonstrate clinical efficacy. Two clinical trials are in an advanced phase; oral masitinib and intravenous edaravone, and may soon be approved for clinical use (Petrov et al., 2017).

1.10 GENE SILENCING STRATEGIES FOR ALS

1.10.1 Gene knockdown through RNA interference (RNAi)

RNA interference (RNAi) exploits one of the endogenous cell capabilities to regulate gene expression. The target RNA is cleaved into a 21-23 nucleotide long double stranded RNA that binds to the RNA-induced silencing complex (RISC) complex in the cell. Upon loading to the RISC complex one of the RNA stands is degraded and the guide strand remains loaded (Ku et al., 2016). In this way it is able to cleave target transcripts repeatedly.

The complex is able to bind target RNA sequences through complementary Watson-Crick base pairing and induces the cleavage and degradation of the target RNA molecule in a highly specific manner. The exclusive presence of the RISC complex in the cytoplasm makes RNAi a uniquely cytoplasmic event (Ku et al., 2016).

There are two ways of achieving targeted gene repression 1. Through the expression of hairpin structures that are then processed by the cell and loaded into the RISC complex in a similar way as endogenous micro RNAs (miRNAs) are. This is known as small hairpin RNA (shRNA) and it achieves robust and highly accurate gene silencing. 2. Therapeutic RNA duplexes can be delivered directly without the need of processing by the cell; this is known as small interfering RNA (siRNA) (Walton et al., 2010).

1.10.1.1 SOD1

The availability of a reliable mouse model of *SOD1*-linked disease made it possible to develop RNAi strategies. Initially, different studies were able to show the feasibility of using siRNA-mediated SOD1 knockdown in G93A mouse models. Raoul *et al.* (2015) showed a delay in the symptom onset and degrease in progression rate by administering a single injection of lentiviral delivered SOD1 shRNA. Additionally, Ralph *at al.* (2015) were able to obtain similar results by injecting pseudotyped lentivirus expressing SOD1 shRNA into various muscle groups (hind limb, diaphragm, intercostal, facial and tongue). A single dose of injection was performed into multiple sites of the muscle. These authors were able to show that lentiviral-delivered SOD1 shRNA delayed the symptom onset by over 100%, increasing life span and rotarod performance. Both studies demonstrated the feasibility and safety of using lentivirus to deliver SOD1 siRNAs (Ralph et al., 2005; Raoul et al., 2005).

Later in 2013 the feasibility of delivering SOD1 shRNA in an AAV9 vector was shown by Foust and colleagues (2013). AAV9 are advantageous as they achieve high expression in the CNS from a single intravenous injection of AAV9 containing SOD1 shRNA which was able to reduce mutant SOD1 protein levels by 40- 60%, delaying disease onset by 39% and disease progression in a G73R SOD1 mouse model. When the AAV9 SOD1 shRNA was administered at post-natal day 21 there was no improvement in rotarod performance but there was a 30% of increase life span. Finally, they showed that intravenous delivery of AAV9 SOD1 shRNA

achieved a high level of motor neuron transduction and demonstrated the safety of using this strategy in non-human primates (Foust et al., 2013).

1.10.1.2 TDP-43

TDP-43 homozygous knockout mice are not viable and die at 7.5 days of embryonic development (Kraemer et al., 2010). Additionally, there have been many identified mutations in the *TARDBP* gene linked to ALS. These two reasons make TDP-43 silencing a challenging strategy. Any gene silencing strategy would have to involve targeting the mutant allele while not degrading the wild type allele (Picher-Martel et al., 2016). Nishimura and colleagues (2014) performed a siRNA screen and identified two siRNAs that selectively reduced the levels of the M377V mutant transcript. They then tested the siRNA in neural stem cells derived from two individuals carrying the M377V mutation and were able to show that cytosolic TDP-43 was reduced by 30% compared to cells transfected with a scrambled siRNA. Further work should be carried out to assess the feasibility of this strategy in mice (Nishimura et al., 2014).

1.10.1.3 C9ORF72

Several groups have shown that knock out of C9ORF72 protein in mice does not cause any neurological defects; instead mice have enlarged spleens and immunological defects. This may rule out the possibility that haploinsufficiency contributes to the toxicity of *C9ORF72* expansions (Koppers et al., 2015; Sudria-Lopez et al., 2016). The main focus of the field is now to elucidate whether the toxicity arises from the expanded RNA or the abnormally translated DPRs.

The fact that the RISC complex is only present in the cytoplasm and that expanded G4C2 transcripts accumulate in the nucleus does not make the use of a siRNA against the *C9ORF72* expansion a suitable therapeutic strategy. Nevertheless, Lagier-Tourenne and colleagues (2013) have shown that by using a pool of four different siRNAs targeting exons 2

and 4 of the *C9ORF72* gene they were able to obtain a 30% reduction on the total *C9ORF72* transcripts. However, no decrease in the number of RNA foci was detected in fibroblasts from patients carrying the expansion; indicating that toxicity may be due to the presence of expanded transcripts in the nucleus (Lagier-Tourenne et al., 2013).

1.10.1.4 SPT4

SPT4 is a highly conserved transcription elongation factor that upon binding to SPT5 regulates the activity of RNA polymerase II. It has been very recently shown that SPT4 regulates the transcription of both sense and antisense expanded G4C2 transcripts (Kramer et al., 2016). Knockdown of SPT4 in yeast and *C. elegans* overexpression models of the *C9ORF72* expansion repeats resulted in increased survival. Furthermore, siRNA mediated knockdown of SPT4 was able to partially reduce the observed toxicity in an overexpressing model of G4C2 repeats in drosophila eye. Finally, the authors of this study showed that the use of an siRNA against the human homologues of *SUPT4H1* and *SUPT5H* are able to reduce DPR levels in neurons derived from stem cells carrying the *C9ORF72* expansion (Kramer et al., 2016).

1.10.2 Antisense oligonucleotides

Antisense oligonucleotides (ASOs) are short strings of nucleic acids used to target an RNA transcript. ASOs are able to bind to a specific target by means of a standard Watson-Crick base pairing and commonly have a length of 8-50 bases (DeVos and Miller, 2013). ASOs can be chemically modified in order to increase their resistance to nucleases thereby increasing their half-life. Irrespective of their chemical modifications, ASOs are broadly separated into two different categories, described by their mechanism of action; RNAse H dependent; degrading ASOs or 'gapmers' and RNAse H independent ASOs or steric hindering ASOs.

RNAse H dependent ASOs have the ability to bind to target RNA in the nucleus and sequester RNAse H that cleaves the RNA strand in the RNA-DNA heteroduplexes, releasing the intact DNA strand. This allows for the ASO to exert its activity repeatedly, effectively having an enzymatic function (Cerritelli and Crouch, 2009). In order to retain the RNA-se H degrading capability and increase nuclease resistance synthetic chemists have developed "gapmers". Gapmers are ASOs whereby the 2'-modifications together with backbone modifications are introduced at the flanking regions of the ASO, and the centre remains unmodified effectively creating a "gap". In this way high nuclease resistance is achieved and the ability to degrade target transcripts is retained.

Steric hindering ASOs exert their activity by steric blockage upon binding to the target transcript. Chemical modifications in the nucleic acid backbone and the 2'-sugar ring remove the chemical charge of the nucleic acid, thereby make it increasingly resistant to degradation by nucleases, but removing their ability to induce RNAse H activity (DeVos and Miller, 2013). High nuclease resistance and robust affinity to target RNA makes them ideal to target translation inhibition, prevention of accumulation, alter gene splicing and miRNA silencing (DeVos and Miller, 2013).

1.10.2.1 ASO entry mechanism and viability for use in vivo

ASO cellular uptake varies according to the chemical modifications, however it is generally understood that ASOs can bind to proteins in the extracellular medium. ASOs are then internalised through endosomes (Koller et al., 2011). Cellular uptake of uncharged ASOs can be facilitated by coupling to arginine-rich cell-penetrating peptides. Although the mechanism of exit of these vesicles is yet unknown, once internalised in the cell, ASOs can diffuse freely between the nucleus and the cytoplasm (Lorenz et al., 2000). ASOs may maintain their activity for 16 weeks in the case of gapmers or longer in the case of PMOs after cellular internalisation (DeVos and Miller, 2013).

Due to their uncharged nature, some ASOs scarcely cross the blood brain barrier (BBB) making intramuscular and intravenous injections unsuitable methods of delivery to the CNS in order to target neurological conditions. Alternatively, they can be delivered directly into the cerebral spinal fluid (CSF) by means of a single injection or constant diffusion. ASOs show a uniform distribution across the CNS upon direct delivery into the CSF in rodents and rhesus monkeys (Rigo et al., 2014). Additionally, once ASOs are administered into the CSF their tissue half-life is much greater than in peripheral tissues due to the lower presence of endonucleases in the CNS. ASOs were detected 71-206 days and 145-191 days in the brain and the spinal cord, respectively, after a single injection. This contrasts with the 10-65 day presence detected in peripheral tissue (Rigo et al., 2014). However, the fact that ASOs are eventually cleared from the CNS means that there is the possibility of terminating the therapy if necessary. Moreover, it has been shown that it is possible to reverse the beneficial effects of ASOs by injecting a fully complementary ASO, showing that a complementary ASO has the potential to act as an antidote in the case of side effects being detected (Rigo et al., 2014).

Tests in non-human primates have shown that bolus injection into the intrathecal (IT) space achieves a more uniform distribution in the CNS than intramuscular injections, although delivery of ASOs into deeper structures of the brain is harder to achieve (Kordasiewicz et al., 2012). This is a more invasive, costly, painful method but it is well tolerated, and it is a common procedure for delivery of anaesthetics. This method of delivery is relatively costly, meaning that ASO therapies are only being developed against life threatening conditions. For this reason, experts are studying the viability of the use of nanoparticles and coupling ASOs with arginine-rich cell penetrating peptides in order to help ASOs cross the BBB. If successful, it could mean that the cost of delivering ASOs into the CNS could be greatly decreased and making it viable to develop ASO-based therapies against other non-life threatening conditions.

1.10.2.2 Uses of ASOs in muscular and neurological conditions

ASOs have been extensively tested as a possible therapy for many neuromuscular disorders. A main disadvantage of oligonucleotide-based therapies is achieving high concentrations of ASO in the target organ, however, in this case neurological conditions have the advantage that once in the CSF, ASOs escape the degradation by the liver and are rapidly taken by neurons (Butler et al., 2005).

The use of ASOs has been pioneered in two muscular disorders; Myotonic dystrophy and Duchenne's muscular dystrophy. In both cases steric hindering ASOs have been used but for very different purposes. Myotonic dystrophy, a hereditary degenerative disease, is caused by the presence of an expanded trinucleotide CTG repeat in the DM protein kinase (DMPK) gene. The expanded RNA causes the RNA to accumulate in the nucleus, sequestering the RNA-binding protein Mucleblind like 1 (MBNL1). Steric hindering ASOs have been used to prevent the sequestration of MBNL1 into RNA foci; mitigating the toxicity of the CUG repeats (Wheeler et al., 2012). In Duchenne's muscular dystrophy, ASOs have been used to induce the exon skipping of a mutation carrying exon. The disease-causing mutation codes for a stop codon and leads to the translation of a short, inactive dystrophin protein. By targeting the intron boundary with steric hindering ASOs, incorporation of the mutation-containing exon is prevented. In this way, exon skipping is induced and a shorter, but functional protein is translated that does not include the mutated exon. This approach has yielded very promising results showing a restoration of up to 97% of dystrophin protein and is currently in a phase III clinical trial (Goemans et al., 2011; Kinali et al., 2009; van Deutekom et al., 2007).

In Alzheimer's disease, gapmers have been used to decrease the amount of amyloid precursor protein (APP) showing a slight improvement in transgenic mice (Farr et al., 2014) and to reduce the levels of TAU protein encoded by the MAPT gene (Sud et al., 2014).

Gapmers have also been used in AD to specifically target mutated β-secretase, which is responsible for APP cleavage, showing a decrease in toxic amyloid beta (Aβ) levels (Chauhan and Siegel, 2007).

Huntington's disease is an autosomal dominant neurodegenerative disorder due to the expansion of a trinucleotide CAG repeat in the huntingtin gene. The CAG expansion is translated into a protein with an expanded poly-Q. Degrading ASOs could not be used to target the CAG expansion as poly-Q repeats are known to carry out many important cellular functions. Degrading ASOs have therefore been used to knock out both murine and human forms of huntingtin in transgenic mice showing a 75% reduction of transcript and a significant improvement in motor performance and survival (Kordasiewicz et al., 2012). The use of steric hindering ASOs has also been tested for Huntington's showing an attenuation of neurotoxicity *in vivo* and *in vitro* (Sun et al., 2014).

Additionally antisense oligonucleotides have been tested as a possible therapy for spinal muscular atrophy (SMA). SMA is an autosomal recessive condition that leads to the loss of motor neurons in the anterior horn of the spinal cord in a similar fashion to ALS. SMA is usually caused by the deletion of exon 7 in the SMN1 gene. The deletion is not usually embryonic lethal as humans uniquely express the almost identical SMN2 gene. However, the majority of SMN2 transcripts lack exon 7 due to a silent mutation that leads to the skipping of exon 7 and the translation of a shorter unstable SMN protein. Current strategies involve the use of steric hindering ASOs to modulate the splicing of exon 7 and increase its inclusion (Bogdanik et al., 2015; Lorson et al., 2010). Pre-clinical studies have shown that the use of ASOs targeting SMN2 are safe and are currently being taken into clinical trial. Children and adults suffering with SMA were treated with SMN2 targeting ASO showed a 5.9 fold increase in motor performance (n=84) compared to sham controls (n=42).

1.10.2.3 Uses of ASOs in ALS - SOD1

RNAse H-dependent ASOs have been used to degrade SOD1 in G93A SOD1 rat model, showing that a 50% decrease in the total SOD1 protein can increase the lifespan by 8.8% (10 days) compared to scrambled ASO although no effect was observed on disease onset (Smith et al., 2006). Intrathecal delivery of ASO was well tolerated in rats as well as non-human primates and a good ASO distribution throughout the CNS was achieved. This study also concluded that ASOs were safe to use as no adverse effects where reported with the highest doses (Smith et al., 2006).

Following this study, a phase I clinical trial was carried out to test the safety, tolerability and pharmacokinetics of the therapeutic ASO – ISIS333611- which was completed in 2012 (Miller et al., 2013b). The study was carried out in a randomised, placebo-controlled way. The ASO was delivered by intrathecal infusion using an external pump over 11.5 h at increasing doses (0.15 mg, 0.50 mg, 1.50 mg, 3.00 mg) to four cohorts of eight patients with SOD1-positive amyotrophic lateral sclerosis. No dramatic decrease in SOD1 level in the CSF of treated cases was observed. The authors suggest, however, that this is because a low dose was administered in order to assess ASO safety (Miller et al., 2013b).

The study concluded that, in order to achieve satisfactory SOD1 decrease a greater dose and longer infusion time would be necessary. The inability of the ASO to cross the blood brain barrier makes it an ideal candidate to treat CNS related conditions. ASOs may be administered intrathecally and not affect organs other than the CNS. Additionally, there were no reported adverse effect when using the ASO compared to placebo (Miller et al., 2013b). Overall this study constitutes a significant, but not conclusive advance in the implementation of ASOs as a possible therapy.

1.10.2.4 Uses of ASOs in ALS - C9ORF72

There have been a number of *in vitro* studies exploring the used of mostly RNase-H dependent ASOs, although steric hindering ASOs have also been tested. Donnelly and colleagues (2013) have tested both RNAse-H dependent ASOs and steric hindering ASOs. Four degrading ASOs targeting the G4C2 repeat, the repeat-intron boundary and introns 1 and 2 of the *C9ORF72* gene were tested. All four ASOs showed a decrease in the number of detectable RNA foci but only the ASO targeting exon 2 showed a decrease in the total levels of *C9ORF72* mRNA. All degrading ASOs as well as the steric hindering ASO were able to reduce the impact of glutamate susceptibility shown by iPSC-derived from expansion carriers (Donnelly et al., 2013). Another study generated iPSC-derived motor neurons from *C9ORF72* expansion carriers showing that they have diminished capacity to fire continuous spikes upon depolarization. These deficits were reversed upon treatment with antisense oligonucleotides which reduced both the number of RNA foci and C9ORF72 protein levels (Sareen et al., 2013). Lastly, ASOs targeting the *C9ORF72* transcript were shown to reduce the number of detectable RNA foci in fibroblasts carrying the repeat expansion. Furthermore, ASOs were intrathecally administered to mice without any toxicity observed, thereby showing the potential safety of knocking down the C9ORF72 protein and arguing against the possibility haploinsufficiency contributes to the toxicity of *C9ORF72* expansions (Lagier-Tourenne et al., 2013).

A single dose of degrading ASO was intraventricularly administered to 3 month old mice expressing a *C9ORF72* bacterial artificial construct (BAC) with 450 G4C2 repeats. Tissues were collected 4 weeks after injection and the authors reported a decrease of 40% in repeat-containing RNA in the cortex and the spinal cord. Administration of the ASO also resulted in over 50% decrease of RNA foci and almost complete depletion of poly-GP and poly-GR. A different ASO targeting the repeat-exon boundary was shown to improve age dependent behavioural deficits when tested 6 months post administration (Jiang et al., 2016).

1.10.2.5 Uses of ASOs in ALS - Other targets

ALS cases have been shown to have increased acetylcholinesterase enzyme (AChE) serum levels, making it a potential therapeutic target (Gotkine et al., 2013; Rasool et al., 1983; Rodriguez-Ithurralde et al., 1998). Moreover, the effects of a potential therapeutic strategy can be easily monitored. ASOs targeting AChE mRNA have been shown to lead to a 10% increased life span in G93A SOD1 mice, as well as a decrease motor neuron loss (Gotkine et al., 2013).

Additionally, it has been reported that the micro RNA, miRNA-155 is upregulated in sporadic and familial ALS. Although miRNA-155 is constitutively expressed, it is most highly expressed in T-cells and monocytes and have been shown to regulate pro-inflammatory pathways. Koval and colleagues (2013) used steric hindering ASOs to block the effect of miRNA155. G93A SOD1 mice were implanted with osmotic pumps at 60 days containing 20 mg/day anti-miR-155. There was no significant change in the disease onset (measured by weight loss and neurological score), however, the anti-miR-155 ASO treated mice showed a 7.4% (9.5 days) average increase in survival (Koval et al., 2013).

Finally, degrading ASOs targeted at Ataxin-2 have been shown to significantly increase the median lifespan of mice expressing two copies of human TDP-43 by 34% (Becker et al., 2017). The use of this ASO achieved a 77% reduction of Ataxin 2 transcript levels by ICV injection Ataxin ASO at P1. No mice treated with control ASO lived past 32 days; in contrast 2/16 mice treated with Ataxin 2 ASO lived over 120 days. The authors of this study suggest that the improvement in survival and motor performance was due to preventing TDP-43 to be sequestered into stress granules which lead to its aggregation. This study opens an exciting new therapeutic avenue to treat the majority of ALS cases that have TDP-43 inclusions (Becker et al., 2017).

1.10.3 Biological uses of steric hindering ASOs

Steric hindering ASOs bind to the target with high affinity and do not induce degradation, for this reason there have a number of different biological applications. ASOs can be designed such that they bind to the 5'-cap formation site of specific genes in the nucleus in order to prevent polyadenylation and therefore reducing the transcript levels. Alternatively, protein levels can be decreased by using ASOs targeting the ribosomal entry site and inhibiting translation (Evers et al., 2015). Splicing modulation may also be achieved by designing ASOs that bind to the exon-intron boundary, splicing will be prevented achieving the removal of an intron containing a pathogenic mutation (Arechavala-Gomeza et al., 2007; Dominski and Kole, 1993). This has been shown in Duchenne's muscular atrophy and is currently undergoing a phase III clinical trial (Goemans et al., 2011; Kinali et al., 2009; van Deutekom et al., 2007). Finally, ASOs have also been shown to reduce the effects of miRNAs by binding and inhibiting them in the cytoplasm (Davis et al., 2009).

Site of Modification	Chemical modification	Pros cons
Backbone modifications 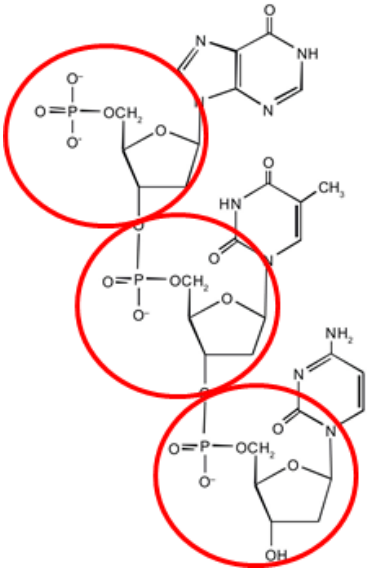	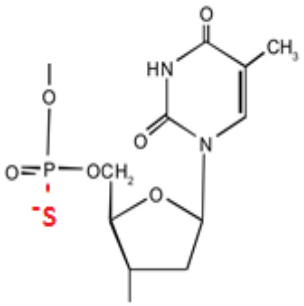 Phosphotioate (PS) oligomer	+ Recruit RNAse H and degrade the target transcript + Possess "enzymatic" activity - Have a short life due to degradation by nucleases - Off target effects
	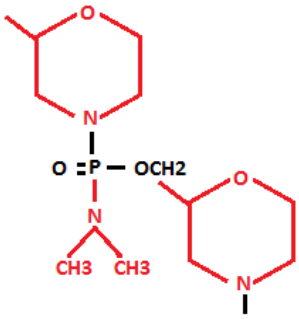 Phosphorodiamidate Morpholino Oligomer (PMO)	+ Good efficacy for translation inhibition + Increased affinity to target + High nuclease resistance - low cellular uptake - Do not degrade the target transcript
2' Carbon modifications 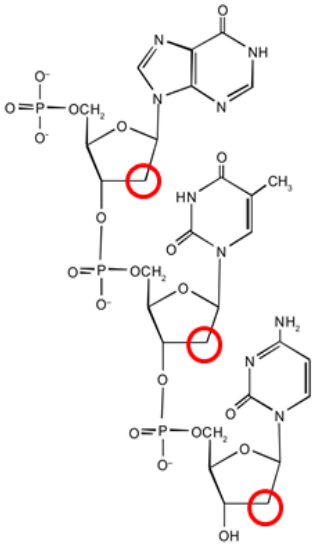	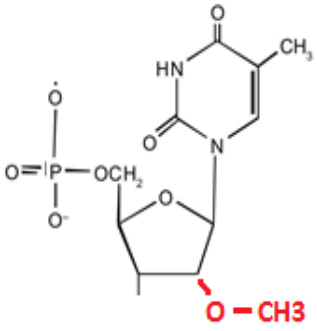 2'-o-methyl (MOE)	+ Moderate cell uptake + Low off target binding - Lower target affinity than PMO - Moderate nuclease resistance
	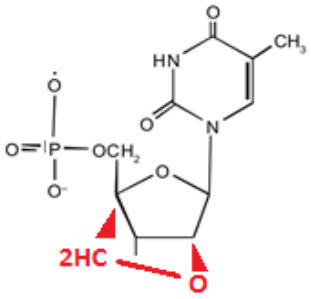 Locked nucleic acid (LNA)	+ Robust binding to target + High binding affinity - High cellular toxicity - Poor cellular uptake

Table 1.2: Review of chemical ASO chemical modifications

1.11 PROJECT RATIONALE

At the time that the present study was designed, the mechanisms of the *C9ORF72* expansion toxicity were relatively unexplored. Three main theories of toxicity; toxic gain-of-function of RNA foci, DPR toxicity or haploinsufficiency, were equally plausible. In my project I tried to address this by quantifying the abundance and distribution of sense and antisense RNA foci, TDP-43 mislocalisation and inclusions from all five DPRs in spinal cord motor neurons of ten *C9ORF72*-ALS cases and compared them to five non-C9 ALS-TDP-43 cases. We have found that sense RNA foci are the most common species in the spinal cord of C9ORF72-ALS cases. Moreover we observed that DPR protein inclusions are rare in the spinal cord and almost absent from the motor neurons of the ten C9ORF72-ALS cases analysed.

We also explored the use of steric hindering ASOs, as they would not cause a decrease in the levels C9ORF72 transcript or protein. Additionally steric hindering ASOs had been shown to have the ability to decrease the number of RNA foci in an *in vivo* model of another repeat-expansion disorder and have been shown to be effective at translation inhibition (Mulders et al., 2009; Wheeler et al., 2009). Further publications have shown that the G4C2 repeats are sufficient to cause cognitive deficits and TDP-43 mislocalisation in mice (Chew et al., 2015b). For this reason, targeting the repeats directly and no other flanking region may be sufficient to mitigate toxicity. Furthermore, *C9orf72* knockout mice show microglia activation and macrophage dysfunction (O'Rourke et al., 2016). This may suggest that using gapmers as a therapeutic strategy may have toxic side effects. By using non-degrading ASOs that target the G4C2 expansion, we aim to mitigate the repeat expansion toxicity as well as reducing any possible side effects that may arise from decreasing the levels of *C9ORF72* mRNA and protein.

A collaboration was initiated with Sarepta plc, a biotechnology company with great expertise in the use of phosphorodiamidate morpholino oligomers (PMOs) for other

neuromuscular conditions. Having a commercial company collaborating in the project satisfied the ambition that the outcome of the project could be clinically explored if the results were satisfactory. Sarepta provided control and G4C2 targeting peptide-coupled PMOs (PPMOs) in order to increase the cellular uptake of PMOs. Additionally, PPMOs have been shown to show a wide distribution throughout the brain upon ICV injection and little toxicity (Du et al., 2011).

2 METHODS

All reagents were purchased from Life Technologies unless otherwise stated

2.1 HUMAN PATHOLOGICAL STUDY

2.1.1 Human post-mortem tissue

A total of thirty spinal cord sections were analysed for the presence of TDP-43 and all DPR inclusions and RNA foci by fluorescent *in situ* hybridisation and/or double immunofluorescence from each individual including ten ALS cases positive for the *C9ORF72* intronic expansion (C9ORF72-ALS). Thirteen sections were also analysed from five ALS cases negative for *C9ORF72*, *FUS* and *SOD1* mutations (365 sections in total). Sections of frontal lobe and cerebellar cortex from a case of C9ORF72-FTD with abundant p62 pathology were chosen as a positive control for DPR staining. All cases were provided by the Medical Research Council London Neurodegenerative Diseases Brain Bank (Institute of Psychiatry, Psychology and Neuroscience, King's College London). Samples were collected and distributed in accordance with local and national research ethics committee approvals. Expansion carriers were identified using repeat primed PCR (Smith et al., 2013) and all of the cases had previously been reported to show characteristic cerebellar p62 and TDP-43 pathology (King et al., 2009; Troakes et al., 2012). Details of the age, sex and post-mortem delay are recorded in the appropriate chapter.

2.1.2 Motor neuron counting and double label immunofluorescence

A total of 30 spinal cord sections were analysed from each C9ORF72-ALS case. Histological examination was performed on 7μm sections prepared from formalin-fixed, paraffin–embedded tissue from spinal cords of all ALS cases. Sections were stained with hematoxylin and eosin to perform motor neuron counts, and sequential sections were

processed for double label immunofluorescence for the DPRs, sense and antisense foci and TDP-43. Prior to double immunofluorescence staining, paraffin was removed with xylene and all sections were rehydrated in an ethanol series (100%, 95%, 70%) for 3 min per step. Slides were incubated in 0.3% Sudan black for 5 min to quench autofluorescence and washed with water. Antigen retrieval was carried out by microwaving for 6 min at maximum power and 12 min at medium power in 100mM sodium citrate buffer (pH 6.0). Non-specific binding sites were then blocked for 20 min using 5% normal donkey serum in PBS.

For double immunofluorescence staining, spinal cord sections were incubated with primary rabbit antibodies against the five different DPRs (poly-GA, GP, GR, PR and PA) at a dilution of 1:100 together with TDP-43 (rat monoclonal TDP-43 Sigma Scientific (SIG-39850) at a dilution of 1:100 antibody was carried out overnight in a humid chamber at 4^{o}C. The DPR antibodies were obtained from Dr. Leonard Petrucelli and colleagues and were previously characterised (Gendron et al., 2013). After 3 washes with PBS, sections were incubated with anti-rabbit (Alexa Fluor 594) and anti-rat (Alexa Fluor 488) secondary antibodies for 1hr at room temperature. DAPI (Sigma) was used to counterstain nuclei. Sections were mounted in Fluorsave. Semi-quantitative and quantitative evaluation of DPR and TDP-43 pathology was performed using Zeiss Axiovert S100 microscope. Aggregates were also imaged using a Leica Confocal SP microscope. A "secondary antibody only" control was introduced in each staining procedure.

2.1.3 Fluorescent *in situ* hybridisation for human sections

Fluorescent *in situ* hybridisation (FISH) was performed in 20 lumbar spinal cord sections from each of ten C9+ve-ALS cases and 13 sections from 5 TDP-43-ALS cases. Human sections were provided as 10% formalin fixed and paraffin-embedded blocks. To perform FISH, paraffin was removed with two 3 minute washes in xylene and sections were rehydrated as described in Lee *et al.(*2013) Cy3-labelled sense ((C4G2)X4) and antisense

((G4C2)x4) LNA probes were used at a concentration of 200ng/µl (Exiqon). Hybridisation was carried out in a humid chamber at 60°C overnight. Sections were washed once in 2XSCC/ 0.1% Tween 20 solution at room temperature and three times with 0.1X SCC solution at 60°C for 5 minutes. Sections were then incubated with 1.25ng/ml DAPI (Sigma) counterstain solution for 5 minutes and mounted in Fluorsave for quantification of RNA foci.

If IHC was performed to assess the co-occurrence of TDP-43 and RNA foci, sections were blocked with 5% Donkey serum-PBS solution for 1 hour and incubated with TDP-43 (mouse polyclonal TDP-43 10782-AP Proteintech) at a dilution of 1:100. Sections were washed three times with PBS and incubated with anti-rabbit AlexaFluor 488 secondary antibody for 1 hour. The sections were then treated with DAPI counterstain and mounted in Floursave.

2.1.4 Semi quantitative and quantitative evaluation of pathology

The presence of sense and antisense foci, DPRs and TDP-43 inclusions were scored in the spinal cord using a previously published semi-quantitative grading scale (Mackenzie et al., 2013b), in which the total number of immunoreactive inclusions, as well as the cytoplasmic inclusions (CI) and the intranuclear inclusions (NI), were rated as follows: **0** – Absent, **0.5** – one or two inclusions in the whole section, **1**- very few, **2**- occasional- easy to find and a few cells are affected, **3**- moderate- many of the cells are affected, inclusions are easy to find, **4**- numerous- nearly all of the cells are affected. Additionally, each section was re-analysed and the number of DPR and TDP-43 inclusions was counted manually in a systematic, blinded manner. The number of DPR aggregates was counted per section and averaged per case.

2.2 CELL CULTURE

2.2.1 Maintenance of Cell lines

HEK-293T cells were grown in DMEM/GlutaMax media, 10% foetal bovine serum, 1% penicillin-streptomycin. Cells were grown T25 flask until 100% confluent and split by washing once with PBS and treating for 2-3minutes or until cells detached with 1ml of trypsin-EDTA reagent. Cells were then collected in 5ml of growth medium and spun at 1000g for 4 minutes. The supernatant was discarded and the pellet was then re-suspended in 6ml of growth medium. 2ml of re-suspended cells were put into a clean T25 flask together with 3ml of growth medium. The remaining re-suspended cells were counted and plated for experiments.

2.2.2 Counting and Plating of Cell lines

Cells were counted using a NucleoCounter NC-300 (Chemometech). Cells were counted following the cell count and viability protocol following the manufacturer's instructions. The number of viable cells was used. Cells were then plated in 500µl of media/well for a 24-well plate and 1ml of media/well for a 12-well plate. Cells used for immunohistochemistry were plated in 13 mm coverslips. Prior to plating, coverslips were coated with poly-d-lysine hydrobromide (1:1000 in PBS) for 1 hour at 37°C and washed once with PBS.

2.2.3 Maintenance of iPSC

Cells were grown in Geltrex (Thermo Fisher Scientific) coated 6-well plates. Induced pluripotent stem cells (iPSC) were every other day with 2 ml of E8-FLEX (STEMCELL Technologies) medium and 5 ml of medium was used to feed iPSCs over the weekend.

Cells were passaged when colonies were large, when the edges of the colonies were in contact with each other or when the centre of the colony changed colour, indicating that the

cells were differentiating. Prior to passaging 6-well plates were coated with 750 µl of Geltrex for one hour and washed once with PBS.

For passaging, cells were incubated for at least one hour with 1X REVTACELL (Life technologies) prior to passaging. Cells were washed once with 500 µl of PBS and incubated for 3 minutes with Versene (Thermo Fisher Scientific). Versene was removed and 2 ml of E8-FLEX medium was then added vigorously on the well in order to detach and break up the colonies. 1 ml was added to 3 wells of a 6-well plate.

2.2.4 *In vitro* differentiation into smooth muscle actin (SMA) positive cells

iPSCs were differentiated into smooth muscle cells (SMA positive) in order to show that they can be differentiated into mesodermal cells. iPSCs were spit as previously described and plated into a 24-well plate containing gelatine/fibronectin coated 5mm coverslips in E8-FLEX (STEMCELL Technologies) culture medium. The next day the medium was removed and substituted for muscle differentiation medium (MDM) as described in table 2.1. The medium was replenished every other day for 10 days until cells were fixed from immunofluorescence.

Component	**Final concentration**
DMEM:F12	1X
Fetal bovine serum (FBS)	15%
GlutaMax	1X
Penicillin-streptomycin	1x
MEM Non-essential amino acids	1x
Monothioglycerol	1mM
Retinoic acid	10 µM

Table 2.1: Muscle differentiation medium (MDM)

2.2.5 *In vitro* differentiation into α-fetoprotein (AFP) positive cells

iPSCs were differentiated into hepatocyte progenitors in order to show their ability to differentiate into endodermal cells as previously described by (Siller et al., 2015). iPSCs were split as previously described and plated into a 24-well plate containing Geltrex-coated 5 mm coverslips in E8-FLEX (STEMCELL Technologies) medium. On Day 0 the medium was removed and replaced by AFP medium 1 (table 2.2). After one day, the medium was removed and replaced by AFP medium 2 (table 2.3). Cells were cultured for one day on AFP medium 2, which was then removed and replaced AFP medium 3 (table 2.4). Cells were cultured for 5 days in AFP medium 3 until fixed as previously described for immunofluorescence.

Component	**Final concentration**
RMPI 1640 GlutaMax	1X
B27 supplement	1X
CHIR99021	4 μM

Table 2.2: AFP medium 1

Component	**Final concentration**
RMPI 1640 GlutaMax	1X
B27 supplement	1X

Table 2.3: AFP medium 2

Component	Final concentration
Knockout DMEM	1X
Knockout serum replacement (KOSR)	20%
GlutaMax	1X
2-Mercaptoethanol	100 µM
MEM Non-essential amino acids	1x
DMSO (Sigma-Aldrich)	1%

Table 2.4: AFP medium 3

2.2.6 *In vitro* differentiation of iPSCs into neuronal progenitor cells

iPSCs were differentiated into neuronal progenitors cells (NPCs) as described elsewhere (Devlin et al., 2015). Briefly, iPSCs were plated at 30–40% confluence in neural conversion media containing DMEM/F12, 1% L-glutamine, , 5 mg/mL BSA (Europa Bio-products, Cambridge, UK), 1 x lipids (Life technologies), 450 µM monothioglycerol (Sigma), 7 µg/ml insulin (Roche), 15 µg/ml transferrin (Roche) 10 µM of SB431542 (Tocris Biosciences, Bristol, UK) and 2 µM of dorsomorphin (Merck) for 7-10 days (CDM1 medium, table 2.5). Cells were cultured in suspension to form neurospheres in the same medium described above, withdrawing SB431542 and dorsomorphin and adding 1µM of Retinoic acid, 2.5 ng/ml of bFGF (Peprotech) and 2.5 ng/ml of heparin for 7-10 days (CDM2 medium, table 2.6). Neurospheres were dissociated with Stem Pro Accutase (Life technologies) and plated on matrigel in NPCs expansion medium containing Advance DMEM:F12, 1% Penicillin/streptomycin (P/S), 1% L-glutamine, 1% N2, 0.001% B27 and 10ng/ml of bFGF until differentiation occurred.

Component	Final concentration
DMEM:F12	1X
L-glutamine (10X)	1x
BSA	5mg/ml (filter sterilize)
Lipid 100x	1x
Monothioglycerol	450 µM
Insulin	7 µg/ml
Transferrin	15 µg/ml
Penicillin-streptomycin	1x
Activin inhibitor	10 µM
Dorsomorphin	2 µM

Table 2.5: Chemically defined medium 1 (CDM1) composition

Component	Final concentration
DMEM:F12	up to 250 ml
L-glutamine (10X)	1x
BSA	5mg/ml (filter sterilize)
Lipid 100x	1x
Monothioglycerol	450 µM
Insulin	7 µg/ml
Transferrin	15 µg/ml
Penicillin-streptomycin	1x
Retinoic Acid	0.1 µM
bFGF	2.5 ng/ml
Heparin	2.5 ng/ml

Table 2.6 Chemically defined medium 1 (CDM2) composition

2.2.7 Maintenance of neuronal progenitor cells

T25 Flasks were coated 1:50 with matrigel at least one day before. Prior to use flasks were placed for one hour at 37°C and washed once with PBS. Neuronal progenitor cells were grown in matrigel coated T25 flasks. Cells were maintained with bFGF-containing expansion media (table 2.7) and changed every two days. Cells were kept at 37°C in a hypoxia incubator to preserve the neuronal identity. Cells were grown until fully confluent and split 1:2. Cells were split by washing once with PBS and adding 1ml of Accutase (Life Technologies) until the cells detached. Cells were then collected in expansion media and pelleted by gentle centrifugation (1000g for 4 min). Cells were then resuspended in 500 µl of expansion media and half of the cells were placed into a fresh matrigel coated T25 flask containing 3 ml of expansion media. The remaining cells were plated for neuronal differentiation.

Component	**Concentration**
Advanced DMEM/F12	1x
L-glutamine	1x
Penicillin-streptomycin	1x
Heparin	2 µg/ml
N2	0.5X
B27	0.1X
bFGF	20 ng/µl

Table 2.7: Neuronal progenitor cell expansion medium

2.2.8 *In vitro* differentiation of neuronal progenitor cells into mature neurons

Neuronal progenitor cells were counted as previously described. Differentiation of neuronal progenitor cells into cortical neurons was driven by removal of bFGF (Preprotech) from the culture medium. Plates were coated with matrigel 1:50 the previous day. Prior to

plating, plates were placed at 37°C for one hour and washed once with PBS. Cells were plated in differentiation medium (table 2.8) at a confluency of $2.5x10^5$ cells/well in a 24-well plate and double that for a 12-well plate. Cells were allowed to differentiate for 7 days in differentiation media. The medium was topped every 3-4 days. The differentiation medium removed 7 days after initiation of neuronal differentiation and replaced by GDNF and BDNF-containing maturation medium (table 2.9). Maturation medium was added every 3-4 days for 5 weeks until the neurons were analysed.

Component	**Concentration**
Advanced DMEM/F12	1x
L-glutamine	1x
Penicillin-streptomycin	1x
Heparin	2 µg/ml
N2	0.5X
B27	0.1X

Table 2.8: Neuronal differentiation medium

Component	Concentration
Advanced DMEM/F12	1x
L-glutamine	1x
Penicillin-streptomycin	1x
Heparin	2 µg/ml
N2	0.5X
B27	0.1X
GDNF	5 ng/ml
BDNF	5 ng/ml

Table 2.9: Neuronal maturation medium

2.2.9 Plasmid maxiprep

Bacteria containing the plasmid of choice was grown over night at 37°C in a shaker in 500 ml Luria-Bertani (LB) media with 1X Ampicillin. Plasmids were isolated using a Plasmid Maxiprep Kit (Quiagen) following the manufacturer's instructions. Plasmid was resuspended in 500µl of DNAse-free water (Ambion) and the concentration of DNA was measured using a microvolume spectrophotometer (Nanodrop, Thermoscientific). DNAse-free water was then added to make up a final concentration of 1µg/µl.

2.2.10 Transfection of cells

300 ng/well in a 24-well plate of plasmid DNA was used to transfect all cells unless otherwise stated. 200 µl of media was removed from each well. 300ng of DNA was mixed with 1 µl of Lipofectamine 2000 and 50µl of OPTIMEM in a sterile 1.5ml tube. The transfection mixture was shaken briefly, spun down and allowed to mix for 20 minutes. 50µl of transfection mixture was added dropwise into the 24-wellplate. Transfection was carried out for 24 hours.

2.2.11 Mycoplasma testing

All cells were tested monthly for mycoplasma infection. 2ml of media was collected and analysed using MycoAlert Mycoplasma Detection Kit (Lonza) following the manufacturer's instructions.

2.2.12 Peptide-coupled PMO information

PPMOs were provided by Sarepta Therapeutics (Cambridge MA). To increase the PMO cellular uptake capability, PMOs were coupled to a CP06062 cell penetrating peptide (PPMO). Peptide-coupled PMOs (PPMOs) and 5' fluorescently labelled protein-coupled PMOs (5FL-PPMOs) where synthesized and by Sarepta Therapeutics (Cambridge, MA) and supplied as a lyophilised powder. PPMOs were resuspended in RNAse-free water to form a stock concentration of 2mM as suggested by the company. PPMOs and 5FL-PPMOs were diluted to the required concentration in cell culture media. A Control-PPMO with a scrambled sequence with no known target and a G4C2-PPMO directly targeting the G4C2 expansion (CCCCGG CCCCGG CCCCGG CCCCGG) were used for all experiments.

2.3 ANALYSES

2.3.1 RNA extraction

Total RNA was isolated from cultures of cell lines with the RNeasy kit (Qiagen) according to manufacturer's instructions. Cells were manually scraped and collected into RNAse-free polypropylene tubes. Cells were centrifuged for 1 minute at 12 000g and cell pellets were kept on ice and washed in PBS three times prior to RNA extraction. RNA was quantified using a microvolume spectrophotometer (Nanodrop, Thermo Scientific).

2.3.2 RT PCR

cDNA was synthesized by using 1 µg of total RNA with the SuperScript® III First-Strand Synthesis System in a 20 µl volume following the manufacturer's instructions. cDNA was diluted to 5ng/µl and standard polymerase chain reactions (PCR) were performed using *Thermophilus aquaticus* (*Taq* DNA polymerase). 25 ng of cDNA of each sample was amplified in a 25µl reaction containing 0.2mM dNTP, PCR primers, 1.5 mM $MgCl_2$, 10x PCR buffer and 0.1 µl Taq DNA polymerase. Amplification was performed at 95°C for 30 seconds, 35 cycles of 58°C or 61°C for 30 seconds and 72°C for 30 seconds, followed by extension at 72°C for 10 minutes. PCR products were electrophoresed in 1% agarose gels.

2.3.3 Quantitative PCR (qPCR)

Total RNA from the appropriate cell type was isolated and cDNA was synthesized as previously described. For quantitative expression analysis, 20µl cDNA samples from SuperScript III reactions were diluted with a further 100 µl of nuclease-free H_2O. Reactions were carried out in a total volume of 12µl, containing diluted cDNA, 1× HOT FIREPol® EvaGreen® q-PCR Mix (Solis Biodyne, Tartu, Estonia) and primers at 200nM, using an MJ Research Chromo 4 (Bio-Rad) and MJ Opticon Monitor analytic software (BioRad). Triplicate qPCR reactions were performed and averaged to measure each gene in each cDNA sample. The mean measures of target genes were normalized against a geometric mean determined from three internal control genes (*GAPDH*, *RPL13A* and *SDHA*) for each cDNA sample to yield a relative target gene expression value for all samples using the Pfaffl method (Pfaffl, 2001).

Pair name	Location	Sequence	Annealing	Extension length
Total *C9ORF72*	Exon 2	For-GCAGAGAGTGGTGCTATAGATG	30 s, 60°C	40 s, 72°C
	Exon 5	Rev-GCCTTCATGACAGCTGTCACC		
SOX2	Exon 1	For-TTCACATGTCCCAGCACTACCAGA	30 s, 60°C	20 s, 72°C
	Exon 1	Rev-TCACATGTGTGAGAGGGGCAGTGTGC		
OCT4	Exon 1	For-ACTTCACTTTCCCTCCAACC	30 s, 60°C	40 s, 72°C
	Exon 3	Rev-AGTTTGTGCCAGGGTTTTTG		
GAPDH	Exon 7	For-GTGGACCTGACCTGCCGTCTAG	30 s, 61°C	30 s, 72°C
	Exon 8	Rev-CCTGTTGCTGTAGCCAAATTCGTTG		
RPLA13A	Exon 1	For-CCTGGAGGAGAAGAGGAAAAG	30 s, 60°C	40 s, 72°C
	Exon 1	Rev-TTGAGGACCTCTGTGTAATTGTC		
SDHA	Exon 1	For-TGGGAACAAGAGGGGCTCTG	30 s, 60°C	40 s, 72°C
	Exon 2	Rev-CAACAACTGCATCAAATTCAT		

Table 2.10: Details of primers used

2.3.4 Gel electrophoresis

Agarose was dissolved in TAE buffer by microwaving until the sample was boiling. 1µl of ethidium bromide was added to 25ml of gel before it set in order to visualise the DNA and the gel was then poured into a casting tray. Samples were mixed with 5X loading buffer and loaded into the gel was allowed to settle for 30 minutes prior to running the samples. Samples were run for 30min – 1hour at 120V on a 1% w/v agarose gel in TAE buffer together with 5µl of 1Kb DNA ladder (New England BioLabs). Gels were removed and placed into the BioDOC-IT Imaging system, an UV transilluminator (UVP Inc., San Gabriel, U.S.A.), and photographed digitally under UV transillumination. The size of the DNA was determined by a 100 base pair (bp) DNA ladder (New England BioLabs).

2.3.5 Cell fixing

Cells were grown in 5mm coverslips. Cells were washed twice with 500µl of PBS and then fixed with 4% paraformaldehyde solution for 20 minutes at room temperature. Cells were then washed twice with 500µl of PBS and stored in PBS until analysis was performed.

2.3.6 Quantitative image analysis

MetaMorph Image System 7.5 (v. 7.7, Molecular Devices) and ImageJ (version 1.45e, NIH, Bethesda, USA, http://rsb.info.nih.gov/ij/) software programs were used for quantitative image analysis. For each analysis, 7-12 images were taken with the same exposure times. Images were then converted into 16-bit images from each biological replicate. Three biological replicates were performed for each experiment. A detailed description of different analyses has been included in the corresponding chapters.

2.3.7 Cell harvesting

In order to harvest cells, cells were washed twice with PBS. Plates were then placed on ice and ice cold 300µl RIPA buffer (table 2.11) containing 1X Complete mini protease (Roche) inhibitors was added. Cells were rigorously pipetted and placed into a sterile 1.5ml tube. Cells were then sonicated 3 times for 10 seconds prior to protein quantification.

Component	**Concentration**
TRIS-HCL pH7.4	50 mM
NaCl	150 mM
Triton X-100	1%
Sodium Deoxycholate	1%
SDS	0.5%

Table 2.11: RIPA buffer composition

2.3.8 Protein assay

Protein concentrations were determined using the *DC* Protein Assay Kit II (BioRad) according to the manufacturer's instructions. 1µl of bovine serum albumin (BSA) standards (0 – 2µg/µl) and samples were used in duplicates and pipetted onto a microtiter plate (Corning). 25 µl of a mixture containing 1ml of Reagent A and 20 µl of Reagent S were added to each well. 200 µl of Reagent B was then added to each well. After 15 minutes at room temperature, absorbance was read with a microplate reader set to 750nm. Protein concentrations were calculated based on the mean absorbance of sample duplicates.

2.3.9 Western blotting

10-20µg of lysates were denatured by boiling with 2X SDS sample buffer for 10 minutes at 100°C. Biological replicates, along with 2µl of Precision Plus Protein Dual Color Standard (BioRad), were run on separate NuPAGE Novex 10% Bis-Tris Midi gels in Morpholinepropanesulfonic acid (MOPS) buffer at 150 V until the samples run completely. The gels were incubated in transfer buffer for 5 minutes and transferred to nitrocellulose membranes using iBlot Transfer Stack and the iBlot Gel Transfer Device for 7.5 minutes. Membranes were washed with phosphate-buffered saline with 0.1% Tween 20 (PBST) (Sigma). Membranes were then blocked with 5% non-fat milk solution in PBS for 1 hour and then probed with primary antibodies diluted in a 2.5% milk solution in PBS rolling at 4°C overnight. Membranes were then washed three times with 5ml of PBST and probed with the relevant IRDye secondary antibodies (Li-Cor) diluted 1:5000 in 2.5% milk solution in TBST for 1 hour at room temperature rolling in the dark. Membranes were washed three times with PBST and the fluorescent signal was detected with the Odyssey Infrared Imaging System (Li-Cor Biosciences). Blots were quantitated using ImageJ (version 1.45e, NIH, Bethesda, USA, http://rsb.info.nih.gov/ij/).

2.3.10 Filter trap assay

An Acetate membrane was washed twice with 100µl of RIPA buffer. An appropriate amount of protein lysate was diluted into 100µl of RIPA buffer and added into each well and made to flow though the membrane by aspirating. The membrane was washed three more times with 100 µl of RIPA buffer per well. Membranes were then blocked with 5% non-fat milk solution in PBS for 1 hour and then probed with primary antibodies diluted in a 2.5% milk solution in PBS at rolling at 4°C overnight. Membranes were then washed three times with 5ml of PBST solution and probed with the relevant secondary antibodies (Li-Cor) diluted 1:5000 in 2.5% milk solution in TBST for 1 hour at room temperature rolling in the dark. Membranes were washed three times with PBST and the fluorescent signal was detected with the Odyssey Infrared Imaging System (Li-Cor Biosciences).

2.3.11 Fluorescent *in situ* hybridisation for RNA probes of cell lines

PBS was removed and cells were permeabilised for 5 minutes with 0.1% Triton-X solution. Cells were then incubated for 15 minutes in pre-hybridisation solution (table 2.12). Probe was diluted to its final concentration (see table 2.14 of FISH probes) in hybridisation solution (table 2.13). Pre-hybridisation solution was discarded and 10µl of diluted probe was added dropwise at the top of the cells. Cells were then covered with circular pieces of parafilm to prevent evaporation. Cells were incubated in a hybridisation oven for the selected period of time at the indicated hybridisation temperature shown in table 2.14. Cells were then washed twice 2X SCC for 15 minutes followed by two washes with PBS at room temperature. Cells were then treated with 0.01% RNAse/PBS solution for 5 minutes in order to reduce background staining. Immunohistochemistry was then performed or cells were incubated with DAPI counterstain (1.25µg/ml) for 5 minutes and mounted on microscope slides (SuperFrost, VWR) using Fluorsave reagent and dried over night at 4°C. Samples were then imaged with a Zeiss inverted phase contrast fluorescent microscope or a Leica laser scanning confocal microscope (TCS-SP5).

Component	Concentration
Formamide	40%
SCC	2X

Table 2.12: Prehybridisation solution

Component	Concentration
Dextransulphate	5%
Fromamide	25%
SCC	2X
tRNA	10 mg/ml

Table 2.13: Hybridisation solution

2.3.12 Fluorescent *in situ* hybridisation for LNA probes

After fixing, the PBS was removed and cells were permeabilised for 5 minutes with 0.1% Triton-PBS solution. Cells were incubated for 15 minutes in pre-hybridisation solution (table 2.12). Probe was diluted to its final concentration (see table 2.14 of FISH probes) in hybridisation solution (table 2.13). Pre-hybridisation solution was discarded and 10µl of diluted probe was added dropwise at the top of the cells. Cells were then covered with circular pieces of parafilm to prevent evaporation. Cells were incubated in a hybridisation oven for the selected period of time at the indicated hybridisation temperature shown in table 2.14. Cells were then washed twice 2X SCC, 0.1% TWEEN solution for 15 minutes followed by two washes with 0.1X SCC solution at 60°C. Immunofluorescence was then performed or cells were incubated with DAPI counterstain (1.25 µg/ml) for 5 minutes and mounted using Fluorsave reagent.

2.3.13 Double fluorescent *in situ* hybridisation

Hybridisation with an EGFP LNA targeting probe (5'TYE–563–ATGATTGTGGCGGATCTTGAAGT) was performed at 66°C in a humid chamber overnight at a concentration of 20nM. Cells were washed 3 times with 2X SCC. A second hybridisation was carried out with an Cy5-(C4G2)x8 RNA probe over night as previously described. When FISH was followed by ICC, cells were kept PBS in the dark at 4°C. ICC was performed as previously described using an hnRNP-H rabbit antibody (ab10374).

FISH probe name	**Sequence**	**Hybridisation temp (°C)**	**Working concentration**	**Composition**
C4G2	(CCC CGG)x8 – Cy3	48	5 ng/µl	RNA
C4G2	(CCC CGG)x8 – Cy5	48	5 ng/µl	RNA
C4G2	(CCC CGG)x4 – Cy3	60	2 ng/µl	LNA
G4C2	(GGG GCC)x4-Cy3	60	2 ng/µl	LNA
EGFP LNA	(ATGTTGTGGCGGATCT TGAAGT) – Cy3	60	20 ng/µl	LNA

Table 2.14: Details of FISH probes

2.3.14 Immunofluorescence

Cells were fixed as previously described, permeabilised in 0.1% Triton-X in PBS at room temperature for 5 minutes and blocked in 5% donkey serum (Sigma) in PBS at room temperature for 20 minutes. Cells were probed with the selected primary antibodies diluted in 2.5% donkey serum overnight at 4°C. Details of the antibodies used are provided in each chapter. AlexaFluor-488, AlexaFluor-550 and AlexaFluor-650-labelled secondary antibodies raised in the appropriate species (Thermo Scientific) were diluted 1:500 in PBS and applied for 1 hour at room temperature in the dark. DAPI (Sigma) counterstaining (1.25µg/ml) was

then applied for 5 minutes at room temperature in the dark. Coverslips were mounted on microscope slides (SuperFrost, VWR) with Fluorsave mounting medium and dried at 4°C overnight before imaging with a Zeiss Axiovert S100 (HB0100) (Carl Zeiss Ltd.) inverted phase contrast fluorescent microscope or a Leica laser scanning confocal microscope (TCS-SP5).

2.3.15 Neurite outgrowth assay

Neuronal progenitor cells were counted using a NucleoCounter (Chemometech). Approximately 1500 cells were plated per well per cell line in triplicate for each condition (no PPMO, control PPMO and G4C2 PPMO) on a 96-well optic plate (Falcon) coated with matrigel in neuronal differentiation medium. PMOs were added to each well shortly after plating. Cells were allowed to differentiate for 7 days in the absence of FGF and fixed in 4% PFA for 15 minutes. Cells were stained with rabbit MAP2 antibody (ab5392) at a dilution of 1:500 at 4°C overnight. Cells were washed twice with PBS and incubated with anti-rabbit AlexaFluor 488 secondary for 1 hour at room temperature. Cells were washed three times with PBS and incubated for 5 minutes with DAPI counterstain solution.

Images were taken by looking at the DAPI counterstain channel for all conditions in all 3 wells until 30-60 MAP2 positive cells were imaged where the neurites did not cross the image boundary using a Zeiss Axiovert S100 microscope at a magnification of X20. The average neurite length per cell was quantified in a blinded manner using Image J simple neurite tracer plugin.

$$Average\ total\ neurite\ length = \frac{total\ neurite\ length}{total\ number\ of\ cells}$$

2.3.16 Alamar Blue assay

Alamar blue assay was performed in 96-well plated. Growth media was removed and an equal volume of medium containing Alamar blue reagent (Thermo Fischer) was added into each well following the manufacturer's instructions. After 3 hours of incubation the

media was collected and analysed using a microplate reader following the manufacturer's indications.

2.3.17 Fluorescent activated cell sorting (FACS) – Cell survival assay

Cell survival of iPSC-derived neurons was measured with FACS soring using the cell death marker Annexin V and the mitochondrial depolarisation marker DICL. iPSC-derived neurons were grown in 12-well plates. The culture media was collected into a 15 ml falcon tube. Cells were washed once with PBS, which was collected and added in the same tube. Cells were dissociated by incubating with 300 µl of Accutase (Life Technologies) dissociation reagent for 7 minutes at 37°C. Accutase was inactivated by adding 700µl of plain culture media and all the cells were collected into the corresponding falcon tube. The cells were pelleted by centrifugation at 1000g for 4 minutes. Cells were dissociated into a single cell suspension in PBS by pipetting gently with a P1000 pipette. Cells were then centrifuged and resuspended in 500µl of warm PBS buffer containing DICL and Annexin V450 at 1:1000 and 1:500 concentrations following the manufacturer's instructions.

FACS was carried out in a Canto II flow cytometer (BD Biosciences). 10 000 cells were sorted for each condition in each experiment. Three biological replicates were performed. Data was analyzed with FlowJo software as previously described (Chen et al., 2016).

3 PATHOLOGICAL STUDIES IN THE SPINAL CORD OF C9ORF72 ALS MUTANT CASES

3.1 INTRODUCTION

The neurotoxic mechanisms of the *C9ORF72* expansion are unknown but three mechanisms have been proposed: loss of C9ORF72 protein function, toxicity due to RNA aggregation, and toxicity due to repeat associated non-ATG (RAN) translation of dipeptide repeat (DPR) proteins. Although the G4C2 expansion does cause a decrease in *C9ORF72* mRNA no null alleles or missense mutations in *C9ORF72* have been identified in ALS or FTD cases (Harms et al., 2013) and homozygous carriers do not have an earlier onset or rapidly progressive form of ALS or FTD to support the loss of C9ORF72 protein function hypothesis (Cooper-Knock et al., 2013; Fratta et al., 2013). We, and others have previously reported that G4C2 repeats generate length-dependent, RNase-resistant, intranuclear RNA foci, which can sequester RNA binding proteins potentially leading to defective RNA processing (Cooper-Knock et al., 2014a; Lee et al., 2013; Mori et al., 2013b). Finally, the G4C2 repeat RNA form stable G-quadruplex secondary structures that can recruit the translation machinery (Zu et al., 2011) and generate five different DPRs; poly-GP, poly-GA and poly-GR from the sense G4C2 repeat and poly-PR, poly-PA and poly-GP from the antisense G4C2 repeat strand (Ash et al., 2013; Gendron et al., 2013; Mori et al., 2013a; Mori et al., 2013c).

Antibodies to specific DPR proteins detect cytoplasmic aggregates of poly-GP, poly-GA and poly-PA and intranuclear aggregates of poly-PR and poly-GR in the cerebellum and frontal cortex of ALS and FTD patients (Mackenzie et al., 2013a; Mann et al., 2013). DPR protein aggregates colocalise with p62 but not with TDP-43 (Mackenzie et al., 2013a; Mann et al., 2013) and the connection between the *C9ORF72* mutation, DPR protein deposition and TDP-43 mislocalisation is unknown. In the present study, we conducted a detailed comparison of the abundance and cellular location of inclusions immuno-reactive for the five

DPR proteins and TDP-43 in the spinal cord of ten C9ORF72-ALS cases. Using double immunofluorescence staining, we show that DPR protein aggregates are uncommon in the spinal cord of *C9ORF72*-ALS cases, rarely co-localise with TDP-43, and are almost absent from motor neurons. The abundance of TDP-43 inclusions in ALS cases with or without a *C9ORF72* repeat expansion was broadly similar. Given that TDP-43 mislocalisation is a recognised cause of lower motor neuron neurodegeneration, and given the lack of DPRs in motor neurons, it is difficult to implicate DPRs in this process.

Moreover, there have been few pathological studies assessing the presence of sense and antisense RNA foci in ALS-C9ORF72 cases. Most of the studies have assessed the presence of sense and antisense foci in the frontal cortex, cerebellum and hippocampus of C9ORF72 ALS/FTD cases (DeJesus-Hernandez et al., 2017; Gendron et al., 2013; Mizielinska et al., 2013). Only one study has comprehensively quantified the number of sense and antisense RNA foci in the spinal cord of ALS cases (Cooper-Knock et al., 2015). Cooper-Knock *et al.* (2015) reported a strong correlation between the presence of antisense, but not sense, RNA foci and TDP-43 nuclear depletion in spinal motor neurons. Their study however only analysed 54 motor neurons from seven C9ORF72 ALS cases. In the present study we have assessed the presence of sense and antisense RNA foci in the spinal cord of ten C9ORF72 ALS cases using a semi quantitative scale. Additionally we have quantified the number of motor neurons containing sense and antisense foci and TDP-43 nuclear depletion. We show that sense and antisense RNA foci are common in the spinal cord of C9ORF72 ALS cases and that there are significantly greater number of motor neurons containing sense than antisense RNA foci.

3.2 AIMS

In the present study we aim to study the presence of all five DPR protein inclusions, as well as sense and antisense RNA foci, in the spinal cord of ten C9ORF72 ALS cases and five C9-ve ALS cases. Moreover, we have quantified the presence of each species and assessed whether their presence correlates with TDP-43 aggregation and nuclear depletion in spinal motor neurons.

3.3 MATERIALS AND METHODS

3.3.1 Cases

Spinal cord sections were analysed for the presence of TDP-43 and all DPR inclusions by double immunofluorescence and TDP-43 and sense and antisense RNA foci from ten ALS cases positive for *C9ORF72* intronic expansion (C9+ve-ALS) and sections from five ALS cases negative for *C9ORF72*, *FUS* and *SOD1* mutations (365 sections in total). Sections of frontal lobe and cerebellar cortex from a case of C9ORF72 FTD with abundant p62 pathology were chosen as a positive control for DPR staining. Expansion carriers were identified using repeat primed PCR (Smith et al., 2013) and all of the cases had previously been reported to show characteristic cerebellar p62 and TDP-43 pathology (Troakes et al., 2012) (Al-Sarraj et al., 2011). Details of the age, sex and post-mortem delay are recorded in table 3.1 and show little difference between cases with and without *C9ORF72* mutations.

Case	Age	SEX	PMD	Diagnosis
1	73	M	42	ALS-TDP
2	70	F	27	ALS-TDP
3	60	M	70	ALS-TDP
4	44	F	24	ALS-TDP
5	68	M	5	ALS-TDP
mean±SEM	63±5		33±11	ALS-TDP
6	59	F	35	ALS-C9+ve
7	70	M	38	ALS-C9+ve
8	59	M	46	ALS-C9+ve
9	43	F	69	ALS-C9+ve
10	53	M	82	ALS-C9+ve
11	70	M	60	ALS-C9+ve
12	55	M	76	ALS-C9+ve
13	58	M	11	ALS-C9+ve
14	64	M	68	ALS-C9+ve
15	51	M	64	ALS-C9+ve
mean±SEM	58±2		55±5	

Table 3.1 Clinical data of cases studied

(PMD) = post mortem delay (hours).

3.3.2 Motor neuron counting and double label immunofluorescence

A total of 30 spinal cord sections from C9+ve-ALS cases were analysed. Histological examination was performed on 7 µm sections prepared from formalin-fixed, paraffin–embedded tissue from the spinal cord of all ALS cases. Sections were stained with hematoxylin and eosin to perform motor neuron counts, and sequential sections were processed for double label immunofluorescence for the DPRs, sense and antisense foci and TDP-43. Immunofluorescence was performed as described in the methods section.

Semi-quantitative and quantitative evaluation of DPR and TDP-43 pathology was performed using Zeiss Axiovert S100 microscope. Aggregates were also imaged using a Leica Confocal SP microscope. A “secondary antibody only” control was introduced in each staining procedure.

3.3.3 Semi quantitative and quantitative evaluation of pathology

The presence of sense and antisense foci and DPR and TDP-43 inclusions were scored in the spinal cord using a previously published semi-quantitative grading scale (Mackenzie et al., 2013a), in which the total number of immuno-reactive inclusions/RNA foci, as well as the cytoplasmic inclusions (CI) and the intranuclear inclusions (NI), were rated as follows: **0** – Absent, **0.5** – one or two inclusions in the whole section, **1**- very few, **2**- occasional- easy to find and a few cells are affected, **3**- moderate- many of the cells are affected, inclusions are easy to find, **4**- numerous- nearly all of the cells are affected. Additionally, each section was re-analysed and the number of DPR and TDP-43 inclusions was counted manually in a systematic, blinded manner. The number of DPR aggregates was counted per section and averaged per case.

3.3.4 Fluorescent *in situ* hybridisation for spinal cord sections

Fluorescent *in situ* hybridisation (FISH) was performed in 20 lumbar spinal cord sections from ten C9+ve-ALS cases and 13 sections from five ALS-TDP-43 cases as described in the methods section.

If IHC was performed to assess the co-occurrence of TDP-43 and RNA foci, sections were blocked with 5% Donkey serum-PBS solution for 1 hour and incubated with TDP-43 (mouse polyclonal TDP-43 10782-AP Proteintech) at a dilution of 1:100. Sections were washed three times with PBS and incubated with anti-rabbit (AlexaFluor 488) secondary antibody for 1 hour. The sections were then treated with DAPI counterstain and mounted in Floursave.

3.4 RESULTS

3.4.1 Appearance of DPR proteins in ALS spinal cords

The appearance and subcellular location of each type of DPR inclusion within the spinal cord was recorded (Table 3.2 and Fig 3.1A-H). There were very few DPR inclusions with poly-GA aggregates being the most abundant DPR detected with a rating of only 0-1.0. Cytoplasmic immuno-reactive inclusions more common than intranuclear inclusions, which is consistent with previous studies in FTD and ALS (Mackenzie et al., 2013a). Cytoplasmic inclusions were characteristically large, irregular and perinuclear whilst nuclear inclusions were much smaller and round. Poly-GP inclusions, the second most common DPR inclusion, were all cytoplasmic and in a perinuclear position (Fig 3.1B). We observed very few cytoplasmic poly-GR inclusions and only one small intra-nuclear aggregate. Poly-PR cytoplasmic aggregates were also rare in the nucleus and cytoplasm (Fig 3.1E, 3.1G). Similarly, we were only able to identify a total of only seven poly-PA inclusions (six cytoplasmic and one nuclear; Fig 3.1D, 2.1H) and four poly-PR inclusions (two cytoplasmic and two nuclear; Fig 3.1E, 3.1G) inclusions in all the analysed cases (Fig 3.1D, 3.1H). No immuno-reactive DPR aggregates were identified in any C9-ve TDP-43 cases confirming the mutation-specificity of these inclusions and validating the antibodies. In a small number of cells that contained DPR aggregates granular TDP-43 staining was seen in the cytoplasm or absent in the nucleus (Fig 3.1) consistent with previous studies (Mackenzie et al., 2013a).

Table 3.2: Scoring of TDP-43 and DPR inclusions

	TDP-43 agg.	Poly-GP			Poly-GA			Poly-GR			Poly-PR			Poly-PA			Diagnosis
case		Cyt.	Nuc.	Tot.	Cyt.	Nuc.	Tot.	Cyt.	Nuc.	Tot.	Cyt.	Nuc.	Tot.	Cyt.	Nuc.	Tot.	
1	3	0	0	0	0	0	0	0	0	0	0	0	0	0	0	0	ALS-TDP
2	3	0	0	0	0	0	0	0	0	0	0	0	0	0	0	0	ALS-TDP
3	2	0	0	0	0	0	0	0	0	0	0	0	0	0	0	0	ALS-TDP
4	3	0	0	0	0	0	0	0	0	0	0	0	0	0	0	0	ALS-TDP
5	3	0	0	0	0	0	0	0	0	0	0	0	0	0	0	0	ALS-TDP
MEAN±SEM	**2.8±0.2**																**ALS-TDP**
6	3	0.5	0	0.5	0	0	0	0.5	0	0.5	0	0	0	0.5	0	0.5	C9+ve-ALS
7	3	0.5	0	0.5	1	0.5	1.5	0	0	0	0	0	0	0	0	0	C9+ve-ALS
8	2	1	0	1	0.5	0	0.5	0.5	0	0.5	0	0	0	0.5	0	0.5	C9+ve-ALS
9	3	1	0	1	1	0.5	1.5	0	0	0	0	0	0	0.5	0.5	1	C9+ve-ALS
10	3	0.5	0	0.5	0.5	0.5	1	0.5	0	0.5	0	0	0	0	0	0	C9+ve-ALS
11	3	1	0	1	1	0.5	1.5	0	0.5	0.5	0.5	0	0.5	0.5	0	0.5	C9+ve-ALS
12	3	0.5	0	0.5	0.5	0	0.5	0.5	0	0.5	0.5	0.5	1	0	0	0	C9+ve-ALS
13	3	1	0	1	1	0.5	1.5	0.5	0	0.5	0	0.5	0.5	0.5	0	0.5	C9+ve-ALS
14	3	1	0	1	0.5	0	0.5	0	0	0	0	0	0	0	0	0	C9+ve-ALS
15	3	0.5	0	0.5	1	0	1	0	0	0	0	0	0	0	0	0	C9+ve-ALS
MEAN±SEM	**2.9±0.1**	**0.7±0.1**	**0.0**	**0.7±0.1**	**0.7±0.1**	**0.2±0.1**	**0.9±0.1**	**0.3±0.1**	**0.0±0.1**	**0.3±0.1**	**0.1±0.1**	**0.0±0.1**	**0.2±0.1**	**0.2±0.1**	**0.0±.01**	**0.3±0.1**	

Table 3.2: Scoring of immunoreactive inclusions of TDP-43 and five DPRs in the spinal cord of 5 ALS-TDP-43 and 10 C9+ve-ALS cases.

Results show that there are very few DPR aggregates in the spinal cord of C9+ve-ALS cases and are absent in ALS-TDP-43 cases. However we observe large numbers of TDP-43 aggregates in all 15 cases analysed. Cyt- cytoplasmic inclusion. Nuc.- Nuclear inclusion. **Scoring criteria: 0** – Absent **0.5** – one or two inclusions in the whole section **1**- very few **2**- occasional- easy to find and a few cells are affected **3**- moderate- many of the cells are affected, inclusions are easy to find **4**- numerous- nearly all of the cells are affected

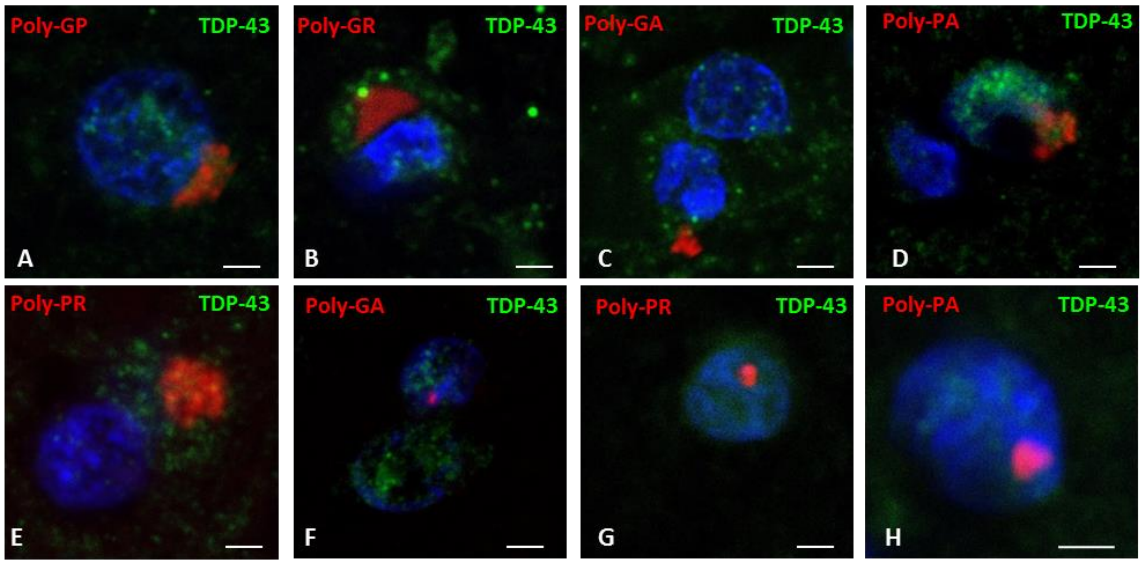

Figure 3.1: Appearance of DPR protein inclusions in the spinal cord of C9+ve-ALS cases

(A-H) Representative immunofluorescence confocal images of DPR (red) and TDP-43 (green) (scale bar=20µm). **(A-E)** Cytoplasmic DPR inclusions, which are often perinuclear. **(F-H)** nuclear DPR inclusions. DPR inclusion (red), TDP-43 (green), Nuclei (blue). Scale bar= 20 µm.

3.4.2 All DPRs are rare and some very rare, but TDP-43 pathology was abundant and consistent

The frequency of each DPR inclusion was initially scored using a semi-quantitative system for each case (table 3.2). DPRs translated from the sense strand (poly-GP, poly-GA and poly-GR) were more abundant than those translated solely from the antisense strand (poly-PR, poly-PA). Although poly-GA and poly-GP were the most abundant immuno-reactive inclusions (scoring of 0.9 and 0.7, respectively) all DPRs were scored as either rare or very rare and there was not a single case that scored above 1.0 (rare) and no more than twelve inclusions of any DPR was observed in any of the cases analysed. No case scored above 0.5 (very rare) for poly-GR, poly-PA and poly-PR inclusions and poly-GR and poly-PR inclusions were absent from several cases. The scoring of DPR aggregates within cases was highly consistent (poly-GA=0.9±0.1, poly-GP=0.7±0.1, poly-GR=0.8±0.21, poly-PA=0.4±0.20 and

poly-PR=0.3±0.1). Of note, there was no significant difference in the scoring of TDP-43 inclusions for ALS cases lacking the *C9ORF72* mutation (2.8±0.2) when compared to those carrying the *C9ORF72* mutation (2.9±0.1). Thus, the presence of DPR inclusions in the spinal cord does not appear to be correlated with the abundance of TDP-43 inclusions.

In order to provide greater detail the number of TDP-43 aggregates in the anterior horn of the spinal cord in each case was quantified in representative sections to explore any correlation between the abundance of DPR and TDP-43 inclusions. An average of 122±8 TDP-43 aggregates was identified per case, which is between 45- and 750- fold greater than the number of any DPRs inclusions These results, graphically depicted in Figure 3.2, demonstrate that the abundance of TDP-43 cytoplasmic inclusions vastly outnumbers the number of DPR inclusions, singly or collectively (note that the Y axis scale is a logarithmic scale). **reversing the formatting error.**

Figure 3.2: Frequency of TDP-43 and DPR inclusion per case.

The number of TDP-43 and DPR immunoreactive inclusions was counted for each case. The graph shows the number of TDP-43 and the five different aggregates in order of abundance. There are many more TDP-43 aggregates than any DPR. Note: The Y axis scale is logarithmic scale. Horizontal bars show mean ±SEM

3.4.3 DPR and TDP-43 inclusions occasionally colocalise

Although all DPRs were rare or very rare, we did see TDP-43 colocalise with 4 of the 12 poly-GR inclusions and 2 of the 7 poly-PA inclusions (Fig 3.3 A-B). Interestingly, the poly-GR immuno-reactive aggregates that did not colocalise were often surrounded by TDP-43 (Fig 3.1B). None of the nuclear poly-GR and poly-PA intranuclear inclusions colocalised with TDP-43. We did not observe any poly-GP, poly-GA or poly-PR immuno-reactive inclusions that colocalised with TDP-43 inclusions.

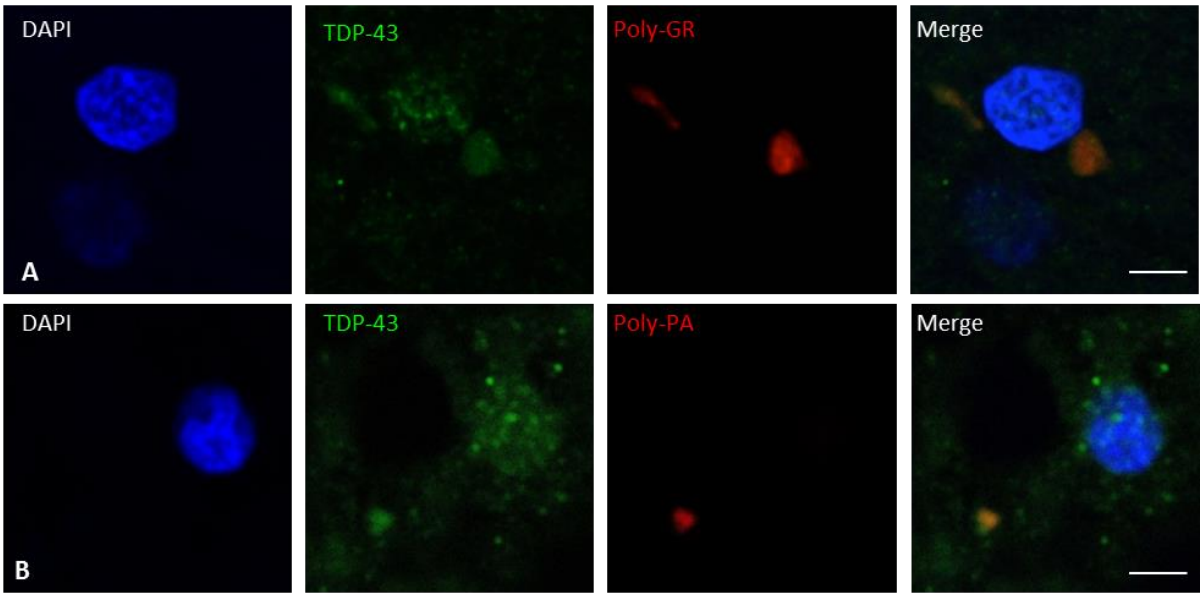

Figure 3.3: DPR and TDP-43 protein inclusions occasionally colocalise

(A-B) Evidence of poly-GR and poly-PA DPR inclusions colocalising with TDP-43. TDP-43 inclusions. DPR inclusion (red), TDP-43 (green), Nuclei (blue). Scale bar= 20 µm.

3.4.4 DPRs are almost absent from motor neurons

ALS is characterised by the loss of lower motor neurons in the anterior horn of the spinal cord. Motor neurons are readily identified as they have large cell bodies and large pale nuclei by H&E staining and by DAPI for immunofluorescence. The total number of motor neurons was counted in order to assess the relative preservation of motor neurons between cases and identify any that contained TDP-43 and DPR immuno-reactive inclusions. In total, of the 786 motor neurons analysed 268 (34%) contained cytoplasmic TDP-43 inclusions (Fig 3.4), which is consistent with classical ALS pathology. In contrast, only one motor neuron contained a DPR inclusion, specifically a cytoplasmic poly-GP aggregate (0.1%) (Fig 3.4B). Occasionally we observed DPR and TDP-43 aggregates in the same cell but never in motor neurons.

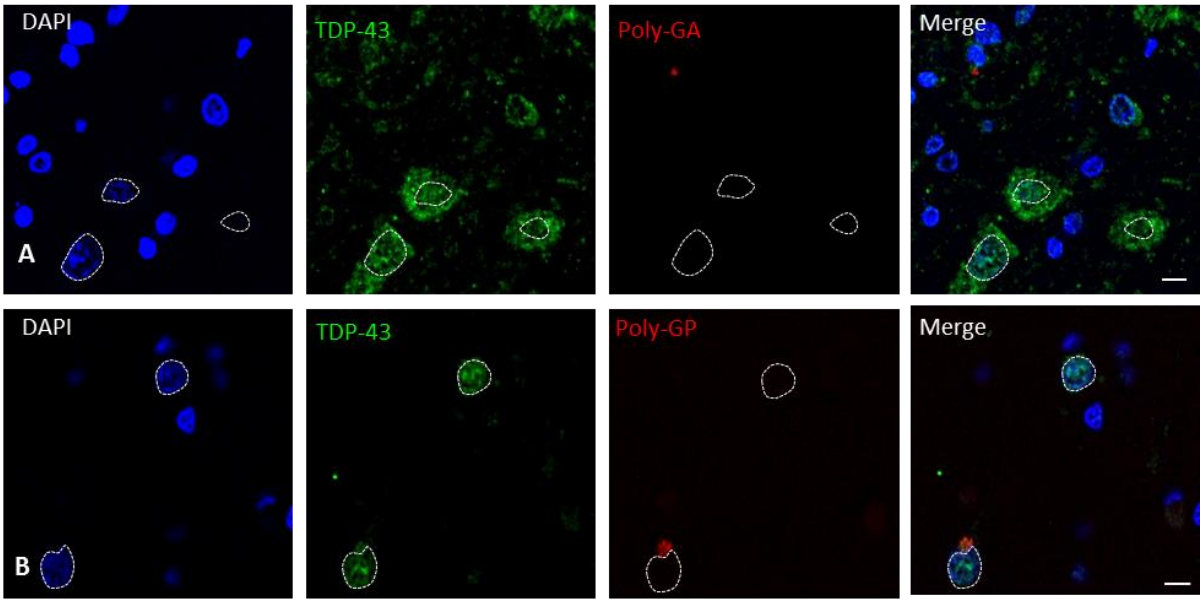

Figure 3.4: DPR inclusions are rare in the spinal cord of C9+ve-ALS cases

(A-B) lower power images of the anterior horn showing the relative abundance of DPR and TDP-43 inclusions. **(A)** poly-GA inclusion, which is not in the motor neurons (dotted lines) that show extensive cytoplasmic TDP deposition. **(B)** poly-GP inclusion within a motor neuron (identified by its large pale nucleus), which does not show cytoplasmic TDP-43 inclusions. DPR inclusion (red), TDP-43 (green), Nuclei (blue) Scale bar= 50 µm.

3.4.5 Sense and antisense RNA foci are common in the spinal cord and motor neurons in ALS cases

We sought to investigate the same cohort of ALS cases and assess the presence of sense and antisense RNA foci. Fluorescent *in situ* hybridisation (FISH) was performed on spinal cord sections in the lumbar region from five TDP-ALS (C9-ve) and ten C9+ve-ALS cases and the presence of sense and antisense RNA foci was quantified using a semi-quantitative scale in a blinded manner. As expected, no RNA foci were observed in any of the ALS-TDP-43 (C9-ve) cases and were therefore used as negative controls. In contrast, all C9+ve-ALS cases had occasional or moderate sense and antisense RNA foci in the anterior horn of the spinal cord and sense foci were more common than antisense foci (Fig 3.5 A and B sense foci score = 2.3 ± 0.3; antisense foci score = 1.8± 0.4). We conclude that sense RNA foci are more common than antisense RNA foci and both species are a consistent pathological hallmark of C9+ve-ALS cases.

A)

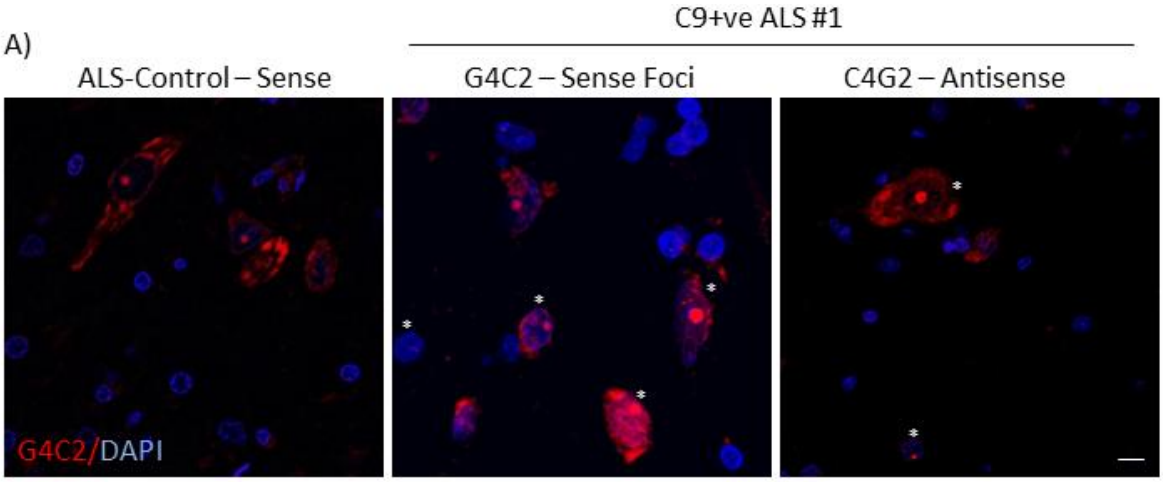

B)

Case	Sense Score	Antisense Score
1	0	0
2	0	0
3	0	0
4	0	0
5	0	0
Average	**0**	**0**
6	2	2
7	2	1
8	3	2
9	2	3
10	2	2
11	2	2
12	3	2
13	3	1
14	2	2
15	2	1
Average	**2.3±0.3**	**1.8±0.4**

Figure 3.5: Sense and antisense RNA foci are common in the spinal cord of C9+ve-ALS cases

(A) Representative images sense and antisense fluorescent *in situ* hybridisation in C9+ve-ALS cases and ALS-TDP. Asterisks (*) indicate the presence of sense and antisense RNA foci. RNA foci (red) and nuclei (blue). Scale bar = 20 μm **(B)** Sense and antisense RNA foci scoring in the spinal cord of *C9ORF72* mutation negative (1-5) and positive ALS cases (6-15). **Scoring criteria: 0** – Absent **0.5** – one or two inclusions in whole section, **1**- very few, **2**- occasional- easy to find and a few cells are affected, **3**- moderate- many of the cells are affected, inclusions are easy to find, **4**- numerous- nearly all of the cells are affected

3.4.6 Sense RNA foci are significantly more common than antisense RNA foci in spinal motor neurons but do not correlate with TDP-43 proteinopathy

ALS is characterised by the loss of motor neurons in the anterior horn of the spinal cord accompanied by nuclear TDP-43 depletion in the spinal cord motor neurons. We investigated the presence of sense and antisense RNA foci in the motor neurons of all ten C9+ve-ALS cases. Our results show that there are a significantly more spinal motor neurons containing sense than antisense RNA foci in the nucleus (Fig 3.6 B: sense foci = 33.8% ± 2.8 vs. antisense 20.7% ± 1.6 over 200 motor neurons; Two-tail t-test, $p<0.001$ **).

Next we sought to investigate whether there is a correlation between the presence of RNA foci (sense and antisense) and TDP-43 nuclear depletion in motor neurons of C9+ve-ALS cases. A FISH analysis followed by immunohistochemistry (IHC) was performed on the same spinal cord samples aforementioned.

TDP-43 nuclear depletion was observed in 38% of motor neurons and sense RNA foci in 33% of all motor neurons identified. Interestingly, 15% of all motor neurons contained both intranuclear RNA foci and showed TDP-43 nuclear depletion (Fig 3.6 A and C-D). This result shows that the burden of sense RNA foci was similar to TDP-43 nuclear depletion in the spinal cord of our C9+ve-ALS cohort. However we did not observe a correlation between the presence of sense RNA foci and loss of nuclear TDP-43 depletion ($X^2 = 3.72$, d.f=1, $p=0.073$) (Fig 3.6 C).

A previous study has reported the correlation between TDP-43 nuclear loss and the presence of antisense RNA foci in spinal motor neurons of C9+ve-ALS cases (Cooper-Knock et al., 2015). We therefore assessed the co-occurrence of antisense RNA foci and TDP-43 nuclear depletion. Only 7% of the analysed motor neurons showed both loss of nuclear TDP-43 and antisense RNA foci. In contrast, 14% of the motor neurons analysed showed the presence of antisense RNA foci but no apparent TDP-43 nuclear loss (Fig 3.6 D) ($X^2 = 0.26$,

d.f=1, p=0.61). Thus we were unable to replicate the previous report correlating antisense RNA foci and the loss of nuclear TDP-43 in spinal motor neurons.

A)

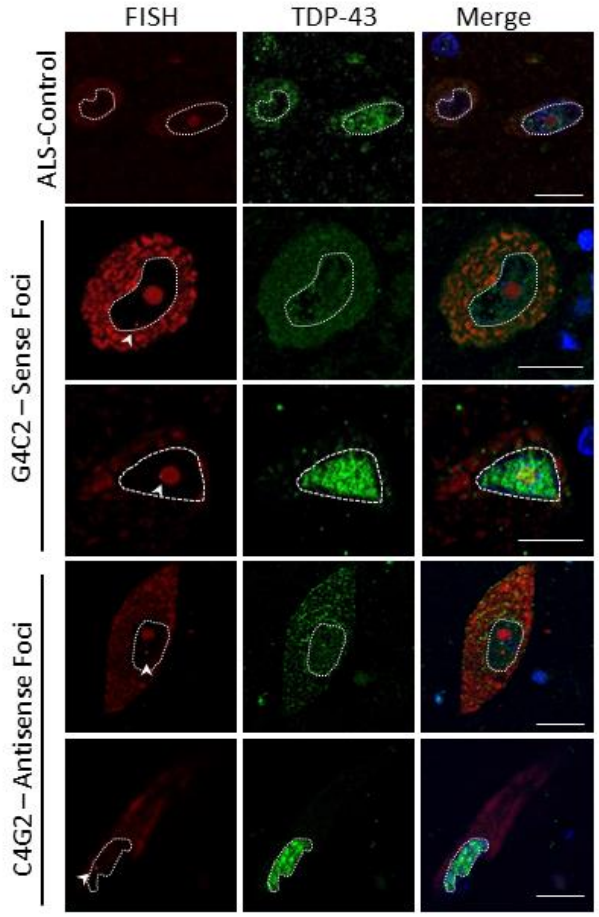

B)

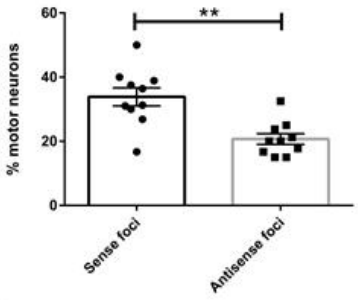

C)

		loss of nuclear TDP-43	
		yes	no
sense foci	yes	33 (15%)	37 (18%)
	no	49 (23%)	93 (44%)

n=213

D)

		loss of nuclear TDP-43	
		yes	no
Antisense foci	yes	20 (7%)	42 (14%)
	no	84 (29%)	148 (50%)

n=294

E)

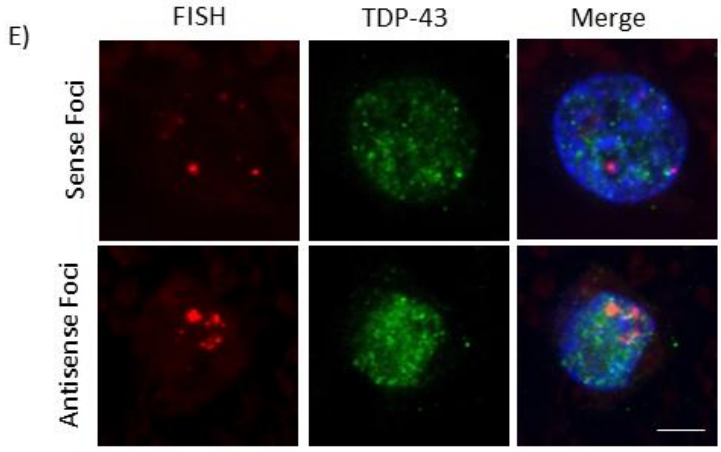

Figure 3.6: Motor neurons containing sense foci are more common than those containing antisense foci

(A) Representative images of sense and antisense fluorescent *in situ* hybridisation and immunohistochemistry on ALS-TDP-43 and C9+ve-ALS spinal cord motor neurons showing the presence of intranuclear sense RNA foci and TDP-43 nuclear clearing. G4C2 foci (red), TDP-43 (green) and nuclei (blue). Scale bar = 50 µm **(B)** The percentage of motor neurons containing sense RNA foci is significantly greater than antisense foci. n=10 over 200 motor neurons. Two-tailed t-test ($p<0.001$ **) **(C)** Results of the quantification of 213 spinal motor neurons of 10 C9+ve-ALS cases for the coincidence of sense RNA foci and TDP-43 nuclear clearing. Total number and percentage of motor neurons containing sense foci and TDP-43 **(D)** Results of the quantification of 294 spinal motor neurons of 10 C9+ve-ALS cases for the coincidence of antisense RNA foci and TDP-43 nuclear clearing. Total number and percentage of motor neurons containing antisense foci and TDP-43. **(E)** Representative images of neurons containing large numbers of sense and antisense foci. Scale bar = 20 µm

3.5 DISCUSSION

The G4C2 repeat mutation in the *C9ORF72* gene is the most common cause of ALS and FTLD known to date. Three mechanisms of toxicity have been proposed, i) loss of C9ORF72 protein due to silencing and degradation of its transcript ii) toxicity though toxic RNA species and iii) toxicity though unconventional translation of G4C2 repeats from the sense and the antisense strand yielding toxic di-peptide repeat proteins (DPRs). In this study we analysed and quantified the presence of sense and antisense foci, all five DPRs known to translate from the sense and the antisense G4C2 strands and TDP-43 in the spinal cord five ALS-TDP-43 (C9-ve) and ten C9+ve-ALS cases.

We have shown that sense RNA foci are more common than antisense foci and are present throughout the spinal cord of C9+ve-ALS cases. We detected very low levels of all DPR protein inclusions in the spinal cords of C9+ve-ALS cases, with poly-GA being the most common followed by poly-GP, poly-GR, poly-PA and poly-PR. The frequency of TDP-43 cytoplasmic inclusions was three to four orders of magnitude higher than DPR inclusions, providing much stronger circumstantial evidence that the accumulation of TDP-43 and not DPRs is the dominant pathogenic process in ALS.

Inclusions for all five DPRs were detected in the spinal cord of C9+ve-ALS cases but they were rare or very rare and it was very uncommon to see DPR and TDP-43 inclusions in the same cell. Poly-GA inclusions, present in the cytoplasm and occasionally the nucleus, were the most common. Poly-GP inclusions were purely cytoplasmic, which is consistent with published reports (Ash et al., 2013; Davidson et al., 2014; Mackenzie et al., 2013a; Mackenzie et al., 2014; Mann et al., 2013; Mori et al., 2013a; Mori et al., 2013c). Of the five DPRs, only poly-GR and poly-PA physically colocalised with TDP-43 inclusions, but this was a very rare event. The total number of TDP-43 inclusions in the spinal cord was between 45- and 750-fold higher than the number of DPR inclusions. We detected only one motor neuron that contained a poly-GP inclusion, whereas on average 34% of motor neurons had cytoplasmic TDP-43 inclusions. Our results are consistent with those published using single staining techniques but were the first to use double labelling with TDP-43 and all five DPRs in the spinal cord of ALS cases (Mackenzie et al., 2013a; Mackenzie et al., 2015). We acknowledge that detection of DPRs by immunofluorescence imaging may be less sensitive than horse radish peroxidase (HRP) but these were abundant in the frontal cortex of our *C9ORF72* mutation positive cases used as a positive control. This study was the first to analyse the presence of all five DPRs in the spinal cord of C9+ve-ALS cases. A separate study also demonstrated the absence of soluble DPRs in the spinal cord of C9+ve-ALS cases (Mackenzie et al., 2015) and the absence of correlation between DPR aggregation and neurodegeneration (Davidson et al., 2016).

Several groups have studied DPR protein toxicity in various cellular models but these have generated conflicting results (May et al., 2014; Tao et al., 2015; Wen et al., 2014; Yamakawa et al., 2015; Zhang et al., 2014b). Some reports describe the greatest toxicity from poly-GR and poly-PR expression in cells (Wen et al., 2014; Yamakawa et al., 2015) and the Drosophila (Mizielinska et al., 2014). Several other studies have suggested that poly-GA is the most toxic DPR *in vitro* (Chang et al., 2016; Schludi et al., 2015; Zhang et al., 2014b) and

in vivo (Schludi et al., 2017; Zhang et al., 2016b). However, these models involve the overexpression of DPRs and no comparison was made with the burden of DPR deposition in human tissues. A landmark study, in which 66 G4C2 repeats were expressed in the central nervous system of mice, has shown that nuclear RNA foci, DPR inclusions *and* TDP-43 pathology were present in the cortex and hippocampus of mice, suggesting that the repeat itself, possibly through foci formation, RAN translation or another mechanisms entirely, caused aberrant TDP-43 deposition (Chew et al., 2015a). We have demonstrated that DPR inclusions are very rare in C9+ve-ALS spinal cords, are infrequently associated with TDP-43 inclusions and almost absent from motor neurons. On this basis we find no pathological evidence that DPR aggregation contributes to lower motor neuron degeneration in C9ORF72 ALS.

While we cannot entirely exclude the possibility that DPR aggregation and toxicity occurs at the sub-microscopic level, perhaps through toxic DPR oligomers, or that all of the motor neurons containing DPR inclusions rapidly degenerated, this explanation seems unlikely as neurotoxic protein aggregates are detected in the affected neurons for all other neurodegenerative diseases. Additionally a separate pathological study has shown the absence of soluble DPRs in the spinal cords of C9+ve-ALS cases (Mackenzie et al., 2015). Moreover some *in vivo* and *in vitro* these studies have shown that DPR aggregation is necessary to induce toxicity (Wen et al., 2014; Zhang et al., 2016b; Zhang et al., 2014b). As the number of TDP-43 inclusions in ALS cases, with and without the *C9ORF72* mutation are nearly identical we can find no evidence that dipeptide repeat proteins are playing a pathogenic role in C9ORF72 ALS.

We next sought to assess the presence of sense and antisense foci in the spinal cord of C9+ve-ALS cases. There have been few studies investigating their presence in the spinal cord, the main site of degeneration of ALS. The majority of studies have focused on screening

RNA foci on different regions of the brain such as the frontal cortex, the cerebellum or the hippocampus, showing that sense and antisense foci are primarily nuclear and in neurons (DeJesus-Hernandez et al., 2017; Mizielinska et al., 2013).

Subsequent FISH analysis revealed a greater abundance of sense than antisense foci in the spinal cord of C9+ve-ALS cases (Fig 3.5 A-B). Moreover, we found that there were a significantly greater number of spinal motor neurons containing sense than antisense foci (Fig 3.6 B). We report that 33.8% of motor neurons investigated contained sense RNA foci contrasting with 20.7% antisense foci and almost no DPR inclusion.

Cooper-Knock *et al.* (2015) reported a correlation between the number of antisense RNA foci and loss of nuclear TDP-43 in the motor neurons of ALS cases (Cooper-Knock et al., 2015). The authors reported that 77% of motor neurons displayed antisense RNA foci combined with loss of nuclear TDP-43. Contrary to their findings we detected no correlation between the number of sense or antisense RNA foci and loss of nuclear TDP-43 in motor neurons. In fact, 15% of motor neurons contained sense RNA foci and loss of nuclear TDP-43. Similarly, 7% of motor neurons contained antisense RNA foci and TDP-43 nuclear depletion. The difference in the number of motor neurons containing both antisense RNA foci and loss of nuclear TDP-43 in motor neurons may be due to the localization of the biopsies from each patient and the number of motor neurons counted for each C9ORF72 patient. The authors also investigated hippocampal CA4 regions and they did not identify a significant correlation between the antisense RNA foci and loss of nuclear TDP-43. Furthermore, we were able to detect neurons with large numbers of intranuclear sense and antisense foci in all cases (Fig 3.6 E). This indicates that our FISH protocol is able to detect the presence of large numbers of RNA foci, but none of these cells were motor neurons.

We have shown that there are a significantly greater number of motor neurons containing sense than antisense RNA foci and that the percentage of motor neurons with

sense RNA foci was similar to the percentage of neurons with nuclear TDP-43 depletion. In contrast we found that DPR inclusions were almost absent from spinal motor neurons in C9+ve-ALS cases. We conclude that the evidence from our pathological studies implicates RNA foci and TDP-43 deposition rather than DPRs as the main contributor to the degeneration of motor neurons in C9ORF72-ALS cases. Other studies have reported the loss of C9ORF72 protein in spinal motor neurons in C9ORF72-ALS (Xiao et al., 2015). The knock down of *C9ORF72* levels in cells results in TDP-43 insolubility and cleavage (Sellier et al., 2016), suggesting that haploinsufficiency may also play an important role in the patho-mechanism of C9ORF72 ALS. Lastly, we and others have reported that all five DPR protein inclusions and soluble DPR are very rare in the spinal cord of ALS cases, and that degeneration in the spinal cord correlates with TDP-43 proteinopathy and not with DPR inclusions (Davidson et al., 2016; Gomez-Deza et al., 2015; Mackenzie et al., 2015).

4 MECHANISM OF ACTION OF PPMOS IN EGFP-72(G4C2) EXPRESSING HEK-293T CELLS

4.1 INTRODUCTION

In the previous chapter, we have shown that motor neurons containing sense RNA foci are significantly more common than those containing antisense RNA foci, and that DPRs are almost absent from motor neurons in the spinal cord of C9ORF72 ALS cases. Additionally we have shown that G4C2 repeats form RNA foci in a length dependent manner that sequester RNA binding proteins and are neurotoxic (Lee et al., 2013). For this reason, we hypothesize that the presence of expanded G4C2 RNA transcripts is the main source of toxicity of the *C9ORF72* expansion.

In order to develop a possible therapeutic strategy to mitigate the toxic effect of G4C2 RNA, we designed non-degrading antisense oligonucleotides, which bind to, but do not degrade the target RNA. Antisense oligonucleotides have been used in other repeat expansion disorders such as myotonic dystrophy, a hereditary degenerative disease, is cause by the presence of an expanded trinucleotide CTG repeat in the DM protein kinase (*DMPK*) gene. The expanded RNA causes the RNA to accumulate in the nucleus, sequestering the RNA-binding protein Mucleblind like 1 (MBNL1). ASOs have been used to prevent the sequestration of MBNL1 into RNA foci; mitigating the toxicity of the CUG repeats (Wheeler et al., 2012).

The use of degrading ASOs (gapmers) has been explored in *in vitro* and *in vivo* models of the *C9ORF72* expansion (Donnelly et al., 2013; Jiang et al., 2016). iPSC-derived neurons from *C9ORF72* expansion carriers show intranuclear RNA foci, increased glutamate toxicity (Donnelly et al., 2013) and diminished capacity to fire continuous spikes upon depolarization (Sareen et al., 2013). The number of RNA foci was reduced and the glutamate toxicity and

diminished firing capability of iPSC-derived neurons was reversed upon treatment with ASOs targeting *C9ORF72* transcripts (Donnelly et al., 2013; Sareen et al., 2013). Gapmers have also been tested in an *in vivo* model of the expansion. A single dose of degrading ASO was intraventricularly administered to 3-month-old *C9ORF72* bacterial artificial construct (BAC) transgenic mice. The authors reported a decrease of 40% in repeat-containing RNA in the cortex and the spinal cord. Administrations of the ASO also resulted in over 50% decrease of RNA foci and almost complete depletion of poly-GP and poly-GR DPRs. A different ASO targeting the repeat-exon boundary was shown to improve age dependent behavioural deficits when tested 6 months post administration (Jiang et al., 2016).

We hypothesised that the use of transcript degrading antisense oligonucleotides may be detrimental if haploinsufficiency played an important role in the *C9ORF72* patho-mechanism. For this reason, we designed phosphorodiamidate morpholino oligomers (PMOs) directly targeted at the G4C2 expansion that would bind to, but do not degrade the target transcript.

4.2 AIMS

In this chapter, we aim to unravel the mechanism of action of PMOs targeting expanded G4C2 RNA transcripts and assess whether they are suitable for studying in iPSC models of the disease. To do so, we transfected HEK-293T cells with EGFP-38(G4C2) and EGFP-72(G4C2) expressing constructs and treated them with G4C2-targeting PPMOs (G4C2 PPMOs). We have shown the presence of intranuclear RNA foci, which sequester RNA binding proteins such as hnRNP-H when HEK-293T cells are transfected with these constructs. Moreover, we have detected the presence of the DPR poly-GP in these cells. We sought to assess the effect of PPMO treatment in the number cells containing RNA foci as well as the levels of poly-GP.

4.3 METHODS

All chemical reagents were purchased from Life Technologies unless otherwise stated.

4.3.1 Protein-coupled PMO synthesis and sequence

Protein-coupled PMOs (PPMOs) and 5' fluorescently labelled protein-coupled PMOs (5FL-PPMOs) where synthesized and by Sarepta Therapeutics (Cambridge, MA) and supplied as a lyophilised powder. PPMOs were resuspended in RNAse free water to form a stock concentration of 2mM as suggested by the company. PPMOs and 5FL-PPMOs were diluted to the required concentration in cell culture media. Further information is provided in the methods section.

4.3.2 Cell culture and transfection

Human embryonic kidney (HEK-239T) cells were maintained and plated as described in the methods section. 100,000 cells per well were plated in a 24-well plate, unless otherwise stated. Prior to transfection 300 ng of DNA with 1 µl of Lipofectctamine transfection reagent and 50 µl of Optimem per well for 30 minutes at room temperature. 250 µl of cellular medium was removed and 50 µl of transfection mixture was added dropwise into the well (volumes were doubled for 12-well plates). One day after plating, cells were transfected for 24 hours. The transfection mix was then removed and PPMOs were added at the appropriate concentration in 500 µl of growth media.

4.3.3 Fluorescence *in situ* hybridisation and immunofluorescence

Fluorescent *in situ* hybridisation and immunofluorescence was carried out was previously described in the methods section. Details of the FISH probes used can be found in table 4.1. hnRNP-H antibody (Sigma, sc15387) was used at a 1:250 dilution in 2.5% donkey serum/PBS solution.

Name	Hybridisation temperature	Hybridisation length	Sequence	Concentration	Chemistry
Sense-Cy3	48°C	Over-night	$(C4G2)_8$	10 nM	RNA
Sense-Cy5	48°C	Over-night	$(C4G2)_8$	10 nM	RNA
EGFP-probe	60°C	Over-night	ATGTTGTGGCGG ATCTTGAAGT	30 nM	LNA

Table 4.1: Details of FISH probes used

4.3.4 Imaging and quantification of images

Representative images were taken using a Leica laser scanning confocal microscope (TCS-SP5). For quantification of the number of RNA foci, 7-9 images were taken randomly per condition per biological replicate using a Leica CTR5000 microscope and 40X magnification by only looking at the DAPI counterstain using the same settings for all images. Image files were then renamed and the number of foci and foci-positive cells counted in a blinded manner. The number of total nuclei was quantified using MetaMorph Image System 7.5 (v. 7.7, Molecular Devices). The percentage of foci per cell was then calculated.

4.3.5 Western blotting

Western blotting analysis was carried out as previously described in the methods section. Poly-GP (own production by Eurogentech and validated in Lee et al. 2013) antibody was used at a 1:5000 dilution. GAPDH (Abcam, UK) antibody was used at a 1:2000 dilution. Membranes were detected using an Odyssey CLx system. Protein levels were calculated using Image J (version 1.45e, NIH, Bethesda, USA, http://rsb.info.nih.gov/ij/). Levels of poly-Glycine-Proline (poly-GP) were normalised to the levels of GAPDH.

4.3.6 Statistics

Statistical analysis was carried out using GraphPad Prism 7. Chosen statistical analysis is detailed in the figure legend for each experiment. Data is presented as mean ± SEM. Statistical significance was considered at $p<0.05$ (*), $p<0.01$ (**) and $p<0.001$ (***).

4.4 RESULTS

4.4.1 Choice of experimental design for PPMO efficacy and mechanism testing

In order to test the efficacy and mechanism of action of PPMOs targeting the G4C2 expansion we used a previously validated ectopic expression model where EGFP-38(G4C2) and EGFP-72(G4C2) expressing constructs are transfected into HEK-293T cells. Cells transfected with the constructs have shown to reliably model some aspects of the disease pathology. Intranuclear RNA foci are present in a length-dependent manner and sequester pathologically relevant proteins such as hnRNP-H and the repeats can be translated through RAN translation yielding the dipeptide repeat protein poly-GP (Lee et al., 2013). Cells were transfected for 24 hours prior to incubation with PPMOs as it would be a more accurate model of the disease, whereby the RNA foci and the RAN translation products are present prior to treatment. A schematic representation of the experimental procedure is depicted in figure 4.1. Cells were incubated for three days with PPMOs following the advice given by Sarepta Therapeutics. Given that the G4C2-targeting PPMOs and the RNA detection probe have the same sequence, there was a high probability that any effect seen on the number of G4C2 RNA foci was due to a competition between the PMO and the detection probe when performing FISH. The EGFP sequence in the expression vector allowed us the possibility to test the efficacy of the PMOs with a non-competing fluorescent *in situ* hybridisation (FISH) probe targeting the EGFP sequence of the vector.

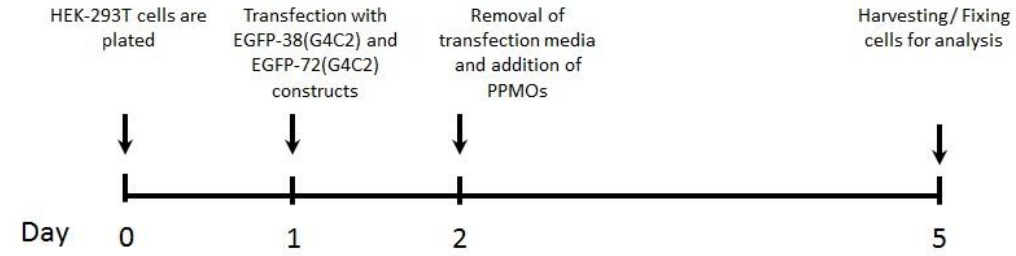

Figure 4.1: Schematic representation of the experimental design.

4.4.2 Uptake of 5FL-PPMOs by HEK-293T cells

In order to show the PPMO cellular uptake 5'-Cy3 labelled protein-coupled PMOs (5FL-PPMOs) were synthesized, 100% of HEK-293T cells uptake similar levels of 5FL-PPMOs after 1-3 days of incubation (Figure 4.2).

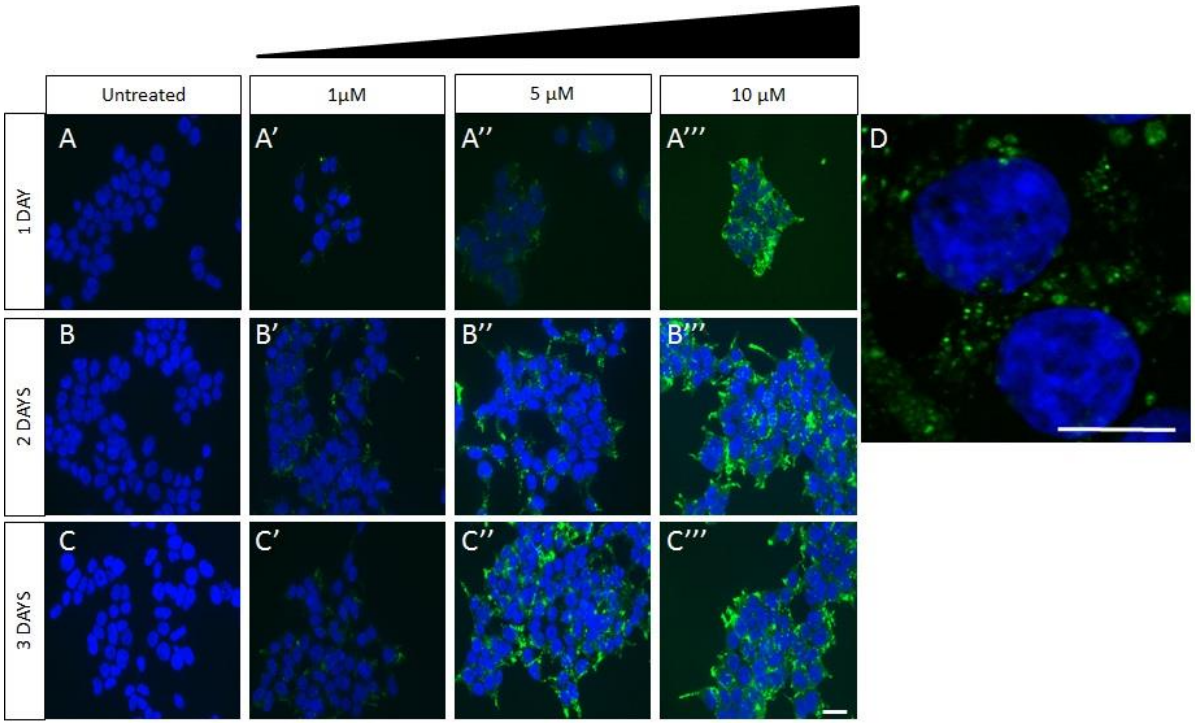

Figure 4.2: Uptake of PPMOs by HEK-293T cells

(A-C) Representative images of HEK-293T cells 1-3 days after incubation with increasing concentrations of 5'-Cy3 labelled peptide-coupled PMOs (5FL-PPMO). **(D)** Higher

magnification image of 3 day 5 µM incubation of 5-FL PPMO showing the subcellular distribution. Scale bar = 20 µm

Additionally there are greater levels of 5FL-PPMOs with increasing concentrations and increasing duration of the incubation. Although there is some presence of the PMO in the nucleus, the cellular distribution is mostly cytoplasmic (Fig. 4.2 D). Previous studies have shown that once the PPMO is internalised, the cell penetrating peptide is cleaved off the PMO and diffuses homogenously throughout the nucleus and the cytoplasm (Lehto et al., 2014). We therefore concluded that PPMOs are internalised by HEK-293T cells.

4.4.3 Effect of PPMOs on the number of RNA foci detectable using a C4G2 FISH probe.

HEK-293T cells were transfected with EGFP-72(G4C2) expressing constructs and treated with PPMOs for three days as explained in figure 4.1. Previous studies in our laboratory have shown the ability of this construct to model some aspects of the pathology as explained in the introduction. Fluorescent *in situ* hybridisation (FISH) was carried out using a $(C4G2)_8$ probe. The presence of large intranuclear RNA foci in EGFP-positive cells was observed (Fig 4.3 Avii). Upon treatment with increasing concentrations of G4C2 PPMO, the number of detectable foci was reduced in a concentration-dependent manner. A significant reduction in the percentage of foci-positive cells was observed in cells treated with 5µM and 10µM G4C2 PPMO but not 1µM compared to untreated (UT) and control PPMO treatment in EGFP-72(G4C2) transfected cells. (Figure 4.3; UT = 22.7±1.5; control PPMO 1µM = 20.0% ± 4.0; 5µM = 21.2% ± 3.9; 10µM = 20.3% ± 0.5; G4C2 PPMO 1µM = 16.2% ± 1.2; 5µM = 4.3% ± 0.5 and 10µM = 1.9% ± 1.0. UT vs all control PPMO concentrations n.s., UT vs 1µM G4C2 PPMO ns., UT vs 5µM and 10µM G4C2 PPMO $p<0.001$ ***; 5µM control vs 5µM C9ORF72 $p<0.001$ ***; 10µM control vs 10µM C9ORF72 PMO $p<0.001$ ***).

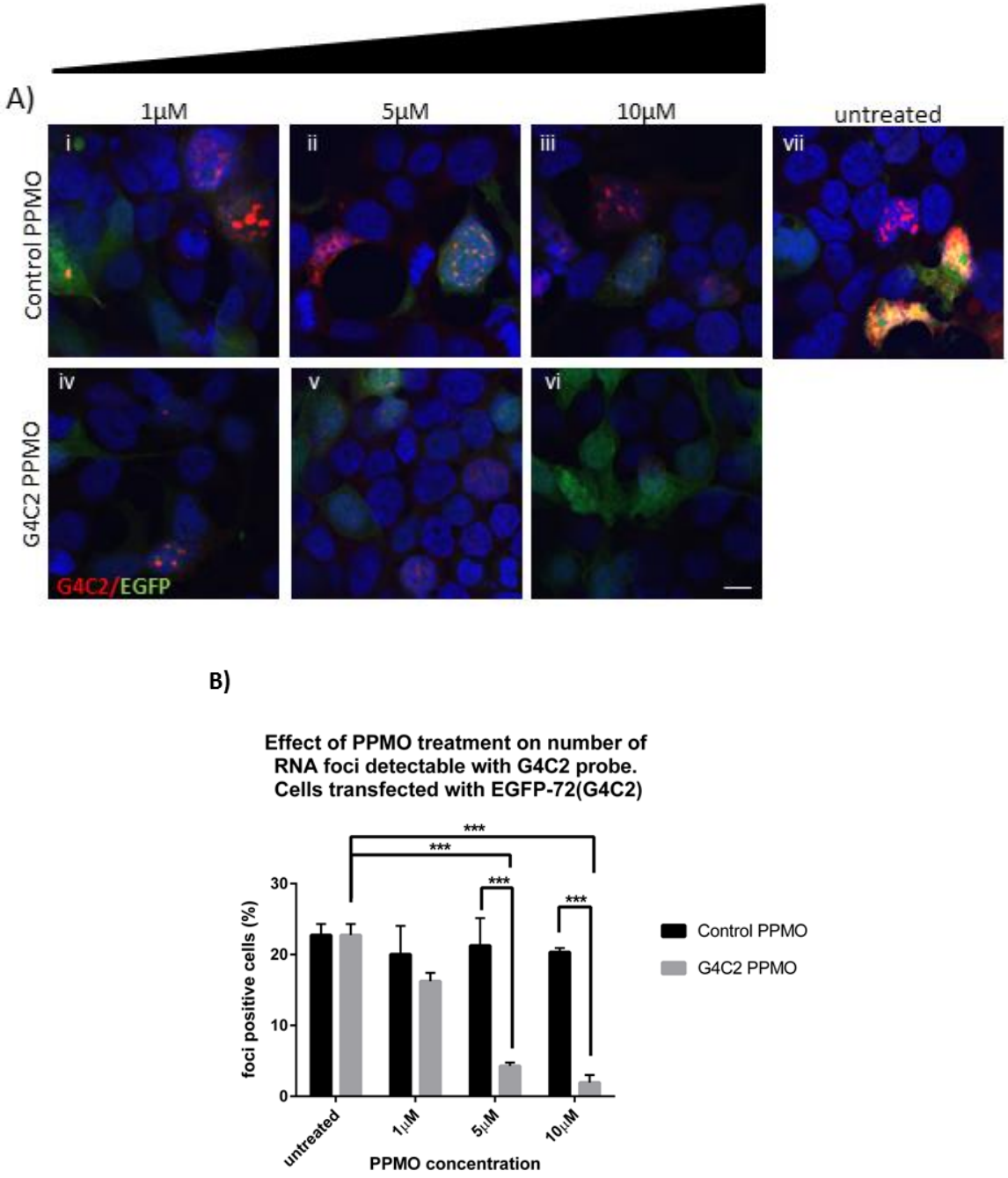

Figure 4.3: PPMO treatment reduces the percentage of foci-positive cells with G4C2 foci in a concentration-dependent manner.

(A i-vii) Representative images of fluorescent *in situ* hybridisation (C4G2 probe) of HEK-293T cells transfected with EGFP-72(G4C2) expressing constructs and treated with increasing concentrations of control and G4C2 PPMO. **(B)** Quantification of the effect of control and G4C2 PPMOs on the percentage of cells containing G4C2 RNA foci in EGFP-72(G4C2) transfected cells. Data represents mean ± SEM. Significance levels were determined by two-way ANOVA with Bonferroni multiple comparisons, selected pairs. (*** $p<0.001$; >2100 cells per condition from three independent replicates). Scale bar = 20 µm

This data not only shows that the G4C2 PPMO binds to the RNA foci and does so in a concentration-dependent manner, it is also able to bind to already existing RNA foci in live cells, thereby making it clinically relevant. Although we observed a significant reduction in the percentage of RNA foci per cell with 5µM G4C2 PPMO, 10µM concentration was selected for the following experiments as no cellular toxicity was observed.

4.4.4 Validation of alternative FISH probe to study the effect of PPMOs on RNA foci.

Given that the $(C4G2)_8$ FISH detection probe and the G4C2 PPMO share the same target sequence, there was the possibility that the observed reduction was due to a masking of the foci and not a real reduction in the number of foci (Figure 4.4). We designed a detection probe outside the G4C2 repeats, targeting the EGFP sequence of the constructs. This would allow us to study the effect of the PPMOs on the number of RNA foci with no interference. Furthermore, the new detection probe has a higher hybridisation temperature of 60°C that the $(C4G2)_8$ probe. At this temperature, EGFP is denatured and partially loses its fluorescent ability. We exploited these two aspects to perform double fluorescent *in situ* hybridisation on EGFP-72(G4C2) transfected HEK-293T cells followed by immunofluorescence. An EGFP Cy3-labelled detection probe and a different C4G2-Cy5 labelled detection probes were used showing that both detection probes colocalise with the pathologically relevant protein hnRNP-H (Fig 4.5 A). Quantification of percentage of foci-positive cells using the EGFP-targeting probe in cells transfected with EGFP and EGFP-72(G4C2) constructs showed that there is significantly more RNA foci when cells were transfected with EGFP-72(G4C2) (Fig 4.5 C; EGFP = 2.9% ± 1.7; Untreated = 18.1% ± 1.3. $p<0.01$ **). Additionally the number of foci hybridising with both EGFP and G4C2 probes was 91.6% ± 2.4 (Fig 4.5 B).

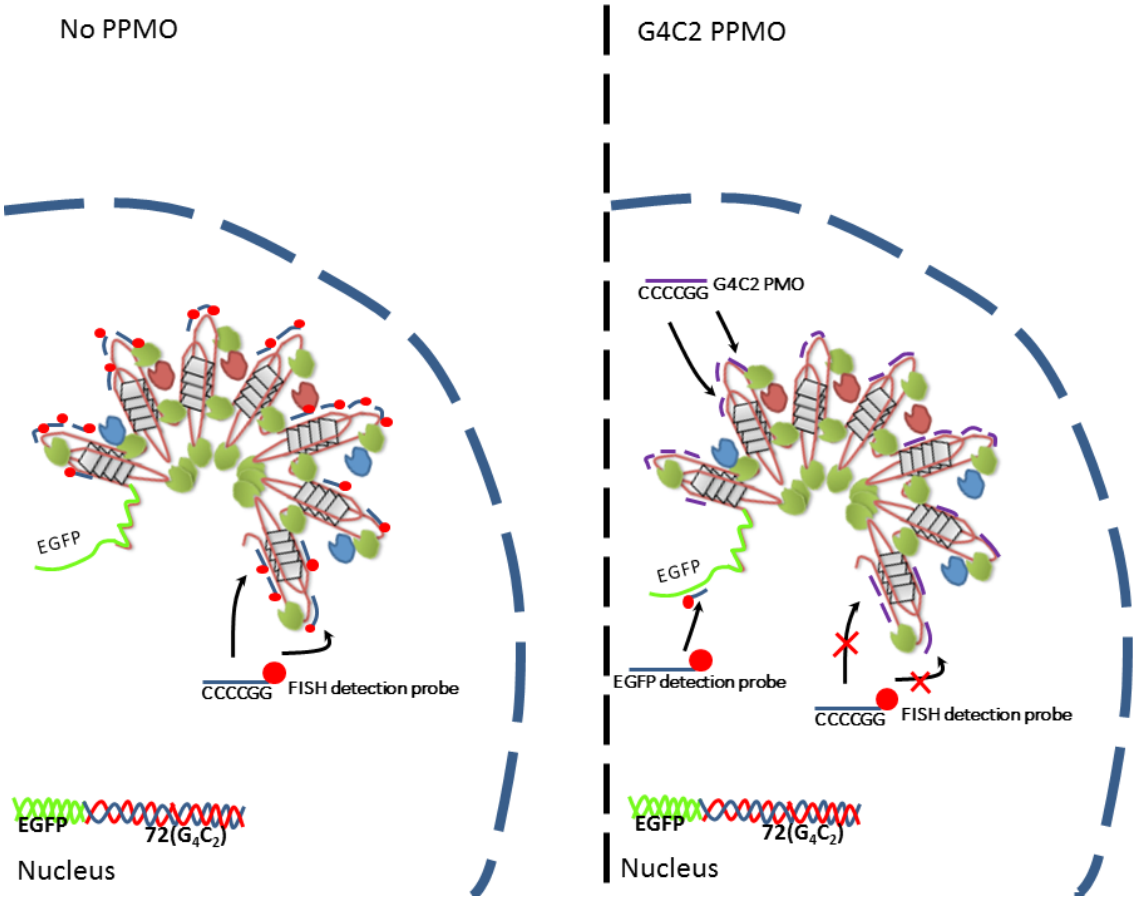

Figure 4.4: Schematic representation of competition of PPMO and C4G2 FISH detection probe

This shows that the RNA foci resulting from the expressing vectors contain the EGFP sequence as well as the G4C2 sequence; they can be reliably detected with EGFP detection probe and have the ability to sequester pathologically relevant RNA-binding proteins such as hnRNP-H. Figure adapted from (Lee et al., 2013).

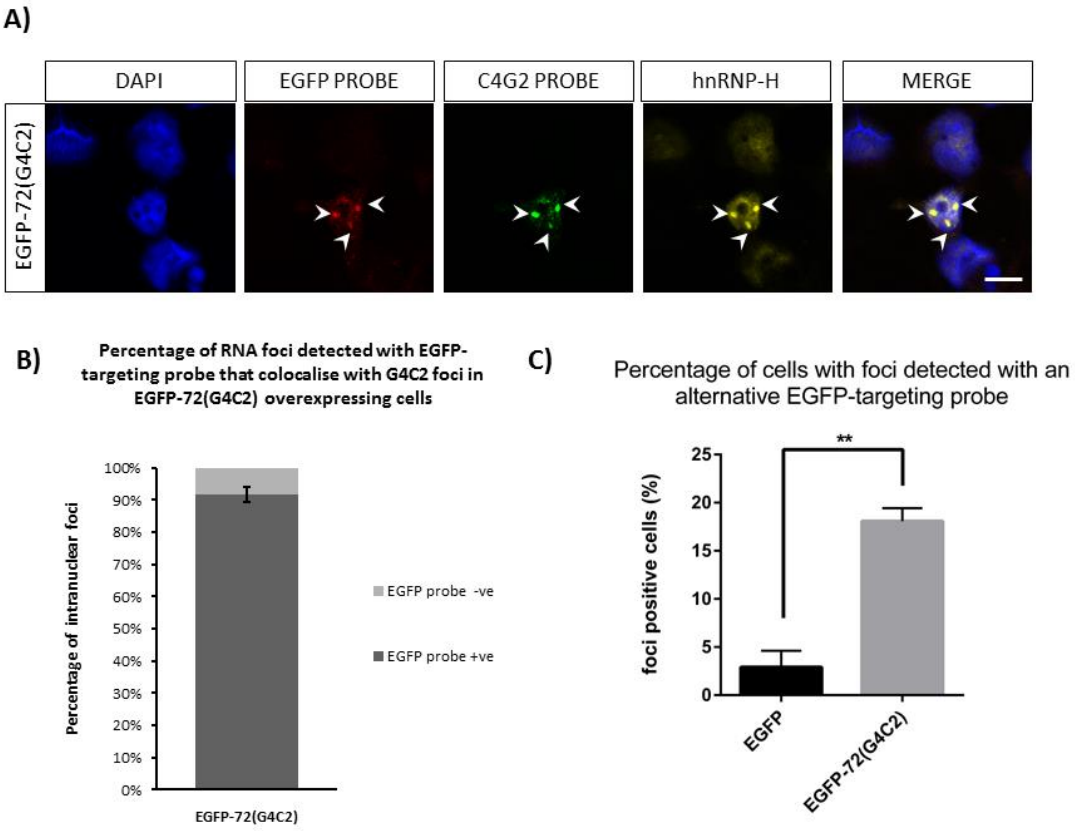

Figure 4.5: Validation of an alternative EGFP targeting FISH probe

(A) Representative image of double fluorescent *in situ* hybridisation followed by immunofluorescence showing that EGFP-targeting probe can detect G4C2 RNA foci, which sequester clinically relevant proteins. **(B)** Percentage of foci-positive cells detected with EGFP-targeting probe that colocalise with G4C2 foci in EGFP-72(G4C2) expressing cells. n=300 G4C2-detectable RNA foci from three independent experiments. **(C)** Percentage of foci-positive cells detected using an alternative EGFP-targeting probe. Data represents mean ± SEM. Significance levels were determined by two-tailed t-test. (** $p<0.01$; >300 cells per condition from three independent replicates). Scale bar = 20 µm

4.4.5 Effect of PPMOs on RNA foci using an EGFP-targeting detection probe

Having shown the feasibility of using an EGFP-targeting detection probe to detect RNA foci, HEK-293T cells were transfected with EGFP-72(G4C2) expressing constructs and treated with 10 µM control and G4C2 PPMO for three days (Fig 4.1). Fluorescent *in situ* hybridisation was performed using an EGFP-targeting probe and the percentage of foci-positive cells was quantified. We observed a significant reduction in the percentage of foci-

positive cells detected with the EGFP-targeting probe upon treatment with G4C2 PPMO compared to Control PPMO (Fig 4.6; Untreated = 18.1% ± 1.3; Control PPMO = 20.4% ± 3.2; G4C2 PPMO 8.0% ± 2.2. Control PPMO vs G4C2 PPMO $p<0.05$ *).

Altogether, the data shows that the G4C2 PPMO significantly reduces the percentage of foci-positive cells in HEK-293T cells transfected with EGFP-72(G4C2), not only bind to them, and thereby possibly mitigate their toxicity.

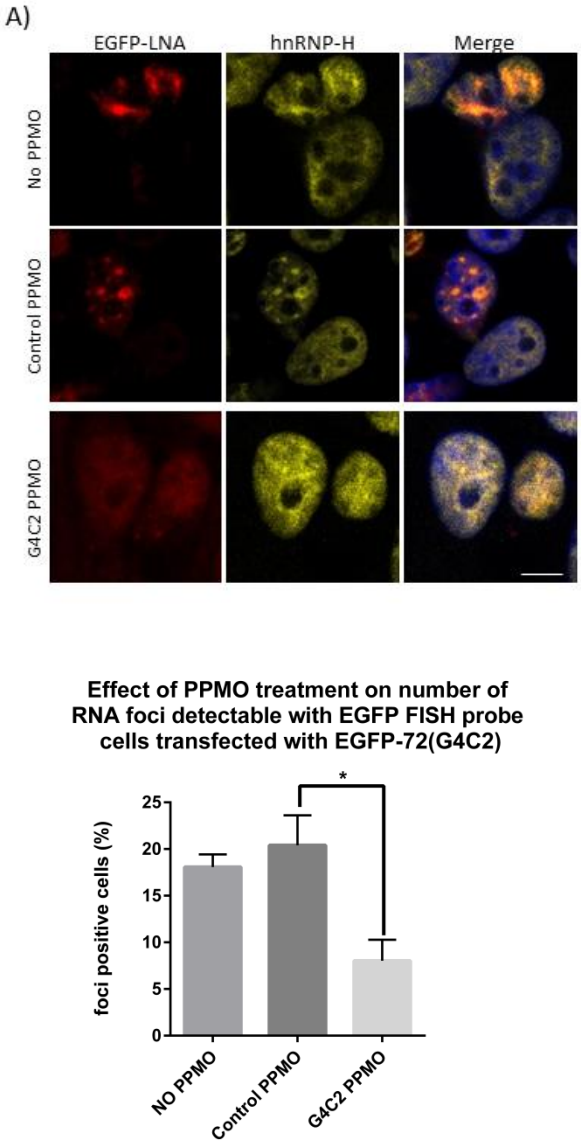

Figure 4.6: PPMO treatment reduced the percentage of foci-positive cells

(A i-vi) Representative images of fluorescent *in situ* hybridisation probing with an alternative EGFP-targeting probe of cells transfected with EGFP-72(G4C2) for 24 hours. Cells were then treated with 10µM Control and G4C2 PPMO. **(B)** Quantification of the effect of Control and

G4C2 PPMOs on the percentage foci-positive cells detected with an EGFP-targeting probe. Cells transfected with EGFP-72(G4C2). Data represents mean ± SEM. Significance levels were determined by one-way ANOVA with Tukey's multiple comparisons. (* $p<0.05$; >500 cells per condition from three independent replicates)

4.4.6 Effect of PPMO on the levels of poly-GP

The C9ORF72 expansion is translated into dipeptide repeat proteins *in vivo* (Mori et al., 2013c). Previous work carried out in our laboratory has shown that EGFP-38(G4C2) and EGFP-72(G4C2) expressing constructs undergo translation, yielding poly-GP protein. The effect of the G4C2 PPMO on the levels of poly-GP that are RAN translated from the two constructs was investigated. We carried out the same experimental procedure previously explained. Quantification of the levels of poly-GP/GAPDH showed a very slight but not significant decrease of the levels of poly-GP normalised to treatment with control PPMO in cells transfected with both EGFP-38(G4C2) and EGFP-72(G4C2) and treated with 10 µM G4C2 PPMO (Fig 4.7; 0.88 A.U. ± 0.1 and 0.86 A.U. ± 0.1 respectively). This suggests that although the G4C2 PPMO may be interacting with the G4C2 RNA in the cytoplasm, it does not significantly reduce the levels of RAN translation.

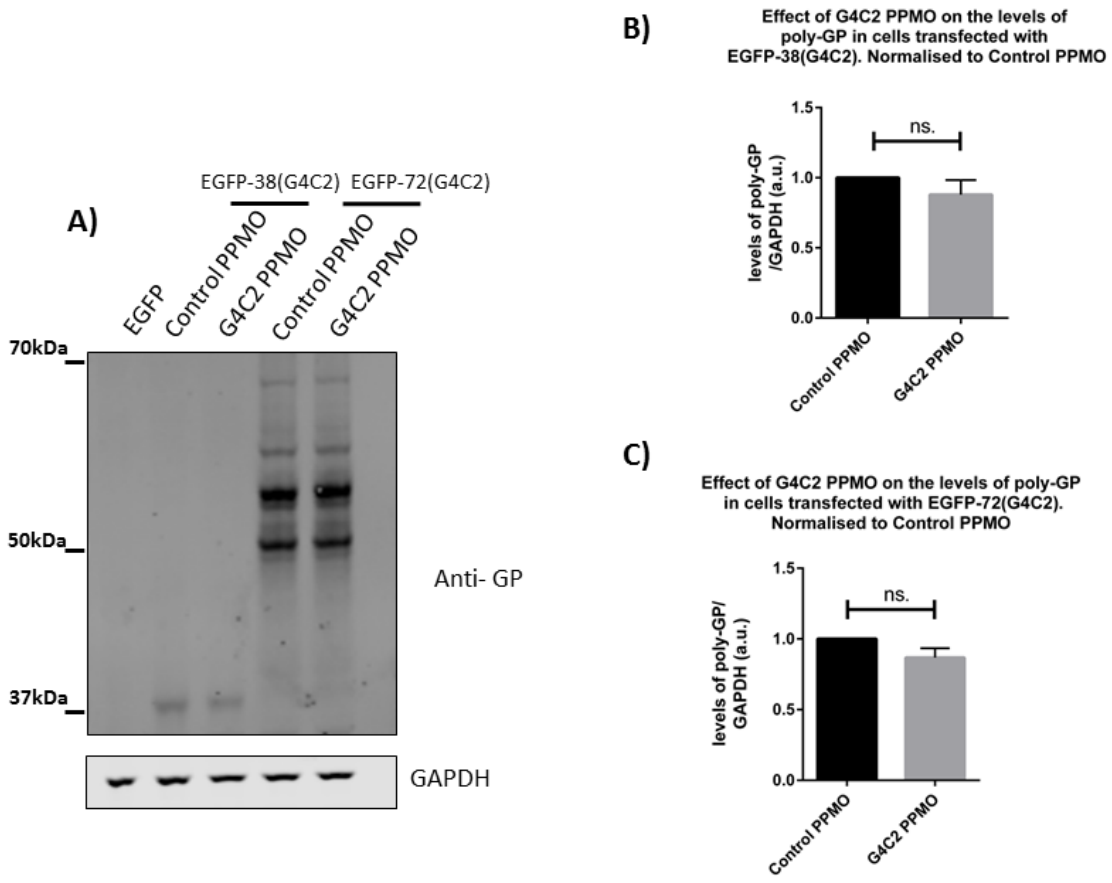

Figure 4.7: PPMO treatment does not reduce the levels of poly-GP.

(A) Western blot showing the levels of poly-GP expressed in EGFP, EGFP-38(G4C2) and EGFP-72(G4C2) transfected cells. Cells there treated for three days with 10 µM control and G4C2 PPMO after 24-hour transfection. **(B)** Levels of poly-GP in EGFP-38(G4C2) transfected cells normalised to control PPMO. **(C)** Levels of poly-GP in EGFP-72(G4C2) transfected cells normalised to control PPMO. Data represents mean ± SEM. (Two-tailed t-test. n.s. = not significant. Three independent experiments measured)

4.5 DISCUSSION

In the present study, we have shown what the G4C2 PPMO significantly reduces the number of RNA foci, thereby reducing their ability to sequester RNA-binding proteins and potentially mitigate their toxicity. Additionally we have shown that although it may interact with G4C2 repeats in the cytoplasm it is not able to block the translation of the repeats into di-peptide repeat (DPR) proteins. However, we do not rule out the possibility that there is no detectable reduction of the levels of poly-GP because the expression of poly-GP takes place for 72 hours and the repeats are greatly overexpressed.

Although we used an artificial ectopic expression system, there it served as an alternative to study the mechanism of action of "blocking" PMOs as it has been shown that the foci detected in iPSC-derived neurons are only formed by the G4C2 repeats and not any other flanking RNA region. Furthermore, this model presents obvious advantages; HEK-293T cells have high transfection efficiencies, there is no observable toxicity upon transfection of the EGFP-38(G4C2) and EGFP-72(G4C2) constructs and the presence of the EGFP sequence allows the study of the mechanism of the G4C2 PPMO effect by using a non-competing detection FISH probe. Additionally, this ectopic expression model recapitulates other aspects of the disease pathology such as the presence of di-peptide repeat proteins or the sequestration of hnRNP-H into RNA foci (Lee et al., 2013).

Although the use of steric hindering antisense oligonucleotide have been previously reported in the literature, showing that their use reduces C9ORF72 iPSN increased glutamate toxicity, our study presents the first comprehensive insight into the mechanism of action of steric hindering ASOs in a G4C2-expressing model. As a unit this study does not constitute an important breakthrough in the field, however, the unravelling of the mechanism of action is essential for the interpretation of the results that may arise from the testing of the G4C2 PPMO in iPSC-derived neurons from *C9ORF72* expansion carriers.

We therefore conclude that the G4C2 PPMOs interact with the G4C2 RNA repeats in the nucleus and are able to reduce the number of RNA foci that arise from the repeats. Furthermore, the G4C2 PPMOs do not reduce the levels of RAN translation in our ectopic expressing model. This may be due to the fact that the levels of RAN translation is too high to observe a decrease three days after transfection or that the PMOs are unable block the assembly of the translation machinery.

5 TREATMENT OF C9ORF72 IPSN WITH G4C2 PPMOS

5.1 BACKGROUND

The use of iPSC-derived neurons (iPSN) has proven to be crucial in unravelling the mechanisms of toxicity for the *C9ORF72* expansion mutation. All studies involving C9ORF72-ALS iPSN report the presence of intranuclear RNA foci which can sequester RNA binding proteins such as hnRNP-H or ADARB2 (Donnelly et al., 2013; Sareen et al., 2013), but the detection of DPR is inconsistent (Almeida et al., 2013; Donnelly et al., 2013; Sareen et al., 2013). Several additional changes have been reported including: elevated p62 levels and dysfunction of the proteasome system (Almeida et al., 2013), increased sensitivity to glutamate-induced stress (Donnelly et al., 2013), diminished capacity to fire continuous spikes upon depolarization (Sareen et al., 2013), hyper-methylation of the *C9ORF72* promoter (Esanov et al., 2016), decreased neurite (Burguete et al., 2015) and axonal outgrowth (Sivadasan et al., 2016), altered ER calcium homeostasis and increased cell death (Dafinca et al., 2016) mitochondrial stress and DNA damage (Lopez-Gonzalez et al., 2016), decreased levels of *C9ORF72* transcript and protein levels (Aoki et al., 2017) and nucleocytoplasmic transport deficits (Zhang et al., 2015). Some of these deficits have been reversed with the *in vivo* and *in vitro* use of antisense oligonucleotides that facilitate the degradation of the target RNA (Aoki et al., 2017; Donnelly et al., 2013; Jiang et al., 2016; Sareen et al., 2013; Zhang et al., 2015).

Neurons derived from iPSCs also present a suitable model in order to test potential therapies; iPSN derived from Alzheimer's disease (AD) patients are resistant to therapeutically relevant concentrations of NSAID-Based GSMs that failed in clinical trials but had an effect on mouse models of the disease (Mertens et al., 2013). Moreover, iPSN from patients with bipolar disorder are responsive to therapeutically relevant lithium levels in the culture medium (Mertens et al., 2015b). The potential to test therapies has also been shown

in iPSN derived from ALS cases: mutant *SOD1*-IPSC derived motor neurons (iPSMN) show a loss of excitability and increased ER stress, deficits which were reversed following treatment with the FDA approved drug 4-aminopyridine (Naujock et al., 2016). Our group were the first to report that mutant TDP-43 iPSMNs develop detergent resistant, cytoplasmic TDP-43 aggregates and reduced survival in long term culture (Bilican et al., 2012). Another study showed that some iPSMN phenotypes could be reversed with the histone acetyl transferase inhibitor anacardic acid (Egawa et al., 2012).

5.2 AIM

In the previous chapter we have shown that PPMOs directly targeting G4C2 repeats reduce the number of RNA foci in HEK-293T cells expressing EGFP-72(G4C2) constructs and prevent the sequestration of RNA binding proteins. In this study we generated iPSC from three healthy individuals and four C9ORF72-ALS cases and differentiated them into mature neurons in order to test the potential use of PPMOs as a therapeutic strategy.

5.3 METHODS

5.3.1 Fluorescent *in situ* hybridisation and immunofluorescence

Fluorescent *in situ* hybridisation and immunofluorescence was carried out was previously described in the methods section. Antibodies were used at the concentrations shown in table 5.1. All antibodies were diluted in 2.5% Donkey serum.

Antigen	Concentration	Manufacturer
MAP2	1:250	Abcam (ab5392)
βIII tubulin	1:500	Abcam (ab78078)
SMA	1:300	Abcam (ab5694)
AFP	1:200	Santa Cruz (C-19)
OCT4	1:200	Santa Cruz (SC-8628)
NANOG	1:250	Abcam (ab80892)

Table 5.1 List of antibodies

5.3.2 Filter trap

Filter trap assay was performed as described in the methods section. 20 µg of protein lysate was added to 100 µl of RIPA buffer and loaded into each well. 5 µg of HEK-293T cells transfected for 48 hours with ply-(GP)x125, poly-(GA)x125, poly-(GR)x125, poly-(PA)x125 and poly-(PR)x125 overexpressing constructs was used as a positive control for the presence of dipeptide repeat proteins.

5.3.3 Maintenance of iPSCs

Induced pluripotent stem cells were maintained as described in the methods section. iPSCs were cultured in E8-Flex media and fed every other day. Colonies were split by washing aspirating the media and washing once with PBS. 1ml of Versene was then added for 3-5 minutes. Versene was aspirated and 2ml of E8-Flex was added. Colonies were scraped and split 1:3 into geltrex coated 6-well plates.

5.3.4 *In vitro* differentiation and maintenance of iPSC-derived neuronal progenitor cells

iPSC lines from three healthy controls and four *C9ORF72* expansion carriers were differentiated into neuronal progenitor cells (NPCs) as previously described. Neuronal progenitor cells were growth in T12.5 falcon flasks until 100% confluent and transferred into T25 flasks by dissociating with Accutase. Cells were passaged until 80%-90% of the cells

showed a neuronal progenitor-like morphology. NPCs were maintained as previously described in expansion medium containing FGF.

5.3.5 *In vitro* differentiation of neuronal progenitor cells into mature neurons

Neuronal progenitor cells were differentiated into mature neurons as described in the methods section. Cells were differentiated for 5 weeks to obtain mature neurons. Cells were differentiated in 24-well for FISH and ICC, in 12 well plates for western/dot blot analysis and 6 well plates for RNA extraction. All plates were coated with Matrigel at least one hour prior to plating and an appropriate number of cells were plated in for each experiment as described in the methods section

5.3.6 RNA extraction

Cells were manually scraped and collected into RNAse-free polypropylene tubes. Cells were centrifuged for 1 minute at 12 000 g and cell pellets were kept on ice and washed in PBS three times prior to RNA extraction. Total RNA was isolated from cultures of cell lines with the RNeasy kit (Qiagen) according to manufacturer's instructions. RNA was quantified using a microvolume spectrophotometer (Nanodrop, Thermo Scientific).

5.3.7 qRT-PCR

Quantitative reverse transcriptase PCR was performed as described in the methods section. Primers were used at a concentration of 10pM. qRT-PCR was performed simultaneously for all samples and the same amount of DNA was used for each of the primer conditions.

5.3.8 Gel electrophoresis

Gel electrophoresis was performed as described in the methods section. RT PCR products were run in 2% agarose gels for 20 minutes and imaged using a UV transiluminator.

5.3.9 Alamar blue assay

Control expansion carrier lines were differentiated in a 96-well plate for 5 weeks. Cells were incubated with appropriate concentrations of control and C9ORF72 targeting PPMOs for 7 days prior to carrying out the assay. Growth media was removed and an equal volume of medium containing Alamar blue reagent was added into each well following the manufacturer's instructions. After 3 hours of incubation the media was collected and analysed using a microplate reader following the manufacturer's indications. Results from the effect of PPMO incubation in each cell line were averaged.

5.3.10 Neurite outgrowth Assay

The Neurite outgrowth assay was performed as previously described in the methods section. The mean total neurite length per cell was measured for each cell line without PPMO treatment and by treating with 5µM of Control and G4C2 PPMO for 7 days in a blinded manner.

$$Average\ total\ neurite\ length = \frac{total\ neurite\ length}{total\ number\ of\ cells}$$

5.3.11 Fluorescently activated cell sorting (FACS) – Cell survival assay

Cell survival of iPSC-derived neurons was measured with FACS soring using the cell death marker Annexin V and the mitochondrial depolarisation marker DICL. iPSC-derived neurons were grown in 12-well plates. The culture media was collected. Cells were washed once with PBS, which was collected and added in the same tube. Cells were dissociated by incubating with 300µl of Accutase (Life Technologies) dissociation reagent for 7 minutes at 37°C. Accutase was inactivated by adding 700µl of plain culture media and all the cells were collected into the corresponding falcon tube. The cells were pelleted by centrifugation at 1000 rpm for 4 minutes. Cells were dissociated into a single cell suspension in PBS by pipetting gently with a P1000 pipette. Cells were then centrifuged and resuspended in 500µl

of warm PBS buffer containing DICL and Annexin V450 at 1:1000 and 1:500 concentrations respectively following the manufacturer's instructions.

5.4 RESULTS

5.4.1 Characterisation of iPSCs

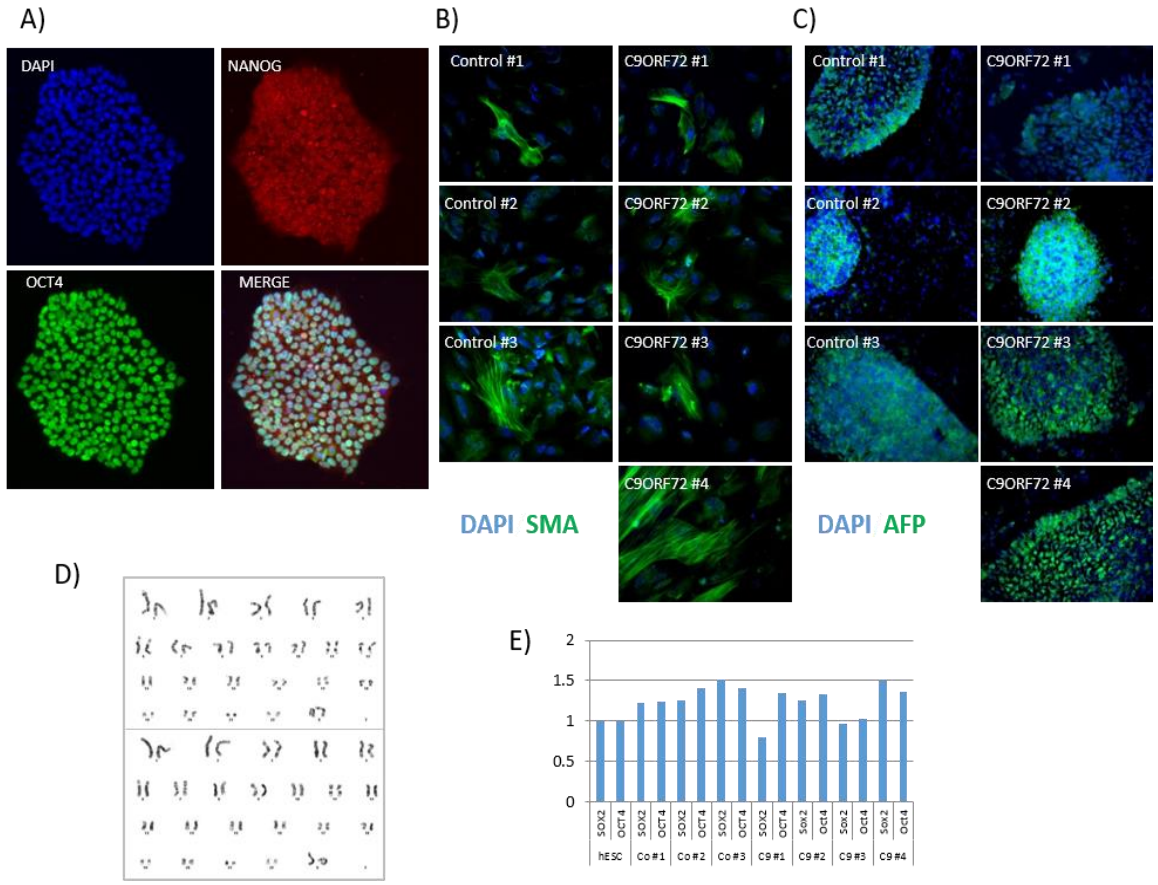

Figure 5.1: Characterisation of iPSCs.

(A) Representative images of iPSC colonies stained for the pluripotency markers NANOG and OCT4. All iPSC lines differentiate into **(B)** SMA positive cells (mesoderm) and **(C)** AFP positive cells (endoderm). **(D)** Representative Karyotyping of control and C9ORF72 #4. All cells maintained normal karyotype **(E)** qPCR analysis of SOX2 and OCT4 pluripotency markers for all iPSC lines normalised to human embryonic stem cell (hESC).

In order to study the pathophysiology of the *C9ORF72* expansion, we generated induced pluripotent stem cells (iPSCs) from unaffected individuals (controls #1-3) and four C9ORF72-ALS patients (C9ORF72 #1-4) from fibroblasts. Induced pluripotent stem cells were

derived by transduction of lentiviral vectors containing the four Yamanaka factors (OCT4, SOX2, KLF4 and cMYC) of human fibroblasts as described in (Bilican et al., 2012). All iPSCs expressed pluripotency makers and were differentiated into three germ layers (Fig 5.1B SMA - mesoderm, Fig 5.1C α-fetoprotein (AFP) - endoderm and Fig 5.3A- βIII-tubulin - ectoderm). All cells showed normal karyotyping (Fig. 5.1D). Silencing of the transduced SOX2 and OCT4 transcription factors after reprogramming was confirmed by quantitative RT-PCR (qRT-PCR) by comparing to the levels observed in human embryonic stem cells (hESCs).

5.4.2 C9ORF72 ALS patient information and confirmation of the presence of the expansion

A)

ID	sex	Age of onset	survival (months)	Diagnosis	SALS/FALS	iPSC method
C9ORF72 #1	male	59	32	ALS	FALS	retrovirus
C9ORF72 #2	male	65	36	ALS	FALS	retrovirus
C9ORF72 #3	female	39	31	ALS/FTD	FALS	retrovirus
C9ORF72 #4	male	58	NA	ALS	SALS	retrovirus

B)

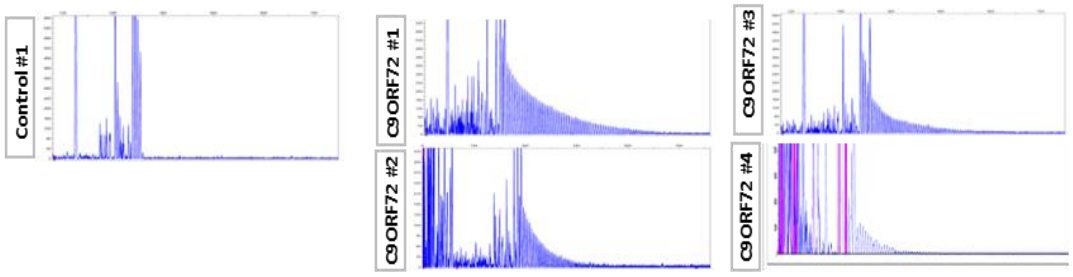

Figure 5.2: ALS patient information and confirmation of the presence of the expansion

(A) Clinical information of patients from which iPSCs where derived. **(B)** Electropherograms of repeat-prime PCR of control and C9ORF72 iPSC lines to confirm the presence of the G4C2 expansion. Experiments were carried out Dr. Agnes Nishimura, Dr. Bradley Smith and Ms. Nada Alahmady.

iPSCs were derived from human fibroblasts from four C9ORF72-ALS expansion carriers as described (Bilican et al., 2012). Clinical data from all C9ORF72 ALS cases is

summarised in figure 5.2A. Repeat primed PCR, carried out by Dr. Agnes Nishimura, Dr. Bradley Smith and Ms. Nada Alahmady as described in (Al-Sarraj et al., 2011), shows the presence of the expansion on iPSCs derived from the four C9ORF72-ALS cases and absent from iPSC control #1 (Fig 5.2 B).

5.4.3 Neuronal differentiation of control and C9ORF72 iPSCs into mature neurons

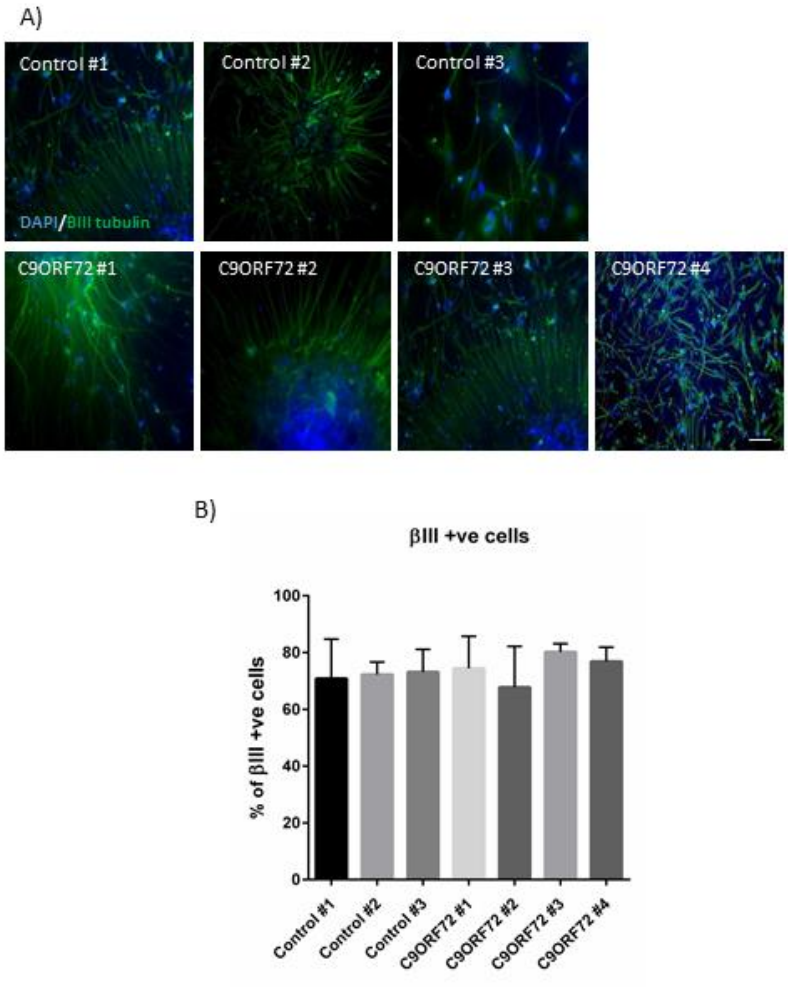

Figure 5.3: Neuronal differentiation of Control and C9ORF72 iPSCs

(A) Representative images of 5-week old iPSN from Controls #1-3 and C9ORF72 #1-4 stained with βIII-tubulin (green) and DAPI (blue). **(B)** Quantification of percentage of βIII-tubulin +ve cells of 5-week differentiation of Controls #1-3 and C9ORF72 #1-4 iPSN. n=3. Over 200 cells were quantified per differentiation. Data is represented as mean ± SEM.

After characterisation, iPSCs were differentiated into neuronal progenitor cell (NPCs) lines from all seven iPSCs lines. Neuronal progenitor cells were differentiated for 5 weeks and stained for pan neuronal marker βIII-tubulin to assess the percentage of neurons in each differentiation batch (Fig 5.3 A-B). A high percentage of neurons was obtained (Fig 5.3 B; 67%-81%) from all differentiated cell lines showing no significant difference between control and C9ORF72-positive cell lines (Control #1 = 67.5% ± 13.9; Control #2 = 72.6% ± 4.5; Control #3 = 77.5% ± 8.0; C9ORF72 #1 = 75.6% ± 11.3; C9ORF72 #2 = 72.9% ± 14.4; C9ORF72 #3 = 81.8% ± 2.9 C9ORF72 #4 = 76.8% ± 5.1). We therefore concluded that we could reliably achieve a high percentage of mature neurons from all cell lines.

5.4.4 Effective internalisation of PPMOs into cells and lack of toxicity

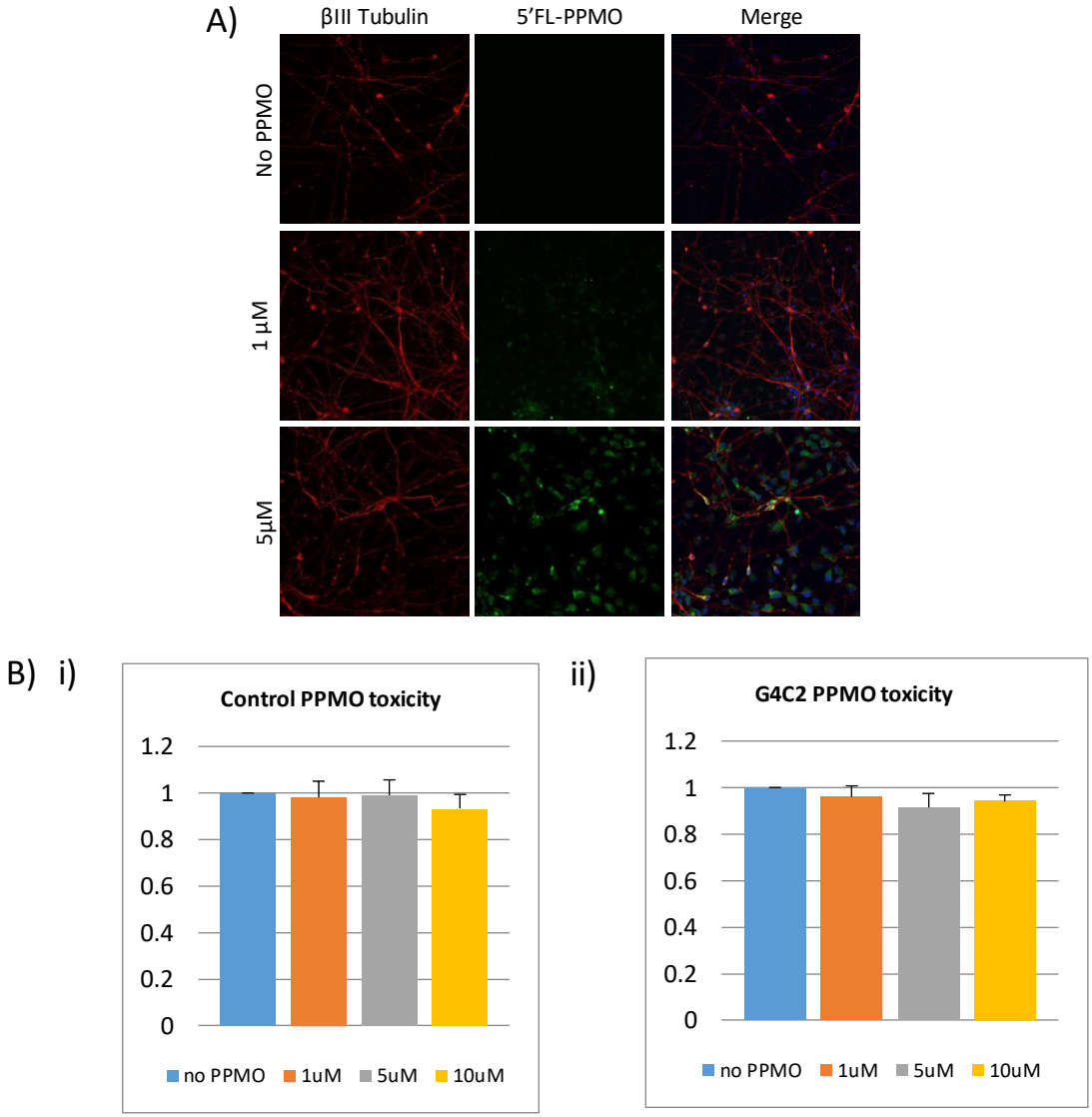

Figure 5.4: PPMO internalisation and toxicity.

(A) All cells internalise 5'FL-PPMO after 7 day incubation. Representative images of Control #1 5week old iPSN were incubated with 0, 1 µM and 5 µM 5'FL-PPMO for 7 days in order to show the uptake of PPMOs by mature neurons. Cells were immunostained with βIII-tubulin (red) and DAPI (blue) and 5'FL-PPMO (green). **(B)** 7 day PPMO treatment does not induce cell death in 5-week differentiated control #1-3 iPSN. Cells were treated with 0, 1µM, 5µM and 10µM control **(B i)** and G4C2 PPMO **(B ii)** for 7 days. ALAMAR blue toxicity assay was carried out. n=3. 3 wells of a 96-well plate were averaged per iPSN line and normalised to PPMO treatment. Data is represented as mean ± SEM; no significant differences were observed.

Mature neurons were incubated with 0, 1 and 5µM Control and G4C2-targeting 5FL-PPMOs (previously described in chapter 2) for 7 days in order to show the efficiency of PPMO uptake. A 100% of PPMO internalisation was obtained upon incubation of neurons with 5 µM control and G4C2 PPMOs (Fig 5.4). Unlike HEK-293T cells where the staining was concentrated, mature neurons showed a diffuse distribution. Furthermore, we observed a concentration-dependent increase in the amount of fluorescence in cells, showing clear concentration dependent uptake. Additionally, we observed that all cells internalised PPMOs, not only mature neurons (Fig 5.4A).

The potential toxic effect of incubating mature neurons with PPMOs was assessed by Alamar blue assay. The assay exploits the ability of live cells to maintain a reducing environment. Cells are incubated with a compound that is able to cross the extracellular membrane. If cells are healthy, the compound will be reduced and a fluorescent by-product created. Cell health and viability can be therefore measured by measuring the fluorescence of such product. A decrease in the fluorescence detected is indicative of cell death due to the loss of reducing activity by unhealthy or dead cells.

Control iPSC-derived neurons were incubated with 0, 1, 5 and 10 µM PPMO for 7 days. Results were normalised to those of untreated cells. No significant levels of toxicity was observed upon incubation with any concentration of control PPMO (Fig 5.4 Bi; 1µM = 0.98 ± 0.07; 5µM = 0.99 ± 0.07; 10µM = 0.93 ± 0.05) or C9ORF72 targeting PPMO (Fig 5.4Bii; 1µM = 0.95 ± 0.05; 5µM = 0.91 ± 0.06; 10µM = 0.93 ± 0.02).

5.4.5 C9ORF72 neuronal progenitor cells show neurite outgrowth deficits

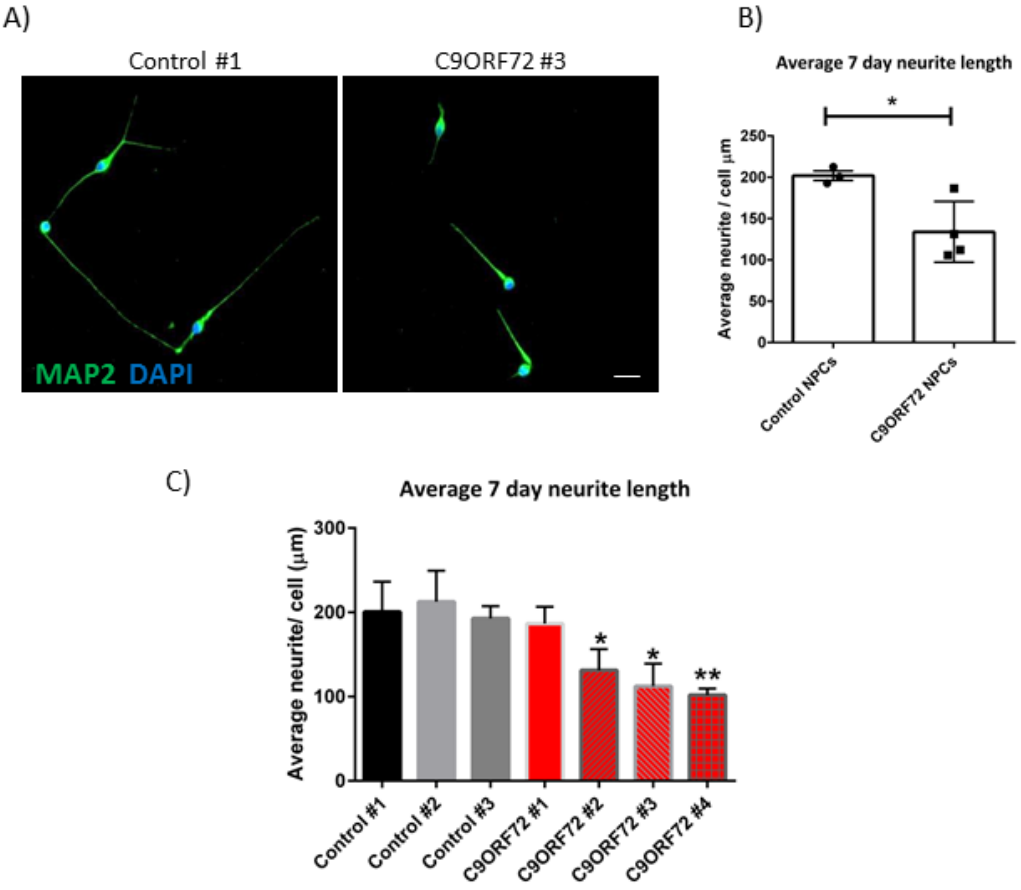

Figure 5.5: C9ORF72 neuronal progenitor cells show reduced neurite outgrowth.

(A) Representative images of 7 day neurite outgrowth deficits in NPCs derived from control #1 and C9ORF72 #3. MAP2 (green) and DAPI (blue). Scale bar = 40 µm **(B)** NPCs derived from C9ORF72 expansion carriers show reduced 7 day neurite outgrowth compared to control NPCs. Each point represents the mean neurite length per cell of each line. Results are represented as mean ± SEM. n=3 two-tailed t-test ($p<0.05$ *) **(C)** Average 7 day neurite outgrowth of individual control and C9ORF72 NPC lines. Data is represented as mean ± SEM. n=3. One-way ANOVA with Tukey's multiple comparisons ($p<0.05$ *, $p<0.01$**).

We investigated the ability of control and C9ORF72 NPC lines to grow neurites upon the removal of FGF from the growth media. Cells were plated at a low confluency and neurite projection was allowed for 7 days after the removal of FGF. Cells were then fixed and stained for MAP2. Images from all conditions were taken in a blinded manner and 30-60 cells were analysed per condition. Three individual replicates were carried out and averaged. The total

length of all neurites was added and divided by the number of cells in order to calculate the average neurite length per cells.

Dendritic and synaptic loss and distal axonal degeneration are early and consistent features of all neurodegenerative disorders, affecting predominantly, but not exclusively, the motor neurons in ALS. Our results show that the average neurite length of C9ORF72 neurons was ~25% shorter than controls (Fig 5.5 A-B; C9ORF72 #1-4 = 141.1µm ± 20.2 and Control #1-3 = 204.2µm ± 4.2; C9ORF72 #1-4 vs. Controls #1-3 $p<0.05$ *. Two-tail t-test). Further analysis shows that only three out of the four C9ORF72 neuronal progenitor cell lines showed neurite outgrowth deficits (Fig 5.5 C; Control #1 = 200 .5µm ± 15.6; Control #2 = 212.5µm ± 16.4; Control #3 = 199.2 µm ± 12.3; C9ORF72 #1 = 180.1µm ± 16.9; C9ORF72 #2 = 131.2µm ± 10.6; C9ORF72 #3 = 112.2µm ± 12.2; C9ORF72 #4 = 101.8µm ± 3.2; All Controls vs. C9ORF72 #1 $p>0.05$ ns; All Controls vs. C9ORF72 #2 $p<0.05$ *, All Controls vs. C9ORF72 #3 $p<0.05$ * All Controls vs. C9ORF72 #4 $p<0.01$ **. One-way ANOVA with Tukey's multiple comparisons).

5.4.6 C9ORF72 iPSN have intranuclear RNA foci but no DPR proteins

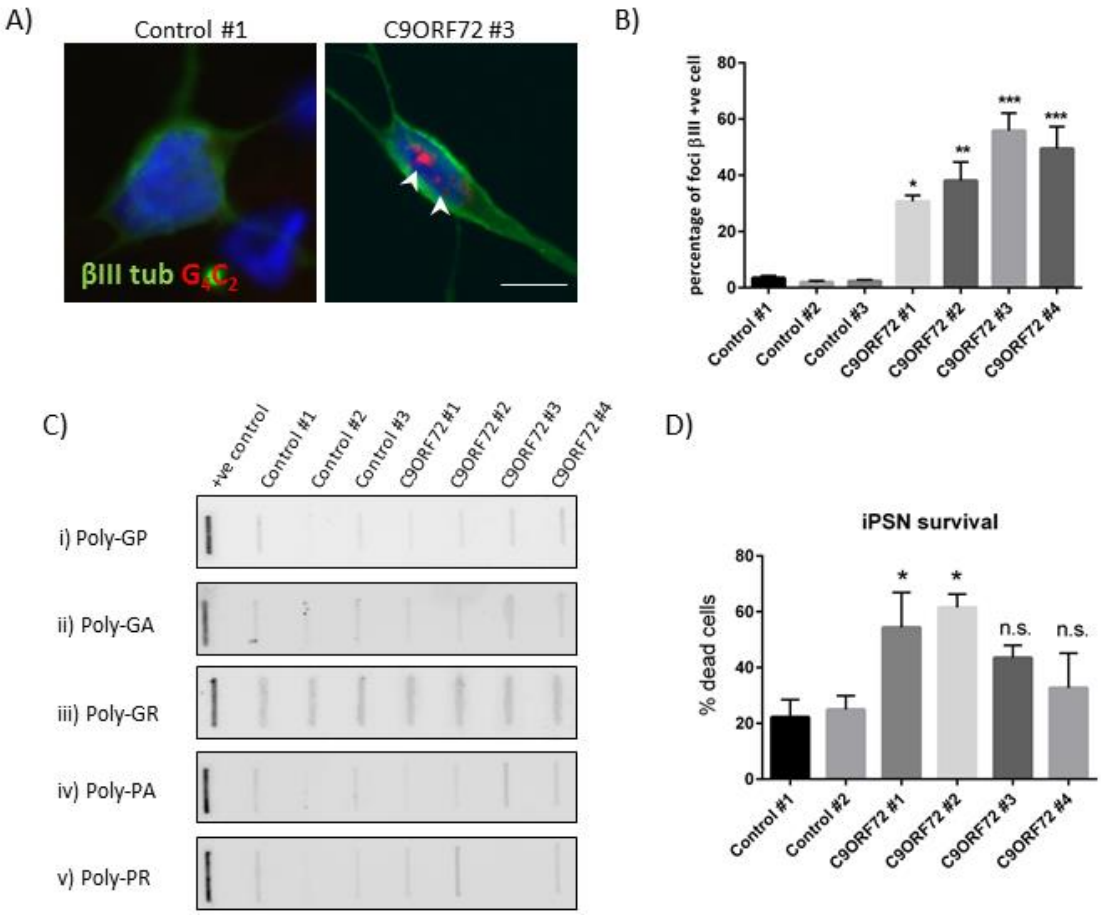

Figure 5.6: C9ORF72 iPSN contain intranuclear RNA foci and increased cell death but we are unable to detect DPR proteins.

(A) Representative images of G4C2 intranuclear RNA foci detected in C9ORF72 iPSN but not in controls. βIII-tubulin (green), G4C2 (red) and DAPI (blue). Scale bars = 20 µm **(B)** Intranuclear G4C2 RNA foci are detected in C9ORF72 iPSN. Results are represented as mean ± SEM. n=3 One-way ANOVA with Tukey's multiple comparisons ($p<0.05$ *, $p<0.01$**, $p<0.001$ ***) **(C)** DPRs are not detected in C9ORF72 or Control iPSN through slot blot analysis. HEK-293T expressing DPRs are used as a positive control. (i) poly-GP (ii) poly-GA (iii) poly-PR (iv) poly-PA and (v) poly-PR. **(D)** iPSN neurons derived from *C9ORF72* expansion carriers show decreased survival. Results are represented as mean ± SEM. one-way ANOVA, with Tukey's multiple comparisons ($p<0.05$ *). Survival assay carried out by Dr. Agnes Nishimura and Dr. Han-Jou Chen.

We next generated neurons from the seven iPSC (iPSN) lines and performed fluorescent *in situ* hybridisation for G4C2 repeat RNA. All quantification was carried out in a

blinded manner. We detected intranuclear sense RNA foci in ~30% to ~60% of neurons generated from C9ORF72-ALS patients (Fig 5.6 A-B; Control #1 = 3.5% ± 1.1; Control #2 = 2.0% ± 0.7; Control #3 = 2.4% ± 0.6; C9ORF72 #1 = 30.7 ± 3.4; C9ORF72 #2 = 38.1% ± 9.4; C9orf72 #3 = 55.8% ± 8.8; C9orf72 #4 = 49.5% ± 10.9, Controls #1-3 vs C9ORF72 #1 $p<0.05$ *, Controls #1-3 vs C9ORF72 #2 $p<0.01$ ** Controls #1-3 vs C9ORF72 #3-4 $p<0.001$ ***. No significance observed within controls #1-3 or C9ORF72 #1-4 lines). Intranuclear RNA foci have been extensively reported in iPSN and are known to recruit several RNA binding proteins such as ADARB2 or hnRNP-H and are one of the pathological hallmarks of C9ORF72-linked ALS/FTD (Cooper-Knock et al., 2014a; Lee et al., 2013; Mizielinska et al., 2013; Prudencio et al., 2015).

The presence of DPR proteins generated through RAN translation from the G4C2 repeats was assessed by performing filter trap assay in neurons differentiated for 75 days. We used lysates from cells HEK-293T cells transfected with constructs capable of generating all five DPR proteins as a positive control. Using this methodology, none of the five DPR proteins were detected in mature iPSN (Fig 5.6 C).

The death of neurons is a defining feature of ALS and FTD pathology. In order to assess the neuronal survival we performed fluorescent activated cell sorting (FACS) of iPSN from control and C9ORF72 lines. The iPSN from C9ORF72-ALS cases (#1 and #2) showed a significant increase of cell death (Fig 5.6 D, Results generated by Dr. Agnes Nishimura with the help of Dr. Han-Jou Chen). We therefore chose assays of neurite outgrowth and cell death as two robust parameters to test the efficacy of PPMOs as a potential therapeutic strategy for C9ORF72-ALS.

5.4.7 PPMOs treatment reduces RNA foci but does not reduce the level of C9orf72 transcripts

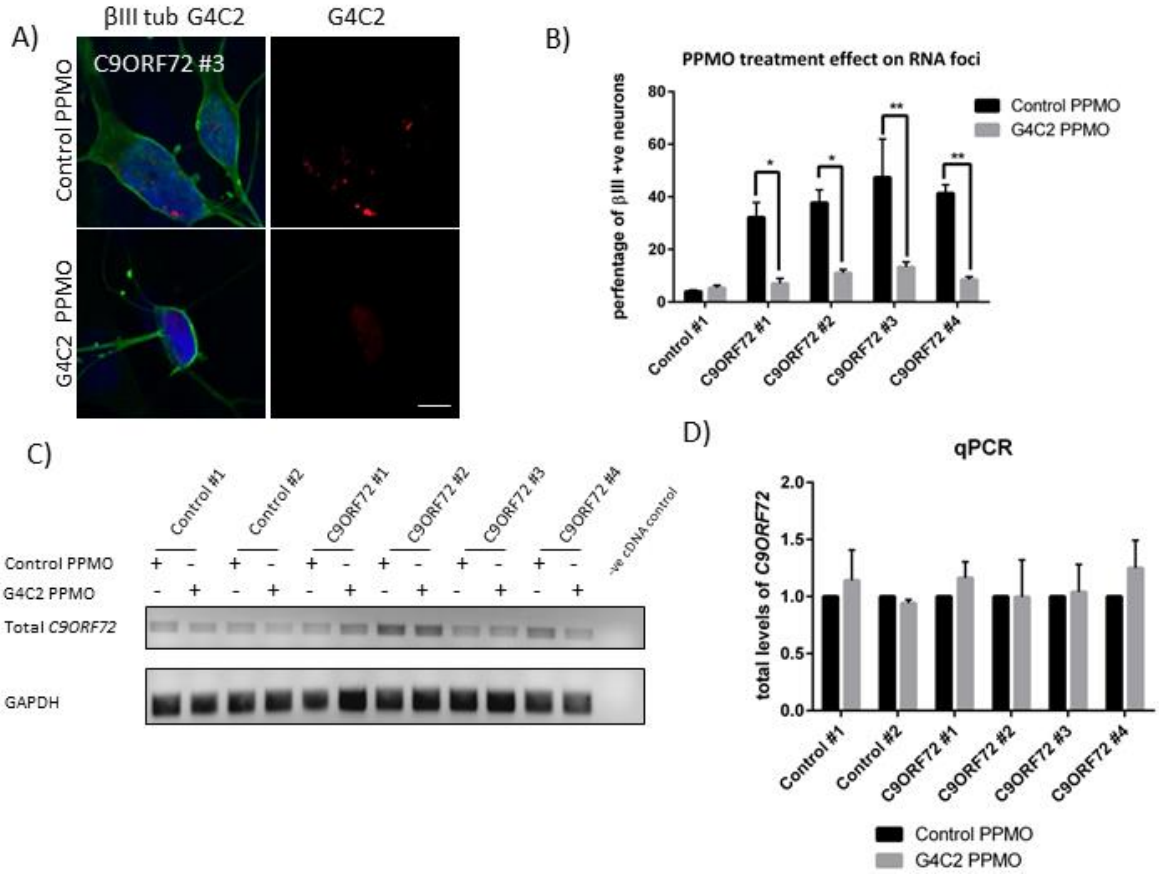

Figure 5.7: Treatment with G4C2 PPMO significantly reduces the number of RNA foci in iPSN but does not reduce the total levels of *C9ORF72* transcripts.

(A) Representative images of iPSN derived from C9ORF72 expansion carriers treated with control and G4C2 PPMO. βIII-tubulin (green), G4C2 (red) and DAPI (blue). Scale bar = 20 µm **(B)** Treatment of iPSN with G4C2 PPMO significantly reduces the number of detectable G4C2 RNA foci in C9ORF72 iPSN. Results are represented as mean ± SEM. Two-way ANOVA with Tukey's multiple comparisons, selected pairs ($p<0.05$ *, $p<0.01$**) **(C)** G4C2 PPMO treatment does not alter the levels of total *C9ORF72* transcript. Representative RT-PCR results. GAPDH was used as a loading control. **(D)** Quantification of the effect of PPMO treatment on the levels of total *C9ORF72* transcripts compared to control PPMO treatment. Results are represented as mean ± SEM. Two-way ANOVA with Tukey's multiple comparisons, selected pairs. Not significant.

In order to test the efficacy of using PPMOs as a therapeutic strategy we treated iPSN derived from control and C9ORF72 expansion carriers for 7 days with control and G4C2 PPMOs. The effect of G4C2 PPMO treatment on the number of detectable RNA foci was assessed, showing a significant decrease in all four C9ORF72 iPSN lines when compared to control PPMO (Fig 5.7 A-B; Control #1: Control PPMO = 4.1% ± 0.5, G4C2 PPMO = 5.4% ± 1.0; C9ORF72 #1: Control PPMO = 32.2% ± 5.6, G4C2 PPMO = 7.0 % ± 1.9; C9ORF72 #2: Control PPMO = 37.8% ± 4.9, G4C2 PPMO = 11.1 % ± 1.3; C9ORF72 #3: Control PPMO = 52.3% ± 10.0, G4C2 PPMO = 13.3 % ± 2.0; C9ORF72 #4: Control PPMO = 41.4% ± 3.3, G4C2 PPMO = 8.5% ± 1.6; C9ORF72 #1: Control PPMO vs G4C2 PPMO $p<0.05$ *; C9ORF72 #2: Control PPMO vs G4C2 PPMO $p<0.05$ *; C9ORF72 #3: Control PPMO vs G4C2 PPMO $p<0.01$ **; C9ORF72 #4: Control PPMO vs G4C2 PPMO $p<0.01$ ** Two way ANOVA with Tukey's multiple comparisons). This result shows that PPMOs are internalised into mature iPSN, bind G4C2 expanded transcripts and reduce the number of RNA foci.

The effect of PPMO treatment on the total levels of *C9ORF72* transcript levels was assessed by qRT-PCR. As expected, treatment of control and C9ORF72 iPSN with lines with control and G4C2 PPMO resulted in no significant change in the levels of total *C9ORF72* transcript (Fig 5.7 C-D).

5.4.8 PPMO treatment rescues C9ORF72 NPC neurite outgrowth deficits

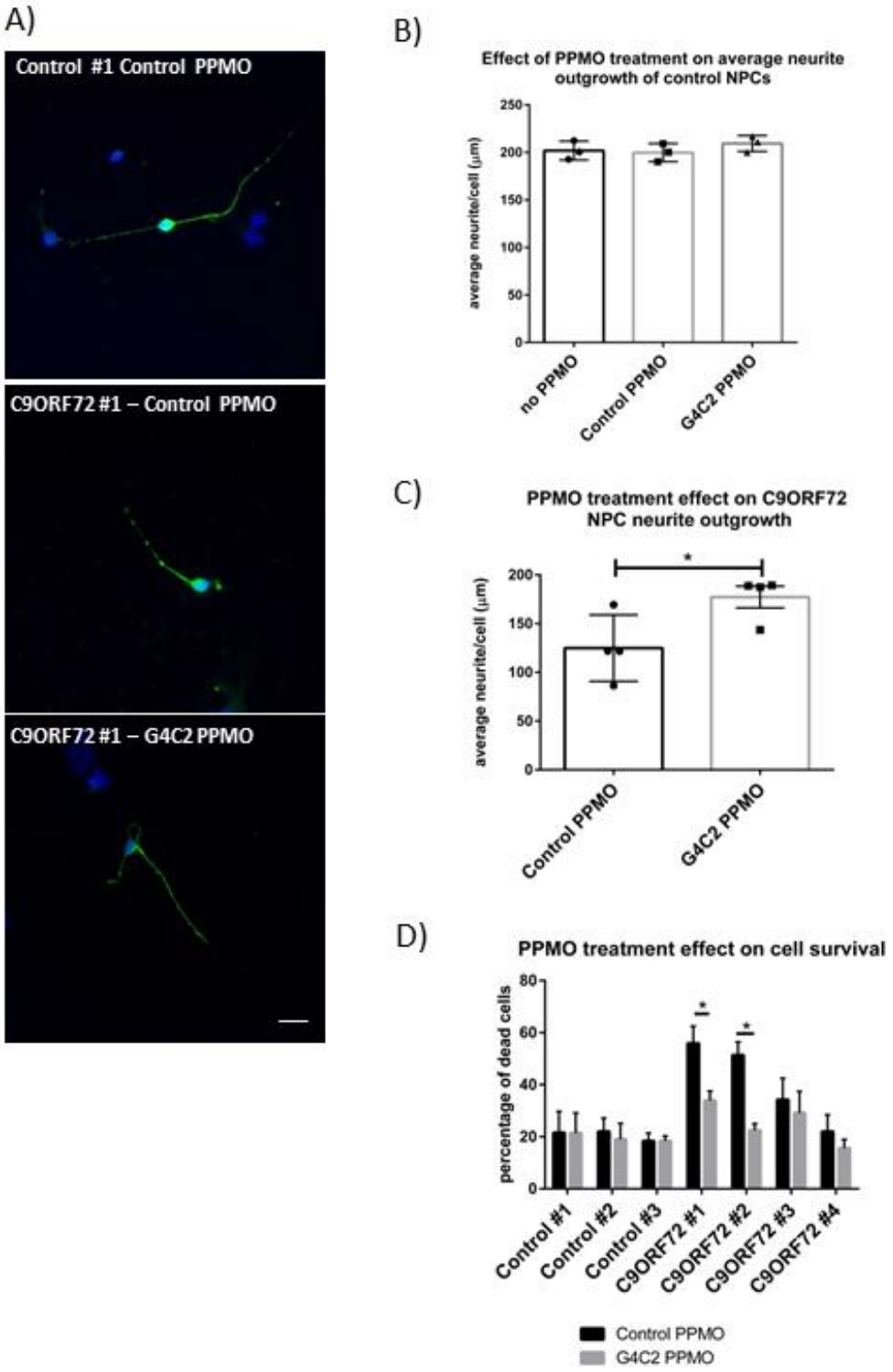

Figure 5.8: PPMOs rescue NPC neurite outgrowth deficits and improve survival of C9ORF72 iPSN.

(A) Representative images of PPMO treatment on 7 day neurite outgrowth NPCs derived from control #1 and C9ORF72 #3. MAP2 (green) and DAPI (blue). Scale bar = 40 µm **(B)** PPMO treatment does not affect 7 day neurite outgrowth in control NPCs. Cells were treated with 5µM control and G4C2 PPMO, or untreated. Each point represents the average neurite length of each control line. n=3. 30-60 NPCs were analysed per condition. No significant differences were observed. **(C)** Treatment of iPSN with G4C2 PPMO reverses neurite outgrowth deficits in C9ORF72 NPCs. Results are represented as mean ± SEM. Each point represents the mean neurite length per cell of each line. Results are represented as mean ± SEM. n=3 two-tailed t-test ($p<0.05$ *) **(D)** PPMO treatment increases cell survival of C9ORF72 iPSN. Results are represented as mean ± SEM. Two-way ANOVA with Tukey's multiple comparisons, selected pairs ($p<0.05$ *).

Prior to investigating the effect of PPMO treatment on the average neurite length in C9ORF72 NPCs, we tested them in all three control lines. Control cell lines of the same passage were incubated for 7 days with 5µM control and G4C2 PPMO at the same time as FGF was removed from the culture media. Control cell lines showed no significant difference in the average neurite outgrowth upon incubation with G4C2 PPMO and control PPMO compared to no PPMO control. Three individual replicates were carried out for cell line (Figure 5.8 A and B; No PPMO = 201.9 µm ± 5.7; Control PPMO = 199.8 µm ± 5.5; G4C2 PPMO = 209.4 µm ± 4.8). We therefore concluded that PPMO treatment has no effect on the ability of NPC lines to grow neurites and that any effect observed in C9ORF72 NPC lines may be due to the effect of the PPMO and not the cell penetrating peptide.

5.4.9 PPMOs rescue neurite outgrowth deficits in C9ORF72 neuronal progenitor lines

Having established that PPMOs are internalised by iPSN and bind expanded G4C2 repeats we tested the effect of treating NPCs and iPSNs derived from C9ORF72-ALS patients with PPMOs and assess the impact on the neurite outgrowth and decreased cell survival.

Control and C9ORF72 NPCs were treated with 5µM PPMO for the duration of the differentiation protocol. Treatment of C9ORF72 lines with G4C2 PPMO resulted in a rescue event on the neurite length by ~33% compared to control treatment (Fig 5.8 C). Moreover, treatment of control NPCs with control and G4C2 PPMO had no effect on the average neurite

length (Fig 5.8 B), showing that the PPMO binding expanded RNA transcripts is responsible for the phenotypic recovery.

5.4.10 Treatment with PPMO improves survival of C9ORF72 ALS iPSC-derived neurons

The ultimate aim of antisense oligonucleotides is to mitigate the toxic effect of the expanded G4C2 transcripts and increase cell survival. We treated mature iPSN with control and G4C2 PPMOs and performed FACS analysis. There was no significant difference in cell survival upon treatment of control iPSN with control and G4C2 PPMOs (Fig 5.8 D), confirming what was observed by ALAMAR blue assay (Fig 5.4 B). Treatment of mature iPSN with G4C2 PPMO resulted in a significant decrease in cell death in two out of the four C9ORF72 iPSN studied (C9ORF72 #1 and #2) (Fig 5.8 D). Although we observed a slight decrease in cell death in the other two C9ORF72 iPSN lines (#3 and #4) the effect was not enough to reach statistical significance. Although the results were variable, reflecting the heterogeneity of human patient-derived cells they demonstrate the potential therapeutic use of PPMOs to mitigate the toxic effect of the *C9ORF72* expansion.

5.5 DISCUSSION

In the present study we analysed iPSC-derived neurons from three health controls and four C9ORF72-ALS expansion mutation carriers. We have shown that C9ORF72 ALS iPSN contain intranuclear G4C2 RNA foci but we were unable to detect any DPRs by filter trap assay. C9ORF72 ALS neuronal progenitor cells showed impaired neurite outgrowth compared to control lines and reduced cell survival by FACS analysis. We demonstrated that treatment with G4C2-targeting PPMOs reversed the neurite outgrowth deficits in C9ORF72 neuronal progenitor cell lines and improved cell survival in mature iPSNs.

Several studies investigating iPSCs from C9ORF72 ALS patients report a variety of pathological phenotypes including impaired ubiquitin proteosome system function (Almeida

et al., 2013), increased sensitivity to glutamate toxicity (Donnelly et al., 2013), reduced neurite outgrowth (Burguete et al., 2015), impaired nucleocytoplasmic transport (Zhang et al., 2015) and increased cell death (Dafinca et al., 2016). We confirmed reduced neurite outgrowth in neuronal progenitor cells. We chose to analyse immature neurons due to the complexity of the neurite arbour of more mature neurons and because they can be rapidly analysed after a short period of culture. Post mortem studies of C9ORF72 ALS cases reveal dystrophic neurites in *C9ORF72* spinal motor neurons (Simon-Sanchez et al., 2012), indicating that this phenotype in neuronal progenitor cells may be relevant to disease pathology. However, the fact NPCs may not be entirely relevant as ALS is a late onset disease and not a developmental disorder. The use of these cells may provide a fast drug discovery assay which is should be explored in the future with the use of high throughput assays. This will be discussed in greater detail in the discussion section. We have also shown that 2/4 iPSN lines derived from *C9ORF72* expansion carriers show a significant reduced cell survival by FACS analysis, which is consistent with previously published studies (Dafinca et al., 2016; Donnelly et al., 2013). We were unable to detect the presence of any DPR in neurons cultured for 75 days, suggesting that any phenotype observed in iPSN is due to an RNA gain-of-function toxicity. We are aware of the limitations of this assay and we acknowledge that the use of a Meso Scale Discovery-based poly-GP immuno-assay (Gendron et al., 2017) could be used to detect the presence of poly-GP in a more accurate manner. In the absence of detectable DPRs we hypothesize that toxicity in iPSN is due to the presence of expanded G4C2 RNA transcripts that recruit RNA binding proteins and may disturb many steps in the processing of RNA from splicing, transport and translation.

Previous studies exploring the use of antisense oligonucleotides to mitigate the C9ORF72 expansion toxicity have yielded promising results, reversing *C9ORF72*-specific increased glutamate sensitivity and splicing dysregulation (Donnelly et al., 2013; Sareen et al., 2013) and *C9ORF72*BAC transgenic mice (Jiang et al., 2016). It must be noted that

Donnelly *et al.* 2013 reverses C9ORF72-specific phenotypes in iPSN using degrading ASOs but does not report a decrease in the total levels of *C9ORF72* transcripts. However, the ASOs used by Jiang et al. 2015 that reverse C9ORF72-specific phenotypes in C9ORF72 BAC mice achieve ~50% reduction in the total levels of *C9ORF72* transcript levels. Degrading the target mRNA may not be a suitable therapeutic strategy if haploinsufficiency of C9ORF72 plays a pathogenic role in C9ORF72 ALS neurodegeneration. Using of non-degrading PPMOs that target the G4C2 expansion we were able to reverse neurite outgrowth deficits in C9ORF72 ALS neuronal progenitors (Fig 5.8 A and C) and significantly improve the survival of mature C9ORF72 ALS neurons (Fig 5.8 D).

It must be mentioned that the use of iPSN is used to model a late-onset neurodegenerative disorder. Clearly, the few months of cell culture do not compare to years of aging in the adult nervous system. Moreover, recent studies have suggested that iPSN are transcriptionally closer to fetal human neurons than to mature human neurons (Mertens et al., 2015a). Additionally, the timescale of the differentiation protocol is likely to be a critical parameter. Some studies have used neurons differentiated for up to 365 days in an attempt to model MAPT-linked FTD (Sposito et al., 2015). The potential of iPSN to model late--onset conditions will be explored in greater detail in the general discussion.

Our results strengthen the hypothesis that expanded G4C2 RNA transcripts are the main contributor to toxicity in C9ORF72 ALS and that PPMOs targeting G4C2 repeats can reverse pathogenic phenotypes. The lack of detectable DPRs in C9ORF72 ALS iPSC-derived neurons in culture and their virtual absence in C9ORF72 ALS spinal motor neurons at post mortem tissues challenges a major role in disease pathogenesis.

Finally, we have shown the promising therapeutic potential of non-degrading PMOs to mitigate G4C2 toxicity in cell culture setting. We have shown that PMO treatment is able to rescue specific phenotypes linked to *C9ORF72* by blocking and not degrading the G4C2

expanded RNA. This opens a new and exciting therapeutic avenue that must be tested further using *in vivo* models of the disease.

6 GENERAL DISCUSSION

6.1 DPR INCLUSIONS ARE EXTREMELY RARE IN C9ORF72-ALS SPINAL MOTOR NEURONS

The presence of aggregated protein inclusions is a feature common to all neurodegenerative conditions. In Alzheimer's disease the presence of extracellular aggregates of amyloid-β peptides, intracellular inclusions of microtubule-associated protein tau forming neurofibrillary tangles and neuritic plaques are pathological hallmarks of the disease (Canter et al., 2016). α-synuclein aggregates form in dopaminergic neurons in the substantia nigra in Parkinson's disease (Spillantini et al., 1997) and are more widely distributed in Dementia with Lewy bodies (Baba et al., 1998). Similarly, cytoplasmic TDP-43 inclusions are the pathological hallmark of ALS and tau-negative FTD (Neumann et al., 2006). The presence of cytoplasmic, poly-ubiquitinated, hyper-phosphorylated TDP-43 aggregates correlates closely with the site of symptomatic neurodegeneration in ALS and FTD (Davidson et al., 2016). For C9ORF72 ALS however another set of inclusions are present, due to repeat associated non-ATG translation of G4C2 transcripts to generate DPRs of poly GA, GP, GR from the sense strand and PA and PR from antisense. Cytoplasmic and intra-nuclear DPR inclusions are abundant in the cerebellum, frontal and temporal lobes and have been shown to be toxic in a range of cellular and *in vivo* studies. This has implicated them in driving the neurodegeneration seen in C9ORF72 ALS and FTD.

In this study we sought to quantify the number of inclusions present in the spinal cord of C9ORF72 ALS cases. We used highly specific DPR antibodies that had been previously extensively validated by others in FTD cases (Chew et al., 2015b; Gendron et al., 2013). Using a previously published semi-quantitative scale (Mackenzie et al., 2013b) to estimate the

relative abundance of TDP-43 inclusions in the spinal cord we observed no difference in the scores for TDP-43 aggregation between C9+ve ALS and C9-ve ALS cases, confirming previous reports (Murray et al., 2011). Having confirmed that our anti-DPR antibodies were sensitive in detecting DPR inclusions in the cortex and cerebellum in C9ORF72-FTD we analysed the spinal cord of ten C9+ve ALS and 5 C9-ve ALS cases. The number of DPR aggregates was highly consistent within cases and all DPRs were scored as either rare, very rare or absent and no more than twelve inclusions of any DPR was observed in any of the cases analysed. DPRs translated from the sense strand (poly-GP, GA and GR) were more abundant than those translated solely from the antisense strand (poly-PR, PA). In contrast TDP-43 inclusions were detected in 38% of surviving motor neurons. It is impossible to exclude the possibility that neurons with toxic DPRs had died and been removed or that toxic DPR species are too small to be detected by confocal microscopy but this would be at variance with all other neurodegenerative disorders where the neurotoxic proteins are readily detected. ~~Our study provides strong circumstantial evidence that it is TDP-43 aggregation or mislocalisation, and not DPRs, that plays a dominant mechanistic role in motor neuron degeneration in C9ORF72 ALS.~~ Others have suggested that the presence DPRs may gradually trigger TDP-43 pathology and subsequent region-specific neurodegeneration in a cascade similar to amyloid-β peptide in Alzheimer's disease (Edbauer et al., 2016). In order to test this hypothesis, mouse models of each DPR may provide useful to understand the distribution of DPRs throughout the disease process. Furthermore it is possible that neurons containing DPR aggregates have died.

Our study was the first to quantify all five DPRs in the spinal cord of ALS cases, which is the main site of neurodegeneration in ALS (Gomez-Deza et al., 2015). Since that publication, other studies have confirmed our findings (Davidson et al., 2016; Mackenzie et al., 2015). Additional evidence comes from a separate study showing that the levels of all

soluble DPRs are very low in the spinal cord of C9+ve ALS cases, casting doubt on their role in causing neurodegeneration (Mackenzie et al., 2015).

Models of the DPR toxicity have not always provided consistent results. Most *in vitro* and *in vivo* studies have reported that poly-GP and poly-PA are not toxic and that the arginine-rich poly-GR and poly-PR DPR proteins are the main source of toxicity (Mizielinska et al., 2014; Wen et al., 2014) although others suggest that poly-GA is the main driver of cell death (Schludi et al., 2017; Zhang et al., 2016b). Additionally only cellular models expressing poly-GA reproduce the typical p62 positive, neuronal cytoplasmic aggregates observed in human post-mortem tissue (Schludi et al., 2015). Perhaps unsurprisingly, adding arginine rich poly-GR and poly-PR to the cell culture medium results in these DPRs being internalised by cells going to the nucleolus (Kwon et al., 2014) since arginine rich peptides have been exploited commercially as cell-penetrating peptides to facilitate the internalisation of a wide range of cargos into cells (Guidotti et al., 2017).

The modelling of DPR protein toxicity has been carried out using DPRs of varying lengths which show different subcellular localisations (Bennion Callister et al., 2016). Therefore elucidating the length of the DPRs present in post mortem tissue may help develop better models of the DPR toxicity. Additionally, the lack of TDP-43 pathology in most of these *in vitro* and *in vivo* models suggests that the toxicity observed is due to the high level of DPR expression of these proteins and do not fully model the disease pathology. Finally, two studies have reported the necessity for poly-GA (Zhang et al., 2016b) and poly-PR (Wen et al., 2014) to aggregate in order induce toxicity, strengthening our observation that DPR protein inclusions are not the main source of toxicity in C9ORF72 ALS.

Whilst we cannot entirely exclude the possibility that DPR aggregation and toxicity occurs at the sub-microscopic level, or that all motor neurons containing DPR inclusions were lost, this explanation seems unlikely as neurotoxic protein aggregates are detected in the

affected neurons for all other neurodegenerative diseases. As the number of TDP-43 inclusions in ALS cases, with and without the *C9ORF72* mutation are nearly identical we can find no evidence that dipeptide repeat proteins are playing a strong pathogenic role in C9ORF72 ALS.

6.2 Sense and antisense RNA foci are abundant in the spinal cord of ALS cases

We have shown that both sense and antisense RNA foci are common in C9+ve-ALS spinal cords, with sense RNA foci being significantly more common than antisense foci. Most of the studies quantifying the number of sense and antisense RNA foci in C9ORF72 ALS and FTD have focussed on the frontal cortex (DeJesus-Hernandez et al., 2017; Gendron et al., 2013; Mizielinska et al., 2013) and the hippocampus (Cooper-Knock et al., 2014a). These studies have provided valuable information showing that sense and antisense RNA foci are present in the central nervous system of *C9ORF72*-FTD cases and are primarily located in the nucleus of neurons (DeJesus-Hernandez et al., 2017; Mizielinska et al., 2013).

Only two studies by the same group (Cooper-Knock et al., 2015; Cooper-Knock et al., 2014a) have attempted to quantify sense and antisense foci in the spinal cord motor neurons in C9+ve-ALS. These publications however report on a small number of patients (n=7) and a small number of motor neurons (n=54). Cooper-Knock *et al.* (2014) compared the presence of foci-positive neurons in the granule neurons with spinal motor neurons in only one C9ORF72-ALS/FTD and three C9ORF72-ALS cases. They concluded that there were a significantly greater number of sense foci-positive motor neurons than granule neurons. Subsequently they reported that the number of antisense and not sense RNA foci, or poly-GA aggregates that correlated with TDP-43 nuclear depletion (Cooper-Knock *et al.* 2015) but they analysed only 54 spinal motor neurons in seven C9+ve-ALS cases. We therefore sought

to replicate and validate their findings in a larger sample size by analysing almost 300 spinal motor neurons in 10 C9+ve-ALS cases. We observed that both sense and antisense RNA foci were commonly detected in spinal cord motor neurons but sense foci were more common than antisense foci. We did not observe a significant correlation between the presence of sense or antisense RNA foci and TDP-43 nuclear depletion. We attribute the differences in our results from the earlier studies to case to case variation and stand by our results which analysed a much larger number of neurons and cases reducing the influence of case to case variation commonly seen in post mortem studies.

In summary, we showed that sense RNA foci are the most common pathological feature in the spinal cord and motor neurons of C9ORF72-ALS cases, followed by antisense RNA foci and DPR protein inclusions. Based on circumstantial evidence we suggest that the presence of sense RNA foci are more likely to contribute to pathogenesis of C9+ve-ALS driven principally by TDP-43 aggregation or nuclear depletion. However the strong cellular animal evidence showing DPR toxicity suggests that DPR toxicity may be also be an important contributing factor to neurodegeneration.

6.3 Antisense oligonucleotides targeting G4C2 reduce RNA foci but not DPRs

We next investigated the potential of using non-degrading PMOs to bind and block G4C2 repeats without inducing the degradation of the target transcript. Several groups have reported that the use of ASOs which degrade the *C9ORF72* transcript and reduce the levels of DPRs and RNA foci *in vitro* (Donnelly et al., 2013; Lagier-Tourenne et al., 2013; Sareen et al., 2013) reversing *C9ORF72*-specific phenotypes such as increased glutamate toxicity, and *in vivo* reducing anxiety-like behaviour of transgenic mice expressing the full *C9ORF72* gene with 450 repeats (Jiang et al., 2016). The ASOs used in these studies however also reduce the

level of total *C9ORF72* transcripts. Decreasing the C9ORF72 protein levels may be counterproductive as it has been shown to play in important role in the immune system (Atanasio et al., 2016; O'Rourke et al., 2016) and one of the proposed toxic mechanisms of C9ORF72-ALS/FTD is haploinsufficiency (DeJesus-Hernandez et al., 2011).

We have previously reported that G4C2 repeats are neurotoxic in a length-dependent manner (Lee et al., 2013). Cells expressing EGFP-G4C2 repeats contain intranuclear G4C2 foci which sequester proteins such as hnRNP-H and undergo RAN translation yielding DPR proteins such as poly-GP. Here I have shown that G4C2-targeting PPMOs reduce the number of RNA foci in a concentration-dependent manner in cells expressing 38X and 72X repeats. In order to exclude the possibility that PPMOs were merely masking the detection of RNA foci we designed an alternative, non-competing FISH probe targeting the EGFP sequence in the EGFP-G4C2 transcript, a strategy previously applied in other repeat expansion disorders (Wheeler et al., 2009). Using this probe, we showed that G4C2-targetted PMOs also reduce the number of EGFP foci confirming their clearance from the nucleus although the mechanism by which this occurs is uncertain. Given that cells are transfected for 24 hours prior to PMO treatment, we hypothesize that PMOs dissociate the RNA foci, however it is possible that the PMOs also prevents the formation of RNA foci.

Although RNA foci were reduced we did not observe a significant decrease in the total levels of poly-GP following PPMO treatment. PMOs are known to efficiently block translation (DeVos and Miller, 2013) so we hypothesize that this may be due to the fact that cells were transfected with G4C2 constructs one day prior to the PPMO treatment and that PPMOs are slowly internalised over 24 hours (DeVos and Miller, 2013) so that DPR synthesis may have already taken place. Moreover, it is also possible that binding of PMO does not affect the structural motifs required to initiate RAN translation. It would be of interest to investigate

whether PMOs have the ability of preventing the formation of secondary RNA structures such as G-quadruplexes.

We concluded that the use of non-degrading PPMOs targeted at the G4C2 repeats reduce the number of G4C2 RNA foci and that their potential therapeutic use should be tested in a physiologically relevant model of the disease such as iPSC-derived neurons (iPSN) from *C9ORF72* expansion carriers.

6.4 C9ORF72-ALS iPSC NEURONS HAVE INTRANUCLEAR RNA FOCI, DECREASED NEURITE OUTGROWTH AND SURVIVAL

We generated iPSCs from C9ORF72 ALS cases and controls and have shown that iPS-derived neurons carrying the G4C2 expansion have an abnormal phenotype. All studies that have generated C9ORF72-iPSN have reported the presence of RNA foci which are able to recruit RNA binding proteins such as hnRNP-H (Sareen et al., 2013) and ADARB2 (Donnelly et al., 2013). The presence of insoluble DPRs in C9ORF72 iPSNs has not been consistently reported; Almeida *et al.* (2013) detected DPRs in 28 day old cortical neurons by filter trap analysis, Donnelly *et al.* (2013) identified poly-GP by immunofluorescence but Sareen *et al.* (2013) was unable to detect them by dot blot analysis or immunofluorescence. We were also unable to detect any of the five DPR proteins by filter trap assay in cortical neurons cultured over 75 days or immunocytochemistry. This discrepancy may be due differences in the C9ORF72 ALS cell lines, differentiation protocols and time in culture.

The use of iPSN has been instrumental in the study of the *C9ORF72* expansion. A variety of important phenotypes have been observed in C9ORF72 iPSN including; impaired UPS function (Almeida et al., 2013), neurite outgrowth (Burguete et al., 2015) and nucleocytoplasmic transport (Zhang et al., 2015), as well as increased sensitivity to glutamate

toxicity (Donnelly et al., 2013) and cell death (Dafinca et al., 2016). Here we have shown that the average total neurite length of C9ORF72 neuronal progenitor cells (NPCs) is ~33% shorter than control NPCs. We chose to analyse neurites from immature neurons due to the complex structure of more mature neurons and the short time taken to grow NPCs is suitable for high-throughput drug discovery assays.

Dendritic and synaptic loss and distal axonal degeneration are early and consistent features of all neurodegenerative disorders, affecting predominantly, but not exclusively, the motor neurons in ALS. Neurite outgrowth deficits have been previously reported in FUS (Kabashi et al., 2011), TDP-43 (Egawa et al., 2012) and *C9ORF72* (Burguete et al., 2015) *in vitro* and *in vivo* models of ALS. Neurite outgrowth depends on a complex interplay between extracellular guiding cues and intracellular signaling pathways. Extracellular cues are detected by molecules expressed on the surface of neurons, and transduced to activate cell signaling and gene transcription inside the cell (Hansen et al., 2008).

Precisely how G4C2 transcripts affect the behaviour and survival of neurons is unknown and it is important to acknowledge that iPSNs are immature cells grown for short time intervals in a non-physiological environment and to avoid making direct correlations to the human pathology which occurs over many years in an aging and complex nervous system. Given that several groups have demonstrated a reversal of the abnormal phenotype using G4C2 targeted ASOs these cellular events are likely to genuinely reflect G4C2-driven neuronal dysfunction. It is possible that RNA foci leads to the sequestration of RNA binding proteins and aberrant RNA processing affecting a wide range of cellular functions. Transcripts containing G4C2 repeats have been detected in the neurites of C9ORF72 iPSN (Burguete et al., 2015) and it is therefore possible that they may bind RNA binding proteins and alter axonal transport and peripheral translation of mRNA including TDP-43 itself. The G4C2 repeats form G-quadruplexes *in vitro* (Fratta et al., 2012) and *in vivo* (Conlon et al.,

2016a). Moreover TDP-43 binds to G-quadruplexes in neurites of iPSC-derived neurons (Ishiguro et al., 2016) and IPSN derived from patients carrying *TARDBP* mutations show impaired axonal transport (Alami et al., 2014). Regardless of the mechanism, motor neurons are the most polarised cell in the body with axons reaching a meter in length, abnormal neurite outgrowth and cargo transport might be especially relevant in predisposing these cells to degeneration as is seen in ALS.

The dysfunction and death of neurons is fundamental to the irreversible progression of ALS and FTD. We have shown that 2/4 C9ORF72 iPSN lines investigated show significant reduced cell survival. Our results are consistent with other published studies (Dafinca et al., 2016; Donnelly et al., 2013). The loss of neurons has been widely reported in animal models of TDP-43 (Mitchell et al., 2015), FUS (Mitchell et al., 2013) and *C9ORF72* (Chew et al., 2015b; Liu et al., 2016). Dafinca *et al.* (2016) reported that C9ORF72 iPSN decreased survival is correlates with disrupted calcium homeostasis and ER dysfunction. We observed a similar rate of neuronal cell death in our C9ORF72 iPSNs as reported by Dafinca *et al.* (2016). The fact that RNA foci are abundant and DPRs are absent in our C9ORF72 IPSNs and suggests that the increased cell death observed is likely to be driven by expanded G4C2 RNA transcripts and not DPRs.

Because C9ORF72 NPCs and iPSN replicate some aspects of human pathology, such as the presence of intranuclear RNA foci (DeJesus-Hernandez et al., 2011; Mizielinska et al., 2013), neurite outgrowth deficits (Simon-Sanchez et al., 2012) and neuronal death we believe that they are a useful model to test the therapeutic potential of G4C2 targeting PPMOs.

6.5 G4C2 PPMOs DECREASE THE NUMBER OF RNA FOCI BUT NOT THE LEVELS OF *C9ORF72* TRANSCRIPTS

We have shown that G4C2 PPMOs are internalised into mature iPSN and that upon doing so they reduce the number of detectable RNA foci without decreasing the total *C9ORF72* transcripts levels. This result demonstrates that G4C2 PMOs bind to G4C2 RNA in iPSN. RNA foci in C9ORF72 iPSNs have been reported to solely comprise G4C2 repeats edited out from the *C9ORF72* transcript (Donnelly et al., 2013). Although we did not confirm this with probes for neighbouring intronic or exonic sequence the results from our EGFP-G4C2 transfection studies strongly suggest that the PMOs are reducing the number of G4C2 foci and not just masking them, which would not be predicted to reverse the abnormal cellular phenotypes we and others have observed.

Previous studies exploring the use of antisense oligonucleotides to mitigate the *C9ORF72* expansion have yielded promising results, reversing *C9ORF72* specific phenotypes in iPSN (Donnelly et al., 2013; Sareen et al., 2013) and C9ORF72 mouse model (Jiang et al., 2016). These ASOs however degrade the target mRNA, which may not be a suitable therapeutic strategy if haploinsufficiency plays a role in the pathogenic mechanism of C9ORF72-ALS. More broadly they can have important side effects as the knockdown of *C9ORF72* has shown to cause important immunological deficits in mice (Atanasio et al., 2016; O'Rourke et al., 2016). In these experiments we have shown that the number of RNA foci can be decreased without reducing the total levels of *C9ORF72*. The lack of *C9ORF72* knockdown may therefore reduce possible side effects then administering the PMO.

6.6 G4C2 PMOs REVERSE DISEASE-SPECIFIC PHENOTYPES

We have shown that the neurite outgrowth deficits observed in C9ORF72 ALS NPCs is reversed by treatment with G4C2 targeting PPMOs. Moreover, we have shown that PMO treatment significantly reduces cytotoxicity in mature C9ORF72 iPSN. From a mechanistic point of view, the absence of detectable DPRs and the presence of intranuclear RNA foci suggests that C9ORF72 ALS toxicity is due to a gain-of-function arising from the RNA transcripts and possibly the foci themselves. We and others have shown that G4C2 repeats are neurotoxic (Lee et al., 2013; Stopford et al., 2017) and that they sequester numerous RNA binding proteins (Cooper-Knock et al., 2014a; Lee et al., 2013). Moreover the presence of G4C2 RNA transcripts in neurites suggests that toxicity may also be driven by expanded transcripts in the cytoplasm (Burguete et al., 2015). Our results show that PMOs bind G4C2 repeats and disrupt RNA foci; however we have also shown that after internalisation, PMOs uniformly distribute in the nucleus and the cytoplasm. It is therefore possible that the binding of PMOs to expanded G4C2 transcripts in the cytoplasm at very low levels, as well as the disruption of RNA foci, may contribute to the improvement in neurite outgrowth and decreased cell death observed. For this reason it would interesting to investigate the effect G4C2 repeat RNA that localise in the cytoplasm and neurites of neurons and their binding partners. Although we did observe occasional RNA foci in the cytoplasm of C9ORF72 iPSN, it was technically challenge to detect RNA foci in the neurites given that iPSN grow in dense networks making it difficult to identify the neurites arising from an individual neuron. It is also possible that expanded G4C2 repeats present in the cytoplasm of neurites and able to exert a toxic effect even though they do not form classical quadruplex structures and visible RNA foci.

It must be noted that Donnelly *et al.* (2013) explored the effect of treating C9ORF72 iPSN with a blocking ASO of a different backbone chemical modification to ours. They show that

this MOE ASO does significantly reduce the sensitivity of C9ORF72 iPSN to glutamate excitotoxicity, but less effectively than the other degrading ASOs tested. This may be due to poor uptake of iPSN due to the MOE ASO but no data on this was reported. However, their results confirm that non-degrading ASOs can reverse *C9ORF72*-specific phenotypes in other laboratories and further validates our results.

From a therapeutic and drug discovery perspective, our results highlight a novel therapeutic approach which consists in blocking the G4C2 expanded RNA transcripts but not degrading them. This may be important given that haploinsufficiency of C9ORF72 protein may also be a component of the C9ORF72 ALS pathogenic mechanism. Our study also highlights the potential of iPSC-derived neurons for drug testing, which has been previously described for ALS (Egawa et al., 2012).

It would be of great interest to assess the efficacy of G4C2 PPMOs in a mouse model of the disease. Several *C9ORF72* transgenic mouse models have been developed with inconsistent results. Two studies that generated *C9ORF72* mouse models expressing the full *C9ORF72* human gene reported the presence of DPRs and sense and antisense RNA foci but observed no neuronal loss or phenotypic deficits (O'Rourke et al., 2015; Peters et al., 2015). Another group has reported that *C9ORF72* transgenic mice have sense and antisense RNA foci, DPR proteins aggregates as well as TDP-43 aggregates in the main sites of neurodegeneration (Liu et al., 2016). These mice show strong dose and gender-dependent phenotypic differences. Jiang *et al.* (2016) showed that the neuronal loss and FTD-like anxiety phenotypes observed in *C9ORF72* transgenic mice can be recovered with a single dose of G4C2-targeting ASO. These mice however did not show any TDP-43 pathology which may be due to difference in the length of repeats expressed of background mouse strains. Finally, Chew *at al.* (2015) showed that 66X G4C2 repeats expressed in the central nervous system of mice, lead to nuclear RNA foci, DPR inclusions and TDP-43 pathology in the cortex and

hippocampus of mice, suggesting that the repeat itself, possibly through foci formation, RAN translation or another mechanisms entirely, caused aberrant TDP-43 deposition (Chew et al., 2015b). This would be a suitable model to test the potential therapeutic use of G4C2 PPMOs as it consistently replicates the pathological features observed in *C9ORF72*-linked ALS and FTD.

6.7 LIMITATIONS OF OUR PATHOLOGICAL STUDY

The current pathological study assessing the abundance of DPR protein inclusions in the spinal cord of C9ORF72 cases was limited by the availability of commercial antibodies that detect DPR proteins. At the time the study was conducted there were no commercially available DPR antibodies but we were fortunate to receive a panel of extensively validated antibodies from Dr. Leonard Petrucelli. The small quantities of antibody we received however meant that we had to focus on assessing the presence of DPR protein inclusion in only the spinal cord and we could not run western blots to quantify soluble DPRs. Moreover, our results would be more robust if several different antibodies that recognised the same DPR had been used to quantify the number of DPR protein aggregates. Nevertheless, the antibodies used have been validated (Chew et al., 2015b; Gendron et al., 2013) and a section of the frontal cortex of ALS and FTD cases. Our results have since been replicated by two independent studies (Davidson et al., 2016; Mackenzie et al., 2015) which increases our confidence that this data is correct.

The DAB IHC protocol used by some groups may be more sensitive in detecting specific DPR protein aggregates but we performed double immunofluorescent histochemistry in order to assess the co-aggregation and co-occurrence of DPR and TDP-43 pathology. Because we have extensive experience in ALS pathology and can reliably identify motor neurons by their large pale nucleus, it would however have been desirable to use a motor neuron specific

antigen (such as CHAT) to determine more precisely which cells contained DPR inclusions as well as sense and antisense RNA foci. Finally, although we were able to detect cells with large numbers of sense and antisense RNA foci, and therefore validating our FISH protocol, it would have been of interest to obtain tissue from the cases published by Cooper-Knock *et al.* 2015 showing large numbers of antisense foci as a positive control in our FISH protocol.

6.8 LIMITATIONS OF *IN VITRO* DISEASE MODELLING AND PPMO TESTING

It must be mentioned that the use of iPSN is used to model a late-onset neurodegenerative disorder. Clearly, the few months of cell culture do not compare to years of aging in the adult nervous system. A potential strategy to address this limitation is to promote premature aging in cell culture. Hutchinson-Gilford progeria syndrome (HGPS) is a human premature ageing disease that is caused by a single point mutation in the lamin A gene (*LMNA*) (Eriksson et al., 2003). Mutations in *LMNA* result in the production of a shorter transcript known as progerin. Miller *et al.* 2013 showed that overexpression of progerin induces multiple aging-related processes and characteristics in iPSC-derived neurons. Furthermore, this study reported multiple progerin-induced neurodegenerative phenotypes in Parkinson's disease patient iPSC-derived neurons that were not observed otherwise (Miller et al., 2013a).

Another limitation of this project is phenotypic variability arising from *in vitro* differentiation of iPSNs. We and others working in the field consistently observe heterogeneity of cell lines through all stages of differentiation. It is possible that subtle differences in the percentage of cells at different stages of maturation could result in non-cell autonomous effects that are not accounted for. In our study 2/4 C9ORF72 iPSN showed significant increased cell death and 1/4 of the C9ORF72 NPCs did not show any neurite outgrowth deficits. Although this may be representative of the heterogeneity observed in

human populations, the way to overcome this problem is by increasing the number of iPSC lines from C9ORF72 ALS cases and controls. Another possible solution is to generate isogenic lines and introducing point mutations or removing the G4C2 repeats using CRISPR-Cas9 technology (Cong et al., 2013), although this might be more challenging that it is initially thought as PAM sequences requited for CRISPR cleavage are not always present adjacent to the mutation insertion site or the CRISPR cleavage is not efficient, meaning many rounds of selection are likely to be necessary.

Another aspect to consider is to what extent are iPSC-derived neurons are representative of human adult neurons. Recent studies have suggested that iPSN are transcriptionally closer to fetal human neurons than to mature human neurons (Mertens et al., 2015a) and that iNeurons generated by direct reprogramming of fibroblasts by the knockdown of PTB reproduce aging phenotypes better than iPSN. iNeurons differentiated in this way also preserved epigenetic information while iPSN do not. Additionally, the timescale of the differentiation protocol is likely to be a critical parameter. Some studies have used neurons differentiated for up to 365 days in an attempt to model MAPT-linked FTD (Sposito et al., 2015). Although it may be seen as a limitation, iPSN can be used as a disease progression model. The same line of neurons differentiated for different lengths of time could be compared in order to assess the burden of a mutation as the neuron matures. Moreover a study has showed that neurons differentiated for 150 days show detectable levels of insoluble DPRs (Lopez-Gonzalez et al., 2016). We differentiated neurons for 75 days and were unable to detect any DPR by filter trap assay. Recent studies have reported the used of Meso Scale Discovery-based immunoassay to detect low levels of DPR protein (e.g. poly-GP) in the CSF pre-symptomatic and symptomatic *C9ORF72* expansion carriers (Gendron et al., 2017; Lehmer et al., 2017). It would be of great interest to use this system to assess the presence of poly-GP in our C9ORF72-iPSN and to assess the effect of PPMO treatment in the levels of DPRs, if detected. However it must be noted that this assay

measures the abundance of poly-GP that has not shown to be toxic in any *in vitro* or *in vivo* study.

6.9 FUTURE DIRECTIONS

Our pathological study analysed one of the largest samples of C9ORF72 ALS spinal cords published to date which allowed us to reduce the influence of case-to-case variability. In the future, it would be of great interest to analyse the specific cell type in which DPRs and foci are present with the use of neuronal sub-type specific markers. Although sense and antisense RNA foci are mostly present in neuronal cells in the frontal cortex of FTD patients (DeJesus-Hernandez et al., 2017; Mizielinska et al., 2013) it would be interesting to discover whether this is also true in the spinal cord of C9ORF72 ALS cases.

Furthermore, with the improvement in imaging methods, it would be interesting to analyse in greater subcellular detail cells containing DPRs or foci and other phenotypes that have been reported in C9ORF72 iPSN. In a recently published study, Mizielinsta *et al.* (2017) shows that neurons containing arginine-rich DPR aggregates and sense RNA foci in the frontal cortex of *C9ORF72*-FTD cases have enlarged nucleoli (Mizielinska et al., 2017). Laser-capture of these cells, followed by transcriptomic analysis could be carried out to elucidate the cellular response to DPR aggregates of RNA foci or to reveal cell-specific differences to explain why is it that, although many cells contain foci or DPR aggregates, it is the motor neurons that mostly degenerate in ALS.

We have shown that C9ORF72 NPCs exhibit reduced neurite outgrowth compared to control cells and that these deficits can be reversed by treatment with G4C2 PPMO. This paradigm could be modified in order to develop a high throughput assay for drug discovery purposes. Control NPCs and G4C2 PPMO treated NPCs could be used as a positive control as it has already been tested (Yeyeodu et al., 2010). Candidate compounds could then be

validated in more complex models of the disease such as *Drosophila* (Xu et al., 2013) or mice (Chew et al., 2015b). The generation of a high sensitivity high throughput protocol would allow for more subtle and relevant phenotypes, such as neurite branching or neurite area to be studied.

We generated neurons from iPSCs following a published protocol (Devlin et al., 2015). The majority of neurons generated with this protocol are cortical neurons. We consider that this is suitable to study the impact of the *C9ORF72* expansion as it affects ALS and FTD patients. However, recent protocols have shown that the generation of motor neurons from iPSCs can be achieved rapidly, yielding a high percentage of CHAT positive cells (Du et al., 2015). Generating motor neurons using such a protocol and assess cell-specific differences may provide valuable information about the disease mechanism. The decrease in cost of transcriptomic analysis techniques has made it possible to perform this analysis in a much larger number of neurons. Performing transcriptomic analysis on neurons treated with control and G4C2 PPMOs could provide an answer about the cellular mechanism responsible for the phenotypic recoveries that we report.

Finally, given that we have shown that G4C2 PPMOs reduce the number of RNA foci and reverse C9ORF72-specific phenotypes in human NPCs and iPSN, the potential therapeutic use of these PMOs should be tested in G4C2 mouse models of the disease. Mouse models expressing the C9ORF72 full gene do not fully replicate all aspects of the disease (Jiang et al., 2016). It would be of interest to test the PMOs in the mouse model developed by Chew *et al.* (2015) as these mice replicate most aspects of the human pathology, including sense RNA foci, TDP-43 and DPR aggregates and behavioural and motor deficits.

6.10 CONCLUSIONS

Collectively, our results implicate expanded G4C2 RNA transcripts foci and TDP-43 aggregation, rather than DPRs, as being the main contributor to neurotoxicity in C9ORF72 ALS. We have shown that sense RNA foci are the most common species in spinal cord motor neurons in C9ORF72 ALS cases and C9ORF72 iPSC neurons in culture but DPRs are extremely rare in spinal motor neurons and undetectable in C9ORF72 iPSC neurons. The limitations of post mortem and cell culture studies are acknowledged and our results do not exclude a contribution from haploinsufficiency and DPR toxicity in C9ORF72 linked ALS and FTD. Our evidence that PMOs targeting G4C2 repeats are able to dramatically decrease the number of RNA foci and reverse deficits in neurite outgrowth and improve neuronal survival in iPSNs implies that RNA foci may directly contribute to G4C2-mediated toxicity. Therefore, PPMOs directly targeting G4C2 offer a promising therapeutic strategy for C9ORF72-mediated disease.

7 REFERENCES

Abalkhail, H., J. Mitchell, J. Habgood, R. Orrell, and J. de Belleroche, 2003, A New Familial Amyotrophic Lateral Sclerosis Locus on Chromosome 16q12.1-16q12.2: The American Journal of Human Genetics, v. 73, p. 383-389.

Al-Chalabi, A., P. M. Andersen, P. Nilsson, B. Chioza, J. L. Andersson, C. Russ, C. E. Shaw, J. F. Powell, and P. N. Leigh, 1999, Deletions of the heavy neurofilament subunit tail in amyotrophic lateral sclerosis: Hum Mol Genet, v. 8, p. 157-64.

Al-Saif, A., F. Al-Mohanna, and S. Bohlega, 2011, A mutation in sigma-1 receptor causes juvenile amyotrophic lateral sclerosis: Ann Neurol, v. 70, p. 913-9.

Al-Sarraj, S., A. King, C. Troakes, B. Smith, S. Maekawa, I. Bodi, B. Rogelj, A. Al-Chalabi, T. Hortobagyi, and C. E. Shaw, 2011, p62 positive, TDP-43 negative, neuronal cytoplasmic and intranuclear inclusions in the cerebellum and hippocampus define the pathology of C9orf72-linked FTLD and MND/ALS: Acta Neuropathol, v. 122, p. 691-702.

Alami, N. H., R. B. Smith, M. A. Carrasco, L. A. Williams, C. S. Winborn, S. S. Han, E. Kiskinis, B. Winborn, B. D. Freibaum, A. Kanagaraj, A. J. Clare, N. M. Badders, B. Bilican, E. Chaum, S. Chandran, C. E. Shaw, K. C. Eggan, T. Maniatis, and J. P. Taylor, 2014, Axonal transport of TDP-43 mRNA granules is impaired by ALS-causing mutations: Neuron, v. 81, p. 536-43.

Almeida, S., E. Gascon, H. Tran, H. J. Chou, T. F. Gendron, S. Degroot, A. R. Tapper, C. Sellier, N. Charlet-Berguerand, A. Karydas, W. W. Seeley, A. L. Boxer, L. Petrucelli, B. L. Miller, and F. B. Gao, 2013, Modeling key pathological features of frontotemporal dementia with C9ORF72 repeat expansion in iPSC-derived human neurons: Acta Neuropathol, v. 126, p. 385-99.

Amick, J., A. Roczniak-Ferguson, and S. M. Ferguson, 2016, C9orf72 binds SMCR8, localizes to lysosomes, and regulates mTORC1 signaling: Mol Biol Cell, v. 27, p. 3040-3051.

Aoki, Y., R. Manzano, Y. Lee, R. Dafinca, M. Aoki, A. G. Douglas, M. A. Varela, C. Sathyaprakash, J. Scaber, P. Barbagallo, P. Vader, I. Mager, K. Ezzat, M. R. Turner, N. Ito, S. Gasco, N. Ohbayashi, S. El Andaloussi, S. Takeda, M. Fukuda, K. Talbot, and M. J. Wood, 2017, C9orf72 and RAB7L1 regulate vesicle trafficking in amyotrophic lateral sclerosis and frontotemporal dementia: Brain.

Arechavala-Gomeza, V., I. R. Graham, L. J. Popplewell, A. M. Adams, A. Aartsma-Rus, M. Kinali, J. E. Morgan, J. C. van Deutekom, S. D. Wilton, G. Dickson, and F. Muntoni, 2007, Comparative analysis of antisense oligonucleotide sequences for targeted skipping of exon 51 during dystrophin pre-mRNA splicing in human muscle: Hum Gene Ther, v. 18, p. 798-810.

Armstrong, G. A., and P. Drapeau, 2013, Loss and gain of FUS function impair neuromuscular synaptic transmission in a genetic model of ALS: Hum Mol Genet, v. 22, p. 4282-92.

Ash, P. E., K. F. Bieniek, T. F. Gendron, T. Caulfield, W. L. Lin, M. Dejesus-Hernandez, M. M. van Blitterswijk, K. Jansen-West, J. W. Paul, 3rd, R. Rademakers, K. B. Boylan, D. W. Dickson, and L. Petrucelli, 2013, Unconventional translation of C9ORF72 GGGGCC expansion generates insoluble polypeptides specific to c9FTD/ALS: Neuron, v. 77, p. 639-46.

Ash, P. E., Y. J. Zhang, C. M. Roberts, T. Saldi, H. Hutter, E. Buratti, L. Petrucelli, and C. D. Link, 2010, Neurotoxic effects of TDP-43 overexpression in C. elegans: Hum Mol Genet, v. 19, p. 3206-18.

Atanasio, A., V. Decman, D. White, M. Ramos, B. Ikiz, H. C. Lee, C. J. Siao, S. Brydges, E. LaRosa, Y. Bai, W. Fury, P. Burfeind, R. Zamfirova, G. Warshaw, J. Orengo, A. Oyejide, M. Fralish, W. Auerbach, W. Poueymirou, J. Freudenberg, G. Gong, B. Zambrowicz, D. Valenzuela, G. Yancopoulos, A. Murphy, G. Thurston, and K. M. Lai, 2016, C9orf72

ablation causes immune dysregulation characterized by leukocyte expansion, autoantibody production, and glomerulonephropathy in mice: Sci Rep, v. 6, p. 23204.

Atkin, J. D., M. A. Farg, B. J. Turner, D. Tomas, J. A. Lysaght, J. Nunan, A. Rembach, P. Nagley, P. M. Beart, S. S. Cheema, and M. K. Horne, 2006, Induction of the Unfolded Protein Response in Familial Amyotrophic Lateral Sclerosis and Association of Protein-disulfide Isomerase with Superoxide Dismutase 1: Journal of Biological Chemistry, v. 281, p. 30152-30165.

Atkinson, R. A., C. M. Fernandez-Martos, J. D. Atkin, J. C. Vickers, and A. E. King, 2015, C9ORF72 expression and cellular localization over mouse development: Acta Neuropathol Commun, v. 3, p. 59.

Atsumi, T., 1981, The ultrastructure of intramuscular nerves in amyotrophic lateral sclerosis: Acta Neuropathol, v. 55, p. 193-8.

Baba, M., S. Nakajo, P. H. Tu, T. Tomita, K. Nakaya, V. M. Lee, J. Q. Trojanowski, and T. Iwatsubo, 1998, Aggregation of alpha-synuclein in Lewy bodies of sporadic Parkinson's disease and dementia with Lewy bodies: Am J Pathol, v. 152, p. 879-84.

Baborie, A., T. D. Griffiths, E. Jaros, R. Perry, I. G. McKeith, D. J. Burn, M. Masuda-Suzukake, M. Hasegawa, S. Rollinson, S. Pickering-Brown, A. C. Robinson, Y. S. Davidson, and D. M. Mann, 2014, Accumulation of dipeptide repeat proteins predates that of TDP-43 in Frontotemporal Lobar Degeneration associated with hexanucleotide repeat expansions in C9ORF72 gene: Neuropathol Appl Neurobiol.

Baloh, R. H., 2012, How do the RNA-binding proteins TDP-43 and FUS relate to amyotrophic lateral sclerosis and frontotemporal degeneration, and to each other?: Curr Opin Neurol, v. 25, p. 701-7.

Bannwarth, S., S. Ait-El-Mkadem, A. Chaussenot, E. C. Genin, S. Lacas-Gervais, K. Fragaki, L. Berg-Alonso, Y. Kageyama, V. Serre, D. G. Moore, A. Verschueren, C. Rouzier, I. Le Ber, G. Auge, C. Cochaud, F. Lespinasse, K. N'Guyen, A. de Septenville, A. Brice, P. Yu-Wai-Man, H. Sesaki, J. Pouget, and V. Paquis-Flucklinger, 2014, A mitochondrial origin for frontotemporal dementia and amyotrophic lateral sclerosis through CHCHD10 involvement: Brain, v. 137, p. 2329-45.

Baumer, D., S. Z. East, B. Tseu, A. Zeman, D. Hilton, K. Talbot, and O. Ansorge, 2014, FTLD-ALS of TDP-43 type and SCA2 in a family with a full ataxin-2 polyglutamine expansion: Acta Neuropathol, v. 128, p. 597-604.

Baumer, D., D. Hilton, S. M. Paine, M. R. Turner, J. Lowe, K. Talbot, and O. Ansorge, 2010, Juvenile ALS with basophilic inclusions is a FUS proteinopathy with FUS mutations: Neurology, v. 75, p. 611-8.

Becker, L. A., B. Huang, G. Bieri, R. Ma, D. A. Knowles, P. Jafar-Nejad, J. Messing, H. J. Kim, A. Soriano, G. Auburger, S. M. Pulst, J. P. Taylor, F. Rigo, and A. D. Gitler, 2017, Therapeutic reduction of ataxin-2 extends lifespan and reduces pathology in TDP-43 mice: Nature, v. 544, p. 367-371.

Bennion Callister, J., S. Ryan, J. Sim, S. Rollinson, and S. M. Pickering-Brown, 2016, Modelling C9orf72 dipeptide repeat proteins of a physiologically relevant size: Hum Mol Genet, v. 25, p. 5069-5082.

Bhinge, A., S. C. Namboori, X. Zhang, A. M. VanDongen, and L. W. Stanton, 2017, Genetic Correction of SOD1 Mutant iPSCs Reveals ERK and JNK Activated AP1 as a Driver of Neurodegeneration in Amyotrophic Lateral Sclerosis: Stem Cell Reports.

Bilican, B., A. Serio, S. J. Barmada, A. L. Nishimura, G. J. Sullivan, M. Carrasco, H. P. Phatnani, C. A. Puddifoot, D. Story, J. Fletcher, I. H. Park, B. A. Friedman, G. Q. Daley, D. J. Wyllie, G. E. Hardingham, I. Wilmut, S. Finkbeiner, T. Maniatis, C. E. Shaw, and S. Chandran, 2012, Mutant induced pluripotent stem cell lines recapitulate aspects of TDP-43 proteinopathies and reveal cell-specific vulnerability: Proc Natl Acad Sci U S A, v. 109, p. 5803-8.

Blokhuis, A. M., E. J. Groen, M. Koppers, L. H. van den Berg, and R. J. Pasterkamp, 2013, Protein aggregation in amyotrophic lateral sclerosis: Acta Neuropathol, v. 125, p. 777-94.

Boeynaems, S., E. Bogaert, D. Kovacs, A. Konijnenberg, E. Timmerman, A. Volkov, M. Guharoy, M. De Decker, T. Jaspers, V. H. Ryan, A. M. Janke, P. Baatsen, T. Vercruysse, R. M. Kolaitis, D. Daelemans, J. P. Taylor, N. Kedersha, P. Anderson, F. Impens, F. Sobott, J. Schymkowitz, F. Rousseau, N. L. Fawzi, W. Robberecht, P. Van Damme, P. Tompa, and L. Van Den Bosch, 2017, Phase Separation of C9orf72 Dipeptide Repeats Perturbs Stress Granule Dynamics: Mol Cell, v. 65, p. 1044-1055 e5.

Boeynaems, S., E. Bogaert, E. Michiels, I. Gijselinck, A. Sieben, A. Jovicic, G. De Baets, W. Scheveneels, J. Steyaert, I. Cuijt, K. J. Verstrepen, P. Callaerts, F. Rousseau, J. Schymkowitz, M. Cruts, C. Van Broeckhoven, P. Van Damme, A. D. Gitler, W. Robberecht, and L. Van Den Bosch, 2016a, Drosophila screen connects nuclear transport genes to DPR pathology in c9ALS/FTD: Sci Rep, v. 6, p. 20877.

Boeynaems, S., E. Bogaert, P. Van Damme, and L. Van Den Bosch, 2016b, Inside out: the role of nucleocytoplasmic transport in ALS and FTLD: Acta Neuropathol, v. 132, p. 159-73.

Bogdanik, L. P., M. A. Osborne, C. Davis, W. P. Martin, A. Austin, F. Rigo, C. F. Bennett, and C. M. Lutz, 2015, Systemic, postsymptomatic antisense oligonucleotide rescues motor unit maturation delay in a new mouse model for type II/III spinal muscular atrophy: Proc Natl Acad Sci U S A, v. 112, p. E5863-72.

Borghero, G., M. Pugliatti, F. Marrosu, M. G. Marrosu, M. R. Murru, G. Floris, A. Cannas, L. D. Parish, T. B. Cau, D. Loi, A. Ticca, S. Traccis, U. Manera, A. Canosa, C. Moglia, A. Calvo, M. Barberis, M. Brunetti, A. E. Renton, M. A. Nalls, B. J. Traynor, G. Restagno, A. Chio, Italsgen, and S. consortia, 2015, ATXN2 is a modifier of phenotype in ALS patients of Sardinian ancestry: Neurobiol Aging, v. 36, p. 2906 e1-5.

Brenner, D., K. Muller, T. Wieland, P. Weydt, S. Bohm, D. Lule, A. Hubers, C. Neuwirth, M. Weber, G. Borck, M. Wahlqvist, K. M. Danzer, A. E. Volk, T. Meitinger, T. M. Strom, M. Otto, J. Kassubek, A. C. Ludolph, P. M. Andersen, and J. H. Weishaupt, 2016, NEK1 mutations in familial amyotrophic lateral sclerosis: Brain, v. 139, p. e28.

Brettschneider, J., V. M. Van Deerlin, J. L. Robinson, L. Kwong, E. B. Lee, Y. O. Ali, N. Safren, M. J. Monteiro, J. B. Toledo, L. Elman, L. McCluskey, D. J. Irwin, M. Grossman, L. Molina-Porcel, V. M. Lee, and J. Q. Trojanowski, 2012, Pattern of ubiquilin pathology in ALS and FTLD indicates presence of C9ORF72 hexanucleotide expansion: Acta Neuropathol, v. 123, p. 825-39.

Brooks, B. R., 1999, Diagnostic dilemmas in amyotrophic lateral sclerosis: J Neurol Sci, v. 165 Suppl 1, p. S1-9.

Bruijn, L. I., M. K. Houseweart, S. Kato, K. L. Anderson, S. D. Anderson, E. Ohama, A. G. Reaume, R. W. Scott, and D. W. Cleveland, 1998, Aggregation and motor neuron toxicity of an ALS-linked SOD1 mutant independent from wild-type SOD1: Science, v. 281, p. 1851-4.

Buchan, J. R., 2014, mRNP granules. Assembly, function, and connections with disease: RNA Biol, v. 11, p. 1019-30.

Burguete, A. S., S. Almeida, F. B. Gao, R. Kalb, M. R. Akins, and N. M. Bonini, 2015, GGGGCC microsatellite RNA is neuritically localized, induces branching defects, and perturbs transport granule function: Elife, v. 4, p. e08881.

Burkhardt, M. F., F. J. Martinez, S. Wright, C. Ramos, D. Volfson, M. Mason, J. Garnes, V. Dang, J. Lievers, U. Shoukat-Mumtaz, R. Martinez, H. Gai, R. Blake, E. Vaisberg, M. Grskovic, C. Johnson, S. Irion, J. Bright, B. Cooper, L. Nguyen, I. Griswold-Prenner, and A. Javaherian, 2013, A cellular model for sporadic ALS using patient-derived induced pluripotent stem cells: Mol Cell Neurosci, v. 56, p. 355-64.

Butler, M., C. S. Hayes, A. Chappell, S. F. Murray, T. L. Yaksh, and X. Y. Hua, 2005, Spinal distribution and metabolism of 2'-O-(2-methoxyethyl)-modified oligonucleotides after intrathecal administration in rats: Neuroscience, v. 131, p. 705-15.

Canete-Soler, R., D. G. Silberg, M. D. Gershon, and W. W. Schlaepfer, 1999, Mutation in neurofilament transgene implicates RNA processing in the pathogenesis of neurodegenerative disease: J Neurosci, v. 19, p. 1273-83.

Canter, R. G., J. Penney, and L. H. Tsai, 2016, The road to restoring neural circuits for the treatment of Alzheimer's disease: Nature, v. 539, p. 187-196.

Cerritelli, S. M., and R. J. Crouch, 2009, Ribonuclease H: the enzymes in eukaryotes: FEBS J, v. 276, p. 1494-505.

Chang, Y. J., U. S. Jeng, Y. L. Chiang, I. S. Hwang, and Y. R. Chen, 2016, The Glycine-Alanine Dipeptide Repeat from C9orf72 Hexanucleotide Expansions Forms Toxic Amyloids Possessing Cell-to-Cell Transmission Properties: J Biol Chem, v. 291, p. 4903-11.

Chauhan, N. B., and G. J. Siegel, 2007, Antisense inhibition at the beta-secretase-site of beta-amyloid precursor protein reduces cerebral amyloid and acetyl cholinesterase activity in Tg2576: Neuroscience, v. 146, p. 143-51.

Cheah, B. C., S. Vucic, A. V. Krishnan, and M. C. Kiernan, 2010, Riluzole, neuroprotection and amyotrophic lateral sclerosis: Curr Med Chem, v. 17, p. 1942-199.

Chen, H., K. Qian, Z. Du, J. Cao, A. Petersen, H. Liu, L. W. t. Blackbourn, C. L. Huang, A. Errigo, Y. Yin, J. Lu, M. Ayala, and S. C. Zhang, 2014, Modeling ALS with iPSCs reveals that mutant SOD1 misregulates neurofilament balance in motor neurons: Cell Stem Cell, v. 14, p. 796-809.

Chen, H. J., J. C. Mitchell, S. Novoselov, J. Miller, A. L. Nishimura, E. L. Scotter, C. A. Vance, M. E. Cheetham, and C. E. Shaw, 2016, The heat shock response plays an important role in TDP-43 clearance: evidence for dysfunction in amyotrophic lateral sclerosis: Brain, v. 139, p. 1417-32.

Chen, Y. Z., C. L. Bennett, H. M. Huynh, I. P. Blair, I. Puls, J. Irobi, I. Dierick, A. Abel, M. L. Kennerson, B. A. Rabin, G. A. Nicholson, M. Auer-Grumbach, K. Wagner, P. De Jonghe, J. W. Griffin, K. H. Fischbeck, V. Timmerman, D. R. Cornblath, and P. F. Chance, 2004, DNA/RNA helicase gene mutations in a form of juvenile amyotrophic lateral sclerosis (ALS4): Am J Hum Genet, v. 74, p. 1128-35.

Chew, J., T. F. Gendron, M. Prudencio, H. Sasaguri, Y. J. Zhang, M. Castanedes-Casey, C. W. Lee, K. Jansen-West, A. Kurti, M. E. Murray, K. F. Bieniek, P. O. Bauer, E. C. Whitelaw, L. Rousseau, J. N. Stankowski, C. Stetler, L. M. Daughrity, E. A. Perkerson, P. Desaro, A. Johnston, K. Overstreet, D. Edbauer, R. Rademakers, K. B. Boylan, D. W. Dickson, J. D. Fryer, and L. Petrucelli, 2015a, C9ORF72 repeat expansions in mice cause TDP-43 pathology, neuronal loss, and behavioral deficits: Science.

Chew, J., T. F. Gendron, M. Prudencio, H. Sasaguri, Y. J. Zhang, M. Castanedes-Casey, C. W. Lee, K. Jansen-West, A. Kurti, M. E. Murray, K. F. Bieniek, P. O. Bauer, E. C. Whitelaw, L. Rousseau, J. N. Stankowski, C. Stetler, L. M. Daughrity, E. A. Perkerson, P. Desaro, A. Johnston, K. Overstreet, D. Edbauer, R. Rademakers, K. B. Boylan, D. W. Dickson, J. D. Fryer, and L. Petrucelli, 2015b, Neurodegeneration. C9ORF72 repeat expansions in mice cause TDP-43 pathology, neuronal loss, and behavioral deficits: Science, v. 348, p. 1151-4.

Chio, A., G. Logroscino, B. J. Traynor, J. Collins, J. C. Simeone, L. A. Goldstein, and L. A. White, 2013, Global epidemiology of amyotrophic lateral sclerosis: a systematic review of the published literature: Neuroepidemiology, v. 41, p. 118-30.

Chow, C. Y., J. E. Landers, S. K. Bergren, P. C. Sapp, A. E. Grant, J. M. Jones, L. Everett, G. M. Lenk, D. M. McKenna-Yasek, L. S. Weisman, D. Figlewicz, R. H. Brown, and M. H. Meisler, 2009, Deleterious variants of FIG4, a phosphoinositide phosphatase, in patients with ALS: Am J Hum Genet, v. 84, p. 85-8.

Chow, C. Y., Y. Zhang, J. J. Dowling, N. Jin, M. Adamska, K. Shiga, K. Szigeti, M. E. Shy, J. Li, X. Zhang, J. R. Lupski, L. S. Weisman, and M. H. Meisler, 2007, Mutation of FIG4 causes neurodegeneration in the pale tremor mouse and patients with CMT4J: Nature, v. 448, p. 68-72.

Cirulli, E. T., B. N. Lasseigne, S. Petrovski, P. C. Sapp, P. A. Dion, C. S. Leblond, J. Couthouis, Y. F. Lu, Q. Wang, B. J. Krueger, Z. Ren, J. Keebler, Y. Han, S. E. Levy, B. E. Boone, J. R. Wimbish, L. L. Waite, A. L. Jones, J. P. Carulli, A. G. Day-Williams, J. F. Staropoli, W. W. Xin, A. Chesi, A. R. Raphael, D. McKenna-Yasek, J. Cady, J. M. Vianney de Jong, K. P. Kenna, B. N. Smith, S. Topp, J. Miller, A. Gkazi, F. S. Consortium, A. Al-Chalabi, L. H. van den Berg, J. Veldink, V. Silani, N. Ticozzi, C. E. Shaw, R. H. Baloh, S. Appel, E. Simpson, C. Lagier-Tourenne, S. M. Pulst, S. Gibson, J. Q. Trojanowski, L. Elman, L. McCluskey, M. Grossman, N. A. Shneider, W. K. Chung, J. M. Ravits, J. D. Glass, K. B. Sims, V. M. Van Deerlin, T. Maniatis, S. D. Hayes, A. Ordureau, S. Swarup, J. Landers, F. Baas, A. S. Allen, R. S. Bedlack, J. W. Harper, A. D. Gitler, G. A. Rouleau, R. Brown, M. B. Harms, G. M. Cooper, T. Harris, R. M. Myers, and D. B. Goldstein, 2015, Exome sequencing in amyotrophic lateral sclerosis identifies risk genes and pathways: Science, v. 347, p. 1436-41.

Ciura, S., S. Lattante, I. Le Ber, M. Latouche, H. Tostivint, A. Brice, and E. Kabashi, 2013, Loss of function of C9orf72 causes motor deficits in a zebrafish model of Amyotrophic Lateral Sclerosis: Ann Neurol.

Coelho, M. B., J. Attig, N. Bellora, J. Konig, M. Hallegger, M. Kayikci, E. Eyras, J. Ule, and C. W. Smith, 2015, Nuclear matrix protein Matrin3 regulates alternative splicing and forms overlapping regulatory networks with PTB: EMBO J, v. 34, p. 653-68.

Cong, L., F. A. Ran, D. Cox, S. Lin, R. Barretto, N. Habib, P. D. Hsu, X. Wu, W. Jiang, L. A. Marraffini, and F. Zhang, 2013, Multiplex genome engineering using CRISPR/Cas systems: Science, v. 339, p. 819-23.

Conlon, E. G., L. Lu, A. Sharma, T. Yamazaki, T. Tang, N. A. Shneider, and J. L. Manley, 2016a, The C9ORF72 GGGGCC expansion forms RNA G-quadruplex inclusions and sequesters hnRNP H to disrupt splicing in ALS brains: Elife, v. 5.

Conlon, E. G., L. Lu, A. Sharma, T. Yamazaki, T. Tang, N. A. Shneider, and J. L. Manley, 2016b, The C9ORF72 GGGGCC expansion forms RNA G-quadruplex inclusions and sequesters hnRNP H to disrupt splicing in ALS patient brains: Elife, v. 5.

Cooper-Knock, J., C. Hewitt, J. R. Highley, A. Brockington, A. Milano, S. Man, J. Martindale, J. Hartley, T. Walsh, C. Gelsthorpe, L. Baxter, G. Forster, M. Fox, J. Bury, K. Mok, C. J. McDermott, B. J. Traynor, J. Kirby, S. B. Wharton, P. G. Ince, J. Hardy, and P. J. Shaw, 2012, Clinico-pathological features in amyotrophic lateral sclerosis with expansions in C9ORF72: Brain, v. 135, p. 751-64.

Cooper-Knock, J., A. Higginbottom, N. Connor-Robson, N. Bayatti, J. J. Bury, J. Kirby, N. Ninkina, V. L. Buchman, and P. J. Shaw, 2013, C9ORF72 transcription in a frontotemporal dementia case with two expanded alleles: Neurology, v. 81, p. 1719-21.

Cooper-Knock, J., A. Higginbottom, M. J. Stopford, J. R. Highley, P. G. Ince, S. B. Wharton, S. Pickering-Brown, J. Kirby, G. M. Hautbergue, and P. J. Shaw, 2015, Antisense RNA foci in the motor neurons of C9ORF72-ALS patients are associated with TDP-43 proteinopathy: Acta Neuropathol, v. 130, p. 63-75.

Cooper-Knock, J., M. J. Walsh, A. Higginbottom, J. Robin Highley, M. J. Dickman, D. Edbauer, P. G. Ince, S. B. Wharton, S. A. Wilson, J. Kirby, G. M. Hautbergue, and P. J. Shaw, 2014a, Sequestration of multiple RNA recognition motif-containing proteins by C9orf72 repeat expansions: Brain.

Cooper-Knock, J., M. J. Walsh, A. Higginbottom, J. Robin Highley, M. J. Dickman, D. Edbauer, P. G. Ince, S. B. Wharton, S. A. Wilson, J. Kirby, G. M. Hautbergue, and P. J. Shaw,

2014b, Sequestration of multiple RNA recognition motif-containing proteins by C9orf72 repeat expansions: Brain, v. 137, p. 2040-51.

Cox, L. E., L. Ferraiuolo, E. F. Goodall, P. R. Heath, A. Higginbottom, H. Mortiboys, H. C. Hollinger, J. A. Hartley, A. Brockington, C. E. Burness, K. E. Morrison, S. B. Wharton, A. J. Grierson, P. G. Ince, J. Kirby, and P. J. Shaw, 2010, Mutations in CHMP2B in lower motor neuron predominant amyotrophic lateral sclerosis (ALS): PLoS One, v. 5, p. e9872.

D'Angelo, M. A., M. Raices, S. H. Panowski, and M. W. Hetzer, 2009, Age-dependent deterioration of nuclear pore complexes causes a loss of nuclear integrity in postmitotic cells: Cell, v. 136, p. 284-95.

Dafinca, R., J. Scaber, N. Ababneh, T. Lalic, G. Weir, H. Christian, J. Vowles, A. G. Douglas, A. Fletcher-Jones, C. Browne, M. Nakanishi, M. R. Turner, R. Wade-Martins, S. A. Cowley, and K. Talbot, 2016, C9orf72 Hexanucleotide Expansions Are Associated with Altered Endoplasmic Reticulum Calcium Homeostasis and Stress Granule Formation in Induced Pluripotent Stem Cell-Derived Neurons from Patients with Amyotrophic Lateral Sclerosis and Frontotemporal Dementia: Stem Cells, v. 34, p. 2063-78.

Dal Canto, M. C., and M. E. Gurney, 1995, Neuropathological changes in two lines of mice carrying a transgene for mutant human Cu,Zn SOD, and in mice overexpressing wild type human SOD: a model of familial amyotrophic lateral sclerosis (FALS): Brain Res, v. 676, p. 25-40.

Daoud, H., S. Dobrzeniecka, W. Camu, V. Meininger, N. Dupre, P. A. Dion, and G. A. Rouleau, 2013, Mutation analysis of PFN1 in familial amyotrophic lateral sclerosis patients: Neurobiol Aging, v. 34, p. 1311 e1-2.

Daoud, H., S. Zhou, A. Noreau, M. Sabbagh, V. Belzil, A. Dionne-Laporte, C. Tranchant, P. Dion, and G. A. Rouleau, 2012, Exome sequencing reveals SPG11 mutations causing juvenile ALS: Neurobiol Aging, v. 33, p. 839 e5-9.

Davidson, Y., A. C. Robinson, X. Liu, D. Wu, C. Troakes, S. Rollinson, M. Masuda-Suzukake, G. Suzuki, T. Nonaka, J. Shi, J. Tian, H. Hamdalla, J. Ealing, A. Richardson, M. Jones, S. Pickering-Brown, J. S. Snowden, M. Hasegawa, and D. M. Mann, 2016, Neurodegeneration in frontotemporal lobar degeneration and motor neurone disease associated with expansions in C9orf72 is linked to TDP-43 pathology and not associated with aggregated forms of dipeptide repeat proteins: Neuropathol Appl Neurobiol, v. 42, p. 242-54.

Davidson, Y. S., H. Barker, A. C. Robinson, J. C. Thompson, J. Harris, C. Troakes, B. Smith, S. Al-Saraj, C. Shaw, S. Rollinson, M. Masuda-Suzukake, M. Hasegawa, S. Pickering-Brown, J. S. Snowden, and D. M. Mann, 2014, Brain distribution of dipeptide repeat proteins in frontotemporal lobar degeneration and motor neurone disease associated with expansions in C9ORF72: Acta Neuropathol Commun, v. 2, p. 70.

Davis, S., S. Propp, S. M. Freier, L. E. Jones, M. J. Serra, G. Kinberger, B. Bhat, E. E. Swayze, C. F. Bennett, and C. Esau, 2009, Potent inhibition of microRNA in vivo without degradation: Nucleic Acids Res, v. 37, p. 70-7.

De Vos, K. J., G. M. Morotz, R. Stoica, E. L. Tudor, K. F. Lau, S. Ackerley, A. Warley, C. E. Shaw, and C. C. Miller, 2012, VAPB interacts with the mitochondrial protein PTPIP51 to regulate calcium homeostasis: Hum Mol Genet, v. 21, p. 1299-311.

DeJesus-Hernandez, M., N. A. Finch, X. Wang, T. F. Gendron, K. F. Bieniek, M. G. Heckman, A. Vasilevich, M. E. Murray, L. Rousseau, R. Weesner, A. Lucido, M. Parsons, J. Chew, K. A. Josephs, J. E. Parisi, D. S. Knopman, R. C. Petersen, B. F. Boeve, N. R. Graff-Radford, J. de Boer, Y. W. Asmann, L. Petrucelli, K. B. Boylan, D. W. Dickson, M. van Blitterswijk, and R. Rademakers, 2017, In-depth clinico-pathological examination of RNA foci in a large cohort of C9ORF72 expansion carriers: Acta Neuropathol.

DeJesus-Hernandez, M., I. R. Mackenzie, B. F. Boeve, A. L. Boxer, M. Baker, N. J. Rutherford, A. M. Nicholson, N. A. Finch, H. Flynn, J. Adamson, N. Kouri, A. Wojtas, P. Sengdy, G. Y. Hsiung, A. Karydas, W. W. Seeley, K. A. Josephs, G. Coppola, D. H. Geschwind, Z. K. Wszolek, H. Feldman, D. S. Knopman, R. C. Petersen, B. L. Miller, D. W. Dickson, K. B. Boylan, N. R. Graff-Radford, and R. Rademakers, 2011, Expanded GGGGCC hexanucleotide repeat in noncoding region of C9ORF72 causes chromosome 9p-linked FTD and ALS: Neuron, v. 72, p. 245-56.

Deng, H. X., W. Chen, S. T. Hong, K. M. Boycott, G. H. Gorrie, N. Siddique, Y. Yang, F. Fecto, Y. Shi, H. Zhai, H. Jiang, M. Hirano, E. Rampersaud, G. H. Jansen, S. Donkervoort, E. H. Bigio, B. R. Brooks, K. Ajroud, R. L. Sufit, J. L. Haines, E. Mugnaini, M. A. Pericak-Vance, and T. Siddique, 2011, Mutations in UBQLN2 cause dominant X-linked juvenile and adult-onset ALS and ALS/dementia: Nature, v. 477, p. 211-5.

Devlin, A. C., K. Burr, S. Borooah, J. D. Foster, E. M. Cleary, I. Geti, L. Vallier, C. E. Shaw, S. Chandran, and G. B. Miles, 2015, Human iPSC-derived motoneurons harbouring TARDBP or C9ORF72 ALS mutations are dysfunctional despite maintaining viability: Nat Commun, v. 6, p. 5999.

DeVos, S. L., and T. M. Miller, 2013, Antisense oligonucleotides: treating neurodegeneration at the level of RNA: Neurotherapeutics, v. 10, p. 486-97.

Diaper, D. C., Y. Adachi, L. Lazarou, M. Greenstein, F. A. Simoes, A. Di Domenico, D. A. Solomon, S. Lowe, R. Alsubaie, D. Cheng, S. Buckley, D. M. Humphrey, C. E. Shaw, and F. Hirth, 2013, Drosophila TDP-43 dysfunction in glia and muscle cells cause cytological and behavioural phenotypes that characterize ALS and FTLD: Hum Mol Genet, v. 22, p. 3883-93.

Dimos, J. T., K. T. Rodolfa, K. K. Niakan, L. M. Weisenthal, H. Mitsumoto, W. Chung, G. F. Croft, G. Saphier, R. Leibel, R. Goland, H. Wichterle, C. E. Henderson, and K. Eggan, 2008, Induced pluripotent stem cells generated from patients with ALS can be differentiated into motor neurons: Science, v. 321, p. 1218-21.

Dominski, Z., and R. Kole, 1993, Restoration of correct splicing in thalassemic pre-mRNA by antisense oligonucleotides: Proc Natl Acad Sci U S A, v. 90, p. 8673-7.

Donnelly, C. J., P. W. Zhang, J. T. Pham, A. R. Haeusler, N. A. Mistry, S. Vidensky, E. L. Daley, E. M. Poth, B. Hoover, D. M. Fines, N. Maragakis, P. J. Tienari, L. Petrucelli, B. J. Traynor, J. Wang, F. Rigo, C. F. Bennett, S. Blackshaw, R. Sattler, and J. D. Rothstein, 2013, RNA toxicity from the ALS/FTD C9ORF72 expansion is mitigated by antisense intervention: Neuron, v. 80, p. 415-28.

Dormann, D., and C. Haass, 2011, TDP-43 and FUS: a nuclear affair: Trends Neurosci, v. 34, p. 339-48.

Dormann, D., T. Madl, C. F. Valori, E. Bentmann, S. Tahirovic, C. Abou-Ajram, E. Kremmer, O. Ansorge, I. R. Mackenzie, M. Neumann, and C. Haass, 2012, Arginine methylation next to the PY-NLS modulates Transportin binding and nuclear import of FUS: EMBO J, v. 31, p. 4258-75.

Dormann, D., R. Rodde, D. Edbauer, E. Bentmann, I. Fischer, A. Hruscha, M. E. Than, I. R. Mackenzie, A. Capell, B. Schmid, M. Neumann, and C. Haass, 2010, ALS-associated fused in sarcoma (FUS) mutations disrupt Transportin-mediated nuclear import: EMBO J, v. 29, p. 2841-57.

Du, L., R. Kayali, C. Bertoni, F. Fike, H. Hu, P. L. Iversen, and R. A. Gatti, 2011, Arginine-rich cell-penetrating peptide dramatically enhances AMO-mediated ATM aberrant splicing correction and enables delivery to brain and cerebellum: Hum Mol Genet, v. 20, p. 3151-60.

Du, Z. W., H. Chen, H. Liu, J. Lu, K. Qian, C. L. Huang, X. Zhong, F. Fan, and S. C. Zhang, 2015, Generation and expansion of highly pure motor neuron progenitors from human pluripotent stem cells: Nat Commun, v. 6, p. 6626.

Egawa, N., S. Kitaoka, K. Tsukita, M. Naitoh, K. Takahashi, T. Yamamoto, F. Adachi, T. Kondo, K. Okita, I. Asaka, T. Aoi, A. Watanabe, Y. Yamada, A. Morizane, J. Takahashi, T. Ayaki, H. Ito, K. Yoshikawa, S. Yamawaki, S. Suzuki, D. Watanabe, H. Hioki, T. Kaneko, K. Makioka, K. Okamoto, H. Takuma, A. Tamaoka, K. Hasegawa, T. Nonaka, M. Hasegawa, A. Kawata, M. Yoshida, T. Nakahata, R. Takahashi, M. C. Marchetto, F. H. Gage, S. Yamanaka, and H. Inoue, 2012, Drug screening for ALS using patient-specific induced pluripotent stem cells: Sci Transl Med, v. 4, p. 145ra104.

Elden, A. C., H. J. Kim, M. P. Hart, A. S. Chen-Plotkin, B. S. Johnson, X. Fang, M. Armakola, F. Geser, R. Greene, M. M. Lu, A. Padmanabhan, D. Clay-Falcone, L. McCluskey, L. Elman, D. Juhr, P. J. Gruber, U. Rub, G. Auburger, J. Q. Trojanowski, V. M. Lee, V. M. Van Deerlin, N. M. Bonini, and A. D. Gitler, 2010, Ataxin-2 intermediate-length polyglutamine expansions are associated with increased risk for ALS: Nature, v. 466, p. 1069-75.

Engelhardt, J. I., and S. H. Appel, 1990, IgG reactivity in the spinal cord and motor cortex in amyotrophic lateral sclerosis: Arch Neurol, v. 47, p. 1210-6.

Eriksson, M., W. T. Brown, L. B. Gordon, M. W. Glynn, J. Singer, L. Scott, M. R. Erdos, C. M. Robbins, T. Y. Moses, P. Berglund, A. Dutra, E. Pak, S. Durkin, A. B. Csoka, M. Boehnke, T. W. Glover, and F. S. Collins, 2003, Recurrent de novo point mutations in lamin A cause Hutchinson-Gilford progeria syndrome: Nature, v. 423, p. 293-298.

Esanov, R., K. C. Belle, M. van Blitterswijk, V. V. Belzil, R. Rademakers, D. W. Dickson, L. Petrucelli, K. B. Boylan, D. M. Dykxhoorn, J. Wuu, M. Benatar, C. Wahlestedt, and Z. Zeier, 2016, C9orf72 promoter hypermethylation is reduced while hydroxymethylation is acquired during reprogramming of ALS patient cells: Exp Neurol, v. 277, p. 171-7.

Evers, M. M., L. J. Toonen, and W. M. van Roon-Mom, 2015, Antisense oligonucleotides in therapy for neurodegenerative disorders, Adv Drug Deliv Rev, v. 87: Netherlands, 2015. Published by Elsevier B.V., p. 90-103.

Farg, M. A., K. Y. Soo, S. T. Warraich, V. Sundaramoorthy, I. P. Blair, and J. D. Atkin, 2013, Ataxin-2 interacts with FUS and intermediate-length polyglutamine expansions enhance FUS-related pathology in amyotrophic lateral sclerosis: Hum Mol Genet, v. 22, p. 717-28.

Farr, S. A., M. A. Erickson, M. L. Niehoff, W. A. Banks, and J. E. Morley, 2014, Central and peripheral administration of antisense oligonucleotide targeting amyloid-beta protein precursor improves learning and memory and reduces neuroinflammatory cytokines in Tg2576 (AbetaPPswe) mice: J Alzheimers Dis, v. 40, p. 1005-16.

Fecto, F., J. Yan, S. P. Vemula, E. Liu, Y. Yang, W. Chen, J. G. Zheng, Y. Shi, N. Siddique, H. Arrat, S. Donkervoort, S. Ajroud-Driss, R. L. Sufit, S. L. Heller, H. X. Deng, and T. Siddique, 2011, SQSTM1 mutations in familial and sporadic amyotrophic lateral sclerosis: Arch Neurol, v. 68, p. 1440-6.

Ferrante, R. J., S. E. Browne, L. A. Shinobu, A. C. Bowling, M. J. Baik, U. MacGarvey, N. W. Kowall, R. H. Brown, Jr., and M. F. Beal, 1997, Evidence of increased oxidative damage in both sporadic and familial amyotrophic lateral sclerosis: J Neurochem, v. 69, p. 2064-74.

Foust, K. D., D. L. Salazar, S. Likhite, L. Ferraiuolo, D. Ditsworth, H. Ilieva, K. Meyer, L. Schmelzer, L. Braun, D. W. Cleveland, and B. K. Kaspar, 2013, Therapeutic AAV9-mediated suppression of mutant SOD1 slows disease progression and extends survival in models of inherited ALS: Mol Ther, v. 21, p. 2148-59.

Fratta, P., S. Mizielinska, A. J. Nicoll, M. Zloh, E. M. Fisher, G. Parkinson, and A. M. Isaacs, 2012, C9orf72 hexanucleotide repeat associated with amyotrophic lateral sclerosis and frontotemporal dementia forms RNA G-quadruplexes: Sci Rep, v. 2, p. 1016.

Fratta, P., J. M. Polke, J. Newcombe, S. Mizielinska, T. Lashley, M. Poulter, J. Beck, E. Preza, A. Devoy, K. Sidle, R. Howard, A. Malaspina, R. W. Orrell, J. Clarke, C. H. Lu, K. Mok, T. Collins, M. Shoaii, T. Nanji, S. Wray, G. Adamson, A. Pittman, A. E. Renton, B. J. Traynor, M. G. Sweeney, T. Revesz, H. Houlden, S. Mead, A. M. Isaacs, and E. M. Fisher, 2015, Screening a UK amyotrophic lateral sclerosis cohort provides evidence of multiple origins of the C9orf72 expansion: Neurobiol Aging, v. 36, p. 546 e1-7.

Fratta, P., M. Poulter, T. Lashley, J. D. Rohrer, J. M. Polke, J. Beck, N. Ryan, D. Hensman, S. Mizielinska, A. J. Waite, M. C. Lai, T. F. Gendron, L. Petrucelli, E. M. Fisher, T. Revesz, J. D. Warren, J. Collinge, A. M. Isaacs, and S. Mead, 2013, Homozygosity for the C9orf72 GGGGCC repeat expansion in frontotemporal dementia: Acta Neuropathol, v. 126, p. 401-9.

Freibaum, B. D., Y. Lu, R. Lopez-Gonzalez, N. C. Kim, S. Almeida, K. H. Lee, N. Badders, M. Valentine, B. L. Miller, P. C. Wong, L. Petrucelli, H. J. Kim, F. B. Gao, and J. P. Taylor, 2015, GGGGCC repeat expansion in C9orf72 compromises nucleocytoplasmic transport: Nature, v. 525, p. 129-33.

Freischmidt, A., K. Muller, A. C. Ludolph, J. H. Weishaupt, and P. M. Andersen, 2016, Association of Mutations in TBK1 With Sporadic and Familial Amyotrophic Lateral Sclerosis and Frontotemporal Dementia: JAMA Neurol.

Freischmidt, A., T. Wieland, B. Richter, W. Ruf, V. Schaeffer, K. Muller, N. Marroquin, F. Nordin, A. Hubers, P. Weydt, S. Pinto, R. Press, S. Millecamps, N. Molko, E. Bernard, C. Desnuelle, M. H. Soriani, J. Dorst, E. Graf, U. Nordstrom, M. S. Feiler, S. Putz, T. M. Boeckers, T. Meyer, A. S. Winkler, J. Winkelman, M. de Carvalho, D. R. Thal, M. Otto, T. Brannstrom, A. E. Volk, P. Kursula, K. M. Danzer, P. Lichtner, I. Dikic, T. Meitinger, A. C. Ludolph, T. M. Strom, P. M. Andersen, and J. H. Weishaupt, 2015, Haploinsufficiency of TBK1 causes familial ALS and fronto-temporal dementia: Nat Neurosci, v. 18, p. 631-6.

Frey, D., C. Schneider, L. Xu, J. Borg, W. Spooren, and P. Caroni, 2000, Early and Selective Loss of Neuromuscular Synapse Subtypes with Low Sprouting Competence in Motoneuron Diseases: The Journal of Neuroscience, v. 20, p. 2534-2542.

Gascon, E., K. Lynch, H. Ruan, S. Almeida, J. M. Verheyden, W. W. Seeley, D. W. Dickson, L. Petrucelli, D. Sun, J. Jiao, H. Zhou, M. Jakovcevski, S. Akbarian, W. D. Yao, and F. B. Gao, 2014, Alterations in microRNA-124 and AMPA receptors contribute to social behavioral deficits in frontotemporal dementia: Nat Med, v. 20, p. 1444-51.

Gellera, C., C. Tiloca, R. Del Bo, L. Corrado, V. Pensato, J. Agostini, C. Cereda, A. Ratti, B. Castellotti, S. Corti, A. Bagarotti, A. Cagnin, P. Milani, C. Gabelli, G. Riboldi, L. Mazzini, G. Soraru, S. D'Alfonso, F. Taroni, G. P. Comi, N. Ticozzi, V. Silani, and S. Consortium, 2013, Ubiquilin 2 mutations in Italian patients with amyotrophic lateral sclerosis and frontotemporal dementia: J Neurol Neurosurg Psychiatry, v. 84, p. 183-7.

Gendron, T. F., K. F. Bieniek, Y. J. Zhang, K. Jansen-West, P. E. Ash, T. Caulfield, L. Daughrity, J. H. Dunmore, M. Castanedes-Casey, J. Chew, D. M. Cosio, M. van Blitterswijk, W. C. Lee, R. Rademakers, K. B. Boylan, D. W. Dickson, and L. Petrucelli, 2013, Antisense transcripts of the expanded C9ORF72 hexanucleotide repeat form nuclear RNA foci and undergo repeat-associated non-ATG translation in c9FTD/ALS: Acta Neuropathol, v. 126, p. 829-44.

Gendron, T. F., J. Chew, J. N. Stankowski, L. R. Hayes, Y. J. Zhang, M. Prudencio, Y. Carlomagno, L. M. Daughrity, K. Jansen-West, E. A. Perkerson, A. O'Raw, C. Cook, L. Pregent, V. Belzil, M. van Blitterswijk, L. J. Tabassian, C. W. Lee, M. Yue, J. Tong, Y. Song, M. Castanedes-Casey, L. Rousseau, V. Phillips, D. W. Dickson, R. Rademakers, J. D. Fryer, B. K. Rush, O. Pedraza, A. M. Caputo, P. Desaro, C. Palmucci, A. Robertson, M. G. Heckman, N. N. Diehl, E. Wiggs, M. Tierney, L. Braun, J. Farren, D. Lacomis, S. Ladha, C. N. Fournier, L. F. McCluskey, L. B. Elman, J. B. Toledo, J. D. McBride, C.

Tiloca, C. Morelli, B. Poletti, F. Solca, A. Prelle, J. Wuu, J. Jockel-Balsarotti, F. Rigo, C. Ambrose, A. Datta, W. Yang, D. Raitcheva, G. Antognetti, A. McCampbell, J. C. Van Swieten, B. L. Miller, A. L. Boxer, R. H. Brown, R. Bowser, T. M. Miller, J. Q. Trojanowski, M. Grossman, J. D. Berry, W. T. Hu, A. Ratti, B. J. Traynor, M. D. Disney, M. Benatar, V. Silani, J. D. Glass, M. K. Floeter, J. D. Rothstein, K. B. Boylan, and L. Petrucelli, 2017, Poly(GP) proteins are a useful pharmacodynamic marker for C9ORF72-associated amyotrophic lateral sclerosis: Sci Transl Med, v. 9.

Gijselinck, I., S. Van Mossevelde, J. van der Zee, A. Sieben, S. Engelborghs, J. De Bleecker, A. Ivanoiu, O. Deryck, D. Edbauer, M. Zhang, B. Heeman, V. Baumer, M. Van den Broeck, M. Mattheijssens, K. Peeters, E. Rogaeva, P. De Jonghe, P. Cras, J. J. Martin, P. P. de Deyn, M. Cruts, and C. Van Broeckhoven, 2016, The C9orf72 repeat size correlates with onset age of disease, DNA methylation and transcriptional downregulation of the promoter: Mol Psychiatry, v. 21, p. 1112-24.

Gilpin, K. M., L. Chang, and M. J. Monteiro, 2015, ALS-linked mutations in ubiquilin-2 or hnRNPA1 reduce interaction between ubiquilin-2 and hnRNPA1: Hum Mol Genet, v. 24, p. 2565-77.

Goemans, N. M., M. Tulinius, J. T. van den Akker, B. E. Burm, P. F. Ekhart, N. Heuvelmans, T. Holling, A. A. Janson, G. J. Platenburg, J. A. Sipkens, J. M. Sitsen, A. Aartsma-Rus, G. J. van Ommen, G. Buyse, N. Darin, J. J. Verschuuren, G. V. Campion, S. J. de Kimpe, and J. C. van Deutekom, 2011, Systemic administration of PRO051 in Duchenne's muscular dystrophy: N Engl J Med, v. 364, p. 1513-22.

Gomez-Deza, J., Y. B. Lee, C. Troakes, M. Nolan, S. Al-Sarraj, J. M. Gallo, and C. E. Shaw, 2015, Dipeptide repeat protein inclusions are rare in the spinal cord and almost absent from motor neurons in C9ORF72 mutant amyotrophic lateral sclerosis and are unlikely to cause their degeneration: Acta Neuropathol Commun, v. 3, p. 38.

Gotkine, M., L. Rozenstein, O. Einstein, O. Abramsky, Z. Argov, and H. Rosenmann, 2013, Presymptomatic treatment with acetylcholinesterase antisense oligonucleotides prolongs survival in ALS (G93A-SOD1) mice: Biomed Res Int, v. 2013, p. 845345.

Greenway, M. J., M. D. Alexander, S. Ennis, B. J. Traynor, B. Corr, E. Frost, A. Green, and O. Hardiman, 2004, A novel candidate region for ALS on chromosome 14q11.2: Neurology, v. 63, p. 1936-8.

Gros-Louis, F., R. Lariviere, G. Gowing, S. Laurent, W. Camu, J. P. Bouchard, V. Meininger, G. A. Rouleau, and J. P. Julien, 2004, A frameshift deletion in peripherin gene associated with amyotrophic lateral sclerosis: J Biol Chem, v. 279, p. 45951-6.

Guidotti, G., L. Brambilla, and D. Rossi, 2017, Cell-Penetrating Peptides: From Basic Research to Clinics: Trends Pharmacol Sci, v. 38, p. 406-424.

Hadano, S., C. K. Hand, H. Osuga, Y. Yanagisawa, A. Otomo, R. S. Devon, N. Miyamoto, J. Showguchi-Miyata, Y. Okada, R. Singaraja, D. A. Figlewicz, T. Kwiatkowski, B. A. Hosler, T. Sagie, J. Skaug, J. Nasir, R. H. Brown, Jr., S. W. Scherer, G. A. Rouleau, M. R. Hayden, and J. E. Ikeda, 2001, A gene encoding a putative GTPase regulator is mutated in familial amyotrophic lateral sclerosis 2: Nat Genet, v. 29, p. 166-73.

Hadano, S., S. Mitsui, L. Pan, A. Otomo, M. Kubo, K. Sato, S. Ono, W. Onodera, K. Abe, X. Chen, M. Koike, Y. Uchiyama, M. Aoki, E. Warabi, M. Yamamoto, T. Ishii, T. Yanagawa, H. F. Shang, and F. Yoshii, 2016, Functional links between SQSTM1 and ALS2 in the pathogenesis of ALS: cumulative impact on the protection against mutant SOD1-mediated motor dysfunction in mice: Hum Mol Genet.

Haeusler, A. R., C. J. Donnelly, G. Periz, E. A. Simko, P. G. Shaw, M. S. Kim, N. J. Maragakis, J. C. Troncoso, A. Pandey, R. Sattler, J. D. Rothstein, and J. Wang, 2014, C9orf72 nucleotide repeat structures initiate molecular cascades of disease: Nature, v. 507, p. 195-200.

Hansen, S. M., V. Berezin, and E. Bock, 2008, Signaling mechanisms of neurite outgrowth induced by the cell adhesion molecules NCAM and N-cadherin: Cell Mol Life Sci, v. 65, p. 3809-21.

Harms, M. B., J. Cady, C. Zaidman, P. Cooper, T. Bali, P. Allred, C. Cruchaga, M. Baughn, R. T. Libby, A. Pestronk, A. Goate, J. Ravits, and R. H. Baloh, 2013, Lack of C9ORF72 coding mutations supports a gain of function for repeat expansions in amyotrophic lateral sclerosis: Neurobiol Aging, v. 34, p. 2234 e13-9.

Hart, M. P., J. Brettschneider, V. M. Lee, J. Q. Trojanowski, and A. D. Gitler, 2012, Distinct TDP-43 pathology in ALS patients with ataxin 2 intermediate-length polyQ expansions: Acta Neuropathol, v. 124, p. 221-30.

Helgason, E., Q. T. Phung, and E. C. Dueber, 2013, Recent insights into the complexity of Tank-binding kinase 1 signaling networks: the emerging role of cellular localization in the activation and substrate specificity of TBK1: FEBS Lett, v. 587, p. 1230-7.

Henkel, J. S., D. R. Beers, W. Zhao, and S. H. Appel, 2009, Microglia in ALS: the good, the bad, and the resting: J Neuroimmune Pharmacol, v. 4, p. 389-98.

Hentati, A., K. Bejaoui, M. A. Pericak-Vance, F. Hentati, M. C. Speer, W. Y. Hung, D. A. Figlewicz, J. Haines, J. Rimmler, C. Ben Hamida, and et al., 1994, Linkage of recessive familial amyotrophic lateral sclerosis to chromosome 2q33-q35: Nat Genet, v. 7, p. 425-8.

Higelin, J., M. Demestre, S. Putz, J. P. Delling, C. Jacob, A. K. Lutz, J. Bausinger, A. K. Huber, M. Klingenstein, G. Barbi, G. Speit, A. Huebers, J. H. Weishaupt, A. Hermann, S. Liebau, A. C. Ludolph, and T. M. Boeckers, 2016, FUS Mislocalization and Vulnerability to DNA Damage in ALS Patients Derived hiPSCs and Aging Motoneurons: Front Cell Neurosci, v. 10, p. 290.

Hirano, A., I. Nakano, L. T. Kurland, D. W. Mulder, P. W. Holley, and G. Saccomanno, 1984, Fine structural study of neurofibrillary changes in a family with amyotrophic lateral sclerosis: J Neuropathol Exp Neurol, v. 43, p. 471-80.

Hock, E. M., and M. Polymenidou, 2016, Prion-like propagation as a pathogenic principle in frontotemporal dementia: J Neurochem, v. 138 Suppl 1, p. 163-83.

Holm, I. E., E. Englund, I. R. Mackenzie, P. Johannsen, and A. M. Isaacs, 2007, A reassessment of the neuropathology of frontotemporal dementia linked to chromosome 3: J Neuropathol Exp Neurol, v. 66, p. 884-91.

Hoyer, L. L., and J. E. Hecht, 2000, The ALS6 and ALS7 genes of Candida albicans: Yeast, v. 16, p. 847-55.

Huang, B., Q. Wu, H. Zhou, C. Huang, and X. G. Xia, 2016, Increased Ubqln2 Expression Causes Neuron Death in Transgenic Rats: J Neurochem.

Ichiyanagi, N., K. Fujimori, M. Yano, C. Ishihara-Fujisaki, T. Sone, T. Akiyama, Y. Okada, W. Akamatsu, T. Matsumoto, M. Ishikawa, Y. Nishimoto, Y. Ishihara, T. Sakuma, T. Yamamoto, H. Tsuiji, N. Suzuki, H. Warita, M. Aoki, and H. Okano, 2016, Establishment of In Vitro FUS-Associated Familial Amyotrophic Lateral Sclerosis Model Using Human Induced Pluripotent Stem Cells: Stem Cell Reports, v. 6, p. 496-510.

Iguchi, Y., M. Katsuno, K. Ikenaka, S. Ishigaki, and G. Sobue, 2013a, Amyotrophic lateral sclerosis: an update on recent genetic insights: J Neurol, v. 260, p. 2917-27.

Iguchi, Y., M. Katsuno, J. Niwa, S. Takagi, S. Ishigaki, K. Ikenaka, K. Kawai, H. Watanabe, K. Yamanaka, R. Takahashi, H. Misawa, S. Sasaki, F. Tanaka, and G. Sobue, 2013b, Loss of TDP-43 causes age-dependent progressive motor neuron degeneration: Brain, v. 136, p. 1371-82.

Ihara, Y., K. Nobukuni, H. Takata, and T. Hayabara, 2005, Oxidative stress and metal content in blood and cerebrospinal fluid of amyotrophic lateral sclerosis patients with and without a Cu, Zn-superoxide dismutase mutation: Neurol Res, v. 27, p. 105-8.

Ishiguro, A., N. Kimura, Y. Watanabe, S. Watanabe, and A. Ishihama, 2016, TDP-43 binds and transports G-quadruplex-containing mRNAs into neurites for local translation: Genes Cells, v. 21, p. 466-81.

Jiang, J., Q. Zhu, T. F. Gendron, S. Saberi, M. McAlonis-Downes, A. Seelman, J. E. Stauffer, P. Jafar-Nejad, K. Drenner, D. Schulte, S. Chun, S. Sun, S. C. Ling, B. Myers, J. Engelhardt, M. Katz, M. Baughn, O. Platoshyn, M. Marsala, A. Watt, C. J. Heyser, M. C. Ard, L. De Muynck, L. M. Daughrity, D. A. Swing, L. Tessarollo, C. J. Jung, A. Delpoux, D. T. Utzschneider, S. M. Hedrick, P. J. de Jong, D. Edbauer, P. Van Damme, L. Petrucelli, C. E. Shaw, C. F. Bennett, S. Da Cruz, J. Ravits, F. Rigo, D. W. Cleveland, and C. Lagier-Tourenne, 2016, Gain of Toxicity from ALS/FTD-Linked Repeat Expansions in C9ORF72 Is Alleviated by Antisense Oligonucleotides Targeting GGGGCC-Containing RNAs: Neuron, v. 90, p. 535-50.

Johnson, J. O., J. Mandrioli, M. Benatar, Y. Abramzon, V. M. Van Deerlin, J. Q. Trojanowski, J. R. Gibbs, M. Brunetti, S. Gronka, J. Wuu, J. Ding, L. McCluskey, M. Martinez-Lage, D. Falcone, D. G. Hernandez, S. Arepalli, S. Chong, J. C. Schymick, J. Rothstein, F. Landi, Y. D. Wang, A. Calvo, G. Mora, M. Sabatelli, M. R. Monsurro, S. Battistini, F. Salvi, R. Spataro, P. Sola, G. Borghero, I. Consortium, G. Galassi, S. W. Scholz, J. P. Taylor, G. Restagno, A. Chio, and B. J. Traynor, 2010, Exome sequencing reveals VCP mutations as a cause of familial ALS: Neuron, v. 68, p. 857-64.

Johnson, J. O., E. P. Pioro, A. Boehringer, R. Chia, H. Feit, A. E. Renton, H. A. Pliner, Y. Abramzon, G. Marangi, B. J. Winborn, J. R. Gibbs, M. A. Nalls, S. Morgan, M. Shoai, J. Hardy, A. Pittman, R. W. Orrell, A. Malaspina, K. C. Sidle, P. Fratta, M. B. Harms, R. H. Baloh, A. Pestronk, C. C. Weihl, E. Rogaeva, L. Zinman, V. E. Drory, G. Borghero, G. Mora, A. Calvo, J. D. Rothstein, I. Consortium, C. Drepper, M. Sendtner, A. B. Singleton, J. P. Taylor, M. R. Cookson, G. Restagno, M. Sabatelli, R. Bowser, A. Chio, and B. J. Traynor, 2014, Mutations in the Matrin 3 gene cause familial amyotrophic lateral sclerosis: Nat Neurosci, v. 17, p. 664-6.

Johnston, C. A., B. R. Stanton, M. R. Turner, R. Gray, A. H. Blunt, D. Butt, M. A. Ampong, C. E. Shaw, P. N. Leigh, and A. Al-Chalabi, 2006, Amyotrophic lateral sclerosis in an urban setting: a population based study of inner city London: J Neurol, v. 253, p. 1642-3.

Jovicic, A., J. Mertens, S. Boeynaems, E. Bogaert, N. Chai, S. B. Yamada, J. W. Paul, 3rd, S. Sun, J. R. Herdy, G. Bieri, N. J. Kramer, F. H. Gage, L. Van Den Bosch, W. Robberecht, and A. D. Gitler, 2015, Modifiers of C9orf72 dipeptide repeat toxicity connect nucleocytoplasmic transport defects to FTD/ALS: Nat Neurosci, v. 18, p. 1226-9.

Jovicic, A., J. W. Paul, 3rd, and A. D. Gitler, 2016, Nuclear transport dysfunction: a common theme in amyotrophic lateral sclerosis and frontotemporal dementia: J Neurochem, v. 138 Suppl 1, p. 134-44.

Kabashi, E., V. Bercier, A. Lissouba, M. Liao, E. Brustein, G. A. Rouleau, and P. Drapeau, 2011, FUS and TARDBP but not SOD1 interact in genetic models of amyotrophic lateral sclerosis: PLoS Genet, v. 7, p. e1002214.

Kabashi, E., L. Lin, M. L. Tradewell, P. A. Dion, V. Bercier, P. Bourgouin, D. Rochefort, S. Bel Hadj, H. D. Durham, C. Vande Velde, G. A. Rouleau, and P. Drapeau, 2010, Gain and loss of function of ALS-related mutations of TARDBP (TDP-43) cause motor deficits in vivo: Hum Mol Genet, v. 19, p. 671-83.

Kaneb, H. M., A. W. Folkmann, V. V. Belzil, L. E. Jao, C. S. Leblond, S. L. Girard, H. Daoud, A. Noreau, D. Rochefort, P. Hince, A. Szuto, A. Levert, S. Vidal, C. Andre-Guimont, W. Camu, J. P. Bouchard, N. Dupre, G. A. Rouleau, S. R. Wente, and P. A. Dion, 2015, Deleterious mutations in the essential mRNA metabolism factor, hGle1, in amyotrophic lateral sclerosis: Hum Mol Genet, v. 24, p. 1363-73.

Kenna, K. P., P. T. van Doormaal, A. M. Dekker, N. Ticozzi, B. J. Kenna, F. P. Diekstra, W. van Rheenen, K. R. van Eijk, A. R. Jones, P. Keagle, A. Shatunov, W. Sproviero, B. N. Smith,

M. A. van Es, S. D. Topp, A. Kenna, J. W. Miller, C. Fallini, C. Tiloca, R. L. McLaughlin, C. Vance, C. Troakes, C. Colombrita, G. Mora, A. Calvo, F. Verde, S. Al-Sarraj, A. King, D. Calini, J. de Belleroche, F. Baas, A. J. van der Kooi, M. de Visser, A. L. Ten Asbroek, P. C. Sapp, D. McKenna-Yasek, M. Polak, S. Asress, J. L. Munoz-Blanco, T. M. Strom, T. Meitinger, K. E. Morrison, S. Consortium, G. Lauria, K. L. Williams, P. N. Leigh, G. A. Nicholson, I. P. Blair, C. S. Leblond, P. A. Dion, G. A. Rouleau, H. Pall, P. J. Shaw, M. R. Turner, K. Talbot, F. Taroni, K. B. Boylan, M. Van Blitterswijk, R. Rademakers, J. Esteban-Perez, A. Garcia-Redondo, P. Van Damme, W. Robberecht, A. Chio, C. Gellera, C. Drepper, M. Sendtner, A. Ratti, J. D. Glass, J. S. Mora, N. A. Basak, O. Hardiman, A. C. Ludolph, P. M. Andersen, J. H. Weishaupt, R. H. Brown, Jr., A. Al-Chalabi, V. Silani, C. E. Shaw, L. H. van den Berg, J. H. Veldink, and J. E. Landers, 2016, NEK1 variants confer susceptibility to amyotrophic lateral sclerosis: Nat Genet, v. 48, p. 1037-42.

Khosravi, B., H. Hartmann, S. May, C. Mohl, H. Ederle, M. Michaelsen, M. H. Schludi, D. Dormann, and D. Edbauer, 2016, Cytoplasmic poly-GA aggregates impair nuclear import of TDP-43 in C9orf72 ALS/FTLD: Hum Mol Genet.

Kim, H. J., N. C. Kim, Y. D. Wang, E. A. Scarborough, J. Moore, Z. Diaz, K. S. MacLea, B. Freibaum, S. Li, A. Molliex, A. P. Kanagaraj, R. Carter, K. B. Boylan, A. M. Wojtas, R. Rademakers, J. L. Pinkus, S. A. Greenberg, J. Q. Trojanowski, B. J. Traynor, B. N. Smith, S. Topp, A. S. Gkazi, J. Miller, C. E. Shaw, M. Kottlors, J. Kirschner, A. Pestronk, Y. R. Li, A. F. Ford, A. D. Gitler, M. Benatar, O. D. King, V. E. Kimonis, E. D. Ross, C. C. Weihl, J. Shorter, and J. P. Taylor, 2013, Mutations in prion-like domains in hnRNPA2B1 and hnRNPA1 cause multisystem proteinopathy and ALS: Nature, v. 495, p. 467-73.

Kinali, M., V. Arechavala-Gomeza, L. Feng, S. Cirak, D. Hunt, C. Adkin, M. Guglieri, E. Ashton, S. Abbs, P. Nihoyannopoulos, M. E. Garralda, M. Rutherford, C. McCulley, L. Popplewell, I. R. Graham, G. Dickson, M. J. Wood, D. J. Wells, S. D. Wilton, R. Kole, V. Straub, K. Bushby, C. Sewry, J. E. Morgan, and F. Muntoni, 2009, Local restoration of dystrophin expression with the morpholino oligomer AVI-4658 in Duchenne muscular dystrophy: a single-blind, placebo-controlled, dose-escalation, proof-of-concept study: Lancet Neurol, v. 8, p. 918-28.

King, A., S. Al-Sarraj, and C. Shaw, 2009, Frontotemporal lobar degeneration with ubiquitinated tau-negative inclusions and additional alpha-synuclein pathology but also unusual cerebellar ubiquitinated p62-positive, TDP-43-negative inclusions: Neuropathology, v. 29, p. 466-71.

King, A., C. Troakes, B. Smith, M. Nolan, O. Curran, C. Vance, C. E. Shaw, and S. Al-Sarraj, 2015, ALS-FUS pathology revisited: singleton FUS mutations and an unusual case with both a FUS and TARDBP mutation: Acta Neuropathol Commun, v. 3, p. 62.

Koller, E., T. M. Vincent, A. Chappell, S. De, M. Manoharan, and C. F. Bennett, 2011, Mechanisms of single-stranded phosphorothioate modified antisense oligonucleotide accumulation in hepatocytes: Nucleic Acids Res, v. 39, p. 4795-807.

Komine, O., and K. Yamanaka, 2015, Neuroinflammation in motor neuron disease: Nagoya J Med Sci, v. 77, p. 537-49.

Kon, T., F. Mori, K. Tanji, Y. Miki, Y. Toyoshima, M. Yoshida, H. Sasaki, A. Kakita, H. Takahashi, and K. Wakabayashi, 2014, ALS-associated protein FIG4 is localized in Pick and Lewy bodies, and also neuronal nuclear inclusions, in polyglutamine and intranuclear inclusion body diseases: Neuropathology, v. 34, p. 19-26.

Koppers, M., A. M. Blokhuis, H. J. Westeneng, M. L. Terpstra, C. A. Zundel, R. Vieira de Sa, R. D. Schellevis, A. J. Waite, D. J. Blake, J. H. Veldink, L. H. van den Berg, and R. J. Pasterkamp, 2015, C9orf72 ablation in mice does not cause motor neuron degeneration or motor deficits: Ann Neurol, v. 78, p. 426-38.

Kordasiewicz, H. B., L. M. Stanek, E. V. Wancewicz, C. Mazur, M. M. McAlonis, K. A. Pytel, J. W. Artates, A. Weiss, S. H. Cheng, L. S. Shihabuddin, G. Hung, C. F. Bennett, and D. W. Cleveland, 2012, Sustained therapeutic reversal of Huntington's disease by transient repression of huntingtin synthesis: Neuron, v. 74, p. 1031-44.

Koval, E. D., C. Shaner, P. Zhang, X. du Maine, K. Fischer, J. Tay, B. N. Chau, G. F. Wu, and T. M. Miller, 2013, Method for widespread microRNA-155 inhibition prolongs survival in ALS-model mice: Hum Mol Genet, v. 22, p. 4127-35.

Kovanda, A., M. Zalar, P. Sket, J. Plavec, and B. Rogelj, 2015, Anti-sense DNA d(GGCCCC)n expansions in C9ORF72 form i-motifs and protonated hairpins: Sci Rep, v. 5, p. 17944.

Kraemer, B. C., T. Schuck, J. M. Wheeler, L. C. Robinson, J. Q. Trojanowski, V. M. Lee, and G. D. Schellenberg, 2010, Loss of murine TDP-43 disrupts motor function and plays an essential role in embryogenesis: Acta Neuropathol, v. 119, p. 409-19.

Kramer, N. J., Y. Carlomagno, Y. J. Zhang, S. Almeida, C. N. Cook, T. F. Gendron, M. Prudencio, M. Van Blitterswijk, V. Belzil, J. Couthouis, J. W. Paul, 3rd, L. D. Goodman, L. Daughrity, J. Chew, A. Garrett, L. Pregent, K. Jansen-West, L. J. Tabassian, R. Rademakers, K. Boylan, N. R. Graff-Radford, K. A. Josephs, J. E. Parisi, D. S. Knopman, R. C. Petersen, B. F. Boeve, N. Deng, Y. Feng, T. H. Cheng, D. W. Dickson, S. N. Cohen, N. M. Bonini, C. D. Link, F. B. Gao, L. Petrucelli, and A. D. Gitler, 2016, Spt4 selectively regulates the expression of C9orf72 sense and antisense mutant transcripts: Science, v. 353, p. 708-12.

Ku, S. H., S. D. Jo, Y. K. Lee, K. Kim, and S. H. Kim, 2016, Chemical and structural modifications of RNAi therapeutics: Adv Drug Deliv Rev, v. 104, p. 16-28.

Kwiatkowski, T. J., Jr., D. A. Bosco, A. L. Leclerc, E. Tamrazian, C. R. Vanderburg, C. Russ, A. Davis, J. Gilchrist, E. J. Kasarskis, T. Munsat, P. Valdmanis, G. A. Rouleau, B. A. Hosler, P. Cortelli, P. J. de Jong, Y. Yoshinaga, J. L. Haines, M. A. Pericak-Vance, J. Yan, N. Ticozzi, T. Siddique, D. McKenna-Yasek, P. C. Sapp, H. R. Horvitz, J. E. Landers, and R. H. Brown, Jr., 2009, Mutations in the FUS/TLS gene on chromosome 16 cause familial amyotrophic lateral sclerosis: Science, v. 323, p. 1205-8.

Kwon, I., S. Xiang, M. Kato, L. Wu, P. Theodoropoulos, T. Wang, J. Kim, J. Yun, Y. Xie, and S. L. McKnight, 2014, Poly-dipeptides encoded by the C9orf72 repeats bind nucleoli, impede RNA biogenesis, and kill cells: Science, v. 345, p. 1139-45.

Lagier-Tourenne, C., M. Baughn, F. Rigo, S. Sun, P. Liu, H. R. Li, J. Jiang, A. T. Watt, S. Chun, M. Katz, J. Qiu, Y. Sun, S. C. Ling, Q. Zhu, M. Polymenidou, K. Drenner, J. W. Artates, M. McAlonis-Downes, S. Markmiller, K. R. Hutt, D. P. Pizzo, J. Cady, M. B. Harms, R. H. Baloh, S. R. Vandenberg, G. W. Yeo, X. D. Fu, C. F. Bennett, D. W. Cleveland, and J. Ravits, 2013, Targeted degradation of sense and antisense C9orf72 RNA foci as therapy for ALS and frontotemporal degeneration: Proc Natl Acad Sci U S A, v. 110, p. E4530-9.

Lagier-Tourenne, C., M. Polymenidou, and D. W. Cleveland, 2010, TDP-43 and FUS/TLS: emerging roles in RNA processing and neurodegeneration: Hum Mol Genet, v. 19, p. R46-64.

Lagier-Tourenne, C., M. Polymenidou, K. R. Hutt, A. Q. Vu, M. Baughn, S. C. Huelga, K. M. Clutario, S. C. Ling, T. Y. Liang, C. Mazur, E. Wancewicz, A. S. Kim, A. Watt, S. Freier, G. G. Hicks, J. P. Donohue, L. Shiue, C. F. Bennett, J. Ravits, D. W. Cleveland, and G. W. Yeo, 2012, Divergent roles of ALS-linked proteins FUS/TLS and TDP-43 intersect in processing long pre-mRNAs: Nat Neurosci, v. 15, p. 1488-97.

Landers, J. E., A. L. Leclerc, L. Shi, A. Virkud, T. Cho, M. M. Maxwell, A. F. Henry, M. Polak, J. D. Glass, T. J. Kwiatkowski, A. Al-Chalabi, C. E. Shaw, P. N. Leigh, I. Rodriguez-Leyza, D. McKenna-Yasek, P. C. Sapp, and R. H. Brown, Jr., 2008, New VAPB deletion variant and exclusion of VAPB mutations in familial ALS: Neurology, v. 70, p. 1179-85.

Lattante, S., H. de Calbiac, I. Le Ber, A. Brice, S. Ciura, and E. Kabashi, 2015, Sqstm1 knock-down causes a locomotor phenotype ameliorated by rapamycin in a zebrafish model of ALS/FTLD: Hum Mol Genet, v. 24, p. 1682-90.

Le, N. T., L. Chang, I. Kovlyagina, P. Georgiou, N. Safren, K. E. Braunstein, M. D. Kvarta, A. M. Van Dyke, T. A. LeGates, T. Philips, B. M. Morrison, S. M. Thompson, A. C. Puche, T. D. Gould, J. D. Rothstein, P. C. Wong, and M. J. Monteiro, 2016, Motor neuron disease, TDP-43 pathology, and memory deficits in mice expressing ALS-FTD-linked UBQLN2 mutations: Proc Natl Acad Sci U S A, v. 113, p. E7580-E7589.

Lee, K. H., P. Zhang, H. J. Kim, D. M. Mitrea, M. Sarkar, B. D. Freibaum, J. Cika, M. Coughlin, J. Messing, A. Molliex, B. A. Maxwell, N. C. Kim, J. Temirov, J. Moore, R. M. Kolaitis, T. I. Shaw, B. Bai, J. Peng, R. W. Kriwacki, and J. P. Taylor, 2016, C9orf72 Dipeptide Repeats Impair the Assembly, Dynamics, and Function of Membrane-Less Organelles: Cell, v. 167, p. 774-788 e17.

Lee, S. E., A. M. Khazenzon, A. J. Trujillo, C. C. Guo, J. S. Yokoyama, S. J. Sha, L. T. Takada, A. M. Karydas, N. R. Block, G. Coppola, M. Pribadi, D. H. Geschwind, R. Rademakers, J. C. Fong, M. W. Weiner, A. L. Boxer, J. H. Kramer, H. J. Rosen, B. L. Miller, and W. W. Seeley, 2014a, Altered network connectivity in frontotemporal dementia with C9orf72 hexanucleotide repeat expansion: Brain, v. 137, p. 3047-60.

Lee, W. C., S. Almeida, M. Prudencio, T. R. Caulfield, Y. J. Zhang, W. M. Tay, P. O. Bauer, J. Chew, H. Sasaguri, K. R. Jansen-West, T. F. Gendron, C. T. Stetler, N. Finch, I. R. Mackenzie, R. Rademakers, F. B. Gao, and L. Petrucelli, 2014b, Targeted manipulation of the sortilin-progranulin axis rescues progranulin haploinsufficiency: Hum Mol Genet, v. 23, p. 1467-78.

Lee, Y. B., H. J. Chen, J. N. Peres, J. Gomez-Deza, J. Attig, M. Stalekar, C. Troakes, A. L. Nishimura, E. L. Scotter, C. Vance, Y. Adachi, V. Sardone, J. W. Miller, B. N. Smith, J. M. Gallo, J. Ule, F. Hirth, B. Rogelj, C. Houart, and C. E. Shaw, 2013, Hexanucleotide repeats in ALS/FTD form length-dependent RNA foci, sequester RNA binding proteins, and are neurotoxic: Cell Rep, v. 5, p. 1178-86.

Lehmer, C., P. Oeckl, J. H. Weishaupt, A. E. Volk, J. Diehl-Schmid, M. L. Schroeter, M. Lauer, J. Kornhuber, J. Levin, K. Fassbender, B. Landwehrmeyer, D. German Consortium for Frontotemporal Lobar, M. H. Schludi, T. Arzberger, E. Kremmer, A. Flatley, R. Feederle, P. Steinacker, P. Weydt, A. C. Ludolph, D. Edbauer, and M. Otto, 2017, Poly-GP in cerebrospinal fluid links C9orf72-associated dipeptide repeat expression to the asymptomatic phase of ALS/FTD: EMBO Mol Med.

Lehto, T., A. Castillo Alvarez, S. Gauck, M. J. Gait, T. Coursindel, M. J. Wood, B. Lebleu, and P. Boisguerin, 2014, Cellular trafficking determines the exon skipping activity of Pip6a-PMO in mdx skeletal and cardiac muscle cells: Nucleic Acids Res, v. 42, p. 3207-17.

Lenzi, J., R. De Santis, V. de Turris, M. Morlando, P. Laneve, A. Calvo, V. Caliendo, A. Chio, A. Rosa, and I. Bozzoni, 2015, ALS mutant FUS proteins are recruited into stress granules in induced pluripotent stem cell-derived motoneurons: Dis Model Mech, v. 8, p. 755-66.

Leung, C. L., C. Z. He, P. Kaufmann, S. S. Chin, A. Naini, R. K. Liem, H. Mitsumoto, and A. P. Hays, 2004, A pathogenic peripherin gene mutation in a patient with amyotrophic lateral sclerosis: Brain Pathol, v. 14, p. 290-6.

Li, F., X. Xie, Y. Wang, J. Liu, X. Cheng, Y. Guo, Y. Gong, S. Hu, and L. Pan, 2016a, Structural insights into the interaction and disease mechanism of neurodegenerative disease-associated optineurin and TBK1 proteins: Nat Commun, v. 7, p. 12708.

Li, P. P., X. Sun, G. Xia, N. Arbez, S. Paul, S. Zhu, H. B. Peng, C. A. Ross, A. H. Koeppen, R. L. Margolis, S. M. Pulst, T. Ashizawa, and D. D. Rudnicki, 2016b, ATXN2-AS, a gene antisense to ATXN2, is associated with spinocerebellar ataxia type 2 and amyotrophic lateral sclerosis: Ann Neurol, v. 80, p. 600-15.

Lin, Y., E. Mori, M. Kato, S. Xiang, L. Wu, I. Kwon, and S. L. McKnight, 2016, Toxic PR Poly-Dipeptides Encoded by the C9orf72 Repeat Expansion Target LC Domain Polymers: Cell, v. 167, p. 789-802 e12.

Ling, S. C., M. Polymenidou, and D. W. Cleveland, 2013, Converging mechanisms in ALS and FTD: disrupted RNA and protein homeostasis: Neuron, v. 79, p. 416-38.

Liu, E. Y., J. Russ, K. Wu, D. Neal, E. Suh, A. G. McNally, D. J. Irwin, V. M. Van Deerlin, and E. B. Lee, 2014a, C9orf72 hypermethylation protects against repeat expansion-associated pathology in ALS/FTD: Acta Neuropathol, v. 128, p. 525-41.

Liu, E. Y., J. Russ, K. Wu, D. Neal, E. Suh, A. G. McNally, D. J. Irwin, V. M. Van Deerlin, and E. B. Lee, 2014b, C9orf72 hypermethylation protects against repeat expansion-associated pathology in ALS/FTD: Acta Neuropathol.

Liu, Y., A. Pattamatta, T. Zu, T. Reid, O. Bardhi, D. R. Borchelt, A. T. Yachnis, and L. P. Ranum, 2016, C9orf72 BAC Mouse Model with Motor Deficits and Neurodegenerative Features of ALS/FTD: Neuron, v. 90, p. 521-34.

Lopez-Gonzalez, R., Y. Lu, T. F. Gendron, A. Karydas, H. Tran, D. Yang, L. Petrucelli, B. L. Miller, S. Almeida, and F. B. Gao, 2016, Poly(GR) in C9ORF72-Related ALS/FTD Compromises Mitochondrial Function and Increases Oxidative Stress and DNA Damage in iPSC-Derived Motor Neurons: Neuron, v. 92, p. 383-391.

Lorenz, P., T. Misteli, B. F. Baker, C. F. Bennett, and D. L. Spector, 2000, Nucleocytoplasmic shuttling: a novel in vivo property of antisense phosphorothioate oligodeoxynucleotides: Nucleic Acids Res, v. 28, p. 582-92.

Lorson, C. L., H. Rindt, and M. Shababi, 2010, Spinal muscular atrophy: mechanisms and therapeutic strategies: Hum Mol Genet, v. 19, p. R111-8.

Ludtmann, M. H., C. Arber, F. Bartolome, M. de Vicente, E. Preza, E. Carro, H. Houlden, S. Gandhi, S. Wray, and A. Y. Abramov, 2017, Mutations in valosin-containing protein (VCP) decrease ADP/ATP translocation across the mitochondrial membrane and impair energy metabolism in human neurons: J Biol Chem.

Mackenzie, I. R., T. Arzberger, E. Kremmer, D. Troost, S. Lorenzl, K. Mori, S. M. Weng, C. Haass, H. A. Kretzschmar, D. Edbauer, and M. Neumann, 2013a, Dipeptide repeat protein pathology in C9ORF72 mutation cases: clinico-pathological correlations: Acta Neuropathol, v. 126, p. 859-79.

Mackenzie, I. R., T. Arzberger, E. Kremmer, D. Troost, S. Lorenzl, K. Mori, S. M. Weng, C. Haass, H. A. Kretzschmar, D. Edbauer, and M. Neumann, 2013b, Dipeptide repeat protein pathology in C9ORF72 mutation cases: clinico-pathological correlations: Acta Neuropathol.

Mackenzie, I. R., P. Frick, F. A. Grasser, T. F. Gendron, L. Petrucelli, N. R. Cashman, D. Edbauer, E. Kremmer, J. Prudlo, D. Troost, and M. Neumann, 2015, Quantitative analysis and clinico-pathological correlations of different dipeptide repeat protein pathologies in C9ORF72 mutation carriers: Acta Neuropathol, v. 130, p. 845-61.

Mackenzie, I. R., P. Frick, and M. Neumann, 2014, The neuropathology associated with repeat expansions in the C9ORF72 gene: Acta Neuropathol, v. 127, p. 347-57.

Maharjan, N., C. Kunzli, K. Buthey, and S. Saxena, 2016, C9ORF72 Regulates Stress Granule Formation and Its Deficiency Impairs Stress Granule Assembly, Hypersensitizing Cells to Stress: Mol Neurobiol.

Majcher, V., A. Goode, V. James, and R. Layfield, 2015, Autophagy receptor defects and ALS-FTLD: Mol Cell Neurosci, v. 66, p. 43-52.

Majounie, E., A. E. Renton, K. Mok, E. G. Dopper, A. Waite, S. Rollinson, A. Chio, G. Restagno, N. Nicolaou, J. Simon-Sanchez, J. C. van Swieten, Y. Abramzon, J. O. Johnson, M. Sendtner, R. Pamphlett, R. W. Orrell, S. Mead, K. C. Sidle, H. Houlden, J. D. Rohrer, K. E. Morrison, H. Pall, K. Talbot, O. Ansorge, D. G. Hernandez, S. Arepalli, M. Sabatelli, G. Mora, M. Corbo, F. Giannini, A. Calvo, E. Englund, G. Borghero, G. L. Floris, A. M.

Remes, H. Laaksovirta, L. McCluskey, J. Q. Trojanowski, V. M. Van Deerlin, G. D. Schellenberg, M. A. Nalls, V. E. Drory, C. S. Lu, T. H. Yeh, H. Ishiura, Y. Takahashi, S. Tsuji, I. Le Ber, A. Brice, C. Drepper, N. Williams, J. Kirby, P. Shaw, J. Hardy, P. J. Tienari, P. Heutink, H. R. Morris, S. Pickering-Brown, and B. J. Traynor, 2012, Frequency of the C9orf72 hexanucleotide repeat expansion in patients with amyotrophic lateral sclerosis and frontotemporal dementia: a cross-sectional study: Lancet Neurol, v. 11, p. 323-30.

Mann, D. M., S. Rollinson, A. Robinson, J. Bennion Callister, J. C. Thompson, J. S. Snowden, T. Gendron, L. Petrucelli, M. Masuda-Suzukake, M. Hasegawa, Y. Davidson, and S. Pickering-Brown, 2013, Dipeptide repeat proteins are present in the p62 positive inclusions in patients with frontotemporal lobar degeneration and motor neurone disease associated with expansions in C9ORF72: Acta Neuropathol Commun, v. 1, p. 68.

Martinez, F. J., G. A. Pratt, E. L. Van Nostrand, R. Batra, S. C. Huelga, K. Kapeli, P. Freese, S. J. Chun, K. Ling, C. Gelboin-Burkhart, L. Fijany, H. C. Wang, J. K. Nussbacher, S. M. Broski, H. J. Kim, R. Lardelli, B. Sundararaman, J. P. Donohue, A. Javaherian, J. Lykke-Andersen, S. Finkbeiner, C. F. Bennett, M. Ares, Jr., C. B. Burge, J. P. Taylor, F. Rigo, and G. W. Yeo, 2016, Protein-RNA Networks Regulated by Normal and ALS-Associated Mutant HNRNPA2B1 in the Nervous System: Neuron, v. 92, p. 780-795.

Maruyama, H., H. Morino, H. Ito, Y. Izumi, H. Kato, Y. Watanabe, Y. Kinoshita, M. Kamada, H. Nodera, H. Suzuki, O. Komure, S. Matsuura, K. Kobatake, N. Morimoto, K. Abe, N. Suzuki, M. Aoki, A. Kawata, T. Hirai, T. Kato, K. Ogasawara, A. Hirano, T. Takumi, H. Kusaka, K. Hagiwara, R. Kaji, and H. Kawakami, 2010, Mutations of optineurin in amyotrophic lateral sclerosis: Nature, v. 465, p. 223-6.

May, S., D. Hornburg, M. H. Schludi, T. Arzberger, K. Rentzsch, B. M. Schwenk, F. A. Grasser, K. Mori, E. Kremmer, J. Banzhaf-Strathmann, M. Mann, F. Meissner, and D. Edbauer, 2014, C9orf72 FTLD/ALS-associated Gly-Ala dipeptide repeat proteins cause neuronal toxicity and Unc119 sequestration: Acta Neuropathol, v. 128, p. 485-503.

Mertens, J., A. C. Paquola, M. Ku, E. Hatch, L. Bohnke, S. Ladjevardi, S. McGrath, B. Campbell, H. Lee, J. R. Herdy, J. T. Goncalves, T. Toda, Y. Kim, J. Winkler, J. Yao, M. W. Hetzer, and F. H. Gage, 2015a, Directly Reprogrammed Human Neurons Retain Aging-Associated Transcriptomic Signatures and Reveal Age-Related Nucleocytoplasmic Defects: Cell Stem Cell, v. 17, p. 705-18.

Mertens, J., K. Stuber, P. Wunderlich, J. Ladewig, J. C. Kesavan, R. Vandenberghe, M. Vandenbulcke, P. van Damme, J. Walter, O. Brustle, and P. Koch, 2013, APP processing in human pluripotent stem cell-derived neurons is resistant to NSAID-based gamma-secretase modulation: Stem Cell Reports, v. 1, p. 491-8.

Mertens, J., Q. W. Wang, Y. Kim, D. X. Yu, S. Pham, B. Yang, Y. Zheng, K. E. Diffenderfer, J. Zhang, S. Soltani, T. Eames, S. T. Schafer, L. Boyer, M. C. Marchetto, J. I. Nurnberger, J. R. Calabrese, K. J. Odegaard, M. J. McCarthy, P. P. Zandi, M. Alda, C. M. Nievergelt, S. Pharmacogenomics of Bipolar Disorder, S. Mi, K. J. Brennand, J. R. Kelsoe, F. H. Gage, and J. Yao, 2015b, Differential responses to lithium in hyperexcitable neurons from patients with bipolar disorder: Nature, v. 527, p. 95-9.

Meyer, M. A., and N. T. Potter, 1995, Sporadic ALS and chromosome 22: evidence for a possible neurofilament gene defect: Muscle Nerve, v. 18, p. 536-9.

Meyer, T., A. Schwan, J. S. Dullinger, J. Brocke, K. T. Hoffmann, C. H. Nolte, A. Hopt, U. Kopp, P. Andersen, J. T. Epplen, and P. Linke, 2005, Early-onset ALS with long-term survival associated with spastin gene mutation: Neurology, v. 65, p. 141-3.

Milanese, M., F. Giribaldi, M. Melone, T. Bonifacino, I. Musante, E. Carminati, P. I. Rossi, L. Vergani, A. Voci, F. Conti, A. Puliti, and G. Bonanno, 2014, Knocking down metabotropic glutamate receptor 1 improves survival and disease progression in the

SOD1(G93A) mouse model of amyotrophic lateral sclerosis: Neurobiol Dis, v. 64, p. 48-59.

Miller, Justine D., Yosif M. Ganat, S. Kishinevsky, Robert L. Bowman, B. Liu, Edmund Y. Tu, P. K. Mandal, E. Vera, J.-w. Shim, S. Kriks, T. Taldone, N. Fusaki, Mark J. Tomishima, D. Krainc, Teresa A. Milner, Derrick J. Rossi, and L. Studer, 2013a, Human iPSC-Based Modeling of Late-Onset Disease via Progerin-Induced Aging: Cell Stem Cell, v. 13, p. 691-705.

Miller, J. W., B. N. Smith, S. D. Topp, A. Al-Chalabi, C. E. Shaw, and C. Vance, 2012, Mutation analysis of VCP in British familial and sporadic amyotrophic lateral sclerosis patients: Neurobiol Aging, v. 33, p. 2721 e1-2.

Miller, T. M., A. Pestronk, W. David, J. Rothstein, E. Simpson, S. H. Appel, P. L. Andres, K. Mahoney, P. Allred, K. Alexander, L. W. Ostrow, D. Schoenfeld, E. A. Macklin, D. A. Norris, G. Manousakis, M. Crisp, R. Smith, C. F. Bennett, K. M. Bishop, and M. E. Cudkowicz, 2013b, An antisense oligonucleotide against SOD1 delivered intrathecally for patients with SOD1 familial amyotrophic lateral sclerosis: a phase 1, randomised, first-in-man study: Lancet Neurol, v. 12, p. 435-42.

Mitchell, J., P. Paul, H. J. Chen, A. Morris, M. Payling, M. Falchi, J. Habgood, S. Panoutsou, S. Winkler, V. Tisato, A. Hajitou, B. Smith, C. Vance, C. Shaw, N. D. Mazarakis, and J. de Belleroche, 2010, Familial amyotrophic lateral sclerosis is associated with a mutation in D-amino acid oxidase: Proc Natl Acad Sci U S A, v. 107, p. 7556-61.

Mitchell, J. C., R. Constable, E. So, C. Vance, E. Scotter, L. Glover, T. Hortobagyi, E. S. Arnold, S. C. Ling, M. McAlonis, S. Da Cruz, M. Polymenidou, L. Tessarolo, D. W. Cleveland, and C. E. Shaw, 2015, Wild type human TDP-43 potentiates ALS-linked mutant TDP-43 driven progressive motor and cortical neuron degeneration with pathological features of ALS: Acta Neuropathol Commun, v. 3, p. 36.

Mitchell, J. C., P. McGoldrick, C. Vance, T. Hortobagyi, J. Sreedharan, B. Rogelj, E. L. Tudor, B. N. Smith, C. Klasen, C. C. Miller, J. D. Cooper, L. Greensmith, and C. E. Shaw, 2013, Overexpression of human wild-type FUS causes progressive motor neuron degeneration in an age- and dose-dependent fashion: Acta Neuropathol, v. 125, p. 273-88.

Mitsumoto, H., B. R. Brooks, and V. Silani, 2014, Clinical trials in amyotrophic lateral sclerosis: why so many negative trials and how can trials be improved?: Lancet Neurol, v. 13, p. 1127-38.

Mizielinska, S., S. Gronke, T. Niccoli, C. E. Ridler, E. L. Clayton, A. Devoy, T. Moens, F. E. Norona, I. O. Woollacott, J. Pietrzyk, K. Cleverley, A. J. Nicoll, S. Pickering-Brown, J. Dols, M. Cabecinha, O. Hendrich, P. Fratta, E. M. Fisher, L. Partridge, and A. M. Isaacs, 2014, C9orf72 repeat expansions cause neurodegeneration in Drosophila through arginine-rich proteins: Science, v. 345, p. 1192-4.

Mizielinska, S., T. Lashley, F. E. Norona, E. L. Clayton, C. E. Ridler, P. Fratta, and A. M. Isaacs, 2013, C9orf72 frontotemporal lobar degeneration is characterised by frequent neuronal sense and antisense RNA foci: Acta Neuropathol, v. 126, p. 845-57.

Mizielinska, S., C. E. Ridler, R. Balendra, A. Thoeng, N. S. Woodling, F. A. Grasser, V. Plagnol, T. Lashley, L. Partridge, and A. M. Isaacs, 2017, Bidirectional nucleolar dysfunction in C9orf72 frontotemporal lobar degeneration: Acta Neuropathol Commun, v. 5, p. 29.

Moreira, M. C., S. Klur, M. Watanabe, A. H. Nemeth, I. Le Ber, J. C. Moniz, C. Tranchant, P. Aubourg, M. Tazir, L. Schols, M. Pandolfo, J. B. Schulz, J. Pouget, P. Calvas, M. Shizuka-Ikeda, M. Shoji, M. Tanaka, L. Izatt, C. E. Shaw, A. M'Zahem, E. Dunne, P. Bomont, T. Benhassine, N. Bouslam, G. Stevanin, A. Brice, J. Guimaraes, P. Mendonca, C. Barbot, P. Coutinho, J. Sequeiros, A. Durr, J. M. Warter, and M. Koenig, 2004, Senataxin, the ortholog of a yeast RNA helicase, is mutant in ataxia-ocular apraxia 2: Nat Genet, v. 36, p. 225-7.

Mori, K., T. Arzberger, F. A. Grasser, I. Gijselinck, S. May, K. Rentzsch, S. M. Weng, M. H. Schludi, J. van der Zee, M. Cruts, C. Van Broeckhoven, E. Kremmer, H. A. Kretzschmar, C. Haass, and D. Edbauer, 2013a, Bidirectional transcripts of the expanded C9orf72 hexanucleotide repeat are translated into aggregating dipeptide repeat proteins: Acta Neuropathol, v. 126, p. 881-93.

Mori, K., S. Lammich, I. R. Mackenzie, I. Forne, S. Zilow, H. Kretzschmar, D. Edbauer, J. Janssens, G. Kleinberger, M. Cruts, J. Herms, M. Neumann, C. Van Broeckhoven, T. Arzberger, and C. Haass, 2013b, hnRNP A3 binds to GGGGCC repeats and is a constituent of p62-positive/TDP43-negative inclusions in the hippocampus of patients with C9orf72 mutations: Acta Neuropathol, v. 125, p. 413-23.

Mori, K., Y. Nihei, T. Arzberger, Q. Zhou, I. R. Mackenzie, A. Hermann, F. Hanisch, D. German Consortium for Frontotemporal Lobar, A. Bavarian Brain Banking, F. Kamp, B. Nuscher, D. Orozco, D. Edbauer, and C. Haass, 2016, Reduced hnRNPA3 increases C9orf72 repeat RNA levels and dipeptide-repeat protein deposition: EMBO Rep, v. 17, p. 1314-25.

Mori, K., S. M. Weng, T. Arzberger, S. May, K. Rentzsch, E. Kremmer, B. Schmid, H. A. Kretzschmar, M. Cruts, C. Van Broeckhoven, C. Haass, and D. Edbauer, 2013c, The C9orf72 GGGGCC repeat is translated into aggregating dipeptide-repeat proteins in FTLD/ALS: Science, v. 339, p. 1335-8.

Mulders, S. A., W. J. van den Broek, T. M. Wheeler, H. J. Croes, P. van Kuik-Romeijn, S. J. de Kimpe, D. Furling, G. J. Platenburg, G. Gourdon, C. A. Thornton, B. Wieringa, and D. G. Wansink, 2009, Triplet-repeat oligonucleotide-mediated reversal of RNA toxicity in myotonic dystrophy: Proc Natl Acad Sci U S A, v. 106, p. 13915-20.

Munch, C., A. Rosenbohm, A. D. Sperfeld, I. Uttner, S. Reske, B. J. Krause, R. Sedlmeier, T. Meyer, C. O. Hanemann, G. Stumm, and A. C. Ludolph, 2005, Heterozygous R1101K mutation of the DCTN1 gene in a family with ALS and FTD: Ann Neurol, v. 58, p. 777-80.

Munch, C., R. Sedlmeier, T. Meyer, V. Homberg, A. D. Sperfeld, A. Kurt, J. Prudlo, G. Peraus, C. O. Hanemann, G. Stumm, and A. C. Ludolph, 2004, Point mutations of the p150 subunit of dynactin (DCTN1) gene in ALS: Neurology, v. 63, p. 724-6.

Murray, M. E., M. DeJesus-Hernandez, N. J. Rutherford, M. Baker, R. Duara, N. R. Graff-Radford, Z. K. Wszolek, T. J. Ferman, K. A. Josephs, K. B. Boylan, R. Rademakers, and D. W. Dickson, 2011, Clinical and neuropathologic heterogeneity of c9FTD/ALS associated with hexanucleotide repeat expansion in C9ORF72: Acta Neuropathol, v. 122, p. 673-90.

Nalbandian, A., K. J. Llewellyn, M. Badadani, H. Z. Yin, C. Nguyen, V. Katheria, G. Watts, J. Mukherjee, J. Vesa, V. Caiozzo, T. Mozaffar, J. H. Weiss, and V. E. Kimonis, 2013, A progressive translational mouse model of human valosin-containing protein disease: the VCP(R155H/+) mouse: Muscle Nerve, v. 47, p. 260-70.

Naujock, M., N. Stanslowsky, S. Bufler, M. Naumann, P. Reinhardt, J. Sterneckert, E. Kefalakes, C. Kassebaum, F. Bursch, X. Lojewski, A. Storch, M. Frickenhaus, T. M. Boeckers, S. Putz, M. Demestre, S. Liebau, M. Klingenstein, A. C. Ludolph, R. Dengler, K. S. Kim, A. Hermann, F. Wegner, and S. Petri, 2016, 4-Aminopyridine Induced Activity Rescues Hypoexcitable Motor Neurons from Amyotrophic Lateral Sclerosis Patient-Derived Induced Pluripotent Stem Cells: Stem Cells, v. 34, p. 1563-75.

Neumann, M., L. K. Kwong, E. B. Lee, E. Kremmer, A. Flatley, Y. Xu, M. S. Forman, D. Troost, H. A. Kretzschmar, J. Q. Trojanowski, and V. M. Lee, 2009, Phosphorylation of S409/410 of TDP-43 is a consistent feature in all sporadic and familial forms of TDP-43 proteinopathies: Acta Neuropathol, v. 117, p. 137-49.

Neumann, M., D. M. Sampathu, L. K. Kwong, A. C. Truax, M. C. Micsenyi, T. T. Chou, J. Bruce, T. Schuck, M. Grossman, C. M. Clark, L. F. McCluskey, B. L. Miller, E. Masliah, I. R.

Mackenzie, H. Feldman, W. Feiden, H. A. Kretzschmar, J. Q. Trojanowski, and V. M. Lee, 2006, Ubiquitinated TDP-43 in frontotemporal lobar degeneration and amyotrophic lateral sclerosis: Science, v. 314, p. 130-3.

Niblock, M., B. N. Smith, Y. B. Lee, V. Sardone, S. Topp, C. Troakes, S. Al-Sarraj, C. S. Leblond, P. A. Dion, G. A. Rouleau, C. E. Shaw, and J. M. Gallo, 2016, Retention of hexanucleotide repeat-containing intron in C9orf72 mRNA: implications for the pathogenesis of ALS/FTD: Acta Neuropathol Commun, v. 4, p. 18.

Nishimura, A. L., M. Mitne-Neto, H. C. Silva, A. Richieri-Costa, S. Middleton, D. Cascio, F. Kok, J. R. Oliveira, T. Gillingwater, J. Webb, P. Skehel, and M. Zatz, 2004, A mutation in the vesicle-trafficking protein VAPB causes late-onset spinal muscular atrophy and amyotrophic lateral sclerosis: Am J Hum Genet, v. 75, p. 822-31.

Nishimura, A. L., C. Shum, E. L. Scotter, A. Abdelgany, V. Sardone, J. Wright, Y. B. Lee, H. J. Chen, B. Bilican, M. Carrasco, T. Maniatis, S. Chandran, B. Rogelj, J. M. Gallo, and C. E. Shaw, 2014, Allele-specific knockdown of ALS-associated mutant TDP-43 in neural stem cells derived from induced pluripotent stem cells: PLoS One, v. 9, p. e91269.

Nishimura, A. L., V. Zupunski, C. Troakes, C. Kathe, P. Fratta, M. Howell, J. M. Gallo, T. Hortobagyi, C. E. Shaw, and B. Rogelj, 2010, Nuclear import impairment causes cytoplasmic trans-activation response DNA-binding protein accumulation and is associated with frontotemporal lobar degeneration: Brain, v. 133, p. 1763-71.

Niwa, J.-i., S.-i. Yamada, S. Ishigaki, J. Sone, M. Takahashi, M. Katsuno, F. Tanaka, M. Doyu, and G. Sobue, 2007, Disulfide Bond Mediates Aggregation, Toxicity, and Ubiquitylation of Familial Amyotrophic Lateral Sclerosis-linked Mutant SOD1: Journal of Biological Chemistry, v. 282, p. 28087-28095.

Nordin, A., C. Akimoto, A. Wuolikainen, H. Alstermark, P. Jonsson, A. Birve, S. L. Marklund, K. S. Graffmo, K. Forsberg, T. Brannstrom, and P. M. Andersen, 2015, Extensive size variability of the GGGGCC expansion in C9orf72 in both neuronal and non-neuronal tissues in 18 patients with ALS or FTD: Hum Mol Genet, v. 24, p. 3133-42.

O'Rourke, J. G., L. Bogdanik, A. K. Muhammad, T. F. Gendron, K. J. Kim, A. Austin, J. Cady, E. Y. Liu, J. Zarrow, S. Grant, R. Ho, S. Bell, S. Carmona, M. Simpkinson, D. Lall, K. Wu, L. Daughrity, D. W. Dickson, M. B. Harms, L. Petrucelli, E. B. Lee, C. M. Lutz, and R. H. Baloh, 2015, C9orf72 BAC Transgenic Mice Display Typical Pathologic Features of ALS/FTD: Neuron, v. 88, p. 892-901.

O'Rourke, J. G., L. Bogdanik, A. Yanez, D. Lall, A. J. Wolf, A. K. Muhammad, R. Ho, S. Carmona, J. P. Vit, J. Zarrow, K. J. Kim, S. Bell, M. B. Harms, T. M. Miller, C. A. Dangler, D. M. Underhill, H. S. Goodridge, C. M. Lutz, and R. H. Baloh, 2016, C9orf72 is required for proper macrophage and microglial function in mice: Science, v. 351, p. 1324-9.

Osaka, M., D. Ito, T. Yagi, Y. Nihei, and N. Suzuki, 2015, Evidence of a link between ubiquilin 2 and optineurin in amyotrophic lateral sclerosis: Hum Mol Genet, v. 24, p. 1617-29.

Parkinson, N., P. G. Ince, M. O. Smith, R. Highley, G. Skibinski, P. M. Andersen, K. E. Morrison, H. S. Pall, O. Hardiman, J. Collinge, P. J. Shaw, E. M. Fisher, M. R. C. P. i. A. Study, and F. R. Consortium, 2006, ALS phenotypes with mutations in CHMP2B (charged multivesicular body protein 2B): Neurology, v. 67, p. 1074-7.

Peters, O. M., G. T. Cabrera, H. Tran, T. F. Gendron, J. E. McKeon, J. Metterville, A. Weiss, N. Wightman, J. Salameh, J. Kim, H. Sun, K. B. Boylan, D. Dickson, Z. Kennedy, Z. Lin, Y. J. Zhang, L. Daughrity, C. Jung, F. B. Gao, P. C. Sapp, H. R. Horvitz, D. A. Bosco, S. P. Brown, P. de Jong, L. Petrucelli, C. Mueller, and R. H. Brown, Jr., 2015, Human C9ORF72 Hexanucleotide Expansion Reproduces RNA Foci and Dipeptide Repeat Proteins but Not Neurodegeneration in BAC Transgenic Mice: Neuron, v. 88, p. 902-9.

Petrov, D., C. Mansfield, A. Moussy, and O. Hermine, 2017, ALS Clinical Trials Review: 20 Years of Failure. Are We Any Closer to Registering a New Treatment?: Front Aging Neurosci, v. 9, p. 68.

Pfaffl, M. W., 2001, A new mathematical model for relative quantification in real-time RT-PCR: Nucleic Acids Res, v. 29, p. e45.

Picher-Martel, V., P. N. Valdmanis, P. V. Gould, J. P. Julien, and N. Dupre, 2016, From animal models to human disease: a genetic approach for personalized medicine in ALS: Acta Neuropathol Commun, v. 4, p. 70.

Polymenidou, M., C. Lagier-Tourenne, K. R. Hutt, S. C. Huelga, J. Moran, T. Y. Liang, S. C. Ling, E. Sun, E. Wancewicz, C. Mazur, H. Kordasiewicz, Y. Sedaghat, J. P. Donohue, L. Shiue, C. F. Bennett, G. W. Yeo, and D. W. Cleveland, 2011, Long pre-mRNA depletion and RNA missplicing contribute to neuronal vulnerability from loss of TDP-43: Nat Neurosci, v. 14, p. 459-68.

Porta, S., L. K. Kwong, J. Q. Trojanowski, and V. M. Lee, 2015, Drosha Inclusions Are New Components of Dipeptide-Repeat Protein Aggregates in FTLD-TDP and ALS C9orf72 Expansion Cases: J Neuropathol Exp Neurol, v. 74, p. 380-7.

Pottier, C., K. F. Bieniek, N. Finch, M. van de Vorst, M. Baker, R. Perkersen, P. Brown, T. Ravenscroft, M. van Blitterswijk, A. M. Nicholson, M. DeTure, D. S. Knopman, K. A. Josephs, J. E. Parisi, R. C. Petersen, K. B. Boylan, B. F. Boeve, N. R. Graff-Radford, J. A. Veltman, C. Gilissen, M. E. Murray, D. W. Dickson, and R. Rademakers, 2015, Whole-genome sequencing reveals important role for TBK1 and OPTN mutations in frontotemporal lobar degeneration without motor neuron disease: Acta Neuropathol, v. 130, p. 77-92.

Proudfoot, M., N. J. Gutowski, D. Edbauer, D. A. Hilton, M. Stephens, J. Rankin, and I. R. Mackenzie, 2014, Early dipeptide repeat pathology in a frontotemporal dementia kindred with C9ORF72 mutation and intellectual disability: Acta Neuropathol, v. 127, p. 451-8.

Prudencio, M., V. V. Belzil, R. Batra, C. A. Ross, T. F. Gendron, L. J. Pregent, M. E. Murray, K. K. Overstreet, A. E. Piazza-Johnston, P. Desaro, K. F. Bieniek, M. DeTure, W. C. Lee, S. M. Biendarra, M. D. Davis, M. C. Baker, R. B. Perkerson, M. van Blitterswijk, C. T. Stetler, R. Rademakers, C. D. Link, D. W. Dickson, K. B. Boylan, H. Li, and L. Petrucelli, 2015, Distinct brain transcriptome profiles in C9orf72-associated and sporadic ALS: Nat Neurosci, v. 18, p. 1175-82.

Qian, K., H. Huang, A. Peterson, B. Hu, N. J. Maragakis, G. L. Ming, H. Chen, and S. C. Zhang, 2017, Sporadic ALS Astrocytes Induce Neuronal Degeneration In Vivo: Stem Cell Reports.

Ralph, G. S., P. A. Radcliffe, D. M. Day, J. M. Carthy, M. A. Leroux, D. C. Lee, L. F. Wong, L. G. Bilsland, L. Greensmith, S. M. Kingsman, K. A. Mitrophanous, N. D. Mazarakis, and M. Azzouz, 2005, Silencing mutant SOD1 using RNAi protects against neurodegeneration and extends survival in an ALS model: Nat Med, v. 11, p. 429-33.

Raoul, C., T. Abbas-Terki, J. C. Bensadoun, S. Guillot, G. Haase, J. Szulc, C. E. Henderson, and P. Aebischer, 2005, Lentiviral-mediated silencing of SOD1 through RNA interference retards disease onset and progression in a mouse model of ALS: Nat Med, v. 11, p. 423-8.

Rasool, C. G., W. G. Bradley, B. Connolly, and J. K. Baruah, 1983, Acetylcholinesterase and ATPases in motor neuron degenerative diseases: Muscle Nerve, v. 6, p. 430-5.

Ratti, A., and E. Buratti, 2016, Physiological functions and pathobiology of TDP-43 and FUS/TLS proteins: J Neurochem, v. 138 Suppl 1, p. 95-111.

Reddy, K., M. H. Schmidt, J. M. Geist, N. P. Thakkar, G. B. Panigrahi, Y. H. Wang, and C. E. Pearson, 2014, Processing of double-R-loops in (CAG).(CTG) and C9orf72 (GGGGCC).(GGCCCC) repeats causes instability: Nucleic Acids Res, v. 42, p. 10473-87.

Renton, A. E., E. Majounie, A. Waite, J. Simon-Sanchez, S. Rollinson, J. R. Gibbs, J. C. Schymick, H. Laaksovirta, J. C. van Swieten, L. Myllykangas, H. Kalimo, A. Paetau, Y. Abramzon, A. M. Remes, A. Kaganovich, S. W. Scholz, J. Duckworth, J. Ding, D. W. Harmer, D. G. Hernandez, J. O. Johnson, K. Mok, M. Ryten, D. Trabzuni, R. J. Guerreiro, R. W. Orrell, J. Neal, A. Murray, J. Pearson, I. E. Jansen, D. Sondervan, H. Seelaar, D. Blake, K. Young, N. Halliwell, J. B. Callister, G. Toulson, A. Richardson, A. Gerhard, J. Snowden, D. Mann, D. Neary, M. A. Nalls, T. Peuralinna, L. Jansson, V. M. Isoviita, A. L. Kaivorinne, M. Holtta-Vuori, E. Ikonen, R. Sulkava, M. Benatar, J. Wuu, A. Chio, G. Restagno, G. Borghero, M. Sabatelli, D. Heckerman, E. Rogaeva, L. Zinman, J. D. Rothstein, M. Sendtner, C. Drepper, E. E. Eichler, C. Alkan, Z. Abdullaev, S. D. Pack, A. Dutra, E. Pak, J. Hardy, A. Singleton, N. M. Williams, P. Heutink, S. Pickering-Brown, H. R. Morris, P. J. Tienari, and B. J. Traynor, 2011, A hexanucleotide repeat expansion in C9ORF72 is the cause of chromosome 9p21-linked ALS-FTD: Neuron, v. 72, p. 257-68.

Rigo, F., S. J. Chun, D. A. Norris, G. Hung, S. Lee, J. Matson, R. A. Fey, H. Gaus, Y. Hua, J. S. Grundy, A. R. Krainer, S. P. Henry, and C. F. Bennett, 2014, Pharmacology of a central nervous system delivered 2'-O-methoxyethyl-modified survival of motor neuron splicing oligonucleotide in mice and nonhuman primates: J Pharmacol Exp Ther, v. 350, p. 46-55.

Rodriguez-Ithurralde, D., A. Maruri, and X. Rodriguez, 1998, Motor neurone acetylcholinesterase release precedes neurotoxicity caused by systemic administration of excitatory amino acids and strychnine: J Neurol Sci, v. 160 Suppl 1, p. S80-6.

Rosen, D. R., T. Siddique, D. Patterson, D. A. Figlewicz, P. Sapp, A. Hentati, D. Donaldson, J. Goto, J. P. O'Regan, H. X. Deng, and et al., 1993, Mutations in Cu/Zn superoxide dismutase gene are associated with familial amyotrophic lateral sclerosis: Nature, v. 362, p. 59-62.

Rossi, S., A. Serrano, V. Gerbino, A. Giorgi, L. Di Francesco, M. Nencini, F. Bozzo, M. E. Schinina, C. Bagni, G. Cestra, M. T. Carri, T. Achsel, and M. Cozzolino, 2015, Nuclear accumulation of mRNAs underlies G4C2 repeat-induced translational repression in a cellular model of C9orf72 ALS: J Cell Sci.

Ruddy, D. M., M. J. Parton, A. Al-Chalabi, C. M. Lewis, C. Vance, B. N. Smith, P. N. Leigh, J. F. Powell, T. Siddique, E. Postumus Meyjes, F. Baas, V. De Jong, and C. E. Shaw, 2003, Two Families with Familial Amyotrophic Lateral Sclerosis Are Linked to a Novel Locus on Chromosome 16q: The American Journal of Human Genetics, v. 73, p. 390-396.

Sapp, P. C., B. A. Hosler, D. McKenna-Yasek, W. Chin, A. Gann, H. Genise, J. Gorenstein, M. Huang, W. Sailer, M. Scheffler, M. Valesky, J. L. Haines, M. Pericak-Vance, T. Siddique, H. R. Horvitz, and R. H. Brown Jr, 2003, Identification of Two Novel Loci for Dominantly Inherited Familial Amyotrophic Lateral Sclerosis: The American Journal of Human Genetics, v. 73, p. 397-403.

Sareen, D., J. G. O'Rourke, P. Meera, A. K. Muhammad, S. Grant, M. Simpkinson, S. Bell, S. Carmona, L. Ornelas, A. Sahabian, T. Gendron, L. Petrucelli, M. Baughn, J. Ravits, M. B. Harms, F. Rigo, C. F. Bennett, T. S. Otis, C. N. Svendsen, and R. H. Baloh, 2013, Targeting RNA foci in iPSC-derived motor neurons from ALS patients with a C9ORF72 repeat expansion: Sci Transl Med, v. 5, p. 208ra149.

Scarrott, J. M., S. Herranz-Martin, A. R. Alrafiah, P. J. Shaw, and M. Azzouz, 2015, Current developments in gene therapy for amyotrophic lateral sclerosis: Expert Opin Biol Ther, v. 15, p. 935-47.

Schludi, M. H., L. Becker, L. Garrett, T. F. Gendron, Q. Zhou, F. Schreiber, B. Popper, L. Dimou, T. M. Strom, J. Winkelmann, A. von Thaden, K. Rentzsch, S. May, M. Michaelsen, B. M. Schwenk, J. Tan, B. Schoser, M. Dieterich, L. Petrucelli, S. M. Holter, W. Wurst, H.

Fuchs, V. Gailus-Durner, M. H. de Angelis, T. Klopstock, T. Arzberger, and D. Edbauer, 2017, Spinal poly-GA inclusions in a C9orf72 mouse model trigger motor deficits and inflammation without neuron loss: Acta Neuropathol.

Schludi, M. H., S. May, F. A. Grasser, K. Rentzsch, E. Kremmer, C. Kupper, T. Klopstock, D. German Consortium for Frontotemporal Lobar, A. Bavarian Brain Banking, T. Arzberger, and D. Edbauer, 2015, Distribution of dipeptide repeat proteins in cellular models and C9orf72 mutation cases suggests link to transcriptional silencing: Acta Neuropathol, v. 130, p. 537-55.

Schmid, B., A. Hruscha, S. Hogl, J. Banzhaf-Strathmann, K. Strecker, J. van der Zee, M. Teucke, S. Eimer, J. Hegermann, M. Kittelmann, E. Kremmer, M. Cruts, B. Solchenberger, L. Hasenkamp, F. van Bebber, C. Van Broeckhoven, D. Edbauer, S. F. Lichtenthaler, and C. Haass, 2013, Loss of ALS-associated TDP-43 in zebrafish causes muscle degeneration, vascular dysfunction, and reduced motor neuron axon outgrowth: Proc Natl Acad Sci U S A, v. 110, p. 4986-91.

Scotter, E. L., L. Smyth, J. A. Bailey, C. H. Wong, M. de Majo, C. A. Vance, B. J. Synek, C. Turner, J. Pereira, A. Charleston, H. J. Waldvogel, M. A. Curtis, M. Dragunow, C. E. Shaw, B. N. Smith, and R. L. Faull, 2016, C9ORF72 and UBQLN2 mutations are causes of amyotrophic lateral sclerosis in New Zealand: a genetic and pathologic study using banked human brain tissue: Neurobiol Aging.

Sellier, C., M. L. Campanari, C. Julie Corbier, A. Gaucherot, I. Kolb-Cheynel, M. Oulad-Abdelghani, F. Ruffenach, A. Page, S. Ciura, E. Kabashi, and N. Charlet-Berguerand, 2016, Loss of C9ORF72 impairs autophagy and synergizes with polyQ Ataxin-2 to induce motor neuron dysfunction and cell death: EMBO J, v. 35, p. 1276-97.

Shang, Y., and E. J. Huang, 2016, Mechanisms of FUS mutations in familial amyotrophic lateral sclerosis: Brain Res, v. 1647, p. 65-78.

Shaw, P. J., V. Forrest, P. G. Ince, J. P. Richardson, and H. J. Wastell, 1995a, CSF and plasma amino acid levels in motor neuron disease: elevation of CSF glutamate in a subset of patients: Neurodegeneration, v. 4, p. 209-16.

Shaw, P. J., P. G. Ince, G. Falkous, and D. Mantle, 1995b, Oxidative damage to protein in sporadic motor neuron disease spinal cord: Ann Neurol, v. 38, p. 691-5.

Siller, R., S. Greenhough, E. Naumovska, and G. J. Sullivan, 2015, Small-molecule-driven hepatocyte differentiation of human pluripotent stem cells: Stem Cell Reports, v. 4, p. 939-52.

Simon-Sanchez, J., E. G. Dopper, P. E. Cohn-Hokke, R. K. Hukema, N. Nicolaou, H. Seelaar, J. R. de Graaf, I. de Koning, N. M. van Schoor, D. J. Deeg, M. Smits, J. Raaphorst, L. H. van den Berg, H. J. Schelhaas, C. E. De Die-Smulders, D. Majoor-Krakauer, A. J. Rozemuller, R. Willemsen, Y. A. Pijnenburg, P. Heutink, and J. C. van Swieten, 2012, The clinical and pathological phenotype of C9ORF72 hexanucleotide repeat expansions: Brain, v. 135, p. 723-35.

Simpson, C. L., R. Lemmens, K. Miskiewicz, W. J. Broom, V. K. Hansen, P. W. van Vught, J. E. Landers, P. Sapp, L. Van Den Bosch, J. Knight, B. M. Neale, M. R. Turner, J. H. Veldink, R. A. Ophoff, V. B. Tripathi, A. Beleza, M. N. Shah, P. Proitsi, A. Van Hoecke, P. Carmeliet, H. R. Horvitz, P. N. Leigh, C. E. Shaw, L. H. van den Berg, P. C. Sham, J. F. Powell, P. Verstreken, R. H. Brown, Jr., W. Robberecht, and A. Al-Chalabi, 2009, Variants of the elongator protein 3 (ELP3) gene are associated with motor neuron degeneration: Hum Mol Genet, v. 18, p. 472-81.

Sivadasan, R., D. Hornburg, C. Drepper, N. Frank, S. Jablonka, A. Hansel, X. Lojewski, J. Sterneckert, A. Hermann, P. J. Shaw, P. G. Ince, M. Mann, F. Meissner, and M. Sendtner, 2016, C9ORF72 interaction with cofilin modulates actin dynamics in motor neurons: Nat Neurosci, v. 19, p. 1610-1618.

Smith, B. N., S. Newhouse, A. Shatunov, C. Vance, S. Topp, L. Johnson, J. Miller, Y. Lee, C. Troakes, K. M. Scott, A. Jones, I. Gray, J. Wright, T. Hortobagyi, S. Al-Sarraj, B. Rogelj, J. Powell, M. Lupton, S. Lovestone, P. C. Sapp, M. Weber, P. J. Nestor, H. J. Schelhaas, A. A. Asbroek, V. Silani, C. Gellera, F. Taroni, N. Ticozzi, L. Van den Berg, J. Veldink, P. Van Damme, W. Robberecht, P. J. Shaw, J. Kirby, H. Pall, K. E. Morrison, A. Morris, J. de Belleroche, J. M. Vianney de Jong, F. Baas, P. M. Andersen, J. Landers, R. H. Brown, Jr., M. E. Weale, A. Al-Chalabi, and C. E. Shaw, 2013, The C9ORF72 expansion mutation is a common cause of ALS+/-FTD in Europe and has a single founder: Eur J Hum Genet, v. 21, p. 102-8.

Smith, B. N., N. Ticozzi, C. Fallini, A. S. Gkazi, S. Topp, K. P. Kenna, E. L. Scotter, J. Kost, P. Keagle, J. W. Miller, D. Calini, C. Vance, E. W. Danielson, C. Troakes, C. Tiloca, S. Al-Sarraj, E. A. Lewis, A. King, C. Colombrita, V. Pensato, B. Castellotti, J. de Belleroche, F. Baas, A. L. ten Asbroek, P. C. Sapp, D. McKenna-Yasek, R. L. McLaughlin, M. Polak, S. Asress, J. Esteban-Perez, J. L. Munoz-Blanco, M. Simpson, S. Consortium, W. van Rheenen, F. P. Diekstra, G. Lauria, S. Duga, S. Corti, C. Cereda, L. Corrado, G. Soraru, K. E. Morrison, K. L. Williams, G. A. Nicholson, I. P. Blair, P. A. Dion, C. S. Leblond, G. A. Rouleau, O. Hardiman, J. H. Veldink, L. H. van den Berg, A. Al-Chalabi, H. Pall, P. J. Shaw, M. R. Turner, K. Talbot, F. Taroni, A. Garcia-Redondo, Z. Wu, J. D. Glass, C. Gellera, A. Ratti, R. H. Brown, Jr., V. Silani, C. E. Shaw, and J. E. Landers, 2014, Exome-wide rare variant analysis identifies TUBA4A mutations associated with familial ALS: Neuron, v. 84, p. 324-31.

Smith, R. A., T. M. Miller, K. Yamanaka, B. P. Monia, T. P. Condon, G. Hung, C. S. Lobsiger, C. M. Ward, M. McAlonis-Downes, H. Wei, E. V. Wancewicz, C. F. Bennett, and D. W. Cleveland, 2006, Antisense oligonucleotide therapy for neurodegenerative disease: J Clin Invest, v. 116, p. 2290-6.

Snowden, J. S., S. Rollinson, J. C. Thompson, J. M. Harris, C. L. Stopford, A. M. Richardson, M. Jones, A. Gerhard, Y. S. Davidson, A. Robinson, L. Gibbons, Q. Hu, D. DuPlessis, D. Neary, D. M. Mann, and S. M. Pickering-Brown, 2012, Distinct clinical and pathological characteristics of frontotemporal dementia associated with C9ORF72 mutations: Brain, v. 135, p. 693-708.

Spillantini, M. G., M. L. Schmidt, V. M. Lee, J. Q. Trojanowski, R. Jakes, and M. Goedert, 1997, Alpha-synuclein in Lewy bodies: Nature, v. 388, p. 839-40.

Sposito, T., E. Preza, C. J. Mahoney, N. Seto-Salvia, N. S. Ryan, H. R. Morris, C. Arber, M. J. Devine, H. Houlden, T. T. Warner, T. J. Bushell, M. Zagnoni, T. Kunath, F. J. Livesey, N. C. Fox, M. N. Rossor, J. Hardy, and S. Wray, 2015, Developmental regulation of tau splicing is disrupted in stem cell-derived neurons from frontotemporal dementia patients with the 10 + 16 splice-site mutation in MAPT: Hum Mol Genet, v. 24, p. 5260-9.

Sreedharan, J., I. P. Blair, V. B. Tripathi, X. Hu, C. Vance, B. Rogelj, S. Ackerley, J. C. Durnall, K. L. Williams, E. Buratti, F. Baralle, J. de Belleroche, J. D. Mitchell, P. N. Leigh, A. Al-Chalabi, C. C. Miller, G. Nicholson, and C. E. Shaw, 2008, TDP-43 mutations in familial and sporadic amyotrophic lateral sclerosis: Science, v. 319, p. 1668-72.

Stoica, R., K. J. De Vos, S. Paillusson, S. Mueller, R. M. Sancho, K. F. Lau, G. Vizcay-Barrena, W. L. Lin, Y. F. Xu, J. Lewis, D. W. Dickson, L. Petrucelli, J. C. Mitchell, C. E. Shaw, and C. C. Miller, 2014, ER-mitochondria associations are regulated by the VAPB-PTPIP51 interaction and are disrupted by ALS/FTD-associated TDP-43: Nat Commun, v. 5, p. 3996.

Stopford, M. J., A. Higginbottom, G. M. Hautbergue, J. Cooper-Knock, P. J. Mulcahy, K. J. De Vos, A. E. Renton, H. Pliner, A. Calvo, A. Chio, B. J. Traynor, M. Azzouz, P. R. Heath, I. Consortium, N. Consortium, J. Kirby, and P. J. Shaw, 2017, C9ORF72 hexanucleotide

repeat exerts toxicity in a stable, inducible motor neuronal cell model, which is rescued by partial depletion of Pten: Hum Mol Genet.

Suarez-Calvet, M., M. Neumann, T. Arzberger, C. Abou-Ajram, E. Funk, H. Hartmann, D. Edbauer, E. Kremmer, C. Gobl, M. Resch, B. Bourgeois, T. Madl, S. Reber, D. Jutzi, M. D. Ruepp, I. R. Mackenzie, O. Ansorge, D. Dormann, and C. Haass, 2016, Monomethylated and unmethylated FUS exhibit increased binding to Transportin and distinguish FTLD-FUS from ALS-FUS: Acta Neuropathol, v. 131, p. 587-604.

Sud, R., E. T. Geller, and G. D. Schellenberg, 2014, Antisense-mediated Exon Skipping Decreases Tau Protein Expression: A Potential Therapy For Tauopathies: Mol Ther Nucleic Acids, v. 3, p. e180.

Sudria-Lopez, E., M. Koppers, M. de Wit, C. van der Meer, H. J. Westeneng, C. A. Zundel, S. A. Youssef, L. Harkema, A. de Bruin, J. H. Veldink, L. H. van den Berg, and R. J. Pasterkamp, 2016, Full ablation of C9orf72 in mice causes immune system-related pathology and neoplastic events but no motor neuron defects: Acta Neuropathol, v. 132, p. 145-7.

Suh, E., E. B. Lee, D. Neal, E. M. Wood, J. B. Toledo, L. Rennert, D. J. Irwin, C. T. McMillan, B. Krock, L. B. Elman, L. F. McCluskey, M. Grossman, S. X. Xie, J. Q. Trojanowski, and V. M. Van Deerlin, 2015, Semi-automated quantification of C9orf72 expansion size reveals inverse correlation between hexanucleotide repeat number and disease duration in frontotemporal degeneration: Acta Neuropathol, v. 130, p. 363-72.

Sun, X., L. O. Marque, Z. Cordner, J. L. Pruitt, M. Bhat, P. P. Li, G. Kannan, E. E. Ladenheim, T. H. Moran, R. L. Margolis, and D. D. Rudnicki, 2014, Phosphorodiamidate morpholino oligomers suppress mutant huntingtin expression and attenuate neurotoxicity: Hum Mol Genet, v. 23, p. 6302-17.

Suzuki, N., A. M. Maroof, F. T. Merkle, K. Koszka, A. Intoh, I. Armstrong, R. Moccia, B. N. Davis-Dusenbery, and K. Eggan, 2013, The mouse C9ORF72 ortholog is enriched in neurons known to degenerate in ALS and FTD: Nat Neurosci, v. 16, p. 1725-7.

Takahashi, K., K. Okita, M. Nakagawa, and S. Yamanaka, 2007, Induction of pluripotent stem cells from fibroblast cultures: Nat Protoc, v. 2, p. 3081-9.

Takahashi, K., and S. Yamanaka, 2006, Induction of pluripotent stem cells from mouse embryonic and adult fibroblast cultures by defined factors: Cell, v. 126, p. 663-76.

Takahashi, Y., Y. Fukuda, J. Yoshimura, A. Toyoda, K. Kurppa, H. Moritoyo, V. V. Belzil, P. A. Dion, K. Higasa, K. Doi, H. Ishiura, J. Mitsui, H. Date, B. Ahsan, T. Matsukawa, Y. Ichikawa, T. Moritoyo, M. Ikoma, T. Hashimoto, F. Kimura, S. Murayama, O. Onodera, M. Nishizawa, M. Yoshida, N. Atsuta, G. Sobue, JaCals, J. A. Fifita, K. L. Williams, I. P. Blair, G. A. Nicholson, P. Gonzalez-Perez, R. H. Brown, Jr., M. Nomoto, K. Elenius, G. A. Rouleau, A. Fujiyama, S. Morishita, J. Goto, and S. Tsuji, 2013, ERBB4 mutations that disrupt the neuregulin-ErbB4 pathway cause amyotrophic lateral sclerosis type 19: Am J Hum Genet, v. 93, p. 900-5.

Tao, Z., H. Wang, Q. Xia, K. Li, K. Li, X. Jiang, G. Xu, G. Wang, and Z. Ying, 2015, Nucleolar stress and impaired stress granule formation contribute to C9orf72 RAN translation-induced cytotoxicity: Hum Mol Genet, v. 24, p. 2426-41.

Taylor, J. P., R. H. Brown, Jr., and D. W. Cleveland, 2016, Decoding ALS: from genes to mechanism: Nature, v. 539, p. 197-206.

Teyssou, E., T. Takeda, V. Lebon, S. Boillee, B. Doukoure, G. Bataillon, V. Sazdovitch, C. Cazeneuve, V. Meininger, E. LeGuern, F. Salachas, D. Seilhean, and S. Millecamps, 2013, Mutations in SQSTM1 encoding p62 in amyotrophic lateral sclerosis: genetics and neuropathology: Acta Neuropathol, v. 125, p. 511-22.

Therrien, M., G. A. Rouleau, P. A. Dion, and J. A. Parker, 2013, Deletion of C9ORF72 results in motor neuron degeneration and stress sensitivity in C. elegans: PLoS One, v. 8, p. e83450.

Thys, R. G., and Y. H. Wang, 2015, DNA Replication Dynamics of the GGGGCC Repeat of the C9orf72 Gene: J Biol Chem, v. 290, p. 28953-62.

Ticozzi, N., C. Vance, A. L. Leclerc, P. Keagle, J. D. Glass, D. McKenna-Yasek, P. C. Sapp, V. Silani, D. A. Bosco, C. E. Shaw, R. H. Brown, Jr., and J. E. Landers, 2011, Mutational analysis reveals the FUS homolog TAF15 as a candidate gene for familial amyotrophic lateral sclerosis: Am J Med Genet B Neuropsychiatr Genet, v. 156B, p. 285-90.

Tollervey, J. R., T. Curk, B. Rogelj, M. Briese, M. Cereda, M. Kayikci, J. Konig, T. Hortobagyi, A. L. Nishimura, V. Zupunski, R. Patani, S. Chandran, G. Rot, B. Zupan, C. E. Shaw, and J. Ule, 2011, Characterizing the RNA targets and position-dependent splicing regulation by TDP-43: Nat Neurosci, v. 14, p. 452-8.

Tran, H., S. Almeida, J. Moore, T. F. Gendron, U. Chalasani, Y. Lu, X. Du, J. A. Nickerson, L. Petrucelli, Z. Weng, and F. B. Gao, 2015, Differential Toxicity of Nuclear RNA Foci versus Dipeptide Repeat Proteins in a Drosophila Model of C9ORF72 FTD/ALS: Neuron, v. 87, p. 1207-14.

Troakes, C., S. Maekawa, L. Wijesekera, B. Rogelj, L. Siklos, C. Bell, B. Smith, S. Newhouse, C. Vance, L. Johnson, T. Hortobagyi, A. Shatunov, A. Al-Chalabi, N. Leigh, C. E. Shaw, A. King, and S. Al-Sarraj, 2012, An MND/ALS phenotype associated with C9orf72 repeat expansion: abundant p62-positive, TDP-43-negative inclusions in cerebral cortex, hippocampus and cerebellum but without associated cognitive decline: Neuropathology, v. 32, p. 505-14.

Trotti, D., A. Rolfs, N. C. Danbolt, R. H. Brown, Jr., and M. A. Hediger, 1999, SOD1 mutants linked to amyotrophic lateral sclerosis selectively inactivate a glial glutamate transporter: Nat Neurosci, v. 2, p. 427-33.

Turner, M. R., J. Barnwell, A. Al-Chalabi, and A. Eisen, 2012, Young-onset amyotrophic lateral sclerosis: historical and other observations: Brain, v. 135, p. 2883-91.

Turner, M. R., A. Cagnin, F. E. Turkheimer, C. C. Miller, C. E. Shaw, D. J. Brooks, P. N. Leigh, and R. B. Banati, 2004, Evidence of widespread cerebral microglial activation in amyotrophic lateral sclerosis: an [11C](R)-PK11195 positron emission tomography study: Neurobiol Dis, v. 15, p. 601-9.

Urushitani, M., J. Kurisu, K. Tsukita, and R. Takahashi, 2002, Proteasomal inhibition by misfolded mutant superoxide dismutase 1 induces selective motor neuron death in familial amyotrophic lateral sclerosis: Journal of Neurochemistry, v. 83, p. 1030-1042.

Urwin, H., A. Authier, J. E. Nielsen, D. Metcalf, C. Powell, K. Froud, D. S. Malcolm, I. Holm, P. Johannsen, J. Brown, E. M. Fisher, J. van der Zee, M. Bruyland, F. R. Consortium, C. Van Broeckhoven, J. Collinge, S. Brandner, C. Futter, and A. M. Isaacs, 2010, Disruption of endocytic trafficking in frontotemporal dementia with CHMP2B mutations: Hum Mol Genet, v. 19, p. 2228-38.

van Blitterswijk, M., M. Dejesus-Hernandez, E. Niemantsverdriet, M. E. Murray, M. G. Heckman, N. N. Diehl, P. H. Brown, M. C. Baker, N. A. Finch, P. O. Bauer, G. Serrano, T. G. Beach, K. A. Josephs, D. S. Knopman, R. C. Petersen, B. F. Boeve, N. R. Graff-Radford, K. B. Boylan, L. Petrucelli, D. W. Dickson, and R. Rademakers, 2013, Association between repeat sizes and clinical and pathological characteristics in carriers of C9ORF72 repeat expansions (Xpansize-72): a cross-sectional cohort study: Lancet Neurol, v. 12, p. 978-88.

van Deutekom, J. C., A. A. Janson, I. B. Ginjaar, W. S. Frankhuizen, A. Aartsma-Rus, M. Bremmer-Bout, J. T. den Dunnen, K. Koop, A. J. van der Kooi, N. M. Goemans, S. J. de Kimpe, P. F. Ekhart, E. H. Venneker, G. J. Platenburg, J. J. Verschuuren, and G. J. van Ommen, 2007, Local dystrophin restoration with antisense oligonucleotide PRO051, N Engl J Med, v. 357: United States, 2007 Massachusetts Medical Society., p. 2677-86.

van Es, M. A., J. H. Veldink, C. G. Saris, H. M. Blauw, P. W. van Vught, A. Birve, R. Lemmens, H. J. Schelhaas, E. J. Groen, M. H. Huisman, A. J. van der Kooi, M. de Visser, C. Dahlberg, K. Estrada, F. Rivadeneira, A. Hofman, M. J. Zwarts, P. T. van Doormaal, D. Rujescu, E. Strengman, I. Giegling, P. Muglia, B. Tomik, A. Slowik, A. G. Uitterlinden, C. Hendrich, S. Waibel, T. Meyer, A. C. Ludolph, J. D. Glass, S. Purcell, S. Cichon, M. M. Nothen, H. E. Wichmann, S. Schreiber, S. H. Vermeulen, L. A. Kiemeney, J. H. Wokke, S. Cronin, R. L. McLaughlin, O. Hardiman, K. Fumoto, R. J. Pasterkamp, V. Meininger, J. Melki, P. N. Leigh, C. E. Shaw, J. E. Landers, A. Al-Chalabi, R. H. Brown, Jr., W. Robberecht, P. M. Andersen, R. A. Ophoff, and L. H. van den Berg, 2009, Genome-wide association study identifies 19p13.3 (UNC13A) and 9p21.2 as susceptibility loci for sporadic amyotrophic lateral sclerosis: Nat Genet, v. 41, p. 1083-7.

van Zundert, B., and R. H. Brown, Jr., 2016, Silencing strategies for therapy of SOD1-mediated ALS: Neurosci Lett.

Vance, C., A. Al-Chalabi, D. Ruddy, B. N. Smith, X. Hu, J. Sreedharan, T. Siddique, H. J. Schelhaas, B. Kusters, D. Troost, F. Baas, V. de Jong, and C. E. Shaw, 2006, Familial amyotrophic lateral sclerosis with frontotemporal dementia is linked to a locus on chromosome 9p13.2-21.3: Brain, v. 129, p. 868-76.

Vance, C., B. Rogelj, T. Hortobagyi, K. J. De Vos, A. L. Nishimura, J. Sreedharan, X. Hu, B. Smith, D. Ruddy, P. Wright, J. Ganesalingam, K. L. Williams, V. Tripathi, S. Al-Saraj, A. Al-Chalabi, P. N. Leigh, I. P. Blair, G. Nicholson, J. de Belleroche, J. M. Gallo, C. C. Miller, and C. E. Shaw, 2009, Mutations in FUS, an RNA processing protein, cause familial amyotrophic lateral sclerosis type 6: Science, v. 323, p. 1208-11.

Vance, C., E. L. Scotter, A. L. Nishimura, C. Troakes, J. C. Mitchell, C. Kathe, H. Urwin, C. Manser, C. C. Miller, T. Hortobagyi, M. Dragunow, B. Rogelj, and C. E. Shaw, 2013, ALS mutant FUS disrupts nuclear localization and sequesters wild-type FUS within cytoplasmic stress granules: Hum Mol Genet, v. 22, p. 2676-88.

Veldink, J. H., J. H. Wokke, G. van der Wal, J. M. Vianney de Jong, and L. H. van den Berg, 2002, Euthanasia and physician-assisted suicide among patients with amyotrophic lateral sclerosis in the Netherlands: N Engl J Med, v. 346, p. 1638-44.

Vernay, A., L. Therreau, B. Blot, V. Risson, S. Dirrig-Grosch, R. Waegaert, T. Lequeu, F. Sellal, L. Schaeffer, R. Sadoul, J. P. Loeffler, and F. Rene, 2016, A transgenic mouse expressing CHMP2Bintron5 mutant in neurons develops histological and behavioural features of amyotrophic lateral sclerosis and frontotemporal dementia: Hum Mol Genet.

Waite, A. J., D. Baumer, S. East, J. Neal, H. R. Morris, O. Ansorge, and D. J. Blake, 2014, Reduced C9orf72 protein levels in frontal cortex of amyotrophic lateral sclerosis and frontotemporal degeneration brain with the C9ORF72 hexanucleotide repeat expansion: Neurobiol Aging, v. 35, p. 1779 e5-1779 e13.

Walton, S. P., M. Wu, J. A. Gredell, and C. Chan, 2010, Designing highly active siRNAs for therapeutic applications: FEBS J, v. 277, p. 4806-13.

Watanabe, M., M. Dykes-Hoberg, V. C. Culotta, D. L. Price, P. C. Wong, and J. D. Rothstein, 2001, Histological evidence of protein aggregation in mutant SOD1 transgenic mice and in amyotrophic lateral sclerosis neural tissues: Neurobiol Dis, v. 8, p. 933-41.

Webster, C. P., E. F. Smith, A. J. Grierson, and K. J. De Vos, 2016, C9orf72 plays a central role in Rab GTPase-dependent regulation of autophagy: Small GTPases, p. 1-10.

Wen, X., W. Tan, T. Westergard, K. Krishnamurthy, S. S. Markandaiah, Y. Shi, S. Lin, N. A. Shneider, J. Monaghan, U. B. Pandey, P. Pasinelli, J. K. Ichida, and D. Trotti, 2014, Antisense proline-arginine RAN dipeptides linked to C9ORF72-ALS/FTD form toxic nuclear aggregates that initiate in vitro and in vivo neuronal death: Neuron, v. 84, p. 1213-25.

Westergard, T., B. K. Jensen, X. Wen, J. Cai, E. Kropf, L. Iacovitti, P. Pasinelli, and D. Trotti, 2016, Cell-to-Cell Transmission of Dipeptide Repeat Proteins Linked to C9orf72-ALS/FTD: Cell Rep, v. 17, p. 645-652.

Wheeler, T. M., A. J. Leger, S. K. Pandey, A. R. MacLeod, M. Nakamori, S. H. Cheng, B. M. Wentworth, C. F. Bennett, and C. A. Thornton, 2012, Targeting nuclear RNA for in vivo correction of myotonic dystrophy: Nature, v. 488, p. 111-5.

Wheeler, T. M., K. Sobczak, J. D. Lueck, R. J. Osborne, X. Lin, R. T. Dirksen, and C. A. Thornton, 2009, Reversal of RNA dominance by displacement of protein sequestered on triplet repeat RNA: Science, v. 325, p. 336-9.

White, M. A., and J. Sreedharan, 2016, Amyotrophic lateral sclerosis: recent genetic highlights: Curr Opin Neurol, v. 29, p. 557-64.

Williams, K. L., S. Topp, S. Yang, B. Smith, J. A. Fifita, S. T. Warraich, K. Y. Zhang, N. Farrawell, C. Vance, X. Hu, A. Chesi, C. S. Leblond, A. Lee, S. L. Rayner, V. Sundaramoorthy, C. Dobson-Stone, M. P. Molloy, M. van Blitterswijk, D. W. Dickson, R. C. Petersen, N. R. Graff-Radford, B. F. Boeve, M. E. Murray, C. Pottier, E. Don, C. Winnick, E. P. McCann, A. Hogan, H. Daoud, A. Levert, P. A. Dion, J. Mitsui, H. Ishiura, Y. Takahashi, J. Goto, J. Kost, C. Gellera, A. S. Gkazi, J. Miller, J. Stockton, W. S. Brooks, K. Boundy, M. Polak, J. L. Munoz-Blanco, J. Esteban-Perez, A. Rabano, O. Hardiman, K. E. Morrison, N. Ticozzi, V. Silani, J. de Belleroche, J. D. Glass, J. B. Kwok, G. J. Guillemin, R. S. Chung, S. Tsuji, R. H. Brown, Jr., A. Garcia-Redondo, R. Rademakers, J. E. Landers, A. D. Gitler, G. A. Rouleau, N. J. Cole, J. J. Yerbury, J. D. Atkin, C. E. Shaw, G. A. Nicholson, and I. P. Blair, 2016, CCNF mutations in amyotrophic lateral sclerosis and frontotemporal dementia: Nat Commun, v. 7, p. 11253.

Williamson, T. L., L. B. Corson, L. Huang, A. Burlingame, J. Liu, L. I. Bruijn, and D. W. Cleveland, 2000, Toxicity of ALS-linked SOD1 mutants: Science, v. 288, p. 399.

Winkler, G. S., T. G. Petrakis, S. Ethelberg, M. Tokunaga, H. Erdjument-Bromage, P. Tempst, and J. Q. Svejstrup, 2001, RNA polymerase II elongator holoenzyme is composed of two discrete subcomplexes: J Biol Chem, v. 276, p. 32743-9.

Woerner, A. C., F. Frottin, D. Hornburg, L. R. Feng, F. Meissner, M. Patra, J. Tatzelt, M. Mann, K. F. Winklhofer, F. U. Hartl, and M. S. Hipp, 2016, Cytoplasmic protein aggregates interfere with nucleocytoplasmic transport of protein and RNA: Science, v. 351, p. 173-6.

Wong, P. C., C. A. Pardo, D. R. Borchelt, M. K. Lee, N. G. Copeland, N. A. Jenkins, S. S. Sisodia, D. W. Cleveland, and D. L. Price, 1995, An adverse property of a familial ALS-linked SOD1 mutation causes motor neuron disease characterized by vacuolar degeneration of mitochondria: Neuron, v. 14, p. 1105-16.

Wu, C. H., C. Fallini, N. Ticozzi, P. J. Keagle, P. C. Sapp, K. Piotrowska, P. Lowe, M. Koppers, D. McKenna-Yasek, D. M. Baron, J. E. Kost, P. Gonzalez-Perez, A. D. Fox, J. Adams, F. Taroni, C. Tiloca, A. L. Leclerc, S. C. Chafe, D. Mangroo, M. J. Moore, J. A. Zitzewitz, Z. S. Xu, L. H. van den Berg, J. D. Glass, G. Siciliano, E. T. Cirulli, D. B. Goldstein, F. Salachas, V. Meininger, W. Rossoll, A. Ratti, C. Gellera, D. A. Bosco, G. J. Bassell, V. Silani, V. E. Drory, R. H. Brown, Jr., and J. E. Landers, 2012, Mutations in the profilin 1 gene cause familial amyotrophic lateral sclerosis: Nature, v. 488, p. 499-503.

Xi, Z., I. Rainero, E. Rubino, L. Pinessi, A. C. Bruni, R. G. Maletta, B. Nacmias, S. Sorbi, D. Galimberti, E. I. Surace, Y. Zheng, D. Moreno, C. Sato, Y. Liang, Y. Zhou, J. Robertson, L. Zinman, M. C. Tartaglia, P. St George-Hyslop, and E. Rogaeva, 2014, Hypermethylation of the CpG-island near the C9orf72 G4C2-repeat expansion in FTLD patients: Hum Mol Genet.

Xi, Z., M. Zhang, A. C. Bruni, R. G. Maletta, R. Colao, P. Fratta, J. M. Polke, M. G. Sweeney, E. Mudanohwo, B. Nacmias, S. Sorbi, M. C. Tartaglia, I. Rainero, E. Rubino, L. Pinessi, D. Galimberti, E. I. Surace, P. McGoldrick, P. McKeever, D. Moreno, C. Sato, Y. Liang, J.

Keith, L. Zinman, J. Robertson, and E. Rogaeva, 2015a, The C9orf72 repeat expansion itself is methylated in ALS and FTLD patients: Acta Neuropathol.

Xi, Z., M. Zhang, A. C. Bruni, R. G. Maletta, R. Colao, P. Fratta, J. M. Polke, M. G. Sweeney, E. Mudanohwo, B. Nacmias, S. Sorbi, M. C. Tartaglia, I. Rainero, E. Rubino, L. Pinessi, D. Galimberti, E. I. Surace, P. McGoldrick, P. McKeever, D. Moreno, C. Sato, Y. Liang, J. Keith, L. Zinman, J. Robertson, and E. Rogaeva, 2015b, The C9orf72 repeat expansion itself is methylated in ALS and FTLD patients: Acta Neuropathol, v. 129, p. 715-27.

Xi, Z., L. Zinman, D. Moreno, J. Schymick, Y. Liang, C. Sato, Y. Zheng, M. Ghani, S. Dib, J. Keith, J. Robertson, and E. Rogaeva, 2013, Hypermethylation of the CpG Island Near the GC Repeat in ALS with a C9orf72 Expansion: Am J Hum Genet.

Xiao, S., L. MacNair, P. McGoldrick, P. M. McKeever, J. R. McLean, M. Zhang, J. Keith, L. Zinman, E. Rogaeva, and J. Robertson, 2015, Isoform-specific antibodies reveal distinct subcellular localizations of C9orf72 in amyotrophic lateral sclerosis: Ann Neurol, v. 78, p. 568-83.

Xiao, S., L. MacNair, J. McLean, P. McGoldrick, P. McKeever, S. Soleimani, J. Keith, L. Zinman, E. Rogaeva, and J. Robertson, 2016, C9orf72 isoforms in Amyotrophic Lateral Sclerosis and Frontotemporal Lobar Degeneration: Brain Res, v. 1647, p. 43-9.

Xu, Y. F., T. F. Gendron, Y. J. Zhang, W. L. Lin, S. D'Alton, H. Sheng, M. C. Casey, J. Tong, J. Knight, X. Yu, R. Rademakers, K. Boylan, M. Hutton, E. McGowan, D. W. Dickson, J. Lewis, and L. Petrucelli, 2010, Wild-type human TDP-43 expression causes TDP-43 phosphorylation, mitochondrial aggregation, motor deficits, and early mortality in transgenic mice: J Neurosci, v. 30, p. 10851-9.

Xu, Z., M. Poidevin, X. Li, Y. Li, L. Shu, D. L. Nelson, H. Li, C. M. Hales, M. Gearing, T. S. Wingo, and P. Jin, 2013, Expanded GGGGCC repeat RNA associated with amyotrophic lateral sclerosis and frontotemporal dementia causes neurodegeneration: Proc Natl Acad Sci U S A, v. 110, p. 7778-83.

Yamakawa, M., D. Ito, T. Honda, K. Kubo, M. Noda, K. Nakajima, and N. Suzuki, 2015, Characterization of the dipeptide repeat protein in the molecular pathogenesis of c9FTD/ALS: Hum Mol Genet, v. 24, p. 1630-45.

Yang, C., E. W. Danielson, T. Qiao, J. Metterville, R. H. Brown, Jr., J. E. Landers, and Z. Xu, 2016a, Mutant PFN1 causes ALS phenotypes and progressive motor neuron degeneration in mice by a gain of toxicity: Proc Natl Acad Sci U S A, v. 113, p. E6209-E6218.

Yang, M., C. Liang, K. Swaminathan, S. Herrlinger, F. Lai, R. Shiekhattar, and J. F. Chen, 2016b, A C9ORF72/SMCR8-containing complex regulates ULK1 and plays a dual role in autophagy: Sci Adv, v. 2, p. e1601167.

Yang, Y., A. Hentati, H. X. Deng, O. Dabbagh, T. Sasaki, M. Hirano, W. Y. Hung, K. Ouahchi, J. Yan, A. C. Azim, N. Cole, G. Gascon, A. Yagmour, M. Ben-Hamida, M. Pericak-Vance, F. Hentati, and T. Siddique, 2001, The gene encoding alsin, a protein with three guanine-nucleotide exchange factor domains, is mutated in a form of recessive amyotrophic lateral sclerosis: Nat Genet, v. 29, p. 160-5.

Yeyeodu, S. T., S. M. Witherspoon, N. Gilyazova, and G. C. Ibeanu, 2010, A rapid, inexpensive high throughput screen method for neurite outgrowth: Curr Chem Genomics, v. 4, p. 74-83.

Zamiri, B., M. Mirceta, K. Bomsztyk, R. B. Macgregor, Jr., and C. E. Pearson, 2015, Quadruplex formation by both G-rich and C-rich DNA strands of the C9orf72 (GGGGCC)8*(GGCCCC)8 repeat: effect of CpG methylation: Nucleic Acids Res, v. 43, p. 10055-64.

Zamiri, B., K. Reddy, R. B. Macgregor, Jr., and C. E. Pearson, 2014, TMPyP4 porphyrin distorts RNA G-quadruplex structures of the disease-associated r(GGGGCC)n repeat of the

C9orf72 gene and blocks interaction of RNA-binding proteins: J Biol Chem, v. 289, p. 4653-9.

Zhang, K., C. J. Donnelly, A. R. Haeusler, J. C. Grima, J. B. Machamer, P. Steinwald, E. L. Daley, S. J. Miller, K. M. Cunningham, S. Vidensky, S. Gupta, M. A. Thomas, I. Hong, S. L. Chiu, R. L. Huganir, L. W. Ostrow, M. J. Matunis, J. Wang, R. Sattler, T. E. Lloyd, and J. D. Rothstein, 2015, The C9orf72 repeat expansion disrupts nucleocytoplasmic transport: Nature, v. 525, p. 56-61.

Zhang, K., J. C. Grima, J. D. Rothstein, and T. E. Lloyd, 2016a, Nucleocytoplasmic transport in C9orf72-mediated ALS/FTD: Nucleus, v. 7, p. 132-7.

Zhang, K. Y., S. Yang, S. T. Warraich, and I. P. Blair, 2014a, Ubiquilin 2: a component of the ubiquitin-proteasome system with an emerging role in neurodegeneration: Int J Biochem Cell Biol, v. 50, p. 123-6.

Zhang, Y. J., T. F. Gendron, J. C. Grima, H. Sasaguri, K. Jansen-West, Y. F. Xu, R. B. Katzman, J. Gass, M. E. Murray, M. Shinohara, W. L. Lin, A. Garrett, J. N. Stankowski, L. Daughrity, J. Tong, E. A. Perkerson, M. Yue, J. Chew, M. Castanedes-Casey, A. Kurti, Z. S. Wang, A. M. Liesinger, J. D. Baker, J. Jiang, C. Lagier-Tourenne, D. Edbauer, D. W. Cleveland, R. Rademakers, K. B. Boylan, G. Bu, C. D. Link, C. A. Dickey, J. D. Rothstein, D. W. Dickson, J. D. Fryer, and L. Petrucelli, 2016b, C9ORF72 poly(GA) aggregates sequester and impair HR23 and nucleocytoplasmic transport proteins: Nat Neurosci, v. 19, p. 668-77.

Zhang, Y. J., K. Jansen-West, Y. F. Xu, T. F. Gendron, K. F. Bieniek, W. L. Lin, H. Sasaguri, T. Caulfield, J. Hubbard, L. Daughrity, J. Chew, V. V. Belzil, M. Prudencio, J. N. Stankowski, M. Castanedes-Casey, E. Whitelaw, P. E. Ash, M. DeTure, R. Rademakers, K. B. Boylan, D. W. Dickson, and L. Petrucelli, 2014b, Aggregation-prone c9FTD/ALS poly(GA) RAN-translated proteins cause neurotoxicity by inducing ER stress: Acta Neuropathol, v. 128, p. 505-24.

Zhang, Z., S. Almeida, Y. Lu, A. L. Nishimura, L. Peng, D. Sun, B. Wu, A. M. Karydas, M. C. Tartaglia, J. C. Fong, B. L. Miller, R. V. Farese, Jr., M. J. Moore, C. E. Shaw, and F. B. Gao, 2013, Downregulation of microRNA-9 in iPSC-derived neurons of FTD/ALS patients with TDP-43 mutations: PLoS One, v. 8, p. e76055.

Zhou, Q., C. Lehmer, M. Michaelsen, K. Mori, D. Alterauge, D. Baumjohann, M. H. Schludi, J. Greiling, D. Farny, A. Flatley, R. Feederle, S. May, F. Schreiber, T. Arzberger, C. Kuhm, T. Klopstock, A. Hermann, C. Haass, and D. Edbauer, 2017, Antibodies inhibit transmission and aggregation of C9orf72 poly-GA dipeptide repeat proteins: EMBO Mol Med.

Zu, T., B. Gibbens, N. S. Doty, M. Gomes-Pereira, A. Huguet, M. D. Stone, J. Margolis, M. Peterson, T. W. Markowski, M. A. Ingram, Z. Nan, C. Forster, W. C. Low, B. Schoser, N. V. Somia, H. B. Clark, S. Schmechel, P. B. Bitterman, G. Gourdon, M. S. Swanson, M. Moseley, and L. P. Ranum, 2011, Non-ATG-initiated translation directed by microsatellite expansions: Proc Natl Acad Sci U S A, v. 108, p. 260-5.

Zu, T., Y. Liu, M. Banez-Coronel, T. Reid, O. Pletnikova, J. Lewis, T. M. Miller, M. B. Harms, A. E. Falchook, S. H. Subramony, L. W. Ostrow, J. D. Rothstein, J. C. Troncoso, and L. P. Ranum, 2013, RAN proteins and RNA foci from antisense transcripts in C9ORF72 ALS and frontotemporal dementia: Proc Natl Acad Sci U S A, v. 110, p. E4968-77.